Duality web between little string theories of type A

Brice Bastian

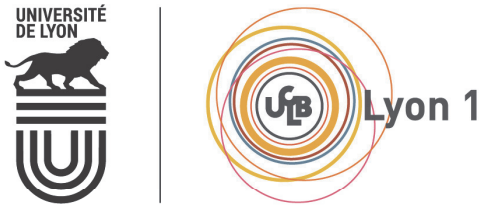

N°d'ordre NNT : 2019LYSE1117

THESE de DOCTORAT DE L'UNIVERSITE DE LYON

opérée au sein de

l'Université Claude Bernard Lyon 1

Ecole Doctorale N° 52

Physique et Astrophysique

Spécialité de doctorat : Physique

Discipline : Physique théorique

Soutenue publiquement le 06/09/2019, par :

Brice BASTIAN

Duality web between little string theories of type A

Devant le jury composé de :

GIERES, François *Professeur* Université de Lyon 1 Président

KASHANI-POOR, Amir-Kian *Maître de Conférences* ENS Paris (Rapporteur)

POMONI, Elli *Tenured staff member* DESY Hamburg (Rapporteure)

GIERES, François *Professeur* Université de Lyon 1 (Examinateur)

MEKAREEYA, Noppadol *Professeur associé* Università Milano-Bicocca (Examinateur)

TSIMPIS, Dimitrios *Professeur* Université de Lyon 1 (Examinateur)

HOHENEGGER, Stefan *Maître de Conférences* Université de Lyon 1 (Directeur de thèse)

To my grandfather,

Pierre Bastian

Acknowledgments

I want to start by thanking my thesis advisor Stefan who made an enriching and gratifying experience out of my thesis. Even with a busy schedule, he always made time for me. Our numerous, sometimes long lasting, discussions provided me with a lot of valuable insights and allowed my to grow as a researcher. Although, I was Stefan's first PhD student, his guidance was impeccable and he presented me with a lot of opportunities. I will always be grateful to him for introducing me to his collaborators Amer Iqbal and Soo-Jong Rey, both to whom I am also grateful for their support. Their vast knowledge made our collaboration a stimulating experience.

I also want to thank the "Institut de physique nucléaire" for being such a welcoming host institution during the completion of my PhD. The theoretical physics group with its permanent members and PhD students provided me with good company that made even the more difficult days enjoyable. I am especially thankful to my longtime office mates, Albert, Bertrand and Robin. I very much enjoyed our discussions in the office.

On a personal note, I want to thank my friends from back home in Luxembourg. Without my longtime friends, I would not be the person I am today. They were always there when I needed to escape the world of physics. They also made me realize that when a physics joke has to be explained, it is probably not funny anymore. My family (where I include of course my newly gained family from my girlfriend's side) always supported me, especially my parents Guy and Leslie. They did not doubt me when I announced that I wanted to change my studies from Economics to Physics, a subject which I basically knew nothing about until I was twenty years old. I am especially grateful to my grandfather, to whom this thesis is dedicated. I have a lot of memories from when I was little where he would sit down with me after school to do my homework. Somehow he was always convinced that I would become an academic one day. Sadly, he passed away before the completion of this thesis but knowing that I was on the right track. Last but not least, an enormous amount of gratitude goes to my wonderful girlfriend Julie. She had to put up with me during these three years. She supported me through the lows but also cheered with me in the good moments, which she made even more special. I consider myself lucky to have her in my life and I am looking forward to our future together.

P.S. A special thank you goes also to our cat Leo, who can lighten up any sad moment by just doing what cats do.

This thesis is based on the following publications:

- B. Bastian, S. Hohenegger, A. Iqbal and S. J. Rey, *Dual little strings and their partition functions,* Phys. Rev. D **97** (2018) no.10, 106004 [arXiv:1710.02455 [hep-th]].
- B. Bastian, S. Hohenegger, A. Iqbal and S. J. Rey, *Triality in Little String Theories,* Phys. Rev. D **97** (2018) no.4, 046004 [arXiv:1711.07921 [hep-th]].
- B. Bastian, S. Hohenegger, A. Iqbal and S. J. Rey, *Beyond Triality: Dual Quiver Gauge Theories and Little String Theories,* JHEP **1811** (2018) 016 [arXiv:1807.00186 [hep-th]].
- B. Bastian, S. Hohenegger, A. Iqbal and S. J. Rey, *Five-Dimensional Gauge Theories from Shifted Web Diagrams,* Phys. Rev. D **99** (2019) no.4, 046012 [arXiv:1810.05109 [hep-th]].
- B. Bastian and S. Hohenegger, *Dihedral Symmetries of Gauge Theories from Dual Calabi-Yau Threefolds,* Phys. Rev. D **99** (2019) no.6, 066013 [arXiv:1811.03387 [hep-th]].

Another work that gave rise to a publication during my thesis:

- B. Bastian and S. Hohenegger, *Five-Brane Webs and Highest Weight Representations,* JHEP **1712** (2017) 020 [arXiv:1706.08750 [hep-th]].

The latter was already partly included in my Master's thesis.

Contents

1 Introduction

The 20th century has seen the development of two physical theories that are immensely successful in describing the world we live in, namely general relativity and quantum field theory. These theories describe the four fundamental forces of nature that we know. Quantum field theory is a framework in which we can build theories that describe the electro-magnetic, weak and strong nuclear force, that govern the world of subatomic particles. In contrast, general relativity describes the force of gravity and how the latter governs the large structures in the universe. Despite the numerous experimental tests passed by these theories, we know that they do not provide us with a complete picture. One of the biggest challenges that we face today is to describe gravity at the quantum level and develop a unified theory that describes all four fundamental forces.

Among the best candidates we have for this endeavor is string theory (see [1–3] for introductory textbooks). The latter is a theory of quantized strings, which can either be open or closed and propagate in ten-dimensional spacetime [4, 5]. This exact number of spacetime dimensions is required for consistency of the theory and is generally referred to as the critical dimension with the propagating strings being called critical strings. As we currently observe only four spacetime dimensions, the others are generally considered to be compact with their characteristic length scale being small. The potential experimental signatures due to the existence of extra dimensions as predicted by string theory is currently a popular topic for phenomenological studies. The particles that we observe arise by the vibrational modes of the quantized strings. The strings define through their length a characteristic mass scale in the theory that we denote by M_s. Together with the string coupling g_s which governs the interactions between strings, they are the only two free parameters in the theory. What got people interested in string theory in the pursuit of a theory of quantum gravity was that is naturally contains the graviton as a specific excitation mode of the closed string. The graviton is the force carrier particle for the gravitational force and thus string theory is a quantum theory which naturally contains gravity. In addition, the other known fundamental forces are also present, thus providing a potential unified framework for all fundamental forces. String theory also contains additional extended objects known as Dp-branes [6] which can be thought of as p-dimensional hyperplanes that serve as endpoints for open strings and also as source/sink for closed strings.

Initially, five different consistent string theories were constructed which seemed unrelated at first. At a later stage, it was realized that these different theories were connected through dualities and unified under an eleven-dimensional description known as M-theory [7]. The latter is not a theory of critical strings but only contains branes, more specifically so called $M2$, $M5$ and $M9$ branes. Two of these five string theories will appear in this thesis and are called type IIA and type IIB respectively and are related by T-duality [8, 9]. This means that when we compactify one space direction in for example the type IIA theory on a circle of radius R, we can equivalently describe the same physics by compactifying the type IIB theory on a circle of radius $(M_s^2 R)^{-1}$. Furthermore type IIA theory is obtained by compactifying one direction in the eleven dimensional M-theory on a circle and shrinking the circle to zero size. Type IIB string theory also enjoys a symmetry known as S-duality [10] which relates its weak coupling to its strong coupling regime, exchanging perturbative and non-perturbative states. It was discovered in [11], that compactifications of type IIB string theory can be described in a more

geometric setting by embedding it in a twelve-dimensional spacetime. This approach is known as F-theory and allows for the use of powerful geometrical tools. A topological version of string theory has also been developed in [12]. In the latter, the correlators of a certain class of operators are independent of the metric tensor of the theory which explains why they are called topological. Topological string theories are interesting for a number of reasons. They provide toy models to understand more about properties of ordinary string theory. Furthermore, they can be used to derive results in the ordinary string theories mentioned above [13, 14]. Finally, they can lead to interesting mathematical results.

As of today, no complete model describing our reality has been constructed in the framework of string theory. Nevertheless, along the way it was realized that string theory can give us valuable insights into a variety of subjects among which is a specific class of quantum field theories by studying the low-energy (small compared to the string scale M_s) worldvolume dynamics of branes, *i.e.* the spacetime along the directions of the brane. The quantum field theories that arise this way naturally enjoy a property known as supersymmetry [15–17]. The latter is an additional symmetry that relates bosons to fermions and vice versa. Bosons and fermions that are related under this symmetry are called superpartners. Supersymmetry transformations are generated by spinors which are referred to as supercharges. A given theory can be invariant under symmetries generated by more than one supercharge, which is generally known as extended supersymmetry. In supersymmetric theories, there exists an interesting class of states, called BPS (Bogomol'nyi–Prasad–Sommerfield) states [18]. Understanding the BPS spectrum of a theory is an essential tool that can lead to exact non-perturbative results. These states are protected by supersymmetry, *i.e.* invariant under deformations of parameters, and as long as supersymmetry remains unbroken they can be safely followed into the strong coupling regime. Even in the absence of experimental confirmation of supersymmetry, its presence in this class of theories provides us with a playground where different methods can be tested in an efficient way. Indeed, supersymmetry provides additional structure, rendering the underlying theory more rigid and making it possible to devise non-perturbative techniques which provide us with exact results. Such techniques are very hard to come by in current models that describe our physical reality but do not enjoy supersymmetry. One could dare to say that when a certain result cannot be calculated in the presence of supersymmetry, there is probably not much hope of achieving it without supersymmetry. It is thus interesting to understand non-perturbative methods in supersymmetric theories and study if they can be applied, or at least part of them, when supersymmetry is broken. The embedding of quantum field theories into string theory provides us with a different viewpoint that often allows us to use powerful geometric tools in order to obtain new results that are inaccessible from conventional methods. This stringy approach makes it possible to unravel hidden dualities or to understand already known ones from a different perspective. In return, as these quantum field theories arise as the low-energy theories in the worldvolume of the branes, we can also gain new insights into string theory itself.

A good illustrative example of the insight string theory can give into supersymmetric quantum field theory is the electro-magnetic Montonen-Olive duality [19] in four-dimensional supersymmetric $\mathcal{N} = 4$ (referring to the number of supercharges) Yang-Mills theory (sYM) [20] (classical pure Yang mills theory completed with the respective superpartners such that it is invariant under the extended supersymmetry), which states that the theory enjoys equivalent descriptions where the role of electric and magnetic quantum number are exchanged and the gauge

coupling constant is inverted. This dual description is very useful in the sense that it established a relation between the weak coupling dynamics (perturbative regime) and the strong coupling dynamics (non-perturbative regime). When one sees the $\mathcal{N} = 4$ sYM theory as the worldvolume theory of $D3$ branes in type IIB string theory, then the Montonen-Olive duality is a direct consequence of S-duality of type IIB string theory [21]. If one further embeds type IIB into M-theory by considering torus compactification of the latter then the $D3$ branes arise from torus compactified $M5$ branes and the S-duality can be understood as the conventional $SL(2, \mathbb{Z})$ action on the torus [22]. We thus see that by embedding the gauge theory into string theory (including M-theory), we gain alternative points of view which can have a more geometric nature as in this example.

An interesting class of quantum theories that are embedded into string theory are the so called little string theories, first discovered two decades ago [23]. Reviews can be found in [24, 25]. These six-dimensional theories were first realized as the worldvolume theory of a stack of $NS5$ branes[1] in the context of Type II string theory through a particular decoupling limit that sends the string coupling constant to zero ($g_s \to 0$) while keeping at the same time the string scale M_s finite. In this limit, the resulting theory remains interacting but the bulk dynamics, *i.e.* strings propagating in the directions orthogonal to the brane, is decoupled, in particular gravity. As their name suggests, they contain strings which are however non-critical as they propagate in a six-dimensional spacetime. The tension of these little strings is proportional to the string scale M_s, which is the only intrinsic scale in the theory. Furthermore, the little string theories enjoy T-duality similar to the critical string theory underlining thus their nature as non-local quantum theories. So the complexity of little string theory thus lies between that of local quantum field theories and full fledged critical string theory. This makes them interesting candidates for studying stringy phenomena in an easier setup where gravity is absent and to learn more about the worldvolume dynamics of the $NS5$ brane. At energies far below the string scale M_s, they have a low-energy description in terms of quiver gauge theories, so their study can also give us insights into these kinds of theories. These types of theories have different gauge groups and a matter content which is coupled to a certain number of them, which is conveniently encoded into a graph known as quiver, where each gauge factor is represented by a node and an edge connecting different nodes represents matter charged under them. This local description breaks down as we reach the scale M_s and we must rely on the full little string theories. They are also intimately related to the famous six dimensional superconformal field theories (SCFTs) [22]. Conformal symmetry refers to the fact that a theory is scale invariant, *i.e.* it cannot have an intrinsic scale, whereas superconformal means that it is in addition also supersymmetric. These theories enjoy a special status as they are the SCFTs in the highest possible dimension [26]. In contrast to the little string theories, which have strings of finite tension, the SCFTs contain tensionless strings. For every little string theory, it is possible to take a limit that gets rid of the string scale and obtain an associated SCFT [27, 28]. We can thus also get new insights about the latter. These two kinds of theories mentioned above have long resisted a systematic study. The reason for this is that they do not have a description in terms of a Lagrangian. This can be understood from the fact that these theories contain self-dual two-forms for which we cannot write down a non-trivial kinetic terms in six dimensions [29]. So the usual field-theoretic methods based on a Lagrangian approach do not apply

[1] These are an additional type of branes present in type IIA and IIB string theory.

when we want to study these theories and we have to rely on their embedding into string theory.

In recent years, there has been a lot of progress in the study of little string theories, for a non-exhaustive list see [28, 30–48]. They have been completely classified by using systematic construction through F-theory compactifications [28, 49]. In this approach, all the physical data of the theories is encoded into the geometry of an elliptically fibered Calabi-Yau threefold, thus allowing for the use of powerful geometric methods for their study. Heuristically, one can think of these elliptically fibered spaces as a torus varying over a two complex dimensional base. In the specific case of little string theories there is an additional torus in the base manifold. The T-duality property of little string theories manifests itself in this F-theory setting by the exchange of the fiber torus with the base torus. More specifically, the six-dimensional theories that are the subject of this thesis are the so called little string theories of type A, where the letter refers to the ADE classification in terms of affine Dynkin diagrams of $\widehat{\mathfrak{a}}_N$[2]. This class of theories is defined by F-theory compactification on an elliptic Calabi-Yau threefold that we denote by $X_{N,M}$, where N and M are two positive integers that are part of the definition of the associated theories. What exactly we mean by this statement will become clear in the main text. In [33], the authors conjectured the existence of a third little string theory engineered by $X_{N,M}$ in addition to two already existing ones. As this third theory is associated with the same Calabi-Yau threefold, it is reasonable that it should be related to the other two resulting in a more intricate duality structure than simply T-duality.

In this thesis we explore and extend the conjectured duality and study its consequences. We also give a proof of the conjecture in a specific case. In order to attack this problem we have different viewpoints at our disposal that each have their own benefits. The first viewpoint is the F-theory construction gives us valuable insights into how the geometry of $X_{N,M}$ translates into the physical parameters of our theories, *i.e.* Coupling constants, Coulomb branch and mass parameters. The Coulomb branch parameters are the vacuum expectation values of the scalars that are related through supersymmetry to the vector field. They parametrize the moduli space of vacua for a given theory. The second viewpoint is a specific M-theory construction of our class of theories in terms of a configuration of $M5$ and $M2$ branes [50, 51, 31]. The little strings are BPS states in the worldvolume theory [53, 54] and one can capture their spectrum by the BPS counting function, which is equivalent to the instanton partition function of the low-energy description of circular quiver gauge theories. Through a remarkable relation, this partition function is equivalent to the topological string partition function associated with the Calabi-Yau geometry $X_{N,M}$ [13, 14, 55]. On the topological string side we have a technique at our disposal that is known as the refined topological vertex formalism [56, 57]. Using the latter we can systematically calculate the topological string partition function from the representation of $X_{N,M}$ as a toric variety. This is where the third viewpoint comes into play. By dualizing the M-theory setup into type IIB string theory we end up with a brane configuration of $D5$ and $NS5$ branes, commonly referred to as (p, q) brane web [58]. The essential information about how the branes intersect in this setup is conveniently encoded into a planar graph of trivalent vertices. Furthermore, this graph encodes the geometric information of $X_{N,M}$ viewed as a toric variety, which is exactly what we need in order to set up the topological vertex calculation in a systematic way for our class of theories. Our strategy for proving the conjecture is to

[2]We explain in the main text how this classification comes about.

explicitly calculate the partition function of the third theory associated with $X_{N,M}$ and show that indeed it corresponds to the BPS counting function of a little string theory or equivalently the instanton partition function of its low-energy description. Due to the non-perturbative nature of the partition function, this matching provides us with an exact result. It directly follows from the topological vertex method that the partition functions of the three theories engineered by $X_{N,M}$ are different series expansions of the same function, which provides us with relations among their physical parameters and allows us to establish a duality map between them. This shows that the geometry $X_{N,M}$ engineers three different little string theories which are dual to each other. We refer to this as *Triality*. To further support our result, we show based on considerations on the (p,q)-brane web diagram that there exist three regions in the Kähler moduli space of $X_{N,M}$ where the weak coupling regime of the respective gauge theory description is realized. From the geometric relations of [33] and our Triality, we show that there is an even larger web of dualities relating theories engineered by different geometries $X_{N,M}$ and $X_{N',M'}$. We formulate the condition for theories to be dual in terms of the positive integer pairs N, M and N', M'. Our analysis naturally leads us to consider a slightly more general class of geometries that we call *shifted web diagrams* and denote by $X^{(\delta)}_{N,M}$ where δ is a positive integer that refers to the shift. We conclude that these geometries engineer a least one little string theory in general. In a second part of this thesis, we analyze the direct consequences of the web of dualities that we established and we find two main result. First, we discover that for the theories associated with the shifted geometries $X^{(\delta)}_{N,M}$ that we encountered in our previous analysis, the question about dimensional reduction form six to five dimensions does not seem so straightforward anymore. Upon searching for a good parametrization of the geometry, we find that as we dimensionally reduce our theories, the gauge group and matter content changes. This is in contrast with the usual case where we simply end up with a five dimensional theory that has the same gauge group and matter content. We show the consistency of these newly found limits by implementing them in the partition function and formulate a general pattern for this reduction procedure. Secondly, we analyze the consequences of the duality web at the level of the partition function. As a consequence of the plethora of different geometries that lead to the same expansion form (from the perspective of a specific gauge theory expansion) of the partition function, we find that the latter enjoys a dihedral symmetry. This symmetry group acts on the Kähler moduli space and relates different terms at different orders in the instanton expansion in a highly non-trivial way.

The outline of this thesis is as follows. In section 2 we introduce some preliminary notions that will be important in the remainder of this thesis. We start by quickly reviewing the notion of Kähler moduli space and Calabi-Yau manifold, as we encounter these concepts frequently. We also introduce the Coulomb branch and pre-potential in the context of $\mathcal{N} = 2$ supersymmetric Yang-Mills (sYM). After this we sketch Nekrasov's calculation for the instanton partition function and its describe its modular structure in terms of contributions of individual vector and matter multiplets. In section 3 we review the different dual constructions of little string theories of type A. We also introduce the partition function and describe its calculation by the refined topological vertex method. In section 4, we prove the Triality and establish the extended web of dualities. In 5 we introduce the non-trivial five-dimensional limits for the shifted geometries. In 6 we explicitly show the manifestation of the hidden dihedral symmetry of the partition function. In section , we comment on the results and discuss research directions for the future. In the appendices, we give some relevant background information that we refer to

when needed.

2 Preliminary notions

In this section, we review some preliminary notions that play a role in the remainder of this thesis. We start with a lightning review of the notions of Kähler moduli space and Calabi-Yau manifold. We explain the notion of BPS states, specifically in six dimensions. Then we introduce the concept of Coulomb branch in supersymmetric gauge theories and discuss the calculation of the so called pre-potential in Seiberg and Witten's work. At last, we review Nekrasov's method to calculate the pre-potential and thereby introduce the Nekrasov partition function and comment on its structure in terms of individual contributions that arise from different types of multiplets. In this context, we also explain the notion of quiver gauge theory.

2.1 Calabi-Yau threefolds and Kähler moduli space

As the notions of Calabi-Yau manifold and Kähler moduli will appear numerous times in the course of this thesis, we briefly review them and refer the reader to physically motivated reviews [59, 60].

Let M be a complex manifold with $\dim(M)_{\mathbb{C}} = m$ and let g denote a Hermitian metric which satisfies

$$g_p(J_pX, J_pY) = g_p(X, Y) \tag{2.1}$$

at each point $p \in M$ and for any vectors in the tangent space $X, Y \in T_pM$. Here J_p is the almost complex structure at the point p. Choosing a basis for T_pM of the form $(\frac{\partial}{\partial z^\mu}, \frac{\partial}{\partial \bar{z}^{\bar{\nu}}})$ it can be shown that $g_{\mu\nu} = g_{\bar{\mu}\bar{\nu}} = 0$. In components the metric takes the form

$$g = g_{\mu\bar{\nu}} dz^\mu \otimes d\bar{z}^{\bar{\nu}} + g_{\bar{\mu}\nu} d\bar{z}^{\bar{\mu}} \otimes dz^\nu \tag{2.2}$$

A complex manifold together with a Hermitian metric is called a Hermitian manifold and denoted by (M, g). For the latter, we can define a specific $(1,1)$-form, called the Kähler form of the hermitian metric g, by its action on $X, Y \in T_pM$, as follows

$$\omega_p(X, Y) = g_p(J_pX, Y) \tag{2.3}$$

When expressed in components the Kähler form can be written as

$$\omega = i g_{\mu\bar{\nu}} dz^\mu \otimes d\bar{z}^{\nu} - i g_{\bar{\nu}\mu} d\bar{z}^{\nu} \otimes dz^\mu = i g_{\mu\bar{\nu}} dz^\mu \wedge d\bar{z}^{\nu} \tag{2.4}$$

Furthermore the Kähler form is a real form, *i.e.* $\omega = \bar{\omega}$. A Kähler manifold is a Hermitian manifold (M, g) whose Kähler form is closed, *i.e* $d\omega = 0$. In this case the Hermitian metric is called a Kähler metric. This is a non-trivial statement as not all complex manifolds admit Kähler metrics. As we are dealing with closed forms we can look at cohomology classes of closed Kähler forms, *i.e.* $[\omega] \in H^{1,1}(M)$, where $[\omega]$ is called the Kähler class of ω. The latter can be expanded in terms of a basis of $H^{1,1}(M)$ as follows

$$[\omega] = \sum_{i=1}^{h^{1,1}} \lambda_i [\omega]^i \,, \tag{2.5}$$

where $h^{1,1} = \dim(H^{1,1}(M))$ and $[\omega]^i$ are the basis elements. The parameters λ_i, known as Kähler parameters, are coordinates in the space $H^{1,1}(M)$ which is called the Kähler moduli space of M. We will have more to say about this space at a later point in this work. From the fact that the Kähler form is closed it can be established that

$$\frac{\partial g_{\mu\bar{\nu}}}{\partial z^{\lambda}} = \frac{\partial g_{\lambda\bar{\nu}}}{\partial z^{\mu}} \quad \text{and} \quad \frac{\partial g_{\mu\bar{\nu}}}{\partial \bar{z}^{\lambda}} = \frac{\partial g_{\lambda\bar{\nu}}}{\partial \bar{z}^{\mu}} \tag{2.6}$$

This suggests and it can indeed be shown [59] that locally on a chart U_i any Kähler metric can be expressed as

$$g_{\mu\bar{\nu}} = \partial_{\mu}\partial_{\bar{\nu}}\mathcal{K}_i \tag{2.7}$$

where the function $\mathcal{K}_i$ is called the Kähler potential. Given two overlapping charts it can be shown that on the intersection $U_i \cap U_j$ the respective Kähler potentials are simply related by

$$\mathcal{K}_i(z,\bar{z}) = \mathcal{K}_j(w,\bar{w}) + \phi_{ij}(w) + \psi_{ij}(\bar{w}) \tag{2.8}$$

They differ by a holomorphic, respectively an anti-holomorphic function. A special class of Kähler manifolds are so called Calabi-Yau manifolds. We say that a Kähler manifold is Calabi-Yau if it has vanishing first Chern class, or equivalently if the canonical bundle[3] is trivial, *i.e.* $\Lambda^{(m,0)}T^*M \cong \mathbb{C} \times M$.

2.2 Supersymmetric gauge theories and Nekrasov partition function

In the previous section we reviewed a few mathematical concepts that we will encounter at different points in the remainder of this thesis. Now, we introduce physical concepts that will also be of importance later on. Due to the lack of a Lagrangian description for the six-dimensional theories that we are interested in, it is useful to review some aspects of four dimensional $\mathcal{N} = 2$ super Yang-Mills (sYM) in order to introduce concepts that are important in this thesis. We look at the Lagrangian description of $\mathcal{N} = 2$ sYM where we introduce the concept of Coulomb branch parameters and briefly discuss the effective low energy solution constructed by Seiberg and Witten [61]. Finally, we discuss the approach taken by Nekrasov and the resulting instanton partition function [62].

2.2.1 $\mathcal{N} = 2$ super Yang-Mills in four dimensions and the notion of Coulomb branch

The goal of this section is to introduce the notion of Coulomb branch and pre-potential from the Lagrangian viewpoint. We only brush over the broad lines of four dimensional Seiberg-Witten theory and refer to the review [63] for further details. The four-dimensional on-shell $\mathcal{N} = 2$ vector multiplet contains a complex scalars ϕ, two Majorana spinors λ and ψ, and a vector field A_μ. With this field content, the $\mathcal{N} = 2$ pure sYM Lagrangian in four dimensions has the

[3]The m-th exterior product of the holomorphic cotangent bundle T^*M of the manifold M. Sections of the canonical bundle are holomorphic m-forms.

following form

$$\begin{aligned}\mathcal{L} =&\frac{1}{4\pi}\mathfrak{Im}\mathrm{Tr}\Big[\int d^2\theta d^2\tilde{\theta}\frac{1}{2}\tau\Psi^2\Big]\\ =&\frac{1}{8\pi}\mathrm{Tr}\Big[\tau\Big(\int d^2\theta W^\alpha W_\alpha + 2\int d^2\theta d^2\bar{\theta}\Phi^\dagger e^{-2V}\Phi\Big)\Big]\\ =&\frac{\theta}{32\pi^2}\mathrm{Tr}F_{\mu\nu}\tilde{F}^{\mu\nu} + \frac{1}{g^2}\mathrm{Tr}\Big(-\frac{1}{4}F_{\mu\nu}F^{\mu\nu} + (D_\mu\phi)^\dagger D^\mu\phi - \frac{1}{2}[\phi^\dagger,\phi]^2\\ &- i\lambda\sigma^\mu D_\mu\bar{\lambda} - i\bar{\psi}\bar{\sigma}^\mu D_\mu\psi - i\sqrt{2}[\lambda,\psi]\phi^\dagger - i\sqrt{2}[\bar{\lambda},\bar{\psi}]\phi\Big)\end{aligned} \tag{2.9}$$

where the trace is normalized as follows in terms of the generators of the gauge group $\mathrm{Tr}(T^aT^b) = \delta^{ab}$. In the first line we wrote the Lagrangian in the $\mathcal{N}=2$ superspace formalism with Ψ being a chiral superfield. The complexified gauge coupling is given by $\tau = \theta/2\pi + 4\pi i/g^2$. The second line corresponds to the Lagrangian written out in terms of $\mathcal{N}=1$ superfields, with Φ being a chiral superfield and V being the vector superfield whose superspace field strength is given by W^α. In the third line, all superspace variables have been integrated over and the Lagrangian is written out in terms of component fields. We give the three completely equivalent descriptions as they all have their own benefits. From (2.9), we see that their is a potential term for the complex scalar field ϕ,

$$V = \frac{1}{2g^2}\mathrm{Tr}\left([\phi^\dagger,\phi]^2\right)\,. \tag{2.10}$$

The vacua are defined by the condition $[\phi^\dagger,\phi]=0$. This implies that ϕ takes values in the Cartan subalgebra H of the gauge group, *i.e.* $\phi = \phi_i H^i$, where the H^i are the generators of the Cartan subalgebra. Concretely for $G=SU(2)$, we can take $\phi = \frac{1}{2}a\sigma^3$, with a being a complex parameter and σ^3 being the third Pauli matrix. This mechanism breaks the gauge group G to the subgroup which is generated by the Cartan elements. Physically equivalent vacua are related by elements in G/H, which correspond to gauge transformations. However, there are elements in G/H which do not take us out of the Cartan subalgebra. These elements belong to the Weyl group. In the specific $SU(2)$ example, they act as $a \mapsto -a$. In order to correctly parametrize the physically distinct vacua, we need to consider Weyl invariant functions of ϕ. In general they can be obtained from the characteristic equation,

$$\det(\eta - \phi) = 0\,, \tag{2.11}$$

This expression is invariant as the Weyl group acts by conjugation. Upon expanding in a formal series in η, the coefficients are Weyl invariant functions. For the specific example of $SU(2)$ a Weyl invariant quantity is $\mathrm{Tr}(\phi) = \frac{1}{2}a^2$. This moduli space of vacua is known as the *Coulomb branch* [4]. Its dimension is equal to $r = \mathrm{rk}(G)$, which is the dimension of the Cartan subalgebra. Away from the origin, the gauge group of the theory is completely broken down to $U(1)^r$. At the origin of the Coulomb branch, *i.e.* where $\phi = 0$, the full gauge group is restored. Until now, the entire discussion has been classical. Quantum mechanically, we parametrize the Coulomb by the vacuum expectation value of the classical Weyl invariant operators. For example, in the case of a $SU(2)$ gauge group the moduli space is parametrized by $u = \langle\mathrm{Tr}(\phi^2)\rangle$, which reduces

[4] The name comes from the fact that the gauge group is completely broken down to $U(1)$ factors.

in the classical limit to $\frac{1}{2}a^2$. As the gauge group is broken, the associated vector fields (and their superpartners) gain mass through the Higgs mechanism. Specifically for $SU(2)$, we get the two massive W-bosons.

Although we introduced the Coulomb branch here for four dimensional $\mathcal{N} = 2$ SYM, the concept is valid for generic supersymmetric gauge theories in d dimensions that have a scalar field in their vector multiplet. To recapitulate: The Coulomb branch corresponds to the moduli space of vacua in a supersymmetric theory parametrized by the vacuum expectation value of the scalar field in the vector multiplet. One should emphasize that not every supersymmetric gauge theory has a Coulomb branch, *e.g.* the six dimensional $\mathcal{N} = (1, 0)$ vector multiplet does not contain any scalar fields. We preferred to introduce the Coulomb branch in this way, because there is an explicit Lagrangian formulation which makes it easier to explain the concept. Later in this thesis, we will encounter the Coulomb branch again, but in this case for theories that do not have a Lagrangian description making the concept maybe less easy to visualize in a first encounter. In this case, the non-zero vacuum expectation value will have a geometric origin in string theory as separation between branes. A related concept that will also make an appearance in this thesis is the *Tensor branch* [22]. As one might already infer from the name, the latter corresponds to the moduli space of vacua parametrized by the vacuum expectation value of the scalar in the supersymmetric tensor multiplet. For completeness, we mention another similar concept, the *Higgs branch* [64], which is the moduli space of vacua parametrized by the vacuum expectation value of the scalar in the supersymmetric hypermultiplet. However, this notion will not be of direct importance to us. As a concluding remark to this very brief overview of moduli spaces of vacua, we would like to mention that there can be simultaneously more than one such branch in a given theory. In general they join each other at the origin. For explicit computations, a choice has to be made. However, there are cases where we can have mixed branches [65].

2.2.2 Low-energy effective action and pre-potential

The Lagrangian in (2.9) is renormalizable as can be seen from standard methods, *e.g.* power counting [66, 67]. However, if we are interested in a Wilsonian effective field-theory[5], renormalizability is not a criterion anymore. Integrating out the fields that gained mass by going on the Coulomb branch produces additional contributions to the Lagrangian. So (2.9) is not the most general Lagrangian we can write down for a $\mathcal{N} = 2$ chiral superfield Ψ, but rather

$$\begin{aligned}\mathcal{L} &= \frac{1}{4\pi}\mathfrak{Im}\mathrm{Tr}\int d^2\theta d^2\tilde{\theta}\mathcal{F}(\Psi)\\ &= \frac{1}{4\pi}\mathfrak{Im}\Big[\int d^2\theta d^2\bar{\theta}\Phi^\dagger\frac{\partial\mathcal{F}(\Phi)}{\partial\Phi} + \int d^2\theta\frac{1}{2}\frac{\partial^2\mathcal{F}(\Phi)}{\partial\Phi^2}W_\alpha W^\alpha\Big]\end{aligned} \tag{2.12}$$

The function $\mathcal{F}$ is known as the $\mathcal{N} = 2$ prepotential and it follows from supersymmetry that it depends on Ψ in a analytic way [67]. In the second line, we wrote the Lagrangian in terms of $\mathcal{N} = 1$ superspace variables. The seminal work of Seiberg and Witten [61] consists in the determination of $\mathcal{F}$, starting from the microscopic theory (2.9) which is quadratic in Ψ.

[5]We integrate out all the massive fields down to an energy scale Λ usually set to correspond to the mass of the lightest massive state. We can then formulate the theory in terms of an effective Lagrangian with massless fields only [61].

At the classical level, the prepotential would simply correspond to $\mathcal{F}_{\text{classical}} = \frac{1}{2}\tau\Psi^2$ and the Coulomb branch has a singularity at $u = 0$. This is the point where some fields that have been integrated out, the massive gauge bosons in this case, become massless again, thus rendering the effective description incorrect because we integrated something out that we should not have. In addition to the classical piece there are quantum corrections, which are both perturbative and non-perturbative in nature. These contributions to the pre-potential are denoted by $\mathcal{F}_{\text{pert}}$ and $\mathcal{F}_{inst}$ respectively, so that complete pre-potential has the following form

$$\mathcal{F} = \mathcal{F}_{\text{classical}} + \mathcal{F}_{\text{pert}} + \mathcal{F}_{\text{inst}} \tag{2.13}$$

As a consequence of a supersymmetric non-renormalization theorem [68], it has been shown, by using the fact that the $U(1)_{\mathcal{R}}$ symmetry of the theory is broken by a chiral anomaly, that $\mathcal{F}_{\text{pert}}$ does not receive any corrections beyond 1-loop order and takes the form

$$\mathcal{F}_{\text{pert}} = i\frac{1}{2\pi}\Phi^2 \ln\frac{\Phi^2}{\Lambda^2} \tag{2.14}$$

In [68], it was argued that the non-perturbative part of the pre-potential coming from instanton contributions is of the form

$$\mathcal{F}_{\text{inst}} = \sum_{k=1}^{\infty} \mathcal{F}_k \left(\frac{\Lambda}{\Phi}\right)^{4k} \Phi^2 \tag{2.15}$$

The first coefficient $\mathcal{F}_1$ was initially calculated in [68] and shown to be non-zero. The achievement of Seiberg and Witten was to devise a method, which allows in principle to calculate all the coefficients $\mathcal{F}_k$. However, while their method is well adapted for a conceptual study, it is not well adapted for the explicit calculation of the actual coefficients $\mathcal{F}_k$. It was only a few years later that another approach was developed that allowed for a more practical calculation of the instanton contributions at each order. This method will be discussed below. What became clear in the work of Seiberg and Witten is that the structure of the quantum moduli space is quite different from the classical picture, having no longer a singularity at $u = 0$ but a rather more intricate singularity structure, which gives rise to non-abelian monodromies on the moduli space. They showed that the singularities arise from specific BPS states (monopoles and Dyons) which become massless at these points. The monodromies together with a electromagnetic dual description of the $\mathcal{N} = 2$ Lagrangian were used to determine the structure of the moduli space, which was given a description in terms of a Riemann surface of genus r together with a specific differential on it. This Riemann surface is now commonly known as Seiberg-Witten curve. The relevant data for the effective $\mathcal{N} = 2$ effective theory can then be extracted as period integrals of the above mentioned differential along the cycles of the Riemann surface. It was also explained in [69], how the Seiberg-Witten curve is related to brane constructions of four dimensional gauge theories in ten dimensional string theory. Roughly speaking, when the discussed brane setups are lifted to M-theory, it becomes a single M5 brane with non-trivial topology, which is the relevant Seiberg-Witten curve. In the context of string compactifications on Calabi-Yau manifolds, the relation to the Seiberg Witten curves was discussed in [70]. Although our discussion was focussed on pure super Yang-Mills, a similar analysis was also performed in [64] when matter multiplets are included. As one would expect, this renders the structure more complicated but it can be done. The point of our discussion is not to give a complete review of Seiberg-Witten theory (a review can be found in [63]), but rather to introduce

the concept of pre-potential and to emphasize that its determination is a quite a non-trivial task. The initial calculation by Seiberg and Witten is very important from a conceptual point of view. In practice, however, for explicit computations of the pre-potential more efficient and more direct methods have since been developed. We shall review one particular method known as instanton counting in the following section.

2.2.3 The Nekrasov partition function

In [62], Nekrasov demonstrated a more direct way of calculating the pre-potential of $\mathcal{N} = 2$ sYM theory using localization techniques suggested in [71, 72]. In this approach, the problem of computing the pre-potential was first converted into the framework of topological quantum field theory [73]. In this formalism, the path integral could be reduced to a finite-dimensional volume integral over the moduli space of instantons. This integral was still plagued by divergences, but they were successfully regularized. The result of this calculation is the so called Nekrasov or instanton partition function from which the pre-potential can be extracted. For a modern review on Nekrasov's work, see [74].

The starting point to the calculation is the partition function, which is nothing but the correlator of the identity in the vacuum labeled by the Coulomb branch parameter that we denote by a,

$$Z = \langle 1 \rangle_a = \int_{|k|<\Lambda} \mathcal{D}X \exp\left(\frac{i}{4\pi} \int d^4x d^2\theta d^2\tilde{\theta} \mathcal{F}(\Psi[X]) \right) \tag{2.16}$$

Here $\mathcal{F}$ is the pre-potential that we already encountered in (2.12), $\mathcal{D}X$ denotes the path integral measure over the collective fields in the theory and $\Psi[X]$ is the $\mathcal{N} = 2$ chiral superfield whose field content consists of the collective fields X. The parameter Λ is the energy scale relevant for the effective Wilsonian action and the remaining integral is over energies below this scale. The first step is to translate this action into the language of topological field theory. This is achieved by the procedure known as topological twisting [73]. The rough idea is that we reinterpret the global symmetry group consisting of the Lorentz group in $\mathbb{R}^4$ and the $\mathcal{N} = 2$ $\mathcal{R}$-symmetry group of the SUSY generators, *i.e.*

$$G_{\text{global}} = SU(2)_L \times SU(2)_R \times SU(2)_{\mathcal{R}} \,. \tag{2.17}$$

We take a diagonal subgroup of the $SU(2)_R \times SU(2)_{\mathcal{R}}$ factor and then redefine what we call the Lorentz group for our theory. Let $SU(2)_{\text{diag}}$ denote this diagonal subgroup, then we declare the new Lorentz group to be

$$SU(2)_L \times SU(2)_{\text{diag}} \tag{2.18}$$

With this redefinition, the transformation properties of the fields in the theory change as well, *e.g.* some fermionic fields are now scalars under the new Lorentz group but are still anti-commuting. We do not provide any details, but only focus on the fact that in the new theory there is a supercharge $\bar{Q}$ which transforms as a scalar and is nilpotent, *i.e.* $\bar{Q}^2 = 0$. Now it can be shown that the action of the topological theory can be written as the sum of a $\bar{Q}$-closed piece $\bar{Q}S_{\text{topo}} = 0$ and a $\bar{Q}$-exact piece, *i.e.* $\bar{Q}$ of something,

$$S = S_{\text{topo}} + \bar{Q}V \tag{2.19}$$

The correlators of observables in the topological theory are not sensitive to the addition of $\bar{Q}$-exact additions to the action. Thus the second term in (2.19) can be dropped without consequences. This also means that we can in principle add any $\bar{Q}$-exact contribution to the action that makes the calculation easier. In particular, we can add a $\bar{Q}$-exact term that depends on an additional parameter t such that the action takes the schematic form

$$S = S_{\text{topo}} + \int d^4x \text{Tr}\left(-t^2(F_{\mu\nu} - \tilde{F}_{\mu\nu})(F^{\mu\nu} - \tilde{F}^{\mu\nu}) + \dots\right) \tag{2.20}$$

where we do not write out terms of order less than t^2. Here $\tilde{F}_{\mu\nu}$ denotes the dual field-strength. As the path integral is invariant under the addition of this term, it does also not depend on the explicit value of the parameter t. So we can take the limit $t \to \infty$, for which the integral localizes onto the configurations for which the Field strength is self-dual, *i.e.* $F_{\mu\nu} = \tilde{F}_{\mu\nu}$. These configurations correspond exactly to instanton solutions [75]. Hence the path integral reduces to an integral over the moduli spaces of instantons and the partition function takes the schematic form

$$Z = \sum_{k=0} Q_g^k \oint_{\mathcal{M}_k} 1 \tag{2.21}$$

where the sum runs over configurations consisting of k-instantons. The parameter Q_g is the exponentiated gauge coupling constant and serves as fugacity for the instanton number. The integral calculates the volume of the k-instanton moduli space $\mathcal{M}_k$. The expression (2.21) is also known as an instanton sum. In order to successfully calculate the integrals, one has to give a correct parametrization of the instanton moduli space. This has been achieved by the so called Atiyah-Drinfeld-Hitchin-Manin (ADHM) construction [76]. The authors gave a systematic construction of instantons by using methods of linear algebra. Even with a adequate parametrization, the integrals in (2.21) are still plagued by divergences that have two different origins. The first one, known as UV non-compactness, is related to the size of an instanton which can go to zero. This problem was regularized by a procedure known as Uhlenbeck compactification in [62]. This appropriately regularized space is denoted by $\widetilde{\mathcal{M}}_k$. The second source of divergences, known as IR non-compactness, are due to the fact that an instanton can wander off tho infinity, *i.e.* the collective coordinates describing their center of mass can go to infinity. This was remedied by the introduction of the Ω-background. We introduce the real regularization parameters ϵ_1 and ϵ_2 that act by rotation on $\mathbb{R}^4 \cong \mathbb{C}^2$ as

$$U(1)_{\epsilon_1} \times U(1)_{\epsilon_2} : (z_1, z_2) \to (e^{2\pi i\epsilon_1} z_1, e^{2\pi i\epsilon_2} z_2) \tag{2.22}$$

This rotation action combined with the Atiyah-Bott-Duistermaat-Heckman formula for equivariant localization [77], makes it possible to evaluate the path integral over the instanton moduli space $\widetilde{\mathcal{M}}_k$. The main idea is that the result of the integral will be a sum of contributions coming from the fixed points of the action (2.22), which is in this case the origin in $\mathbb{R}^4$. In physical terms this means that only instantons at the origin will contribute. As ϵ_1 and ϵ_2 are regularization parameters the result is divergent for $\epsilon_{1,2} \to 0$. An illustrative example would be the regularization of the following divergent integral over the volume of $\mathbb{C}^2$

$$\int dz_1 dz_2 \mapsto \int dz_1 dz_2 e^{-(\epsilon_1|z_1|^2 + \epsilon_2|z_2|^2)} = \frac{1}{\epsilon_1\epsilon_2}\,. \tag{2.23}$$

Once the divergences were all cured, Nekrasov was able to write down an expression for the resulting partition function. The latter is now also commonly known as the Nekrasov partition function $Z_{\text{Nek}}(a, \epsilon_1, \epsilon_2, g)$, where a is the Coulomb branch parameter and $Q_g = e^{-g}$ is the fugacity for the instanton number in (2.21). The relation to the Seiberg-Witten instanton part of the prepotential is given by

$$\mathcal{F}_{\text{inst}} = \lim_{\epsilon_1, \epsilon_2 \to 0} \epsilon_1 \epsilon_2 Z_{\text{Nek}}(a, \epsilon_1, \epsilon_2, g) \tag{2.24}$$

Upon modifying it a little, the same calculation can also be performed if matter is included in the $\mathcal{N} = 2$ theory [78]. It can also be generalized to quiver gauge theories [79]. The latter have multiple gauge groups factors and matter multiplets can be charged under several of them simultaneously. Two types of matter are important for us in this thesis. The first one is bi-fundamental matter which sits in the fundamental representation with respect to one gauge group and in the anti-fundamental representation with respect to another gauge group. The second one is adjoint matter which sits in the adjoint representation of one gauge group. We can also think of adjoint matter as a bi-fundamental where both gauge groups are identified. The content of quiver gauge theories can be conveniently encoded into a quiver graph. In the latter, each node represents a gauge group and charged matter is indicated by edges connecting the gauge groups under which they are charged. In Fig. 1, we show a quiver corresponding to a theory with M $SU(N)$ gauge groups factors with M bi-fundamental matter mutliplets. We refer generally to this as a $\widehat{A}_{M-1}$ type quiver due to its resemblance to the affine Dynkin diagram for the affine non-twisted Lie algebra $\widehat{\mathfrak{a}}_{M-1}$.

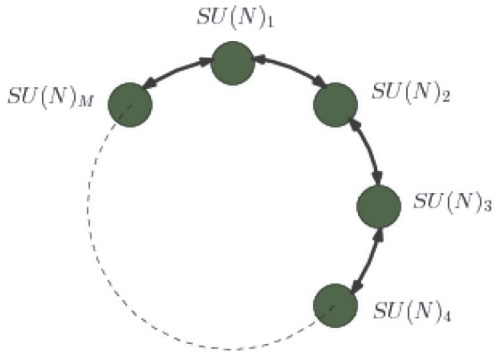

Figure 1: $\widehat{A}_{M-1}$ type quiver composed of $SU(N)$ gauge nodes with M bi-fundamentals. Figure taken from [52].

A powerful feature of the instanton counting technique as described above, is that the individual contribution of vector or matter multiplets can be identified in the resulting partition function. For example, the instanton partition function for a quiver gauge theory consisting of M $SU(N)$ gauge group factors with bi-fundamental matter as shown in Fig. 1 has the schematic

form

$$Z_{\text{Nek}}(\{\vec{a}^{(i)}\},\{m_i\},\{g_i\},\epsilon_{1,2}) = \sum_{\vec{\alpha}^{(1)},\ldots,\vec{\alpha}^{(N)}} \left(\prod_{i=1}^{M} Q_{g_i}^{|\vec{\alpha}^{(i)}|} z_{\text{vec}}(\vec{a}^{(i)},\vec{\alpha}^{(i)}) z_{\text{bif}}(\vec{a}^{(i)},\vec{\alpha}^{(i)};\vec{a}^{(i+1)},\vec{\alpha}^{(i+1)}) \right) \tag{2.25}$$

where $\{\vec{a}^{(i)}\},\{m_i\}$ and $\{g_i\}$, with $i = 1,\ldots,M$, denote the sets of Coulomb branch moduli, mass parameters and coupling constants respectively. The vector $\vec{a}^{(i)} = (a_1^{(1)},\ldots,a_{N-1}^{(M)})$ carries the Coulomb branch parameters of the i-th $SU(N)$ factor. Similarly $\vec{\alpha}_i$ denotes a vector of M integer partitions, see appendix D for their definition and related notions. The sum runs over these integer partitions. The functions z_{vec} and z_{bif} correspond to the contributions to the partition function coming from the vector and bi-fundamental matter multiplets respectively [80]. They are also referred to as Nekrasov subfunctions. The expression for the bi-fundamental contribution has the following form

$$z_{\text{bif}}(\vec{a},\vec{\alpha};\vec{b},\vec{\beta},m) = \prod_{i,j=1}^{M} \prod_{r\in\alpha_i} (E(a_i - b_j,\alpha_i,\beta_j,r) - m) \prod_{s\in\beta_j} (\epsilon_+ - E(b_j - a_i,\beta_j,\alpha_i,t) - m) \tag{2.26}$$

where we defined the functions E that depend on the partition coordinates (i,j) of a given box r in the Young diagram associated with the partition as

$$E(a,\alpha,\beta,r) = a - \epsilon_1(\alpha_j^T - i) + \epsilon_2(\beta_i - j) \tag{2.27}$$

In terms of the bi-fundamental contribution the Nekrasov partition function for the vector multiplet takes the form

$$z_{\text{vec}}(\vec{a},\vec{\alpha}) = \frac{1}{z_{\text{bif}}(\vec{a},\vec{\alpha};\vec{a},\vec{\alpha},0)} \tag{2.28}$$

The contribution of matter in the adjoint representation is simply given by

$$z_{\text{adj}}(\vec{a},\vec{\alpha},m) = z_{\text{bif}}(\vec{a},\vec{\alpha};\vec{a},\vec{\alpha},m)\,. \tag{2.29}$$

The instanton counting method that we briefly sketched in this section can also be performed for five-dimensional supersymmetric gauge theories as was already remarked in [62], where again explicit contributions from the individual multiplets can be identified in the instanton partition function. For five-dimensional theories, alternative methods to calculate the partition function have also been explored. For these theories the partition function can be calculated directly by the use of a technique known as topological vertex, which we will describe in section 3.5.4, that makes it possible to calculate the so called topological string amplitudes for toric Calabi-Yau threefolds, which are related to the respective five-dimensional theories through string theory [81, 13, 14, 55]. Through a remarkable correspondence, the topological string result corresponds to the five-dimensional Nekrasov partition function [82–84]. Unfortunately, the absence of a Lagrangian formulation for the six-dimensional theories we are interested in, makes it impossible to perform an instanton calculation à la Nekrasov. However, the alternative method via topological string theory is still a viable option and indeed gives the correct instanton partition functions [50, 51]. Well will have more to say on this in section 3.5.4. In the remainder of this thesis, we will encounter the elliptic generalizations of the Nekrasov subfunction (2.28), (2.26) and (2.29) when studying the partition function of the six dimensional little string theories (or equivalently their low-energy description in terms of quiver gauge theories) on $\mathbb{R}^4_{\epsilon_1,\epsilon_2} \times T^2$.

3 Little string theories and their partition function

Over the years, there have been various dual construction of little string theories. Each approach has its own benefits and it is therefore useful to use them in a complimentary fashion. We should emphasize that not every class of little string theories admits a description in all the dual frames we are going to present in this section, *i.e.* not all associated non-compact Calabi-Yau geometries have a description as a toric variety. We start by giving a very general description of little string theories as they were first discovered [85, 23, 86]. After this, we describe the different alternative but equivalent viewpoints, among which the approach that we are going to rely on the most in our search for dualities among these theories. For early reviews on the subject see [24, 25].

3.1 Little string theories as worldvolume theories of $NS5$ branes

We can consider a stack of N coincident $NS5$ branes in either of the type II string theories and try to understand their worldvolume theory. Their presence breaks the ten-dimensional Lorentz group down to

$$SO(9,1) \to SO(5,1) \times SO(4) \tag{3.1}$$

where the Lorentz group of the worldvolume theory is now given by $SO(5,1)$. The $SO(4)$ factor corresponds to an internal R-symmetry from the brane point of view. Furthermore, the presence of the branes breaks half of the supersymmetry, *i.e.* from thirty two down to sixteen unbroken supercharges. The six dimensional worldvolume theories will have either chiral $(2,0)$ supersymmetry if we are in type IIA or $(1,1)$ supersymmetry if we are in type IIB [87]. There will be excitations in the worldvolume theories coming from various open strings attached to the branes and interactions with closed strings propagating in the bulk. It is a natural question to ask whether it is possible to decouple the bulk dynamics without taking the low energy limit $E << M_s$, with M_s being the string scale. The processes in which modes living on the fivebranes are emitted into the bulk as closed strings are proportional to the string coupling g_s. Hence decoupling the latter would require taking the string coupling to zero while keeping the string scale fixed,

$$g_s \to 0 \quad \text{and} \quad M_s = \text{fixed}\,. \tag{3.2}$$

One needs to check the consequences of this limit for the couplings of the fields in the worldvolume theory of the $NS5$ branes. To this end we can analyze the low energy dynamics of the brane configurations. If the gauge coupling also goes to zero then we just end up with a trivial non-interacting theory. It turns out that this is not the case and there are indeed non-trivial interacting theories in the worldvolume of $NS5$ branes that are decoupled from the bulk and hence decoupled from gravity [23].

Let us first look at this in the type IIB case. We can use S-duality to relate the configuration described above the a stack of N coincident $D5$ branes. For these we know that the worldvolume theory would have $U(N)$ gauge symmetry with a gauge coupling given by

$$\frac{1}{g_{D5}^2} = \frac{M_s^2}{g_s} \tag{3.3}$$

From the transformation properties of M_s and g_s under S-duality we can deduce that the coupling constant in the $NS5$ worldvolume has the form

$$\frac{1}{g_{NS5}^2} = M_s^2 \tag{3.4}$$

From this we see that the limit $g_s \to 0$ can safely be taken without resulting in trivial low-energy dynamics. At energies of order $E \cong M_S$ the gauge theory description breaks down and there are additional degrees of freedom that play a role. However, since the low energy theory is not free and the full string theory is consistent, also the full six-dimensional theory must be interacting [23]. This six dimensional worldvolume theory with $(1,1)$ supersymmetry is commonly called type IIa little string theory. The moduli space of the latter is controlled by the four real scalars from the six-dimensional $(1,1)$ vector multiplet that parametrize the transverse directions to the N $NS5$ branes

$$\mathcal{M}_{\text{IIa}} = \frac{(\mathbb{R}^4)^N}{S_N} \tag{3.5}$$

A similar analysis can be performed for the worldvolume theory of a stack of $NS5$ branes in type IIA string theory. We get an interacting worldvolume theory with chiral $(2,0)$ supersymmetry that is called the type IIb little string theory. It's moduli space of vacua is described by the five real scalars from the six-dimensional $(2,0)$ tensor multiplet

$$\mathcal{M}_{\text{IIb}} = \frac{(\mathbb{R}^4 \times S_{10}^1)^N}{S_N} \tag{3.6}$$

where the extra compact factor of S_{10}^1 has its origin in the circle which relates type IIA to M-theory [7]. By comparing (3.6) and (3.5), we see that the two moduli space are qualitatively different. This will however change once we consider circle compactifications of these little string theories. To be more specific, we consider the worldvolumes of the $NS5$ branes to be along the $x_0, x_1, x_2, x_3, x_4, x_5$ directions. We choose to compactify the x_1 direction and denote the circle by S_1^1. The compactification of the six dimensional $(1,1)$ vector multiplet gives rise to a scalar in the type IIa coming from the vector field in the multiplet. On the other hand, the compactification of the $(2,0)$ tensor multiplet does not give rise to an additional scalar field [22]. With this in mind, the moduli spaces of the circle compactified little string theories look like

$$\widetilde{\mathcal{M}}_{\text{IIa}} = \frac{(\mathbb{R}^4 \times S_1^1)^N}{S_N} \quad , \quad \widetilde{\mathcal{M}}_{\text{IIb}} = \frac{(\mathbb{R}^4 \times S_{10}^1)^N}{S_N} \tag{3.7}$$

Upon circle compactification, we see that the moduli spaces of the two little string theories are related by exchange of the circles $S_1^1 \leftrightarrow S_{10}^1$. This symmetry is the manifestation of T-duality between the type IIa and type IIb little string theories. At the level of the critical ten-dimensional string theory, T-duality corresponds to inverting the radius R_1 of the circle S_1^1. This sends the circle compactified type IIA $NS5$ brane to the circle compactified type II B $NS5$ brane or vice versa and thus exchanges indeed the respective moduli spaces of the underlying little string theories. The presence of T-duality provides evidence that the full little string theories are not local quantum field theories.

Having discussed the origins of little string theories that enjoy maximal supersymmetry in six dimensions, *i.e.* sixteen supercharges, we briefly review the construction of little string theories with minimal supersymmetry, *i.e.* eight supercharges, that can be obtained by introducing orbifold singularities in the transverse space. These theories have been introduced in [88, 86]. Other such theories with eight supercharges in the setting of heterotic string theory were originally discussed in [23], but we will not talk about these. The $(2,0)$ and $(1,1)$ little string theories in the worldvolume of N $NS5$ branes discussed above admit an alternative description in terms of type IIB, or respectively type IIA, on the orbifold $\mathbb{C}^2/\mathbb{Z}_N$. The idea then was to consider both situations simultaneously and it was shown that N $NS5$ branes in type IIA or IIB with a transverse orbifold singularity $\mathbb{C}^2/\mathbb{Z}_M$ lead to consistent anomaly free six dimensional theories with eight supercharges. The latter are generally referred to as $(1,0)$ little string theories of type IIa or IIb, depending on their origin before introducing the orbifold singularity. Furthermore, it was argued that these theories also enjoy T-duality. The little string theories that we presented here are said to be of class A. The latter makes reference to the orbifold singularity used in the construction, which is commonly known as an A-type singularity due to a correspondence between the smoothed out space and Dynkin diagrams for the A-series. Other little string theories can be obtained by replacing the $\mathbb{Z}_N$ factor in the orbifold quotient by Γ_{ADE} which stands for one of the discrete $SU(2)$ subgroups, which allow for an ADE classification in terms of Dynkin diagrams. In this thesis, we are however solely concerned with the theories of class A.

Having now discussed the origins in terms of $NS5$ branes of the type IIa and IIb little string theories, we now give dual constructions of the latter. Even if the main approach in this thesis is via so called (p,q) brane webs (introduced in section 3.4.1), each point of view has its own benefits and therefore it is worth to go over them in order to give a more complete picture. The argument for T-duality of the little string theories presented above was a purely classical statement about the moduli spaces of the worldvolume theories. It is thus desirable to have an non-perturbative check for this. In [39, 32], the authors confirmed the T-duality by comparing the elliptic genera of the little strings. In section 3.5 we introduce a six dimensional analogue of the Nekrasov partition function that we discussed earlier. We then review how T-duality of the little string theories can be explicitly confirmed using this inherently non-perturbative (being an instanton series) object. Before we come to this we review dual constructions of the class of little string theories that we are interested in.

3.2 Little string theories from F-theory compactification on non-compact Calabi-Yau threefolds $X_{N,M}$

Little string theories, and hence their low-energy description in terms of circular quiver gauge theories can be geometrically constructed in a very efficient way using F-theory [11]. The relevant spaces for F-theory compactification are called elliptic fibrations. The literature on F-theory is immensely vast and a lot is known about how the geometry of elliptic fibrations translates into consequences for the underlying physical theories, see [89, 90] for reviews on the subject. This knowledge and a lot of effort led to a series of papers [91–93] that culminated in a classification of six-dimensional SCFT's [94]. Based upon the latter, the authors of [28] provided an almost complete classification of little string theories.[6]. The goal of this section is

[6]The classification has recently be completed in [49]

not to give a complete review of F-theory neither to describe the classification of little string theories. We would simply like to sketch the construction of little string theories of type A and briefly explain the different objects that are involved. This will allow us to better understand how the F-theory construction of A-type little string theories is related to other dual points of view that are used in this thesis and will be discussed in the coming sections.

3.2.1 A very brief overview of F-theory

In physical terms, F-theory can be understood as non-perturbative reformulation of type IIB compactifications including seven-branes that react back onto the geometry. As is widely known, type IIB string theory enjoys a non-perturbative symmetry relating the weak and strong coupling regime, commonly known as S-duality [10]. This symmetry is implemented by the action of the S-duality group which is $SL(2,\mathbb{Z})$ in IIB string theory[7]. The axion-dilaton field $\tau = C_0 + ie^{-\phi}$ transforms as follows under this symmetry

$$\tau \mapsto \frac{a\tau + b}{c\tau + d} \quad \text{for} \quad \begin{pmatrix} a & b \\ c & d \end{pmatrix} \in SL(2,\mathbb{Z}) \tag{3.8}$$

Furthermore, the NS-NS two-form B_2 and the R-R two-form C_2 of type IIB string theory transform as a doublet,

$$\begin{pmatrix} a & b \\ c & d \end{pmatrix} \begin{pmatrix} B_2 \\ C_2 \end{pmatrix} = \begin{pmatrix} aB_2 + bC_2 \\ cB_2 + dC_2 \end{pmatrix} \tag{3.9}$$

The fundamental string, commonly denoted by $F1$, is electrically charged under B_2, whereas the string like $D1$ brane is electrically charged under C_2. For this reason these two objects are also referred to as $(1,0)^T$ and $(0,1)^T$ strings respectively. In general, for p and q coprime[8], we can have a (p,q) string which is a BPS bound state of p fundamental strings and q D1-strings [95]. The latter electrically couples to $pB_2 + qC_2$. By definition, a $[p,q]$ seven-brane, is a brane where a $(p,q)^T$ string can end. The presence of seven-branes in type IIB string theory induces monodromies for the axion-dilaton field τ when going around a closed path in the space normal to the brane. This can be seen from the seven brane solution in the low-energy type IIB supergravity. The normal space to the brane is two dimensional, hence the harmonic function that specifies the geometry in the presence of the seven-brane has a logarithmic branch-cut [96]. A general $[p,q]$ seven-brane can always be brought into a $[1,0]$ brane by S-duality

$$SL(2,\mathbb{Z}) \ni \begin{pmatrix} r & -s \\ -q & p \end{pmatrix} \begin{pmatrix} p \\ q \end{pmatrix} = \begin{pmatrix} rp - qs \\ 0 \end{pmatrix} = \begin{pmatrix} 1 \\ 0 \end{pmatrix} \tag{3.10}$$

The parameter r and s are not uniquely fixed but they drop out of all physical quantities [97]. However, if multiple seven branes are present with different values of $[p,q]$, there is no $SL(2,\mathbb{Z})$ transformation that transforms them simultaneously into $[1,0]$ branes.

The realization that led to the discovery of F-theory [11] was that the axion-dilaton behavior under $SL(2,\mathbb{Z})$ transformations is identical to the transformation behavior of an elliptic

[7] In contrast, the S-duality group of the low energy type IIB supergravity is $SL(2,\mathbb{R})$. Upon lifting to string theory, the latter is broken down to $SL(2,\mathbb{Z})$ by non-perturbative effects.

[8] If p and q are not coprime the string can decay into n (p',q') strings.

curve[9] $\mathbb{E}_\tau$ under modular transformation. We can think type IIB string theory as being embedded into a twelve dimensional space where over each point in the original ten dimensional space-time, we have an elliptic curve with complex structure specified by the axion-dilaton τ. It must be stressed that the physical degrees of freedom still only propagate in the ten-dimensional spacetime. The elliptic curve serves as a bookkeeping device for the non-trivial variation of the axion-dilaton due to the presence of seven-branes. The volume of the elliptic curve has no physical meaning in F-theory. This can be seen from the duality between type IIB string theory and M-theory which we will review now. Given M-theory on $T^2 = S^1_A \times S^1_B$, with S^1_A being the M-theory circle with radius R_A, we reach type IIA by taking $R_A \to 0$. Then by T-duality we have type IIB on the dual circle $\tilde{S}^1_B$ with radius $\tilde{R}_B = 1/R_B$. In order to restore the full $\mathbb{R}^{1,9}$ spacetime of type IIB we must take the radius of the dual circle to infinity, which means in terms of the original circle in M-theory $R_B \to 0$. To summarize the duality, we have

$$\text{M-theory on } \mathbb{R}^{1,8} \times (S^1_A \times S^1_B)|_{R_A, R_B \to 0} \quad \cong \quad \text{Type IIB theory on } \mathbb{R}^{1,9}$$

By a careful tracing of the effective action of M-theory and type IIB through this limit [98], one can explicitly establish this duality, where the complex structure τ of the M-theory torus corresponds indeed to the axion-dilaton in type IIB. This duality also holds fiberwise if we now consider M-theory on $\mathbb{R}^{1,8-2n} \times Y_{n+1}$, with Y_{n+1} being an elliptic fibration over a n-complex dimensional base B_n, *i.e.* $\dim_{\mathbb{C}}(B_n) = n$ [11]. In terms of the effective theories, we have a theory living in $\mathbb{R}^{1,8-2n}$ from of M-theory compactified on Y_{n+1} which is dual to a theory living in $\mathbb{R}^{1,8-2n}$ from type IIB on $B_n \times \tilde{S}^1_B$. This gives the following relation between the volume of the elliptic curve and the radius of the physical compactification circle

$$\tilde{R}_B \sim \frac{1}{\text{Vol}(\mathbb{E}_\tau)} \tag{3.11}$$

For a finite volume of the M-theory torus, we thus get a $10-2n$ dimensional theory compactified on the dual circle $\tilde{S}_B$. To recover the genuine six dimensional theory living on $\mathbb{R}^{1,9-2n}$ coming from type IIB compactification on B_n, we have to take the limit $\text{Vol}(\mathbb{E}_\tau) \to 0$, also referred to as F-theory limit. Hence only the complex structure τ of the elliptic curve $\mathbb{E}_\tau$ is a dynamical modulus. The volume of the elliptic curve has no physical significance in the genuine $10-2n$ dimensional theory because we recover full type IIB only in the limit where it vanishes.

We now describe in broad lines the geometry of an elliptic fibration. An elliptic curve can be described by a so called Weierstrass model as the vanishing locus of the polynomial

$$P = y^2 - (x^3 + fxz^4 + gz^6)\,, \tag{3.12}$$

where $[x : y : z]$ are homogeneous coordinates in the complex weighted projective space $\mathbb{CP}_{231}$[10]. As a consequence of the variation of τ in the presence of seven-branes, the elliptic curve gives generically a non-trivial fibration over the base space. We can make (3.12) fibered over the

[9] An elliptic curve is a torus T^2 with a marked point. One can define an abelian group law for the points of the elliptic curve. The marked point serves as origin for this group law. We can represent the elliptic curve as the lattice $\mathbb{C}/L = \mathbb{E}_\tau = \{z \in \mathbb{C} \,|\, z \sim z + n + m\tau\}$ where n, m are integers and $\mathfrak{Im}(\tau) > 0$. The marked point can then be identified with $z = 0$.

[10] The space obtained by removing the origin from $\mathbb{C}^3$ and identifying points under the following equivalence relation: $(x, y, z) \sim (\lambda^2 x, \lambda y, \lambda^3 z)$ with $\lambda \in \mathbb{C}^*$.

base by letting the functions f and g depend on the base in a suitable way. This model then defines the elliptic fibration Y_{n+1}. In simple words, the latter is defined as an elliptic curve $\mathbb{E}_\tau$ (basically a torus) varying over a base B_n[11], where $n = \dim_{\mathbb{C}}(B_n)$. For reasons related to supersymmetry, the base B_n cannot be Calabi-Yau [99] while the total space of the fibration Y_{n+1} must be. The Weierstrass model also possesses a holomorphic zero-section, which is a holomorphic function of the base coordinates which gives for every point of the base a point in the fiber. This point in the fiber is defined by setting $z = 0$ in (3.12). Using the scaling from $\mathbb{CP}_{231}$, we can set $x = 1$, resulting in the Weierstrass equation $y^2{=}1$, which has the solution $y = \pm 1$. There is still residual scaling freedom with $\lambda = -1$ that does no affect the choice $x = 1$. So we can set $y = 1$, which means that the point defined by setting $z = 0$ is given by $[1 : 1 : 0]$ in terms of homogeneous coordinates. The zero section defines a divisor[12] in the total space

$$S_0 : \{z = 0\} \tag{3.13}$$

which intersects the elliptic fiber exactly in the point described above. It is this point which serves as the marked point of the elliptic curve. We will not try to develop this subject here in any detail and skip over a lot of subtleties. For the interested reader we refer to the vast mathematical or physical literature on this subject [100]. What is most important to us in this thesis, is the fact that as the elliptic curve varies over the base, it can develop singularities, *i.e.* some cycle of the torus shrinks to zero size. Physically, these points indicate the presence of seven-branes in the type IIB setting with different types of singularities corresponding to different types of seven-branes [89]. In the Weierstrass model, singularities are characterized as points where we simultaneously have

$$P = 0 \quad \text{and} \quad dP = 0\,, \tag{3.14}$$

where the differential is taken with respect to the homogeneous coordinates of $\mathbb{CP}_{2,3,1}$. The singularity cannot be at $z = 0$ since in this case the Weierstrass equation reads $y^2 = x^3$, which would then imply $x = y = 0$, but the point $x = y = z = 0$ does not belong to $\mathbb{CP}_{2,3,1}$. This means that the singularity occurs away from the zero-section. Furthermore, when we are interested in the singularities of the elliptic curve, we can restrict our attention to the coordinate patch where $z = 1$. In this patch, the Weierstrass model takes a simpler form

$$P = y^2 - (x^3 + fx + g) = y^2 - F(x) \tag{3.15}$$

The conditions defining the singularities of the elliptic curve are equivalent to the vanishing of the discriminant $\Delta = 4f^3 + 27g^2$, of the cubic polynomial $F(x)$ defined in (3.15). The points in the base where Δ vanishes define the discriminant locus, which corresponds to a divisor in the base defined by

$$\Sigma : \{\Delta = 0\} \subset B_n \tag{3.16}$$

In general, this divisor might not be irreducible, *i.e.*

$$\Sigma = \cup_I \Sigma_I \tag{3.17}$$

[11]The construction of little string theories actually requires a non-compact base in order to decouple gravity.
[12]A codimension 1 subvariety.

where the Σ_I individually correspond to degeneration loci for which $\Delta = 0$. The singular points of the elliptic curve as defined by (3.14) are not in general singular points of the whole space Y_{n+1}. For this to happen, in addition to the vanishing discriminant Δ also the gradient with respect to the base coordinates must vanish, *i.e.*

$$\frac{dP}{df} = 0 \quad \text{and} \quad \frac{dP}{dg} = 0 \tag{3.18}$$

The specific type of singularities that occur over these points depends on the vanishing orders of f, g and Δ. Fortunately, codimension-one singularities on elliptically fibered surfaces were classified some time ago by Kodaira [101] and Néron [102] and were shown to admit an ADE classification. This classifications carries over to elliptic fibrations over a higher dimensional base. A good overview of the different types of singularities can be found in [89]. Instead of the singular space Y_{n+1}, we can consider its resolution $\widehat{Y}_{n+1}$, which is smooth. Mathematically these two spaces are birationally equivalent. This means that they are isomorphic away from the singular points of Y_{n+1}. The singularities can be resolved by a so called crepant resolution, which might not exist in general but for the examples we are interested in it does. The word crepant refers to the fact that this resolution process does not change the canonical bundle, *i.e.* it preserves the Calabi-Yau condition. Hence if we start with a Calabi-Yau space the resolved space is still Calabi-Yau. An example of a resolution for the so called conifold geometry is given in appendix A. The only relevant singularity type for this thesis will be the so called Kodaira-type I_N, which is related to the affine Dynkin diagram of $\widehat{a}_{N-1}$. As already mentioned, the singular elliptic curve can be thought of as a pinched torus. Topologically the latter is equivalent to a two-sphere with two points identified. To smooth out the I_N-type singularity, it turns out that introducing only a single $\mathbb{CP}^1$ space is not enough but the singular point has to be replaced with a chain of N $\mathbb{CP}^1$ [101, 102]. The resulting picture is that of a periodic chain of two-spheres intersecting their two neighbors in one point respectively. So their is a correspondence between the resolved elliptic curve and the affine Dynkin diagrams of $\widehat{a}_{N-1}$. This picture should give the reader a general idea of how the ADE classification comes about. In physical terms these I_N-type singularities give rise to the gauge groups of the effective theories on $\mathbb{R}^{1,9-2n}$.

In the case where the degeneration locus Σ is not irreducible, it can happen that two loci Σ_I and Σ_J, which are codimension-one in the base, intersect in a codimension-two space in the base. Physically, this corresponds to the intersection of two seven branes in the type IIB picture. Over these codimension-two loci, the singularities get enhanced which is indicated by an increase in the vanishing orders of f, g and Δ. In [103], it was explained that the consequence of these codimension-two singularities is the appearance of charged massless matter. In general there can be intersection loci of even higher co-dimension, which gives rise to different phenomena. However, for the theories we are interested in, the base is only two complex-dimensional and the maximal co-dimension for the intersection loci is thus two.

3.2.2 Construction of little string theories of type A

In this part we will review the general construction of $\mathcal{N} = (1, 0)$ little string theories of type A. This requires a description of the elliptic fibration structure of the Calabi-Yau three-fold $X_{N,M}$ and an explanation on how the geometric ingredients are related to the little string or respectively the effective quiver gauge theories. At the end of this section we will comment on

how the $\mathcal{N} = (2,0)$ and $\mathcal{N} = (1,1)$ little string theories of type A are realized as particular cases of this construction. As we are dealing with non-gravitational theories, we need to decouple gravity in the F-theory framework. In [104–106], it was shown that the Planck scale of F-theory compactifications is set by the volume of the base of the elliptic fibration. In order do decouple gravity one must take a limit for which the base becomes non-compact. In [94], it was argued that the decoupling limit only depends on the metric in a neighborhood of a connected collection of curves on the original compact base, together with a rescaling which takes that neighborhood to infinite volume in an appropriate way. We do not repeat the argument here but simply take it for granted that such a non-compact basis exists in our case. The elliptic Calabi-Yau threefold $X_{N,M}$ has the following description in terms of an elliptic fibration over a complex two-dimensional non-compact base B_2. We consider M compact curves in the base, namely the discriminant loci Σ_I, which are $\mathbb{CP}^1$, of geometric self-intersection number (-2) which intersect in the form of the affine Dynkin diagram of $\widehat{\mathfrak{a}}_{M-1}$ inside the base B_2. As a result their intersection matrix is the negative of the Cartan Matrix of the associated affine Lie algebra and hence is negative semi-definite. The scalars of the six-dimensional $\mathcal{N} = (1,0)$ tensor multiple of the theory, also called tensor branch moduli, are controlled by the volumes of the curves in the base

$$\xi_I = \mathrm{vol}(\Sigma_I) = \int_{\Sigma_I} [\omega]\,, \tag{3.19}$$

where $[\omega]$ is the Kähler form of $X_{N,M}$. The little strings that give their name to the little string theories, arise by the $D3$ branes wrapping these curves in the base and as a consequence their tension is proportional to the tensor branch moduli. There exists a mathematical theorem in algebraic geometry, called the Grauert-Artin contractibility criterion [107, 108], stating that any curve in a complex surface is contractible if and only if the intersection matrix of its irreducible components is negative definite. As we mentioned above, in our case the intersection matrix is minus the affine Cartan matrix of $\widehat{\mathfrak{a}}_{M-1}$, which is negative semi-definite with exactly one null eigenvalue. The latter corresponds to one non-contractible curve in the base, defining an intrinsic scale in the theory. Hence the little strings always retain a finite tension. This is in contrast to the well known six dimensional superconformal field theories [109], which also have string degrees of freedom. However, for these theories the intersection matrix for the base curves is negative definite. As a consequence, the volume of all the base curves can be simultaneously tuned to zero, resulting in tensionless strings. In terms of the construction of little string theories, we can reach a superconformal field theory configuration by taking the volume of one curves in the base to infinity $\Sigma_I \to \infty$, while keeping everything else fixed. This would result in a configuration where the compact curves intersect in the form of the Dynkin diagram of $\mathfrak{a}_{M-1}$. This limit will have a quite natural interpretation in terms of brane web diagrams, as we will see in 3.4. In terms of the effective low-energy six-dimensional, the tensor moduli control the effective gauge coupling constants

$$\frac{1}{g_I^2} \sim \mathrm{vol}(\Sigma_I) \tag{3.20}$$

Hence, each irreducible component Σ_I of the degeneration locus corresponds to a gauge group factor and the intersection structure of the base curves in the form of a Dynkin diagram corresponds to the quiver structure of the effective theory in six dimensions, *i.e.* a circular quiver in the form of the Dynkin diagram of $\widehat{\mathfrak{a}}_{M-1}$, as shown in Fig. 1.

Over each curve Σ_I in the base, the elliptic curve degenerates into a I_N-type Kodaira singularity. The resolution of the latter gives a periodic chain of N $\mathbb{CP}^1$ that intersect in the form of the affine Dynkin diagram of $\widehat{\mathfrak{a}}_{N-1}$. Let us denote the elliptic curve degenerating over a given base curve Σ_I by $\mathbb{E}_I$ and its individual components by C_{i_I} where $i = 0, \ldots, N-1$ and $I = 0, \ldots, M-1$. Over each discriminant locus, the component C_{0_I} denotes the curve that is intersected by the zero-section, *i.e.* the original component of the elliptic curve before the resolution. Each $\mathbb{E}_I$ is also a fibered over the given base curve Σ_I and defines this way through its individual components a total of NM divisors S_{i_I} in the total space $X_{N,M}$. These are also referred to as resolution divisors. The latter will be directly visible as toric divisors in the brane web diagram of $X_{N,M}$, as we will see in section 3.4. The intersection numbers in $X_{N,M}$ between the fiber components C_{i_I} and the resolution divisors S_{i_I} encode the the Lie algebra structure of $\widehat{\mathfrak{a}}_{N-1}$

$$C_{i_I} \circ S_{j_I} = -\delta_{IJ} \widehat{C}_{i_I j_J} \tag{3.21}$$

where $\widehat{C}$ corresponds to the affine Cartan matrix of the affine Lie algebra $\widehat{\mathfrak{a}}_{N-1}$. This structure suggests that on the algebraic level we should identify the resolution divisors S_{i_I} with the coroots and C_{i_I} with the negative of the simple roots of the algebra $\widehat{\mathfrak{a}}_{N-1}$ [110–112]. In this interpretation, we can see C_{0_I} as the affine root of the algebra, *i.e.* the root that extends the finite root system. This correspondence will be picked up again in section 3.4. Similar to (3.19), the volume of the fiber curves is given

$$a_{i_I} = \mathrm{vol}(C_{i_I}) = \int_{C_{i_I}} [\omega] \tag{3.22}$$

The parameters a_{i_I} correspond to Coulomb branch parameters from the M-theory point of view. As discussed before, as long as the F-theory limit is not taken, *i.e.* the volume of the elliptic fiber going to zero, the engineered six-dimensional theory will live on $\mathbb{R}^{1,4} \times S^1$. So the a_{i_I} correspond to Coulomb branch parameters from the point of view of the theory on $\mathbb{R}^{1,4}$. From the perspective of F-theory, the scalars a_{iI} descend from the six-dimensional vector field compactified on a circle. The six-dimensional theory does not have a Coulomb branch as the vector multiplet in six dimensions does not have a scalar field. This fits well with the picture of the F-theory limit, which, through the vanishing fiber volume, would naturally impose $a_{i_I} \to 0\,,\ \forall i_I$.

As mentioned previously, the points in the base where two irreducible curves intersect $P_{IJ} = \Sigma_I \cap \Sigma_J$, give rise to enhanced singularities in codimension-two. At the level of the resolution of the elliptic fiber, each of the component curves C_{i_I} splits into two $\mathbb{CP}^1$ parts, which we call $C_{iI}^{(1)}$ and $C_{iI}^{(2)}$ respectively. As this splitting only occurs over single points, *i.e.* codimension-two in the base, these new curves do not give rise to new divisors. In the effective six-dimensional theory these codimension-two intersection points in the base will give rise to matter [103, 113]. The weight vector defining the representation of the matter multiplet under the J-th gauge group factor is determined from the intersection numbers of the curves $C_{i_I}^{(k)}$ with the resolution divisors S_{j_J}, $j = 1, \ldots, N-1$,

$$w_{i_I}^{k,(J)} = [\lambda_1^{(J)}, \ldots, \lambda_{N-1}^{(J)}] = [-C_{i_I}^{(k)} \circ S_{1_J}, \ldots, -C_{i_I}^{(k)} \circ S_{N-1_J}]\,, k = 1, 2 \tag{3.23}$$

were $\lambda_i^{(J)}$ are the Dynkin labels for the J-th gauge group factor. We will see in section 3.4 from the toric diagram that the intersection numbers of the matter curves form indeed the expected representation, which are in this case in the bifundamental representation.

We briefly described the constructions of little string theories in terms of F-theory compactifications on elliptic Calabi-Yau threefold $X_{N,M}$. In terms of the low-energy description we get circular quiver gauge theories, where the form of the quiver is given by the intersection structure of the curves in the base, which in our case has the form of an affine Dynkin diagram of $\widehat{\mathfrak{a}}_{M-1}$. Each node represents an $U(N)$ gauge group arising from the I_N-type Kodaira singularities over the corresponding base curve. An aspect of the Calabi-Yau geometry $X_{N,M}$ that we have not addressed yet, is its double elliptic fibration structure. Until now, we have described the geometry of $X_{N,M}$ as a elliptic fibration where the fiber degenerates into I_N singularity. However, the total discriminant locus over which this happens, has itself the structure of a resolved I_M singularity. As it turns out, $X_{N,M}$ allows for an equivalent description where the elliptic fiber degenerates into a I_M singularity over a discriminant locus in the base that has the structure of an I_N singularity [28]. We can simply think of this as an exchange of the fiber I_N curve with the base I_M curve. For the physics, this means that the Calabi-Yau $X_{N,M}$ engineers two little string theories, *i.e.* one of type $\widehat{A}_N$ and one of type $\widehat{A}_M$. This geometric exchange property is known as fiber-base duality [94] and it is the manifestation of the T-duality for little string theories that has been discussed in section 3.1. In terms of the underlying gauge theory descriptions this means that a circular quiver theory with N $U(M)$ gauge nodes is dual to a circular quiver theory with M $U(N)$ gauge nodes. From the discussion above and more specifically from (3.19) and (3.22), it can easily be seen that at the level of the parameters of the two dual theories, coupling constants get exchanged with Coulomb branch parameters. In section 3.5, we will see how this duality is confirmed at the level of BPS counting function of the little string or respectively the non-perturbative gauge theory partition function.

The construction outlined above engineers in general little string theories with eight supercharges. In specific instances, where the construction becomes simpler, the resulting little string theories will have the maximal sixteen supercharges. The $\mathcal{N} = (2, 0)$ theory is obtained for a configuration of curves in the base, intersecting in the form of an affine Dynkin diagram but with only a I_1-type Kodaira singularity in the fiber, which corresponds to a nodal curve, *i.e.* a curve with generic self-intersection. This type of degeneration does not correspond to a singularity in the whole space $X_{N,M}$, as it merely corresponds to the vanishing of the discriminant to first order with while the coefficients f an g from (3.15) are maximally generic. From the gauge theory perspective, this corresponds to a circular quiver composed of $U(1)$ nodes. On the other hand, the $\mathcal{N} = (1, 1)$ arises from reversing the fiber and the base curves. So we now have a discriminant locus in the base which has the form of a nodal nodal curve with a I_N-type Kodaira singularity in the fiber. From the gauge theory perspective, this corresponds to a single $U(N)$ gauge node with adjoint matter emanating from the self-intersecting base curve [114].

3.3 Little string theory from M-theory

Little string theories can also be engineered as the worldvolume theories of a stack of M5 branes in a specific geometric background. The little strings in the worldvolume of the M5's are in

this picture given by the intersections with M2 branes that are suspended between the M5 branes [50–52]. The advantage of this approach is that can be used to efficiently study the BPS degeneracies of the little strings. As follows from a relation between topological string theory[13] and M-theory [13, 14, 55, 117], this BPS data is conveniently encoded into the topological string partition function. The latter can be calculated by considering topological strings on a Calabi-Yau threefold. In our case, this Calabi-Yau is exactly the elliptically fibered geometry $X_{N,M}$ that we described in the last section. In the next section we will see how this Calabi-Yau geometry can be efficiently described from the perspective of toric geometry by using dualities relating M-theory to type IIB string theory. However, in order to use the duality between topological strings and M-theory, some geometric modifications have to be made to initial M-theory setup. This calculation has initially been done in [50, 51] for the context of the $(2,0)$ and $(1,0)$ SCFT's and then performed for the little string case in [31]. This BPS counting function is equivalent to the Nekrasov partition function for the effective low-energy quiver gauge theories. It is also possible to calculate the BPS counting function of the little strings by computing the elliptic genus of the worldsheet theory of these strings [50, 51, 31]. We will not consider this approach in this thesis. Our main goal in this section is to go through the necessary steps that allow us to relate the M-theory setup to the topological string. Along the way, we need to introduce parameters that will explicitly appear in the expansion of the partition function as we will see in section 3.5.1.

We start with the setup of N $NS5$ branes in type IIA compactified on S^1_T and probing a transverse orbifold singularity $\mathbb{C}^2/\mathbb{Z}_m$. As discussed, this gives $(1,0)$ type IIb little string theory. In this setup, the little string theories with maximal supersymmetry would either correspond to the special cases of having no $NS5$ branes (giving $(1,1)$ type IIa) or having no transverse orbifold singularity (giving $(2,0)$ type IIb). The compactification on the circle S^1_T gives the T-duality between type IIa and type IIb. The singular transverse space can be smoothed out into a multi Taub-NUT[14] space TN_M [119]. We can now lift this configuration to M-theory where the $NS5$ become $M5$ branes, separated along the M-theory circle $S^1_\perp$ according to the values a_i of the scalar in each $(2,0)$ tensor multiplet which give rise to the S^1 factor in the moduli space description (3.6). The $M5$ branes are still wrapping the S^1_T, so their worldvolume has the form $\mathbb{R}^4_{//} \times S^1_T$. The fundamental strings stretching between the $NS5$ branes become $M2$ branes stretched between the $M5$'s. The intersection of the $M2$ branes with this $M5$ branes inside the worldvolume of the latter gives rise to the little string, which are BPS strings in the worldvolume theory [120]. The tension of these strings is proportional to the $M2$ brane tension. Due to the compact transverse direction, the strings do not become tension-less upon bringing the $M5$ branes on top of each other as there always is an $M2$ brane wound around the circle.

[13] We will not review topological string theory here, but the interested reader can consult [115, 116] for a review.

[14] The multi Taub-NUT space is a solution to Einstein's equations [118] with metric

$$\begin{aligned} ds^2 &= V^{-1}(dt + \vec{A}\cdot d\vec{x})^2 + V d\vec{x}^2 \\ V &= \frac{1}{\lambda^2} + \sum_{i=1}^{N} \frac{1}{|\vec{x} - \vec{x}_i|} \\ -\vec{\nabla} V &= \vec{\nabla} \times \vec{A} \end{aligned}$$

This is in contrast to the SCFT's which are obtained by taking the radius of the transverse circle to infinity. We summarized the configuration in table 1.

	x_0	x_1	x_2	x_3	x_4	x_5	x_6	x_7	x_8	x_9	x_{10}
	$\mathbb{R}$	S^1_T	$\mathbb{R}^4_{//}$				$S^1_\perp$	TN_M			
$M5$	•	•	•	•	•	•	$\{a_i\}$				
$M2$	•	•					•				

Table 1: M-theory configuration after lifting the $NS5$ brane setup with transverse orbifold singularity in type IIB.

The Taub-Nut space being a circle fibration over $\mathbb{R}^3$ has a $U(1)_f$ isometry group which corresponds to the circle fiber. Introducing complex coordinates for the transverse Taub-NUT space,

$$w_1 = x_7 + ix_8 \quad , \quad w_2 = x_9 + ix_{10}\,, \tag{3.24}$$

we can rotate the Taub-NUT space non-trivially as we go along the circle S^1_T in the $M5$ brane worldvolume as follows

$$U(1)_f : (w_1, w_2) \to (e^{2\pi i m} w_1, e^{-2\pi i m} w_2) \tag{3.25}$$

From the point of view of the effective gauge theory in the $M5$ worldvolume, the parameter m corresponds to a mass deformation[15][117]. In order to relate the M-theory setup to topological string theory, we take signature of the spacetime to be euclidean and further compactify the x_0 direction on a circle S^1_t. We can then introduce the Ω-background, briefly discussed in section 2, by fibering the other worldvolume directions $\mathbb{R}^4_{//}$ over this circle. For this, we introduce complex coordinates as follows

$$z_1 = x_2 + ix_3 \quad , \quad z_2 = x_3 + ix_4\,. \tag{3.26}$$

In order to break no additional supersymmetries we also need to fiber the TN_M space over this circle [50, 51]. This results in the following $U(1)$ actions,

$$\begin{aligned} U(1)_{\epsilon_1} \times U(1)_{\epsilon_2} : (z_1, z_2) &\to (e^{2\pi i \epsilon_1} z_1, e^{2\pi i \epsilon_2} z_2) \\ : (w_1, w_2) &\to (e^{-i\pi(\epsilon_1+\epsilon_2)} w_1, e^{-i\pi(\epsilon_1+\epsilon_2)} w_2) \end{aligned} \tag{3.27}$$

From the point of view of the effective gauge theory on $\mathbb{R}^4_{\epsilon_1,\epsilon_2} \times S^1_t \times S^1_T$, the parameters ϵ_1 and ϵ_2 play the role of regularization parameters, as in the four dimensional case discussed in section 2.2.3. We summarize the final brane configuration in table 2.

In addition to the position of the branes, we also indicated the directions the different $U(1)$ actions are acting on. Through the relation with topological string theory mentioned above, we can access the BPS counting function for the little strings, by computing the topological string partition function for the associated non-compact Calabi-Yau geometry $X_{N,M}$. More specifically, we get the partition function for the six-dimensional theories on $\mathbb{R}^4_{\epsilon_1,\epsilon_2} \times T^2$ where $T^2 \cong S^1_t \times S^1_T$. In the next section we will see how to relate the M-theory configuration to a type IIB brane setup which encodes the geometry of $X_{N,M}$ as a toric variety in an efficient way.

[15]The classical example of a mass deformation is four dimensional $\mathcal{N} = 4$ sYM. The latter can be seen as $\mathcal{N} = 2$ sYM with an additional hypermultiplet that sits in the adjoint representation of the gauge group. By introducing a mass term for the adjoint, half of the supersymmetry is broken resulting in the $\mathcal{N} = 2^*$ theory.

	x_0	x_1	x_2	x_3	x_4	x_5	x_6	x_7	x_8	x_9	x_{10}
	S^1_t	S^1_T	$\mathbb{R}^4_{\epsilon_1,\epsilon_2}$				$S^1_\perp$	TN_M			
$M5$	•	•	•	•	•	•	$\{a_i\}$				
$M2$	•	•					•				
ϵ_1			•	•				•	•	•	•
ϵ_2					•	•					
m								•	•	•	•

Table 2: M-theory configuration from table 1 after further compactification and introduction of deformation parameters.

3.4 Type IIB String Theory, (p,q) brane webs and toric diagrams

In this part, we introduce the approach to the little string theories of type A in terms of so called (p, q)-brane webs, shown in Fig. 2. The advantage is that these brane configurations directly encode the geometry of the Calabi-Yau threefold $X_{N,M}$ as a toric variety. This interpretation is crucial in order to be able to systematically calculate the topological string partition function of $X_{N,M}$ and thus from the relation with M-theory, the BPS counting function of the little strings or equivalently the Nekrasov partition function of the underlying gauge theory descriptions.

3.4.1 Duality with (p,q) brane webs and and manifestation of T-duality

The M-theory configuration discussed in the previous section can be dualized into a five-brane configuration in type IIB (without orbifold singularity in this case). For simplicity, we set at first the mass deformation m introduced in (3.25) to zero. It will be reintroduced at a later point. We then take the S^1_T to be the M-theory circle. Upon dimensional reduction, we end up in type IIB where the $M5$ branes become $D4$ branes with fundamental strings stretched in between, coming from the $M2$ branes. The transverse space remains TN_M. In order to reach our desired type IIB setup, we can perform a T-duality along the Taub-NUT circle S^1_{TN} [121], which we take to be along the x_7 direction. In the T-dual type IIB string theory, we obtain M $NS5$ branes in the transverse directions to the initial TN_M space. The latter space is replaced by $\tilde{S}^1_{TN} \times \mathbb{R}^3$, where $\tilde{S}^1_{TN}$ is now the dual circle after the T-duality. The $D4$ branes become $D5$ branes with their newly gained worldvolume direction wrapping the dual Taub-NUT circle. After this chain of dualities, we end up with a brane configuration in type IIB string theory as described in table 3. The branes intersect in an orthogonal fashion in order to break not more

	x_0	x_2	x_3	x_4	x_5	x_6	x_7	x_8	x_9	x_{10}
	S^1_t	$\mathbb{R}^4_{\epsilon_1,\epsilon_2}$				$S^1_\perp$	S^1_{TN}	$\mathbb{R}^3_\perp$		
$D5$	•	•	•	•	•		•			
$NS5$	•	•	•	•	•	•				

Table 3: (p, q) five-brane web in type IIB obtained after dualities from the M-theory setup in table 2.

supersymmetry. If we now turn on the mass deformation m from (3.25), bound states of $D5$ and $NS5$ branes at the intersection are formed [117]. In Fig. 2 we show the configuration in the $x_6 - x_7$ plane. The x_6 and the x_7 direction are compactified on a torus. The $D5$ branes

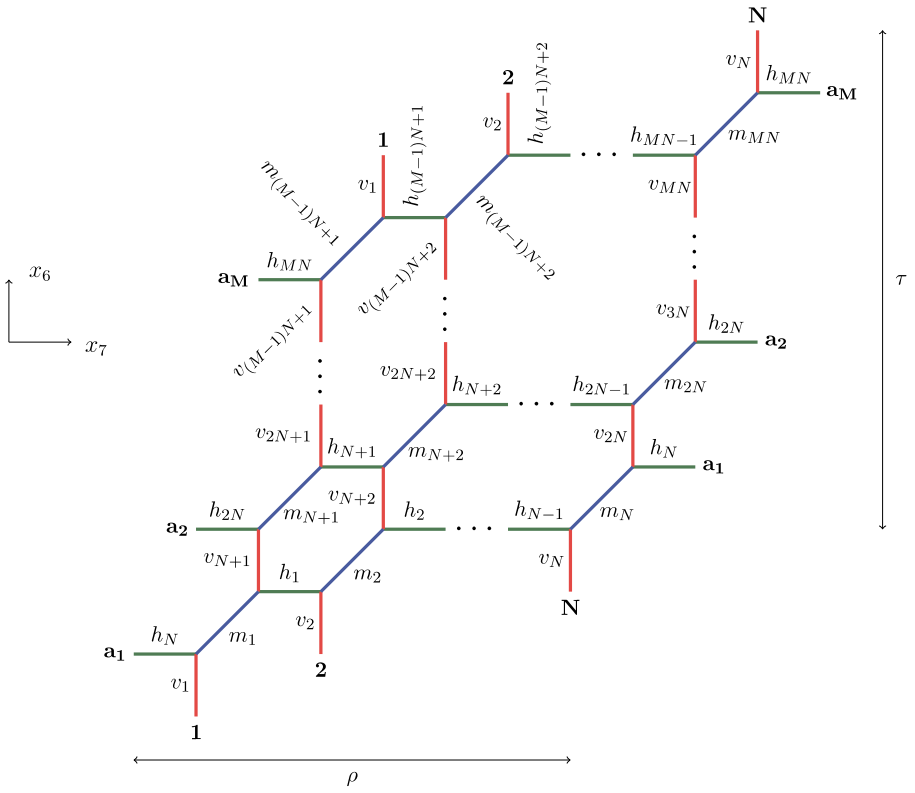

Figure 2: *The 5-brane web corresponding to $X_{N,M}$ with a generic parametrisation of all line segments. Not all variables $\mathbf{h} = (h_1, \ldots, h_{MN})$, $\mathbf{v} = (v_1, \ldots, v_{MN})$ and $\mathbf{m} = (m_1, \ldots, m_{MN})$ are independent, but are subject to $2NM - 2$ consistency conditions.*

are depicted in green, the $NS5$ branes are depicted in red and the bound states correspond to the diagonal blue lines. Such brane configurations of D5's and NS5's are known as (p, q) brane webs [58]. This notation refers again to the charges that transform as a doublet under the type IIB S-duality. This was already discussed in section 3.2.1 for the electric charges of the fundamental string and the $D1$ brane. The objects that are magnetically charged[16] under the B_2 and C_2 fields are the two types of five-branes. So in this notation, the D5 is a $(1, 0)^T$-brane and the NS5 corresponds to a $(0, 1)^T$-brane. The bound states depicted as blue lines in Fig. 2 correspond to $(1, 1)^T$-branes. A general bound state can have charges $(p, q)^T$, which explains the name (p, q) brane web. The relation between the charges and the slopes of individual lines in the web diagram is such that a $(p, q)^T$-brane will be represented by a line that has slope q/p. As for the strings, different types of $(p, q)^T$ branes are mapped into each other by S-duality. A general S-duality transformation acts as

$$\begin{pmatrix} a & b \\ c & d \end{pmatrix} \begin{pmatrix} p \\ q \end{pmatrix} = \begin{pmatrix} ap + bq \\ cp + dq \end{pmatrix} \quad \text{with} \quad \begin{pmatrix} a & b \\ c & d \end{pmatrix} \in SL(2, \mathbb{Z}) \tag{3.28}$$

As already mentioned, the depicted brane web can be thought of as being drawn on a torus where ρ and τ correspond to the length of the two cycles, *i.e.* the radii of the two circles

[16] Given a p-dimensional extended object in a d-dimensional spacetime, it can be electrically charged under a $(p + 1)$-form and magnetically charged under a $(d - p - 3)$-form.

$\tilde{S}^1_{TN}$ and $S^1_\perp$ respectively. The labels on the external legs of the web diagram ($1,\ldots,N$ and $a_1,\ldots,a_M$) indicate the periodic identification of the branes. Each line segment carries a label that parametrizes its length. These $3NM$ length parameters are not completely arbitrary. They are constrained by the fact that the $D5$'s, respectively the $NS5$'s, must remain parallel to each other in order to form a stable supersymmetric configuration [58]. Hence, for each hexagon we get a pair of consistency conditions [50, 32], *e.g.* for the hexagon in the lower left corner Fig. 2 we have for example

$$\begin{aligned} h_1 + m_2 &= h_{N+1} + m_{N+1} \\ v_{N+1} + m_{N+1} &= v_{N+2} + m_2 \end{aligned} \tag{3.29}$$

We thus get a total of $2(NM-1)$ constraints from all the hexagons[17], giving a total of $NM+2$ independent parameters.

We know from the discussion in the beginning of this section that little string theories are the word volume theories for the NS5 branes possibly probing a transverse orbifold singularity and that these theories also enjoy T-duality. In the F-theory setting where our class of little string theories is described by the double elliptically fibered $X_{N,M}$, this duality is simply understood as fiber-base duality, *i.e.* an exchange of the elliptic curve in the fiber with the elliptic curve in the base. In the type IIB (p,q) web setting, T-duality follows from the exchange of $NS5$-branes with $D5$-branes under type IIB S-duality action

$$\begin{pmatrix} 0 & -1 \\ 1 & 0 \end{pmatrix} \in SL(2,\mathbb{Z}) \tag{3.30}$$

which has the following action on the branes

$$\begin{pmatrix} 1 \\ 0 \end{pmatrix} \mapsto \begin{pmatrix} 0 \\ 1 \end{pmatrix} \quad , \quad \begin{pmatrix} 0 \\ 1 \end{pmatrix} \mapsto \begin{pmatrix} -1 \\ 0 \end{pmatrix} \quad , \quad \begin{pmatrix} 1 \\ 1 \end{pmatrix} \mapsto \begin{pmatrix} -1 \\ 1 \end{pmatrix} \tag{3.31}$$

This transformation simply rotates the web diagram by 90 degrees while exchanging D5 with NS5-branes. So we see that T-duality seems also rather natural in the type IIB setting.

3.4.2 Toric Diagrams and Kähler moduli space

What makes the type IIB setting so useful is that the (p,q) brane web in Fig. 2 can be interpreted as the dual toric graph of the toric Calabi-Yau threefold $X_{N,M}$ [122]. The latter is exactly the elliptically fibered geometry that appeared in the F-theory construction of the little string theories in section 3.2.2 and is also the relevant geometry for the relation between M-theory and topological string theory mentioned before. We briefly review the fan construction in toric geometry in appendix A. A classical toric graph is not usually drawn on a torus. From the physical point of view the construction is quite natural as it just corresponds to simple type IIB compactification on a torus. For this reason, it has been around in the physics literature for some time [117]. However, the rigorous mathematical construction of this class of toric varieties is to the best of the authors knowledge quite recent and can be found in [123]. We review some basic aspects of the construction at the level of the toric fan in appendix B. In the toric picture,

[17] Two constraints coming from the hexagons are redundant because of the periodicity of the configuration.

the S-duality of type IIB corresponds simply to a change of basis in the toric fan, *i.e.* the toric geometry does not distinguish between $D5$ and $NS5$ branes. It is just a way of changing the representation of the toric diagram without any effect on the underlying geometry. Each line segment in Fig. 2 corresponds to an irreducible curve in the geometry and the labels are the Kähler parameters which control the area of this curve. As we have reviewed before, a given Kähler parameter λ is related to a curve Σ as

$$\lambda = \int_{\Sigma} [\omega] \,, \qquad [\omega] \in H^{1,1}(X_{N,M}) \tag{3.32}$$

where $[\omega]$ is the Kähler class of the Kähler form of the Calabi-Yau threefold $X_{N,M}$ (see 2.1 for the definition). These Kähler moduli and their respective origins have already been discussed in the F-theory construction, where they have been assigned the more specific roles of coupling constants, Coulomb branch moduli and mass parameters. In the toric diagram, their specific assignment depends on which of the two fiber-base dual theories we are interested in. We already mentioned in 3.2.1 that the roles of coupling constants and Coulomb branch moduli get inverted between the two theories engineered by $X_{N,M}$. Being aware of the parameter counting performed above, we can conclude that the dimension of the Kähler moduli space of $X_{N,M}$ is $\dim(H^{1,1}(X_{N,M})) = NM + 2$, which was also rigorously shown in [123]. This space takes the form of a cone, defined by

$$\int_{\Sigma_i} [\omega] \geq 0 \quad , \quad \int_{S_i} [\omega] \wedge [\omega] \geq 0 \quad , \quad \int_{X_{N,M}} [\omega] \wedge [\omega] \wedge [\omega] \geq 0 \tag{3.33}$$

where Σ_i and S_i are curves respectively divisors in $X_{N,M}$. They were already encountered in the discussion about the F-theory construction. The space defined by (3.33) is generally referred to as the Kähler cone. The points where the bounds are saturated define the walls, where some curves in the geometry shrink to zero size, eventually resulting in a singular space. For example, the diagonal edges are interpreted in the toric picture as curves that resolve otherwise singular points in the geometry. This resolution procedure has a rather simple manifestation at the level of the toric diagram where it just corresponds to finding a complete triangulation of the toric fan. A little more details on this matter are given in appendix A. In general there exist different possible triangulations and as a consequence inequivalent ways of resolving singularities. This fact will be heavily used in later sections of this thesis. In the F-theory picture, the diagonal lines correspond to the curves that resolve the codimension-two singularities that indicate the presence of matter. The mass is controlled by the volume of the curves. The two parameters ρ and τ that control the cycles of the torus on which the web diagram is compactified correspond to the complex structure structure moduli of the two elliptic curves, one in the fiber and one in the base, that appear in the F-theory construction of our class of theories. Hence, their roles get exchanged upon fiber-base duality. Each of the NM hexagons in Fig. 2 corresponds to a toric divisor of $X_{N,M}$[18]. More precisely, they correspond to the resolution divisors S_{i_I} already discussed in the F-theory construction. These arose from the fibering of the resolved elliptic curves over the discriminant locus in the base. From the group theoretic perspective they were identified with the affine co-roots of the gauge group. A divisor that appeared in the F-theory construction but is not represented in the toric diagram, is the divisor related to the zero section

[18]This follows from a standard correspondence in toric geometry between one-dimensional cones in the fan and codimension-one subspaces of the associated variety [124].

(3.13). The latter is non-compact, as it corresponds to an embedding of the base into the whole space $X_{N,M}$ and the reason for its absence is that it is probably not toric in nature, although the author is not aware of any reference for this.

3.4.3 Intersection numbers and charges under the gauge group

In the type of toric fan we consider in this thesis, the intersection numbers between the curves and the divisors in $X_{N,M}$ can be calculated in a practical way. The procedure is reviewed in appendix B. As was explained in section 3.2.1 the geometric intersection numbers are directly related to the charges of vector and matter representations in a given theory. Upon an appropriate choice of divisors $S_i^{(j)}$ that are identified with the non-affine co-roots of the gauge group $[U(N)]^M$, the weight vector associated with a given curve $\mathcal{C}$ under the gauge group is given by the following expression

$$\begin{aligned} w_{\mathcal{C}} :=& \big([-\mathcal{C}\circ S_1^{(1)},\dots,-\mathcal{C}\circ S_{N-1}^{(1)}],\dots,[-\mathcal{C}\circ S_1^{(M)},\dots,-\mathcal{C}\circ S_{N-1}^{(M)}]\big) \\ =& ([\lambda_1^{(1)},\dots,\lambda_{N-1}^{(1)}],\dots,[\lambda_1^{(M)},\dots,\lambda_{N-1}^{(M)}]) \end{aligned} \tag{3.34}$$

where the $\lambda_i^{(j)}$ correspond to the respective Dynkin labels under the j-th factor of the product gauge algebra. To properly parametrize a given theory engineered by $X_{N,M}$ we need to identify three different classes of curves:

- Roots $\widehat{\alpha}_i$: Their intersection numbers with the coroots as in (3.34) should give the adjoint representation under the product gauge group. There are $M(N-1)$ such curves that provide the respective positive simple roots of the gauge algebra and their volumes parametrize the Coulomb branch moduli.

- Coupling constants g_i : Their intersection number with the cooroots as in (3.34) should be uncharged under the product gauge group. There are M such curves and their volumes parametrize the gauge coupling constants.

- Matter curves : Their intersection numbers with the coroots as in (3.34) should give either the bifundamental or the adjoint representation under the gauge group. There are M such curves that provide the respective highest weight states. The other states in the representation are obtained in the usual way by addition of the roots.

Upon fiber-base duality, the coupling constant of one theory can be interpreted as roots (Coulomb branch moduli) for the other dual theory. The same is true for the roots, but only a part of these would appear as coupling constants in the dual theory as there are in general more roots ($M(N-1)$) than coupling constants (M). We also want to remark that upon choosing the finite roots of the algebra, there are also curves that can be interpreted as the affine root $\widehat{\alpha}_0$ of the algebra for a given gauge group factor. When we think in terms of the picture of the periodic chain of spheres (the resolved elliptic curve presented in the F-theory discussion), the affine root corresponds to the initial part of the singular torus before the resolution which is intersected by the zero section divisor as stated before. If the zero section divisor were manifest in the toric diagram the choice of roots would be more or less fixed by this. We can see this freedom as the cyclic rotation symmetry of the affine Dynkin diagram when the affine root is

not fixed. To complete this group theoretic picture, we point out that the elliptic parameters ρ and τ can be interpreted as imaginary roots of the affine algebra as they satisfy

$$\rho = \sum_{i=0}^{N-1} \widehat{\alpha}_i^{(j)} \quad , \quad \tau = \sum_{i=1}^{M} g_i \tag{3.35}$$

where the $\widehat{\alpha}_i$ are the roots corresponding to a single gauge group factor and the g_i are the coupling constants, which can be interpreted as roots in the dual theory. That these relations hold can be easily seen from the web diagram, but these are also the relations between the roots and the imaginary root in the untwisted affine algebras $\widehat{\mathfrak{a}}_{N-1}$ and $\widehat{\mathfrak{a}}_{M-1}$ respectively. As (3.35) for ρ holds for each set of roots for each gauge group factor, *i.e.* for all values of j, the associated affine algebras all share the same imaginary root ρ. Furthermore, ρ and τ have zero intersection with all the resolution divisors S_i (co-roots) which also fits nicely with this picture, as this is also a property of the imaginary roots in the affine extension of the $\mathfrak{a}$ algebras.

The specific example of $X_{2,2}$

In order to illustrate the concepts discussed above, we look at the specific example of $X_{2,2}$ shown in Fig. 3. It is not the most general case because the fiber base dual theories engineered by $X_{2,2}$ are actually the same, *i.e.* $\mathcal{N} = (1,0)$ $\widehat{A}_1$ circular quiver theories with gauge group $U(2)$ or $[U(2)]^2$ for short. The consistency conditions are already imposed, so the $2 \cdot 2 + 2 = 6$ curves labeled by $h_1, h_2, v_1, v_2, m_1, m_2$ form an independent basis. There are four compact divisors labeled by S_i, with $i = 1, 2, 3, 4$, which can be regarded as the coroots of two affine $\widehat{\mathfrak{a}}_1$ algebras. Among these we need to choose which ones correspond to the non-affine coroots. We recall that this liberty of choice is due to the fact that the zero-section divisor is not visible in the toric diagram. We will look at what we call the vertical theory, where the direction refers to the orientation of the curves related to the coupling constants in the web diagram. For the latter, we choose the non-affine coroots to be S_1 and S_2. The weight of a given curve $\mathcal{C}$ under the gauge algebra will thus be given by

$$w_{\mathcal{C}} = ([-\mathcal{C} \circ S_1], [-\mathcal{C} \circ S_2]) = ([\lambda_1], [\lambda_1']) \tag{3.36}$$

with λ_1 and λ_1' being the Dynkin labels under the product gauge algebra. Using the procedure outlined in appendix B, it can be verified that none of the individual curves give the right intersection numbers to be interpreted as roots of the gauge algebra. However, the combinations

$$\widehat{\alpha}_1^{(1)} = m_1 + h_2 \quad , \quad \widehat{\alpha}_1^{(2)} = m_2 + h_2 \tag{3.37}$$

give

$$\begin{aligned} w_{\widehat{\alpha}_1^{(1)}} &= ([-\widehat{\alpha}_1^{(1)} \circ S_1], [-\widehat{\alpha}_1^{(1)} \circ S_2]) = ([2], [0]) \\ w_{\widehat{\alpha}_1^{(2)}} &= ([-\widehat{\alpha}_1^{(2)} \circ S_1], [-\widehat{\alpha}_1^{(2)} \circ S_2]) = ([0], [2]) \end{aligned} \tag{3.38}$$

which are indeed the right weights for roots under the given product algebra. With these definitions the respective affine roots would be given by

$$\widehat{\alpha}_0^{(1)} = m_2 + h_1 \quad , \quad \widehat{\alpha}_0^{(2)} = m_1 + h_1 \tag{3.39}$$

The latter have the following intersections numbers

$$\begin{aligned} w_{\widehat{\alpha}_0^{(1)}} &= ([-\widehat{\alpha}_0^{(1)} \circ S_1], [-\widehat{\alpha}_0^{(1)} \circ S_2]) = ([-2], [0]) \\ w_{\widehat{\alpha}_0^{(2)}} &= ([-\widehat{\alpha}_0^{(2)} \circ S_1], [-\widehat{\alpha}_0^{(2)} \circ S_2]) = ([0], [-2]) \end{aligned} \tag{3.40}$$

From the web diagram it can clearly be seen that $\rho = \widehat{\alpha}_0^{(1)} + \widehat{\alpha}_1^{(1)} = \widehat{\alpha}_0^{(2)} + \widehat{\alpha}_1^{(2)}$, which serves as imaginary root for both gauge group factors and has zero intersection with the gauge divisors. After defining the roots, which control the Coulomb branch moduli, we need to identify the curves which control the coupling constants. These should be uncharged with respect to the gauge algebra. The choice

$$g_1 = m_1 + v_1 \quad , \quad g_2 = m_2 + v_2 \tag{3.41}$$

indeed gives the right weights for being coupling constants

$$\begin{aligned} w_{g_1} &= ([-g_1 \circ S_1], [-g_1 \circ S_2]) = ([0], [0]) \\ w_{g_2} &= ([-g_2 \circ S_1], [-g_2 \circ S_2]) = ([0], [0]) \end{aligned} \tag{3.42}$$

As can easily be seen from the web diagram $\tau = g_1 + g_2$. With the Coulomb branch moduli and coupling constants identified, it remains to check that we indeed have two bifundamentals. The two highest weight states, one for each fundamental representation correspond to the curves m_1 and m_2

$$\begin{aligned} w_{m_1} &= ([-m_1 \circ S_1], [-m_1 \circ S_2]) = ([-1], [1]) \\ w_{m_2} &= ([-m_2 \circ S_1], [-m_2 \circ S_2]) = ([1], [-1]) \end{aligned} \tag{3.43}$$

The remaining states are obtained by adding combinations of simple roots. We thus have

$$\begin{aligned} w_{m_1+\widehat{\alpha}_1} &= ([-(m_1 + \widehat{\alpha}_1) \circ S_1], [-(m_1 + \widehat{\alpha}_1) \circ S_2]) = ([1], [-1]) \\ w_{m_2+\widehat{\alpha}_2} &= ([-(m_2 + \widehat{\alpha}_2) \circ S_1], [-(m_2 + \widehat{\alpha}_2) \circ S_2]) = ([-1], [1]) \end{aligned} \tag{3.44}$$

The weights in (3.43) together with the weight in (3.44) give indeed the right representation for two bifundamentals charged under the product gauge algebra. To summarize, we graphically represent the parametrization for the horizontal $[U(2)]^2$ theory in Fig. 3 (b). For the vertical theory, the discussion would be similar. In that case we could choose the coroots to be S_2 and S_4. Then $\widehat{\alpha}_0^{(2)}$ and $\widehat{\alpha}_1^{(2)}$ will play the role of coupling constants and g_2 would correspond to one finite root. The finite group for the other group factor would be the sum of the curves m_1 and v_2.

3.4.4 F-theory limit and dimensional reduction at the level of the web diagram

The F-theory limit that we mentioned in section 3.2.1 has a simple manifestation at the level of the web diagram. It corresponds to shrinking either the horizontal or vertical compact direction by sending ρ respectively τ in Fig. 2 to zero. Which of the two choices realizes the F-theory limit depends on the description of the theory we are considering. For example, in the vertical description for Fig. 2, the complex structure modulus of the F-theory fiber corresponds to ρ. So from relation (3.11), which states that the radius of the compactification circle is inversely

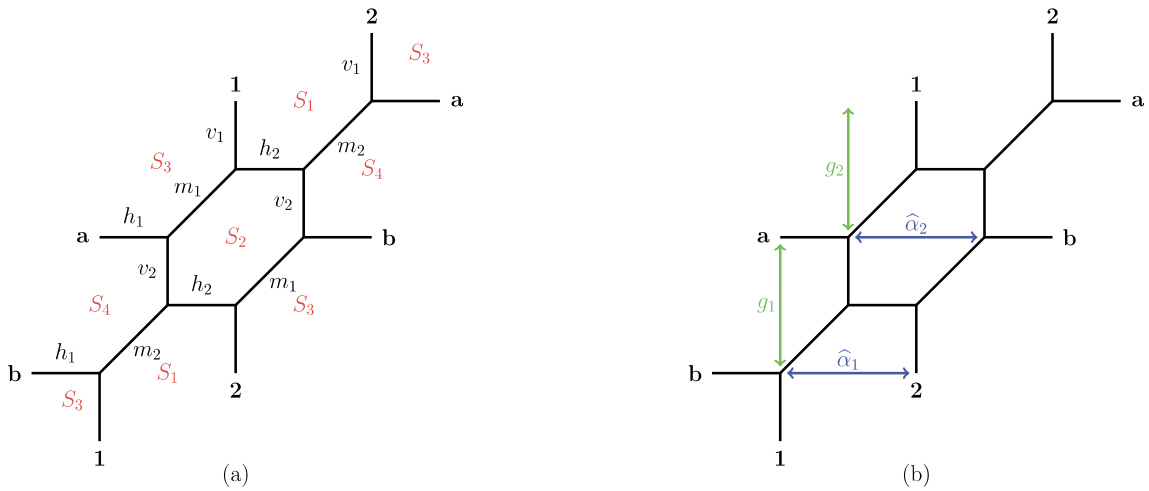

Figure 3: *Toric web diagram for the non-compact Calabi-Yau $X_{2,2}$. (a) Consistency conditions are imposed and each curve is labeled by its associated Kähler parameter. The divisors different divisors are highlighted in red. (b) Choice of curves $\widehat{\alpha}_i$ and g_i parametrizing respectively the Coulomb branch and coupling constants in the horizontal theory.*

proportional to the volume of the elliptic curve, we see that the F-theory limit requires $\rho \to 0$. However, we do not consider this limit in this thesis. In contrast, the dimensional reduction to a theory on $\mathbb{R}^4_{\epsilon_1,\epsilon_2} \times S^1$ can be realized upon taking $\rho \to i\infty$ and hence sending the compactification radius to zero. This is achieved by sending the volume of some curves in the geometry to infinite size. More concretely, in Fig. 3, an example of such a limit for the horizontal theory would be $h_1 \to \infty$ (or equivalently $h_2 \to \infty$). At the level of the web diagram this corresponds to cutting the associated lines. An effective preliminary check for the consistency of this limit is that there are no lines in the web suddenly crossing resulting in an inconsistent brane configuration. These five-dimensional limits will play a role in section 5. From the horizontal perspective, the parameter τ is related to the form of the elliptic curve in the F-theory base or equivalently to the structure of the gauge theory quiver. We can take again appropriate limits where the volume of specific curves goes to infinity and therefore induces $\tau \to i\infty$. Geometrically this would result in a configuration of curves intersecting in the form of a linear quiver with the two curves at the endpoints being non-compact [94]. This would take our little string theory to the associated superconformal field theory which is related to the finite Dynkin diagram of the A series. For the gauge theory description this would open up the circular quiver, resulting in a linear quiver resembling exactly the Dynkin diagram mentioned before. For Fig. 2, this would simply be achieved by $v_1 \to \infty$ or equivalently $v_2 \to \infty$. This type of limits will also come into play in section 5. The same discussion applies to the horizontal description with the roles of ρ and τ inverted.

3.5 The Partition Function

In order to study dualities between the class of little string theories that we have introduced so far, the BPS counting function for little strings, which equals the Nekrasov partition function for the effective gauge theory descriptions, is a powerful tool. For T-dual theories, the latter might

have a different form but it is the same function just expanded in a different set of parameters. As the partition function includes all non-perturbative contributions, its equivalence for two theories gives an exact duality. However, it is not possible to calculate it by using localization methods as in the four or five dimensional case. The reason for this is very simple; There is no Lagrangian description of the theories that we are interested in. Fortunately, the story does not stop here. Alternative methods to devise the instanton partition function have been developed. It can be obtained by computing the elliptic genus of for the worldsheet theories of the little strings [31]. This is however not the approach we are adopting in this thesis. In the previous section we mentioned that the partition function in this case is equal to the topological string partition function on $X_{N,M}$. The latter can be systematically calculated by the so called refined topological vertex method, which we explain at a later point in this section. First we describe the general structure of the partition function and how the different parameters that characterize our theories appear in it.

3.5.1 The general form and Nekrasov subfactors

As we discussed before, the double elliptic Calabi-Yau geometry $X_{N,M}$ gives rise through F-theory compactification to two little string theories of type A which are T-dual to another. These allow for a low energy description in terms of two dual circular quiver gauge theories. These theories admit a description in M-theory and we can use a relation between the latter and topological string theory to compute the partition function. This however requires to consider the six-dimensional space on which the theories are defined to be $\mathbb{R}^4_{\epsilon_1,\epsilon_2} \times T^2$. As there are two dual theories associated with $X_{N,M}$, the underlying partition function has two different but equivalent expressions as an instanton expansion. At a later point, when we introduce the topological vertex formalism to explicitly calculate the partition function, we will see that there is a choice of orientation in the web diagram involved which determines in what expansion form the final result will be. The general form of the partition function for $X_{N,M}$ was given in [31, 32] and in terms of a instanton partition function for a $[U(N)]^M$ circular quiver gauge theory is has the following schematic form

$$\begin{aligned}\mathcal{Z}_{N,M}(\{g_i\},\{a_i^{(j)}\},\{m_i\},\rho,\epsilon_{1,2}) = \sum_{\{\alpha_r^{(s)}\}} \left(\prod_{k=1}^{M}(Q_{g_k})^{\sum_{i=1}^{N}|\alpha_i^{(k)}|}\right) \\ \times \prod_{i}^{M} \widehat{z}^{\text{vec}}(\vec{a}^{(i)},\vec{\alpha}^{(i)};\rho,\epsilon_{1,2})\widehat{z}^{\text{bif}}(\vec{a}^{(i)},\vec{\alpha}^{(i)},\vec{a}^{(i+1)},\vec{\alpha}^{(i+1)},m_i;\rho,\epsilon_{1,2})\end{aligned} \tag{3.45}$$

The three sets $\{g_i\},\{a_i^{(j)}\}$ and $\{m_i\}$ denote respectively the collection of gauge couplings, Coulomb branch moduli and mass parameters. We recall that the parameter ρ controls the radius of the compactification circle, *i.e.* it plays the role of the modulus of the elliptic fiber. We emphasize that τ does only appear implicitly here. Equivalently, we could exchange one of the g_i's for τ through the relation (3.35). The sum runs over the NM integer partitions $\alpha_r^{(s)}$. The definition and notation for the latter is defined in D. The vector notation for Coulomb branch moduli and integer partitions defines N-component vectors, *e.g.* $\vec{a}^{(i)} = (a_1^{(i)},\ldots,a_N^{(i)})$. Also the upper index for these parameters is defined in a periodic fashion, *e.g.* $a_i^{(M+1)} = a_i^{(1)}$. We also introduced the notation $Q_{g_k} = e^{-g_k}$ for the exponentiated coupling constants. The factors

$\widehat{z}^{\text{vector}}$ and $\widehat{z}^{\text{bifund}}$ are the elliptic generalizations of the Nekrasov subfunctions that have been introduced in section 2.2.3 for the four dimensional theories on $\mathbb{R}^4_{\epsilon_1,\epsilon_2}$. Here, the contribution from the vector multiplet takes the following form

$$\widehat{z}^{\text{vec}}(\vec{a},\vec{\alpha};\rho) = \prod_{i,j=1}^{N} \vartheta^{-1}_{\alpha_i\alpha_j}(e^{a_i-a_j+\frac{1}{2}\epsilon_+};\rho) \tag{3.46}$$

with $\epsilon_+ = \epsilon_1 + \epsilon_2$ and the other parameters are defined as above. The $\vartheta_{\alpha\beta}(x;\rho)$-functions are defined in D.11 and D.12 and they contain the Jacobi theta functions θ_1 defined in (C.5). The other contribution that appears in the partition function (3.45) is coming from bifundamental matter and takes the form

$$\widehat{z}^{\text{bif}}(\vec{a},\vec{\alpha},\vec{b},\vec{\beta},m;\rho) = \prod_{i,j=1}^{N} \vartheta_{\alpha_i\beta_j}(e^{a_i-b_j-m+\frac{1}{2}\epsilon_+};\rho)\,. \tag{3.47}$$

Here, a_i and b_j are the Coulomb branch parameters corresponding to the two gauge groups the bi-fundamental matter is coupled to. The parameter m controls the mass of the matter multiplet. Because adjoint matter can be seen as a bi-fundamental coupling to a single gauge node, its expression in the partition function corresponds to a special case of (3.47)

$$\widehat{z}^{\text{adj}}(\vec{a},\vec{\alpha},m;\rho) = \widehat{z}^{\text{bif}}(\vec{a},\vec{\alpha},\vec{a},\vec{\alpha},m;\rho) = \prod_{i,j=1}^{N} \vartheta_{\alpha_i\alpha_j}(e^{a_i-a_j-m+\frac{1}{2}\epsilon_+};\rho)\,. \tag{3.48}$$

The arguments of the ϑ-functions for the contributions of the different multiplets in the theory contain a combination of Kähler parameters which are associated to curves in the web diagram $X_{N,M}$. These curves provide through their intersection numbers (3.34), the appropriate representations for the vector and matter contributions. We can recover the five-dimensional Nekrasov subfunctions for the theory on $\mathbb{R}^4_{\epsilon_1,\epsilon_2}\times S^1$ from (3.46), (3.47) and (3.48) by dimensional reduction. We recall that in terms of the modular parameter this means one has to take the limit $\rho \to i\infty$. These Nekrasov functions can be directly calculated in five dimensions through a localization procedure [62, 78], which provides a cross-check of their correctness. In order to get down to the four-dimensional Nekrasov factors that we have introduced in section 2.2.3, one would need to reinstate the radius of the other compactification circle which we left implicit in our discussion. It was checked in [125, 44] that this gives indeed the expected results. At the level of the partition function, T-duality for the little string theories or duality for the engineered gauge theories, means that the partition function (3.45) can be expanded in two different but equivalent ways. Each expansion than has the structure associated with the specific theory as discussed above. We want to emphasize that this is a rather non-trivial statement from the point of view of the complicated function (3.45). To show the equivalence of two different expansions by brute force one would need to completely expand the ϑ-functions and then re-sum the expression in another set of parameters which serve as the coupling constants of the dual theory.

A specific example

In order to make the discussion more clear we look at the specific example of the partition

function for $X_{2,2}$, whose diagram is shown in Fig. 3. For the horizontal theory the partition function has the following form

$$\begin{aligned}\mathcal{Z}_{2,2} = &\sum_{\alpha_1^{(1)},\alpha_2^{(1)},\alpha_1^{(2)},\alpha_2^{(2)}} (Q_{g_1})^{|\alpha_1^{(1)}|+|\alpha_2^{(1)}|}(Q_{g_2})^{|\alpha_1^{(2)}|+|\alpha_2^{(2)}|} \\ &\times \frac{\vartheta_{\alpha_1^{(1)}\alpha_1^{(2)}}(Q_{m_1})\vartheta_{\alpha_1^{(1)}\alpha_2^{(2)}}(Q_{m_2}\widehat{Q}_1)\vartheta_{\alpha_2^{(1)}\alpha_1^{(2)}}(Q_{m_1}\widehat{Q}_1^{-1})\vartheta_{\alpha_2^{(1)}\alpha_2^{(2)}}(Q_{m_2})}{\vartheta_{\alpha_1^{(1)}\alpha_1^{(1)}}(1)\vartheta_{\alpha_1^{(1)}\alpha_2^{(1)}}(\widehat{Q}_1^{-1})\vartheta_{\alpha_2^{(1)}\alpha_1^{(1)}}(\widehat{Q}_1)\vartheta_{\alpha_2^{(1)}\alpha_2^{(1)}}(1)} \\ &\times \frac{\vartheta_{\alpha_1^{(2)}\alpha_1^{(1)}}(Q_{m_2})\vartheta_{\alpha_1^{(2)}\alpha_2^{(1)}}(Q_{m_1}\widehat{Q}_2)\vartheta_{\alpha_2^{(2)}\alpha_1^{(1)}}(Q_{m_2}\widehat{Q}_2^{-1})\vartheta_{\alpha_2^{(2)}\alpha_2^{(1)}}(Q_{m_1})}{\vartheta_{\alpha_1^{(2)}\alpha_1^{(2)}}(1)\vartheta_{\alpha_1^{(2)}\alpha_2^{(2)}}(\widehat{Q}_2^{-1})\vartheta_{\alpha_2^{(2)}\alpha_1^{(2)}}(\widehat{Q}_2)\vartheta_{\alpha_2^{(2)}\alpha_2^{(2)}}(1)}\,, \end{aligned} \tag{3.49}$$

where the expansion parameters are the exponentiated coupling constants defined in (3.41), $Q_{g_{1,2}} = e^{-g_{1,2}}$ and $\widehat{Q}_i = e^{-\widehat{\alpha}_i}$ are the exponentiated roots defined in (3.37). By looking at the intersection numbers that have been calculated previously in (3.38), (3.43) and (3.44), we can see that indeed the arguments of the ϑ-functions in the numerator encode the matter representations and the ϑ-functions in the denominator encode the vector representation according to general structure presented in (3.45). Even if fiber-base duality is rather trivial for the case of $X_{2,2}$, as both theories have the same structure, the statement at the level of the expression (3.49) is still highly non-trivial. It is not a priori clear that one could completely expand (3.49) and then re-sum it using the parameters $\widehat{\alpha}_1^{(1)}$ and $\widehat{\alpha}_0^{(1)}$ (as defined in (3.37) and (3.39) respectively) such that the final expression has again the same structure with the roles of couplings and roots roughly interchanged.

3.5.2 Modular properties

The topological string partition function $\mathcal{Z}_{N,M}$ that we introduced in (3.45) enjoys modular properties. This can directly be concluded from the presence of the ϑ-functions in the contributions of the different multiplets (3.46), (3.47) and (3.48). The ϑ-functions themselves contain the Jacobi theta function θ_1, which is defined in (C.5) in appendix C. This function is a so called Jacobi form of weight and index $\frac{1}{2}$. They are characterized by a specific transformation behavior under $SL(2,\mathbb{Z})$ action

$$\theta_1\left(\frac{a\rho+b}{c\rho+d}, \frac{z}{c\rho+d}\right) = (c\rho+d)^{\frac{1}{2}} e^{i\pi\frac{cz^2}{c\rho+d}}\theta_1(\rho,z)\,, \quad \begin{pmatrix} a & b \\ c & d\end{pmatrix} \in SL(2,\mathbb{Z}) \tag{3.50}$$

So from this we see that ρ can be interpreted as a modular variable under $SL(2,\mathbb{Z})_\rho$. The subscript is meant to distinguish it from the $SL(2,\mathbb{Z})$ group that provides the S-duality in the (p,q)-brane web setting. The transformation behavior (3.50) is not surprising as we know from the F-theory description that ρ corresponds to the complex structure modulus of an elliptic curve which admits an natural $SL(2,\mathbb{Z})$ action. From the point of view of the partition function the variable z in (3.50) should be viewed as combinations of whatever Kähler parameters that appear in the arguments of the ϑ-functions including the deformation parameters ϵ_1 and ϵ_2. In [31] the authors analyzed the transformation behavior of $\mathcal{Z}_{1,M}$ (note that here $N=1$) under

$$(\mathbf{g},\tau,m,\rho,,\epsilon_1,\epsilon_2) \mapsto (\mathbf{g},\tau,\frac{m}{c\rho+d},\frac{a\rho+b}{c\rho+d},\frac{\epsilon_1}{c\rho+d},\frac{\epsilon_2}{c\rho+d}) \tag{3.51}$$

where $\mathbf{g}$ denotes the collective set of coupling constants as in the expansion (3.45) and τ is related to them as in (3.35). Why we explicitly include both τ and all the $\mathbf{g}$ will become clear as we go on. Here m stands for the only other Kähler parameter that appears in the arguments of the ϑ-function (together with ρ and $\epsilon_{1,2}$) in the expansion (3.45) when $N = 1$. The authors of [31] showed that the partition function has interesting modular properties under the transformation (3.51) when the so called NS limit $\epsilon_2 \to 0$ is taken. A physical interpretation of this limit in this context was given in [126], where the authors compared the BPS counting functions of M- and monopole-string excitations (see also [127]). In this limit, the partition function can be made invariant under the transformation (3.51). Upon specializing to the transformation with $a = d = 0$, $b = 1$ and $c = -1$ the couplings must transform as follows

$$g_i \mapsto g_i - (m^2 - \frac{\epsilon_1^2}{4}) \tag{3.52}$$

which through (3.35) directly implies

$$\tau = \sum_{i=1}^{M} g_i \mapsto \tau - M(m^2 - \frac{\epsilon_1^2}{4}) \tag{3.53}$$

Now, as the partition function enjoys T-duality properties, it can also be expanded in ρ (as here $N = 1$ this is the only expansion parameter). From this perspective, τ can also be interpreted as a modular parameter since it appears now in the arguments of the ϑ-functions. So there is another modular group action $SL(2,\mathbb{Z})_\tau$ which also acts on the partition function as

$$(\mathbf{g}, \tau, m, \rho, , \epsilon_1, \epsilon_2) \mapsto (\frac{\mathbf{g}}{c\tau + d}, \frac{a\tau + b}{c\tau + d}, \frac{m}{c\rho + d}, \rho, \frac{\epsilon_1}{c\rho + d}, \frac{\epsilon_2}{c\rho + d}) \tag{3.54}$$

The explicit transformation of the partition function $\mathcal{Z}_{1,M}$ under (3.54) is more involved as there are now more different parameters in the arguments of the ϑ-functions, *i.e.* there are all the g_i, m, ρ and $\epsilon_{1,2}$. What is important is that the partition function transforms again in a reasonably nice way when ρ behaves as

$$\rho \mapsto \rho - f(m, \mathbf{g}, \epsilon_1, \epsilon_2) \tag{3.55}$$

where f is a function that can in principle be determined by following the partition function through the modular transformation (3.54).

The important point here is that the generic partition function $\mathcal{Z}_{N,M}$ is expected to have reasonable well behaved properties under the action of $SL(2,\mathbb{Z})_\rho \times SL(2,\mathbb{Z})_\tau$. The combined transformations (3.51) and (3.53), or respectively (3.54) and (3.55), are very similar to the transformation properties of so called genus-two modular objects (see [128] for a review). The relation to genus-two modular object is especially clear through mirror symmetry of the underlying Calabi-Yau $X_{N,M}$ [117, 123, 48], where these objects appear naturally. The latter are a function of the period matrix Ω where the two elliptic variables ρ and τ are packaged together in the following way

$$\Omega = \begin{pmatrix} \rho & z \\ z & \tau \end{pmatrix} \tag{3.56}$$

with $z \in \mathbb{C}$ and $\mathfrak{Im}(\Omega)$ positive definite. There is a natural $Sp(4,\mathbb{Z})$ action on the period matrix Ω and hence on the associated genus-two modular objects. The full symmetry group of the partition function G, *i.e.* $SL(2,\mathbb{Z})_\rho \times SL(2,\mathbb{Z})_\tau$ combined with other symmetries, should be such that $SL(2,\mathbb{Z})_\rho \times SL(2,\mathbb{Z})_\tau \subset G \subseteq Sp(4,\mathbb{Z})$[19]. It has been shown in [117, 123] that in the case of $\mathcal{Z}_{1,1}$ there is indeed a $Sp(4,\mathbb{Z})$ symmetry group. In section 6, when we study additional symmetries of the partition function that are a direct consequence of the duality web established in section 4, we also comment on how these additional symmetries together with $SL(2,\mathbb{Z})_\rho \times SL(2,\mathbb{Z})_\tau$ sit inside $Sp(4,\mathbb{Z})$.

3.5.3 The free energy

Another function that is related to $\mathcal{Z}_{N,M}$ and that we will encounter in this work is the so called free energy $\mathcal{F}_{N,M}$ which is defined as the plethystic logarithm of the partition function [129]

$$\begin{aligned}\mathcal{F}_{N,M}(\{g_i\},\{a_i\},\{m_i\},\epsilon_{1,2}) &= \mathrm{PLog}\mathcal{Z}_{N,M}(\{g_i\},\{a_i\},\{m_i\},\epsilon_{1,2}) \\ &= \sum_{k=1}^{\infty}\frac{\mu(k)}{k}\ln\mathcal{Z}_{N,M}(\{kg_i\},\{ka_i\},\{km_i\},k\epsilon_{1,2}) \end{aligned} \tag{3.57}$$

where $\mu(k)$ is the Möbius function. In our context the free energy computes the multiplicities of single little string BPS bound states. As an expansion in the deformation parameters it has the schematic form

$$\mathcal{F}_{N,M} = \frac{1}{\epsilon_1\epsilon_2}\mathcal{F}^{(1)}_{N,M} + \text{(regular terms)} \tag{3.58}$$

This object is thus well behaved in the Nekrasov-Shatashvili (NS) limit (see [130]), which corresponds to $\lim_{\epsilon_2\to 0}\epsilon_2\mathcal{F}_{N,M}$. We will consider this limit when we study the newly found dihedral symmetry [47] in section 6.

3.5.4 Topological vertex

A systematic way to calculate the topological string partition function $\mathcal{Z}_{N,M}$ as given in (3.45) is provided by the topological vertex formalism that has first been introduced in [56]. A refined version was developed by the authors of [57]. In the refined version both deformation parameters ϵ_1 and ϵ_2 are present, whereas the initial unrefined version corresponds to the limit where $\epsilon_1 = -\epsilon_2 = \epsilon$. In this thesis we are working in the refined setting, so even if we refer simply to the topological vertex, it is the refined version that we have in mind, unless stated explicitly otherwise. The underlying idea of the vertex formalism is that the topological string partition function for a given non-compact toric Calabi-Yau threefold can be calculated by using certain elementary building blocks, which have the form of trivalent vertices. The latter can be glued together in order to construct the complete toric diagram corresponding to the Calabi-Yau threefold, *e.g.* as in Fig. 2. Before looking at the explicit algebraic expression of the topological vertex and the procedure on how to glue them together, we try to give a motivation of why one would expect that such a algorithmic procedure would exist in order to calculate the topological string partition function. The method is certainly not limited to the geometries we consider in

[19] It is reasonable to expect that the presence of additional parameters in the partition function breaks part of the full $Sp(4,\mathbb{Z})$ symmetry.

this thesis, but applies to a wide range of toric diagrams, see for example [131–133].

A non-compact toric Calabi-Yau threefold can be described by a non-trivial assembling of $\mathbb{C}^3$ patches that preserves Ricci flatness and hence the Calabi-Yau condition. The simple space $\mathbb{C}^3$ is actually the most basic example of a toric Calabi-Yau threefold. They can be described as a $T^2 \times \mathbb{R}$ fibration over a $\mathbb{R}^3$ base and this structure can be conveniently encoded into a planar graph [56]. Given $(z_1, z_2, z_3) \in \mathbb{C}^3$, we define the three maps

$$\begin{aligned} r_\alpha(z) &= |z_3|^2 - |z_1|^2 \\ r_\beta(z) &= |z_3|^2 - |z_2|^2 \\ r_\gamma(z) &= \mathfrak{Im}(z_1 z_2 z_3) \end{aligned} \tag{3.59}$$

These parametrize the $\mathbb{R}^3$ base of the fibration. The fibers are generated by the action of (3.59) on $\mathbb{C}^3$ via the standard symplectic form $\omega = i \sum_j dz_j \wedge d\bar{z}_j$ and the Poisson brackets

$$\partial_v z_i = \{r_v, z_i\}\,, \quad \text{with } v = \alpha, \beta, \gamma \tag{3.60}$$

More precisely, the T^2 fiber is generated by the circle actions

$$\exp(i\alpha r_\alpha + i\beta r_\beta): \quad (z_1, z_2, z_3) \to (e^{i\alpha} z_1, e^{i\beta} z_2, e^{-i(\alpha+\beta)} z_3)\,, \tag{3.61}$$

while r_γ generates the real line $\mathbb{R}$. We denote the cycles generated by r_α and r_β by $(0,1)$ and $(1,0)$ respectively. These cycles degenerate over certain subspaces of $\mathbb{C}^3$ as can be seen from their explicit form in (3.61). The $(0,1)$ cycle degenerates for example over the $\mathbb{C}^3$ subspace given by $z_1 = z_3 = 0$, which is described in the $\mathbb{R}^3$ base by $r_\alpha = r_\gamma = 0$ and $r_\beta \geq 0$. The $(1,0)$ cycle degenerates over $z_2 = z_3 = 0$ which, in the $\mathbb{R}^3$ base, corresponds to $r_\beta = r_\gamma = 0$ and $r_\alpha \geq 0$. Furthermore there is the one-cycle parametrized by $\alpha + \beta$ which degenerates over $z_1 = z_2 = 0$, or equivalently in the base $r_\alpha - r_\beta = r_\gamma = 0$ with $r_\alpha \leq 0$. These degeneration loci and hence the geometry of $\mathbb{C}^3$ as a $T^2 \times \mathbb{R}$ fibration can be conveniently encoded into a planar graph. For this we choose the $r_\alpha - r_\beta$ plane at $r_\gamma = 0$ in $\mathbb{R}^3$. For a given degenerating $(-q, p)$ cycle of the T^2, we draw a line given by the equation $p r_\alpha + q r_\beta = 0$. Up to a an overall sign ($(p,q) \to (-p,-q)$), this unambiguously associates degeneration loci to lines in the planar graph. The resulting planar graph for $\mathbb{C}^3$ is shown in Fig. 4. It should be emphasized that we merely presented one of numerous possible choices for the generating cycles of T^2. Different choices are related to this one by a $SL(2,\mathbb{Z})$ transformation acting on T^2. From the discussion and the graph Fig. 4, it should become clear that this is just another point of view on the dual toric diagrams, or equivalently the (p,q) brane webs introduced in subsection 3.4.1. The relation will become more clear once we start gluing together the $\mathbb{C}^3$ patches. The choice of basis for the torus cycles corresponds to S-duality for the (p,q) webs in type IIB string theory.

Now that we have presented a description of $\mathbb{C}^3$ as a $T^2 \times \mathbb{R}$ fibration over a base $\mathbb{R}^3$, we want to understand how this picture generalizes when we start patching the $\mathbb{C}^3$'s together in certain ways to form more general Calabi-Yau threefolds. Consider the complex space $\mathbb{C}^{N+3}$ described by coordinates $z_1, \ldots, z_{N+3}$. We must first find a decomposition of the set of coordinates into triplet $U_a = (z_{i_a}, z_{j_a}, z_{k_a})$ that correspond to the decomposition of the Calabi-Yau into $\mathbb{C}^3$ patches. The patching data is provided by the so called moment maps.

$$\sum_i Q_i^a |z_i|^2 = t^a \tag{3.62}$$

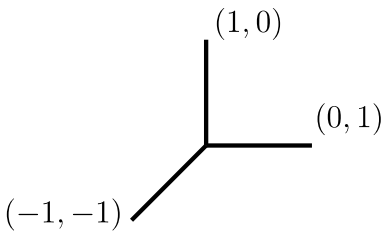

Figure 4: *Degeneration loci of the T^2 fibration in $\mathbb{R}^3$ drawn in the plane given by $r_\gamma = 0$*

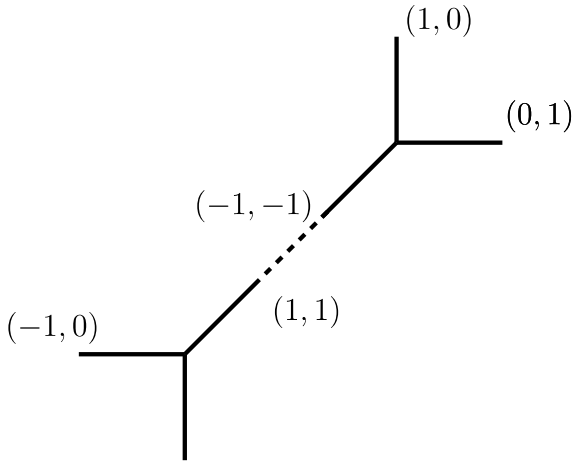

Figure 5: *The degeneration loci graph associated to the resolved conifold $\mathcal{O}(-1)\oplus\mathcal{O}(-1) \to \mathbb{CP}^1$ when seen as a $T^2 \times \mathbb{R}$ fibration over $\mathbb{R}^3$.*

where the t^a correspond to Kähler parameters of the geometry and the Q_i^a are integer coefficients that satisfy

$$\sum_i Q_i^a = 0 \tag{3.63}$$

This is actually the condition for the whole space to be Calabi-Yau. There is furthermore a group action by $G_N = U(1)^N$ that acts as

$$z_k \to e^{iQ_a^k \alpha_a} z_k \tag{3.64}$$

In order to effectively glue together the patches, we start by associating to one patch the two functions r_α and r_β as defined before. These are globally well defined coordinates in the base $\mathbb{R}^3$, so they generate a globally well defined T^2 fiber. The third base coordinate $r_\gamma = \mathfrak{Im}(\prod_{k=1}^{N+3} z_k)$ is manifestly invariant under the action (3.64) and serves as a good coordinate. The moment maps specify how to relate the expressions of r_α and r_β in terms of homogeneous coordinates in two different patches. This explicitly gives the action of r_α and r_β in all the patches.

Specific example

To illustrate all of this we look at the specific example of the resolved conifold[20], *i.e.* local $\mathcal{O}(-1)\oplus\mathcal{O}(-1)\to\mathbb{CP}^1$. For this geometry, we have four homogeneous coordinates z_i and a single moment map that takes the form

$$|z_1|^2-|z_2|^2-|z_3|^2+|z_4|^2=t \tag{3.65}$$

with the single Kähler parameter t.[21] In the first patch $U_1=(z_1,z_2,z_3)$ where $z_4\neq 0$ we can define the following Hamiltonians in terms of the homogeneous coordinates

$$\begin{aligned} r_\alpha &= |z_2|^2-|z_1|^2 \\ r_\beta &= |z_3|^2-|z_1|^2 \end{aligned} \tag{3.66}$$

The latter generate the action

$$\exp(\alpha r_\alpha+\beta r_\beta):\quad (z_1,z_2,z_3)\to(e^{-i(\alpha+\beta)}z_1,e^{i\alpha}z_2,e^{i\beta}z_3) \tag{3.67}$$

which has a $(0,1)$ cycle degenerating over the line $r_\alpha=0$ and $r_\beta\geq 0$. The $(1,0)$ cycle degenerates over $r_\beta=0$ and $r_\alpha\geq 0$. Finally the $(-1,-1)$ cycle degenerates over $r_\alpha-r_\beta=0$. Thus this patch can be represented by the same graph as in Fig. 4. In the other patch $U_2=(z_2,z_3,z_4)$, defined by $z_1\neq 0$, the latter is no longer a good coordinate. Solving for the modulus of z_1 in (3.65), we can re-express the Hamiltonians (3.66) in the U_2 patch as

$$\begin{aligned} r_\alpha &= |z_4|^2-|z_3|^2-t \\ r_\beta &= |z_4|^2-|z_2|^2-t \end{aligned} \tag{3.68}$$

The latter generate the action

$$\exp(\alpha r_\alpha+\beta r_\beta):\quad (z_2,z_3,z_4)\to(e^{-i\beta}z_2,e^{-i\alpha}z_3,e^{i(\alpha+\beta)}z_4) \tag{3.69}$$

which has a degenerating $(0,-1)$ cycle over the line $r_\alpha=-t$ and $r_\beta\leq 0$. A $(-1,0)$ degenerates over $r_\beta=-t$ and $r_\alpha\leq 0$. Finally a $(1,1)$ cycle degenerates over $r_\alpha-r_\beta=0$. This line is the same as the one the $(-1,-1)$ cycle degenerates in the U_1 patch. Hence the two graphs are joined along this edge in the overlapping region where $z_1\neq 0$, $z_4\neq 0$ and $z_2=z_3=0$. The length of this edge corresponds to the Kähler parameter t appearing in (3.65). The associated graph of this construction is shown in Fig. 5.

The fact that the geometry of toric Calabi-Yau threefolds can be encoded into a trivalent graph makes it more plausible that the topological string partition function $\mathcal{Z}_{N,M}$ of for $X_{N,M}$ can be computed by using an algorithmic procedure involving trivalent vertices as building blocks, but it is still far from evident. A rigorous derivation of this fact would be beyond the scope of this thesis. We will simply try to give the very broad lines of the argument here and refer the interested reader to [116] for a review of the subject. The story started with a well motivated conjecture made by Gopakumar and Vafa in [134], which states that Chern-Simons theory on the three sphere S^3 is equivalent to closed topological string theory on the resolved

[20] The conifold and its resolution are also briefly discussed from the algebraic perspective in appendix A

[21] For $z_2=z_3=0$, equation (3.65) describes a $\mathbb{CP}^1$ with area proportional to t. Hence, z_1 and z_4 can be taken as homogeneous coordinates of this $\mathbb{CP}^1$ which is the base of the fibration when viewing the geometry as $\mathcal{O}(-1)\oplus\mathcal{O}(-1)\to\mathbb{CP}^1$ with fiber coordinates z_2 and z_3.

conifold geometry, which is the one represented in Fig. 5. While we are not going to review this conjecture here, we can illustrate how the underlying spaces are related at the geometrical level. The resolved conifold can be taken to its singular point by shrinking the resolving $\mathbb{CP}^1$, which corresponds to the interior edge. Once singular, the conifold singularity can be smoothed out in an alternative way by so called complex structure deformation. This smoothing out procedure makes a three sphere appear in the deformed geometry, which is exactly the one appearing in the conjecture above. The process of passing between the resolved and deformed geometry is known as geometric transition and more specifically in the case of the conifold geometry as conifold transition [135]. The underlying idea of the conjecture is that we can follow the Chern-Simons theory on S^3 in the deformed space through the geometric transition and we end up with topological string theory on the resolved space. Starting with the work of Witten [136], it was clear how to do systematic computations on the Chern-Simons side. So this correspondence was already a step in the right direction. However, it was only a little later in [137] that such a correspondence was established for more complicated geometries than the resolved conifold. This made computations possible, although a little cumbersome as the building block was the resolved conifold geometry, which is not practical in general. It was clear that the fundamental building block should be the simpler $\mathbb{C}^3$ space. A series of works, for example [137, 138, 84, 83] to mention a few, culminated in a deep understanding on how to calculate topological string amplitudes, and thus also gauge theory partition functions, in a systematic fashion with the use of diagrammatic rules. This formalism was then finally made explicit in [56, 57].

After our attempt to motivate the existence of an algorithmic procedure to calculate closed topological string amplitudes, we now simply state the final result. The algebraic expression associated to the refined topological vertex takes the following form

$$C_{\lambda\mu\nu}(t,q) = q^{\frac{||\mu||^2}{2}} t^{-\frac{||\mu^t||^2}{2}} q^{\frac{||\nu||^2}{2}} \tilde{Z}_\nu(t,q) \sum_\eta \left(\frac{q}{t}\right)^{\frac{|\eta|+|\lambda|-|\mu|}{2}} s_{\lambda^t/\eta}(t^{-\xi}q^{-\nu}) s_{\mu/\eta}(q^{-\xi}t^{-\nu^t}) \tag{3.70}$$

where $q = e^{2\pi i\epsilon_1}$ and $t = e^{-2\pi i\epsilon_2}$. The $s_{\mu/\nu}$ are skew Schur functions (defined in D.7) and $\xi = \left\{-\frac{1}{2}, -\frac{3}{2}, -\frac{5}{2}, \ldots\right\}$. Furthermore, we introduced

$$\tilde{Z}_\nu(t,q) = \prod_{(i,j)\in\nu} (1 - t^{\nu_j^t - i + 1} q^{\nu_i - j})^{-1} . \tag{3.71}$$

The refined topological vertex (3.70) does not depend in a symmetric way on the three integer partitions λ, μ and ν, *i.e.* it is not manifestly rotation invariant. When performing calculations we must choose a so called preferred direction for each vertex involved. This choice must be consistent and common to every vertex in the web diagram. When different choices are possible, the partition functions associated to each choice will look different but they are equivalent expansions of the same function [117]. The two different expansions of the partition function that are related through fiber-base duality correspond to two different choices of preferred directions, *i.e.* horizontal and vertical as in Fig. 2. Two topological vertices can be glued along any of their external legs as follows

$$\sum_\lambda (-e^{-h|\lambda|}) C_{\mu_1\nu_1\lambda}(t,q) C_{\mu_2\nu_2\lambda^t}(q,t) \tag{3.72}$$

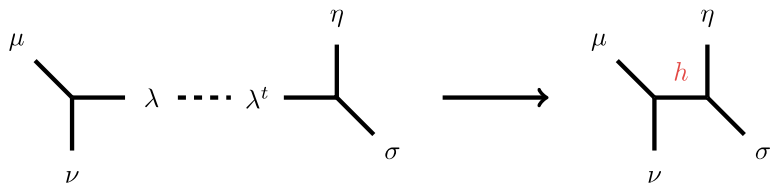

Figure 6: *Gluing of two topological vertices along the legs indexed by λ and λ^t. The Kähler parameter associated to the glued leg is highlighted in red*

where the sum runs over the integer partitions associated to the external legs that are glued. These partitions must be taken to be transpose of another,*e.g.* here λ and λ^t. Furthermore, the roles of the regularization parameters q and t in the individual vertex functions must be inversed with respect to each other. The extra factor inserted into the expression (3.72) is the exponentiated Kähler parameter corresponding to the glued edge, *i.e.* it is the volume of the associated compact curve as defined in (3.32). This procedure is summarized diagrammatically in Fig. 6.

3.5.5 Building Block

In order to calculate the partition function associated to the web diagrams of $X_{N,M}$ in an efficient way, it is useful to derive a general building block. By this, we mean the most general part of the web diagram as shown in Fig. 2 with some of the external legs not glued (still depending on generic integer partitions). This way we can more easily reproduce all web diagrams that are of interest to us. The most generic building block we can devise for our purpose has the form of a periodic strip as depicted in Fig. 7. We recall that the only the relative orientation of the lines counts and different frames are related by $SL(2,\mathbb{Z})$ transformations, thus the fact that in the figure the external legs are diagonal and some of the internal lines are vertical does not play a role. Their respective orientations could simply be inverted by an $SL(2,\mathbb{Z})$ action. Such a building block has for example been derived in [125] for a non-periodic strip geometry and in [36] for a periodic by using the refined topological vertex formalism that we introduced in the previous section. The strip is periodic in the horizontal direction and the diagonal external legs still depend on the two sets of integer partitions $\{\alpha_i\}$ and $\{\beta_i\}$ for $i = 1, \ldots, L$. The partitions $\{\mu_i\}$ and $\{\nu_i\}$ along the internal lines denote the partitions along which the topological vertices have already been glued. We indicate them for clarity when we describe the calculation of the associated algebraic expression. The Kähler parameters corresponding to the horizontal and vertical curves are denoted by $\{h_i\}$ and $\{v_i\}$ respectively. Due to the fact that the external legs are not glued, there are no consistency conditions. Hence, there are no relations between these Kähler parameters at this stage. In order to derive the algebraic expression associated to the building block Fig. 7, we apply the procedure outlined in the preceding section. The gluing rule (3.72) gives us the following expression

$$W^{\alpha_1\ldots\alpha_L}_{\beta_1\ldots\beta_L}(Q_{h_i}, Q_{v_i}, \epsilon_1, \epsilon_2) = \hat{Z} \times \sum_{\substack{\{\mu\}\{\nu\}\\ \{\eta\}\{\tilde{\eta}\}}} \prod_{i=1}^{L} Q_{h_i}^{|\mu_i|} Q_{v_i}^{|\nu_i|} s_{\mu_i/\eta_i}(x_i) s_{\mu_i^t/\tilde{\eta}_{i-1}}(y_{i-1}) s_{\nu_i^t/\tilde{\eta}_i}(w_i) s_{\nu_i/\eta_i}(z_i) \tag{3.73}$$

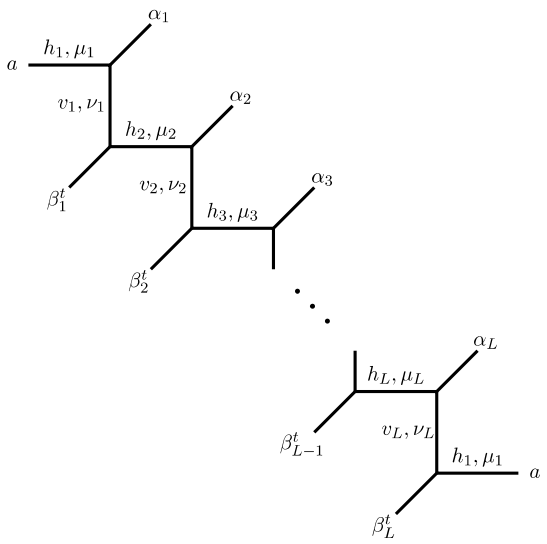

Figure 7: *Periodic strip of length L with a labeling of the Kähler parameters and integer partitions.*

where the sum runs over different sets of integer partitions and the prefactor is given by

$$\hat{Z} = \prod_{i=1}^{L} t^{\frac{||\alpha_k||^2}{2}} q^{\frac{||\alpha_k^t||^2}{2}} \tilde{Z}_{\alpha_k}(q,t) \tilde{Z}_{\alpha_k^t}(t,q)\,, \tag{3.74}$$

and the arguments of skew Schur functions are defined as

$$\begin{aligned} x_i &= q^{-\xi+\frac{1}{2}} t^{-\alpha_i-\frac{1}{2}}\,, & y_i &= t^{-\xi+\frac{1}{2}} q^{-\beta_i^t-\frac{1}{2}}\,, \\ w_i &= q^{-\xi} t^{-\beta_i}\,, & z_i &= t^{-\xi} q^{-\alpha_i^t}\,, \end{aligned} \tag{3.75}$$

where $\xi = \left\{-\frac{1}{2}\,, -\frac{3}{2}\,, -\frac{5}{2}\,, \ldots\right\}$. It is also important to note that the indices are defined cyclically, *e.g.* $y_0 = y_L$. The sum over partitions in (3.73) can be performed explicitly by using the identities on Schur functions (D.8) given in the appendix. The latter allow us to derive a recurrence relation, similar to [50], that makes it possible to write (3.73) as a product. To illustrate the calculation we work with the expression

$$G(\mathbf{x},\mathbf{y},\mathbf{w},\mathbf{z}) = \sum_{\substack{\{\mu\}\{\nu\}\\ \{\eta\}\{\tilde{\eta}\}}} \prod_{i=1}^{L} Q_{h_i}^{|\mu_i|} Q_{v_i}^{|\nu_i|} s_{\mu_i/\eta_i}(x_i) s_{\mu_i^t/\tilde{\eta}_{i-1}}(y_{i-1}) s_{\nu_i^t/\tilde{\eta}_i}(w_i) s_{\nu_i/\eta_i}(z_i) \tag{3.76}$$

which is just (3.73) without the prefactor. We can use the Schur function identities (D.8) to rewrite this expression as follows

$$\begin{aligned} G(\mathbf{x},\mathbf{y},\mathbf{w},\mathbf{z}) = P \times \sum_{\substack{\{\mu\}\{\nu\}\\ \{\eta\}\{\tilde{\eta}\}}} \prod_{i=1}^{L} Q_{h_i}^{|\mu_i|} Q_{v_i}^{|\nu_i|} s_{\mu_{i-1}/\eta_{i-1}}(Q_{h_i} Q_{v_{i-1}} x_i) s_{\mu_{i+1}^t/\tilde{\eta}_i}(\tilde{Q}_i y_{i-1}) \\ \times s_{\nu_{i-1}^t/\tilde{\eta}_{i-1}}(\tilde{Q}_i w_i) s_{\nu_{i+1}/\eta_{i+1}}(Q_{h_{i+1}} Q_{v_i} z_i) \end{aligned} \tag{3.77}$$

where we introduced the notation $\tilde{Q}_i = Q_{h_i} Q_{v_i}$ and

$$P = \prod_{i=1}^{L} \prod_{r,s=1}^{\infty} \frac{(1 - Q_{h_i} x_{i,r} y_{i-1,s})(1 - Q_{v_i} w_{w_{i,r} z_{i,s}})}{(1 - Q_{h_i} Q_{v_{i-1}} x_{i,r} z_{i-1,s})(1 - \tilde{Q}_i y_{i-1,r} w_{i,s})} \times \frac{(1 - Q_{h_i} \tilde{Q}_{i-1} x_{i,r} y_{i-2,s})(1 - Q_{v_i} \tilde{Q}_{i+1} w_{i+1,r} z_{i,s})}{(1 - Q_{h_i} \tilde{Q}_{i-1} Q_{v_{i-2}} x_{i,r} z_{i-2,s})(1 - \tilde{Q}_i \tilde{Q}_{i+1} y_{i-1,r} w_{i+1,s})} \tag{3.78}$$

Up to the prefactor the expression (3.77) is very similar to (3.76) except for the difference that the partitions indexing the Schur functions have been shifted and the arguments modified. By repeating this procedure L times, we obtain again the quantity (3.76), up to a prefactor that we call P_1[22] and a shift of all arguments. More precisely we get the relation

$$G(\mathbf{x}, \mathbf{y}, \mathbf{w}, \mathbf{z}) = P_1 \times G(Q_\rho \mathbf{x}, Q_\rho \mathbf{y}, Q_\rho \mathbf{w}, Q_\rho \mathbf{z}) \tag{3.79}$$

where we defined $Q_\rho = \prod_{i=1}^{L} \tilde{Q}_i$, which will play the role of modular parameter in the partition function. By iterating the procedure that led to the relation (3.79) n times we get the following recursion relation

$$G(\mathbf{x}, \mathbf{y}, \mathbf{w}, \mathbf{z}) = P_n \times G(Q_\rho^n \mathbf{x}, Q_\rho^n \mathbf{y}, Q_\rho^n \mathbf{w}, Q_\rho^n \mathbf{z}) \tag{3.80}$$

where again the explicit form of P_n is not important. Assuming that $\lim_{n\to\infty} Q_\rho^n = 0$[23], we find that

$$\begin{aligned} &\lim_{n\to\infty} G(Q_\rho^n \mathbf{x}, Q_\rho^n \mathbf{y}, Q_\rho^n \mathbf{w}, Q_\rho^n \mathbf{z}) \\ &\quad = \lim_{n\to\infty} \sum_{\substack{\{\mu\}\{\nu\} \\ \{\eta\}\{\tilde{\eta}\}}} \prod_{i=1}^{L} Q_{h_i}^{|\mu_i|} Q_{v_i}^{|\nu_i|} s_{\mu_i/\eta_i}((Q_\rho^2)^n x_i) s_{\mu_i^t/\tilde{\eta}_{i-1}}(y_{i-1}) s_{\nu_i^t/\tilde{\eta}_i}((Q_\rho^2)^n w_i) s_{\nu_i/\eta_i}(z_i) \\ &\quad = \sum_{\{\eta\}\{\tilde{\eta}\}} \prod_{i=1}^{L} Q_{h_i}^{|\eta_i|} Q_{v_i}^{|\tilde{\eta}_i|} s_{\eta_i^t/\tilde{\eta}_{i-1}}(y_{i-1}) s_{\tilde{\eta}_i^t/\eta_i}(z_i) \end{aligned} \tag{3.81}$$

as the only non-vanishing terms in this limit correspond to terms where the partitions take the values $\mu_i = \eta_i$ and $\nu_i^t = \tilde{\eta}_i$, *i.e.* as $s_{\mu/\mu}(x) = s_\emptyset(x) = 1$. The skew Schur functions in (3.81) are only non-zero when $\eta_i \subset \tilde{\eta}_i^t$ and $\tilde{\eta}_i \subset \eta_{i+1}^t$. As inclusion of partitions remains valid when taking the transpose we get the relations $\eta_i \subset \eta_{i+1}$ and $\tilde{\eta}_i \subset \tilde{\eta}_{i+1}$. As the indices are cyclic this simply reduces to the condition $\eta_i = \tilde{\eta}_i = \eta$. As a result we have

$$\lim_{n\to\infty} G(Q_\rho^n \mathbf{x}, Q_\rho^n \mathbf{y}, Q_\rho^n \mathbf{w}, Q_\rho^n \mathbf{z}) = \sum_{\eta} Q_\rho^{|\eta|} = \prod_{k=1}^{\infty} (1 - Q_\rho^k)^{-1} \tag{3.82}$$

which immediately gives

$$G(\mathbf{x}, \mathbf{y}, \mathbf{w}, \mathbf{z}) = P_\infty \times \prod_{k=1}^{\infty} (1 - Q_\rho^k)^{-1} \,. \tag{3.83}$$

[22]The precise form of this factor will not be important and is thus omitted.

[23]This is a reasonable assumption because it will be clear later on that ρ corresponds to the complex structure modulus of the torus in the F-theory construction as described in 3.2.1, *i.e.* $\mathfrak{Im}(\rho) > 0$.

The factor P_∞ is given by

$$P_\infty = \prod_{i,j=1}^{L} \prod_{k,r,s=1}^{\infty} \frac{(1-\widehat{Q}^h_{i,j}\, Q_\rho^{k-1} x_{i,r} y_{i-j,s})(1-\widehat{Q}^v_{i,j} Q_\rho^{k-1} z_{i,s} w_{i+j-1,r})}{(1-\overline{Q}_{i,j} Q_\rho^{k-1} x_{i,r} z_{i-j,s})(1-\dot{Q}_{i,j} Q_\rho^{k-1} y_{i,s} w_{i+j,r})}\,, \tag{3.84}$$

where we introduced some notation to make the equations less heavy. We define

$$\widehat{Q}^h_{i,j} = Q_{h_i} \prod_{k=1}^{j-1} \widetilde{Q}_{i-k}\,, \quad \widehat{Q}^v_{i,j} = Q_{v_i} \prod_{k=1}^{j-1} \widetilde{Q}_{i+k}\,, \quad \overline{Q}_{i,j} = Q_{h_i} Q_{v_{i-j}} \prod_{k=1}^{j-1} \widetilde{Q}_{i-k}\,, \quad \dot{Q}_{i,j} = \prod_{k=1}^{j} \widetilde{Q}_{i+k} \tag{3.85}$$

We have thus expressed the sum over integer partitions in (3.76) as a product. This simplification together with the identities (D.17) from the appendix allows us to write the building block (3.73) in a compact form

$$W^{\alpha_1\dots\alpha_L}_{\beta_1\dots\beta_L} = W_L(\emptyset)\cdot \hat{Z} \cdot \prod_{i,j=1}^{L} \frac{\mathcal{J}_{\alpha_i\beta_j}(\widehat{Q}_{i,i-j};q,t)\mathcal{J}_{\beta_j\alpha_i}((\widehat{Q}_{i,i-j})^{-1}Q_\rho;q,t)}{\mathcal{J}_{\alpha_i\alpha_j}(\overline{Q}_{i,i-j}\sqrt{q/t};q,t)\mathcal{J}_{\beta_j\beta_i}(\dot{Q}_{i,j-i}\sqrt{t/q};q,t)}\,, \tag{3.86}$$

where we introduced the $\mathcal{J}_{\mu\nu}$ functions (defined in the appendix in (D.9) and (D.10)) as well as the so called perturbative part

$$W_L(\emptyset) = \prod_{i,j=1}^{L} \prod_{k,r,s=1}^{\infty} \frac{(1-\widehat{Q}_{i,j}\, Q_\rho^{k-1} q^{r-\frac{1}{2}} t^{s-\frac{1}{2}})(1-\widehat{Q}^{-1}_{i,j} Q_\rho^{k} q^{s-\frac{1}{2}} t^{r-\frac{1}{2}})}{(1-\overline{Q}_{i,j} Q_\rho^{k-1} q^r t^{s-1})(1-\dot{Q}_{i,j} Q_\rho^{k-1} q^{s-1} t^r)}\,. \tag{3.87}$$

The latter is nothing else than the contribution of the building block with all the external legs carrying the empty partition. In terms of five-branes this corresponds to the external branes extending all the way to infinity. The building block (3.86) is now in a convenient form for performing calculations. Upon gluing, we can use the identities (D.13) and (D.14) for the $\mathcal{J}_{\mu\nu}$ functions to convert them into the $\vartheta_{\mu\nu}$ functions that we have already seen in the schematic expansion of the partition function (3.45). In principle, the $\mathcal{J}_{\mu\nu}$ functions in the numerator of (3.86) can readily be combined into $\vartheta_{\mu\nu}$ functions without any gluing of the external legs. However, we prefer to keep the expression (3.86) the way it is until the denominator can also be transformed. It is nevertheless interesting to think about why it does not require gluing to bring the numerator into the 'usual' form. We have seen in section 3.5.1 that the ϑ-functions in the numerator of the partition function are contributions coming from the matter multiplets in our theory (in our case mainly bifundamental or adjoint), whereas the denominator represents contribution from the vector multiplets. This means that the building block (3.86) can be seen as a bifundamental matter contribution which has not yet been associated to definite gauge factors.

4 Duality Web between little string theories of type A

Previously we have reviewed the fact that little string theories enjoy T-duality [39, 31]. As explained, the geometric origin of this duality is the double elliptic fibration structure of the Calabi-Yau threefold $X_{N,M}$ which engineers the respective theories. The instanton partition function is a powerful tool to check this duality explicitly. Due to its non-perturbative nature, it's agreement for two a priori different theories provides us with an exact result. In this section, we argue for an even more intricate web of exact dualities between little string theories of type A and and thus also between their low-energy gauge theory descriptions.

The topological string partition function $\mathcal{Z}_{N,M}$ for a given geometry $X_{N,M}$ can be obtained from a topological vertex calculation as explained in section 3.5.1. The way the partition function is expanded depends on the choice of preferred direction, which has to be the same for every vertex making up the web diagram. The class of toric diagrams we are dealing with (see Fig. 2) thus allows in general for three different choices. The horizontal and vertical choices are known to give instanton partition functions corresponding to T-dual little string theories. One is described by a $\widehat{A}_{N-1}$ quiver composed of $U(M)$ gauge nodes (or $[U(M)]^N$ for short), while the other is described by a $\widehat{A}_{M-1}$ quiver composed of $U(N)$ gauge nodes ($[U(M)^N]$). The choice of the diagonal preferred direction has initially not been studied. One possible explanation is that from the point of view of the five-brane web in type II String Theory, it is a priori not clear what worldvolume theory one should expect on the $(1,1)$ bound state branes. Even upon using S-duality to go to a dual frame where the initially diagonal branes become horizontal or vertical, it is not evident what to expect. In [33], the authors studied this question from the point of view of the toric diagram and conjectured the existence of a third theory which is dual to the other two theories, *i.e.* horizontal and vertical, already known to be engineered by the geometry $X_{N,M}$. Their starting point was the geometric transformation known as flop, which allowed them to relate different web diagrams $X_{N,M}$ and $X_{N',M'}$ with $\gcd(N,M) = k = \gcd(N',M')$ and $NM = N'M'$. This made it possible to establish a connection between the diagonal world volume theory in $X_{N,M}$ on one side and a "conventional" (in the sense that it is known what to expect) world volume theory in $X_{N',M'}$. More precisely, the conjecture was that a given Calabi-Yau threefold $X_{N,M}$, as shown in Fig. 2, engineers three different quiver gauge theories corresponding to the three possible expansions of the topological string partition function. The diagonal theory would be described by an $\widehat{A}_{k-1}$ quiver composed of $U(\frac{NM}{k})$ gauge nodes. A proposal for the duality map relating these theories was also made in [33]. Consequently, in a series of papers [36–38] this conjecture has been verified explicitly at the level of the partition function for the case $\gcd(N,M) = 1$ and further arguments were given for supporting the case when $\gcd(N,M) > 1$ [24]. The presence of three gauge theories engineered by $X_{N,M}$ was dubbed *Triality*. The explicit duality maps relating these theories were given. In contrast to the fiber base duality map, which roughly exchanges Coulomb branch parameters and coupling constants, the duality map of the third theory to either of the other two is highly non-trivial, *i.e.* mixing coupling constants, Coulomb branch and mass parameters. It was also shown that a direct implication of these results was an even larger web of dual theories (more than three) in general.

[24] The duality has recently been proven in [48] for general N and M but only in a specific limit of the Omega background where $\epsilon_1 = -\epsilon_2 \to 0$. The authors used the relation of the partition function to genus 2 Riemann theta functions via mirror symmetry [117] to achieve this.

In this section, we first review the arguments given by the authors of [33] and then we give a proof of their conjecture in the case $\gcd(N, M) = 1$. Furthermore, we give arguments for the validity of the conjecture when $\gcd(N, , M) > 1$ and how the conjecture implies an even larger web of dual theories $[U(N)]^M$ and $[U(N')]^{M'}$ where $NM = N'M'$ and $\gcd(N, M) = \gcd(N', M')$.

4.1 Shifted web diagrams and Flop Transitions

In order to check the conjectured duality put forward in [33], we first need to introduce the notion of shifted web diagram and its relation to conventional web diagrams. For clarity, we focus on the specific example of $X_{3,2}$ as shown in Fig. 8 (a). This easily illustrates how and why one comes to consider such shifted diagrams. From section 3.5, we know that the vertical and horizontal theories associated with this toric diagram are a $\widehat{A}_1$ quiver gauge theory with gauge group $U(3)$ and a $\widehat{A}_2$ quiver gauge theory with gauge group $U(2)$ respectively. It is a priori not known if the diagonal choice of preferred direction gives a meaningful expansion of the topological string partition function, *i.e.* it is not clear if it can be interpreted as the instanton partition function of a third gauge theory or if it is just an inconvenient expansion without a particular meaning. As already mentioned above, when taking the point of view of five-branes in the type IIB setting, it is not clear what theory lives in the world volume of the diagonal bound state branes of $X_{3,2}$. In order to study this question, it is more convenient to look at a different but equivalent representation of the web diagram of $X_{3,2}$ as shown in Fig. 8 (b). Heuristically, this representation is obtained by cutting along the diagonal lines, while keeping them identified and then regluing along the vertical lines. From the point of view of the toric diagrams, this representation is just a different choice of the fundamental domain of the underlying infinite toric fan, as described in appendix B. In this form, we refer to it as *shifted web diagram* and denote it by $X_{6,1}^{(\delta=3)}$, where δ refers to the units the external legs on opposite sides are cyclically rotated with respect to another. In the most general case a shifted web diagram would look like in Fig. 9. One should note that there are in general shifted web diagrams which do not have an equivalent representations in terms of unshifted webs, *i.e.* there is no frame where the external lines have no relative offset. We will be naturally led to consider such configurations when analyzing the extended web of dualities for the engineered theories. An example will be provided at that point. It is important to emphasize that even tough the external legs in Fig. 9 are offset with respect to another, the branes do not cross each other. The diagram can be thought of as being on a torus, so one set of external legs (*e.g.* vertical) being shifted can be allowed without having intersections among branes. However, it is not possible to have at the same time a shift in the other set of external legs as this would necessarily imply intersections. Throughout this work, there will be supporting figures to make clear in what set of external legs the shift δ is. From the example in Fig. 8, it is clear that the notation we introduced has some redundancy from the geometric point of view, *i.e.* $X_{3,2}$ and $X_{6,1}^{(\delta)}$ refer to the same Calabi-Yau threefold. It is nevertheless useful to indicate which presentation of the web diagram we are referring to. Another point worth mentioning is that in Fig. 8 (b) the fact that the external legs are diagonal $(1, 1)$ branes has no special meaning. As explained in appendix A there several possible frames of the toric fan related by $SL(2, \mathbb{Z})$ transformations. Acting with the right group element would simply exchange the diagonal lines with the vertical ones, resulting in a form of the toric diagram that we are more familiar with. Equivalently, the $SL(2, \mathbb{Z})$-action is simply the S-duality in the type IIB con-

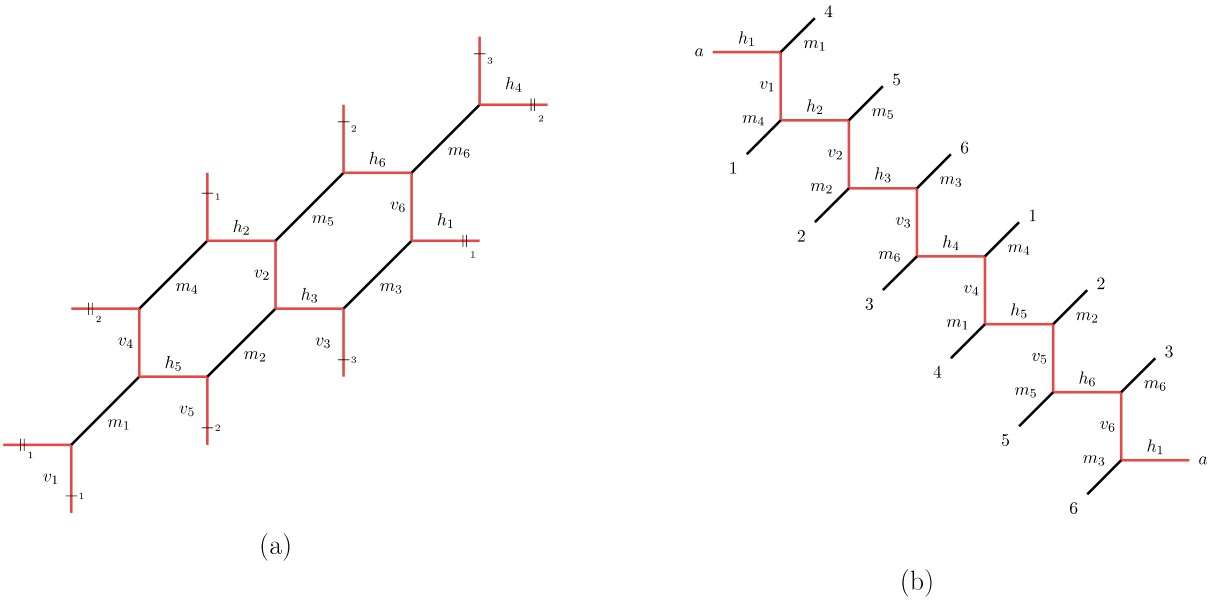

Figure 8: *(a) Web diagram of $X_{3,2}$ where the red line is given as a reference when comparing to Fig. 8 (b). (b) An equivalent representation of the web diagram for $X_{3,2}$ which is more convenient for studying the diagonal preferred direction. In this form we call it shifted web diagram and denote it by $X_{6,1}^{(\delta=3)}$.*

text. We prefer to leave the web in Fig. 8 (b) in this frame to emphasize its relation to Fig. 8 (a).

Now that we have introduced the notion of shifted web diagrams, we describe a kind of geometric transformation, known as flop[25], allowing us to relate different geometries, which in turn will result in relations among the engineered theories. In [33], the authors introduced a useful sequence of flop and $SL(2,\mathbb{Z})$ transformations that cyclically rotates the external legs of a web diagram $X_{N,M}^{(\delta)}$ by $k = \gcd(N,M)$ units. This makes it possible to relate geometries with different shifts δ. A particularly interesting case is when the shift δ is a multiple of the $\gcd(N,M)$ mod N. Then the shifted web $X_{N,M}^{(\delta)}$ can be related to its unshifted counterpart $X_{N,M}$, which makes it plausible that the theories associated with the two geometries are related and thus also the topological string partition functions. The latter will be the main point of investigation in the next section. For now, we first describe the notion of flop in a heuristic way and then explain the aforementioned sequence of flop and $SL(2,\mathbb{Z})$ transformations.

As explained in appendix A, a flop relates different possible resolutions of a singularity. In our case, we have seen in section 3.2.1 that the elliptically fibered Calabi-Yau threefolds $X_{N,M}$ we are considering, are resolutions of singular spaces. In general there are different possibilities of resolving these singularities which result in different smooth spaces. At the level of the toric diagram, different resolutions just correspond to different triangulations of the toric fan (see appendix A). The flop transition can be seen as a continuous process in which the curve that resolves the singularity is shrunk to zero size and then resolved in a different way. As the volumes of the curves are controlled by the Kähler parameters, as described in (3.32), this process describes a path in the Kähler moduli space where we pass through a wall of the Kähler cone

[25]In appendix A, we give an explanation of flops at the level of the toric diagram

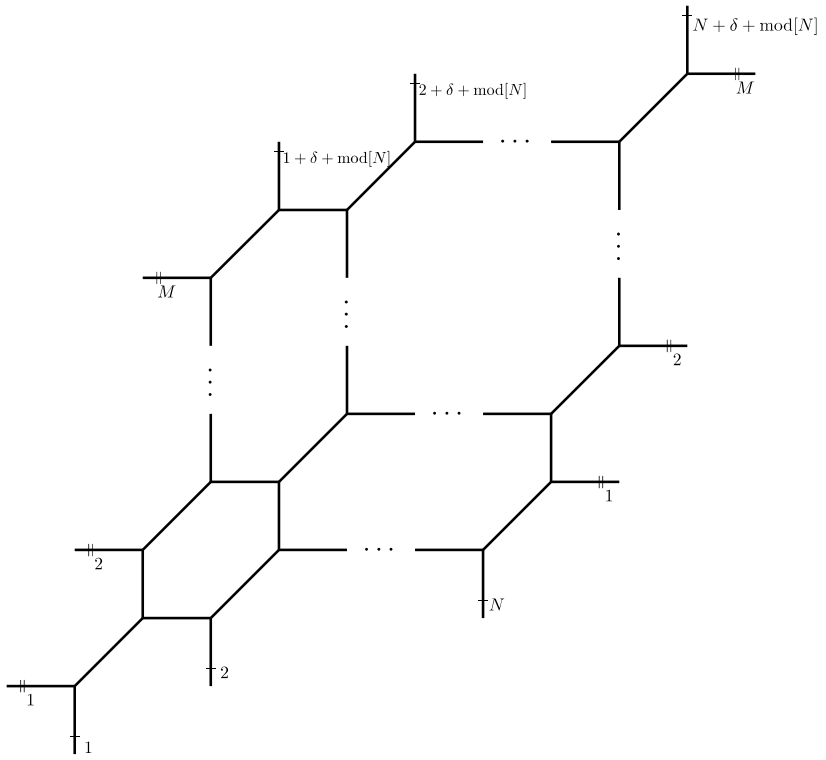

Figure 9: *Shifted toric web diagram of* $X^{(\delta)}_{N,M}$

into an adjacent cone. The wall corresponds exactly to the singular point, where the curve has zero volume, see (3.33). This process is illustrated in Fig. 10. The collection of the different Kähler cones that can be reached through flop transformation is known as the extended moduli space of the Calabi-Yau threefold [139–144]. As flops change in general the geometry of the underlying space, it is natural that the Kähler parameters transform accordingly. This phenomenon is local in the sense that only the Kähler parameters of the adjacent curves that have non-zero intersection with the flopped curve are affected. More concretely, for a local patch of our web diagram, which looks like the space of local $\mathcal{O}(-1)\oplus\mathcal{O}(-1)\to\mathbb{CP}^1$, we have illustrated in Fig. 11 the behavior of the Kähler parameters under flop transformation of the curve labeled by m. This curve corresponds to the base $\mathbb{CP}^1$ in the geometry, as explained in section 3.5.1. The curves adjacent to the flopped curve all pick up the same contribution which is just a positive shift by the Kähler parameter of the flopped curve. In terms of the old Kähler parameters, *i.e.* viewed from the initial cone, the flopped curve now seems to have negative area.

In order to keep things simple, we explain the series of flops and $SL(2,\mathbb{Z})$ transformations that will allow us to shift the external legs, only for the specific case of a periodic strip $X^{(\delta)}_{N,1}$ with some shift δ. This should illustrate the general behavior well enough. An example for $\gcd(N,M)>1$, can be found in [33]. The $SL(2,\mathbb{Z})$ transformations would strictly speaking not be necessary, but they largely simplify the representation in terms of the web diagrams. Indeed, at the level of the toric diagram, flopping a diagonal $(1,1)$ (respectively $(-1,1)$) curve results in replacing it with its orthogonal counterpart $(-1,1)$ (respectively $(1,1)$), thus not introducing

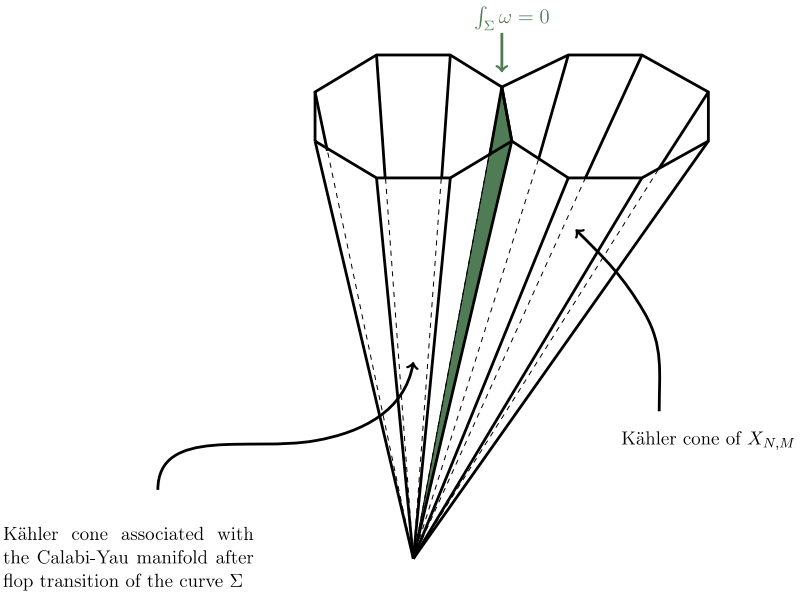

Figure 10: *Kähler cones of two Calabi-Yau manifolds connected through a flop transition of the curve* Σ*.The corresponding wall, along which the cones are glued together, is characterized by* $\int_\Sigma \omega = 0$ *and is shown in green.*

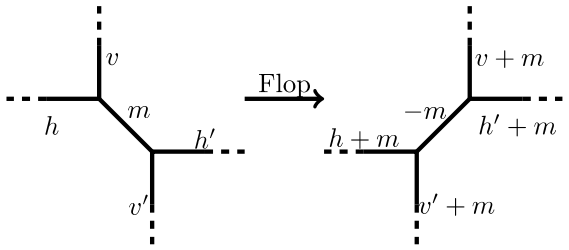

Figure 11: Effect of flop transformation on a patch of the toric diagram which is local $\mathcal{O}(-1) \oplus \mathcal{O}(-1) \to \mathbb{CP}^1$.

lines which have more general slopes, *i.e.* $(p, q) \neq (\pm 1, 1)$. However, flopping a horizontal or vertical curve in a given frame would result in introducing such lines of different slopes[26], which would make the web diagrams distorted and less clear. But the underlying geometry and hence the theories would still be the same. The $SL(2, \mathbb{Z})$ freedom is thus used to go to a frame where the curves we want to flop are represented by diagonal lines.

We show the web diagram for $X^{(\delta)}_{N,1}$ in Fig. 12 with some shift δ and for which we have clearly $\gcd(N, 1) = 1$. The goal is to relate this to the geometry shown in Fig. 14. For this we first use a $SL(2, \mathbb{Z})$ transformation to bring the web diagram into a frame where it is easier to

[26]This can be seen from the toric diagram as shown in Fig. 46 in appendix B by replacing for example a horizontal line with its counterpart such that the diagram is maximally triangulated.

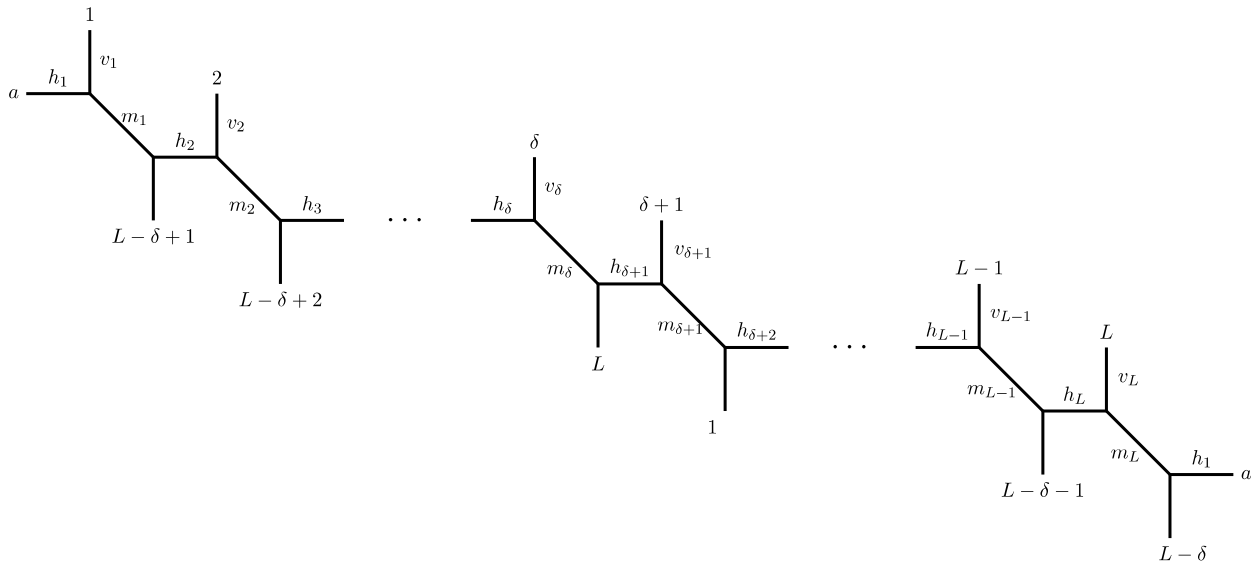

Figure 12: *Shifted strip geometry* $X^{(\delta)}_{N,1}$

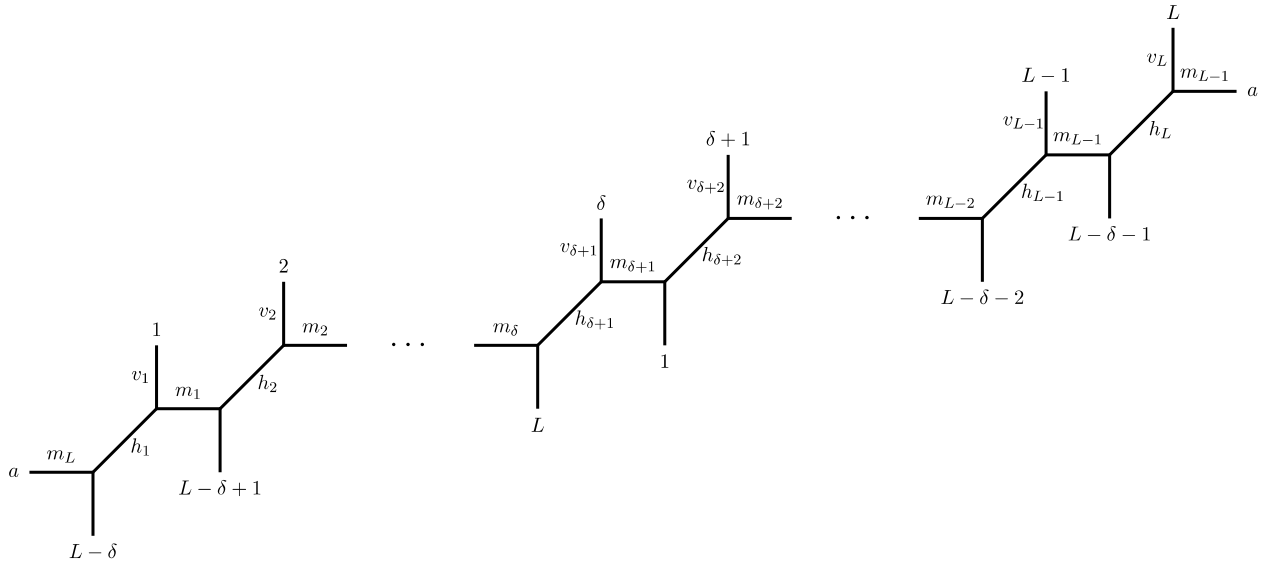

Figure 13: *Web diagram* $X^{(\delta)}_{N,1}$ *from Fig. 12 after appropriate* $SL(2,\mathbb{Z})$ *transformation as well as a cutting along* m_L *and regluing along* h_1.

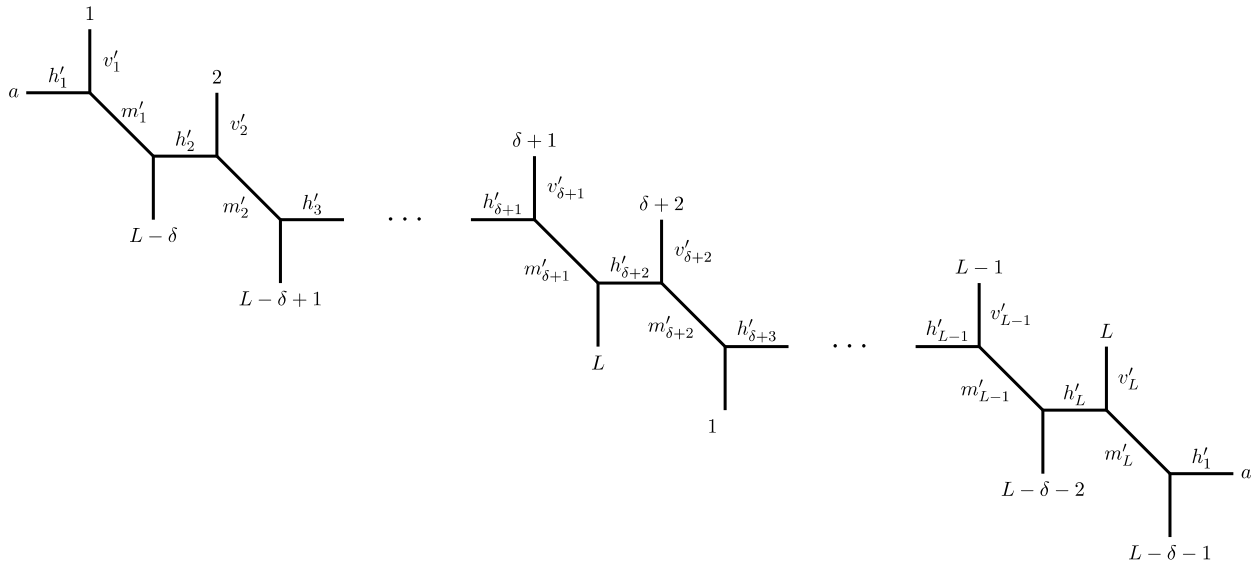

Figure 14: *The web diagram of* $X^{(\delta+1)}_{N,1}$ *obtained from* $X^{(\delta)}_{N,1}$ *in Fig. 12 by performing flop transformations*

visualize the flop transformation. The S-duality transformation associated to the element

$$\begin{pmatrix} 1 & 0 \\ 1 & 1 \end{pmatrix} \in SL(2,\mathbb{Z})\,, \tag{4.1}$$

has the following effect on the (p,q)-branes in Fig. 12

$$\begin{pmatrix} 1 \\ 0 \end{pmatrix} \mapsto \begin{pmatrix} 1 \\ 1 \end{pmatrix} \quad , \quad \begin{pmatrix} 0 \\ 1 \end{pmatrix} \mapsto \begin{pmatrix} 0 \\ 1 \end{pmatrix} \quad , \quad \begin{pmatrix} 1 \\ -1 \end{pmatrix} \mapsto \begin{pmatrix} 1 \\ 0 \end{pmatrix} \tag{4.2}$$

After cutting along the line m_L and regluing along h_1 this gives the web diagram in Fig. 13. We then perform flop transformations on all the diagonal lines with Kähler parameters denoted by h_i. The resulting diagram $X^{(\delta+1)}_{N,M}$ is then indeed Fig. 14, which is parametrized by a new set of Kähler parameters. We can see that it now has shift $\delta+1$. The explicit expression of the latter in terms of the Kähler parameters of the initial setup $X^{(\delta)}_{N,M}$ can be obtained from the local rule explained in Fig. 11. This gives the following map of parameters for $i = 1, \ldots, L$

$$\begin{aligned} h'_i &= h_i + h_{i-1} + m_{i-1} \\ v'_i &= v_i + h_i + h_{i+\delta+1} \\ m'_i &= -h_i \end{aligned} \tag{4.3}$$

where the indices are defined periodically, *e.g.* $h_0 = h_L$. This procedure can be iterated which means that it is possible to relate the web diagram $X^{(\delta)}_{N,1}$ to $X_{N,1}$ by repeating it $L-\delta$ times. The resulting map between the Kähler parameters can then be used to study relation between the instanton partition functions associated to both geometries. In this case, the shift in the external legs increased by one unit at a time according to $\gcd(N,1) = 1$. For an example of this flop sequence when $\gcd(N,M) > 1$, we refer the reader to [33].

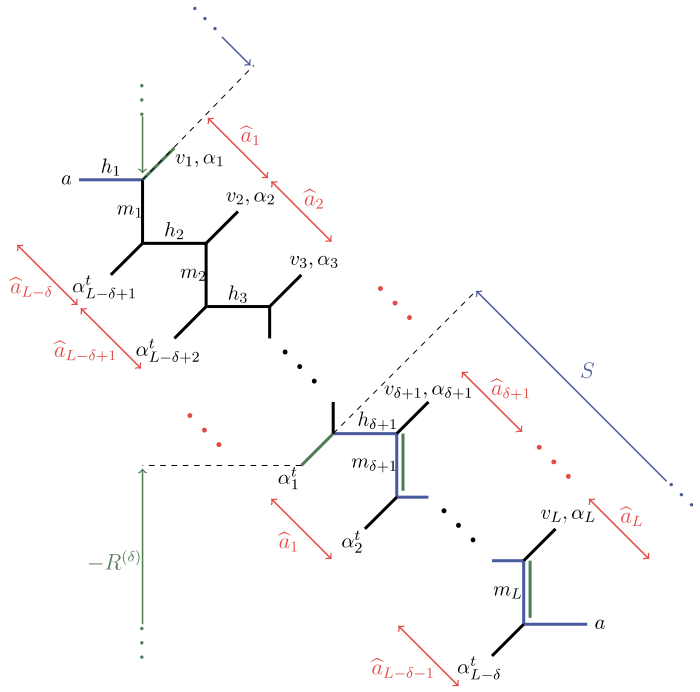

Figure 15: Periodic strip of length L and shift δ with parametrisation suitable for the topological vertex computation.

4.2 Invariance of the partition function

Equipped with the sequence of flop and $SL(2,\mathbb{Z})$ actions introduced in the previous section, we are now ready study how the instanton partition function $\mathcal{Z}_{N,M}$ behaves under these transformations. This calculation was initially performed in [36]. For the sake of simplicity the calculation has been done in the case when the web diagram has the form of a periodic strip of length L as in Fig. 15. For a generic web diagram $X_{N,M}$ the calculation would be similar but more involved.

The partition function for the periodic strip geometry with some shift in the external legs $X^{(\delta)}_{L,1}$ is calculated from the generic building block (3.86) upon suitable gluing of the external legs. Once glued, the $3L$ Kähler parameters associated with the individual curves denoted by $\{h_i, v_i, m_i\}$ are not all independent anymore. They have to satisfy the following $2L-2$ consistency conditions

$$\begin{aligned} v_i + m_i &= v_{i+1} + m_{i+\delta+1}\,, \\ h_{i+1} + m_i &= h_{i+\delta+1} + m_{i+\delta+1}\,, \end{aligned} \tag{4.4}$$

leaving a total of $L+2$ independent parameters. We want to choose a basis in such a way that it can be unambiguously defined for any shift δ and the highest possible number of parameters should be invariant under the flop sequence that we want to study. The remaining parameters should be chosen such that they are easily traceable through flops. From the second line in (4.4), we define

$$\widehat{\alpha}_i = m_i + h_{i+1} = m_{i+\delta+1} + h_{i+\delta+1}\,. \tag{4.5}$$

These L parameters will be the roots of the gauge group and are depicted in red in Fig. 15. They are a natural choice of parameters as they are invariant under the flop transformations that we are interested in, as can be seen by applying the map (4.3),

$$\widehat{\alpha}_i \quad \to \quad \widehat{\alpha}'_i = m'_i + h'_{i+1} = (-h_i) + (h_{i+1} + h_i + m_i) = m_i + h_{i+1} = \widehat{\alpha}_i \,. \tag{4.6}$$

From the $\widehat{\alpha}_i$'s we also define $\rho = \sum_{i=1}^{L} \widehat{\alpha}_i$, which parametrizes the total strip length and will play the role of a modular parameter. Furthermore, we introduce the parameter S, shown as the blue curve in Fig. 15, which measures the distance between identified external legs. There are two ways to measure this distance due to the periodicity of the strip, so this involves making a choice. The two possibilities are simply related at the level of the partition function through ϑ-function identities. Unless stated otherwise we stick to the convention that we go from an upper external leg, indexed by the partition α_i, to the left until we reach its lower counterpart, indexed by α_i^t. As can easily be verified from (4.4), S is the same for any pair of identified legs. In addition, it is well defined for a generic shift which makes it a natural choice for a Kähler parameter. It takes the following form

$$S = h_{i-(L-\delta-1)} + \sum_{r=1}^{L-\delta-1} \widehat{\alpha}_{i-r} \,, \quad i = 1, \ldots, L \tag{4.7}$$

It is also well behaved under flop transformation as can be seen by applying the map (4.3)

$$\begin{aligned} S \quad \to \quad S' =& h'_{i-(L-\delta-1)} + \sum_{r=1}^{L-\delta-1} \widehat{\alpha}_{i-r} = h_{i-(L-\delta)} + \widehat{\alpha}_{i-(L-\delta)} + \sum_{r=1}^{L-\delta-1} \widehat{\alpha}_{i-r} \\ =& h_{i-(L-\delta)} + \sum_{r=1}^{L-\delta} = S \end{aligned} \tag{4.8}$$

where the last equality holds because this is exactly the definition (4.7) of S in the strip obtained after flop with shift $\delta + 1$. By rewriting (4.4), using the parameters $\widehat{\alpha}_i$ and S introduced until now, we get the following recursive relation for v_i

$$v_{i+1} = v_i + \sum_{r=\delta+1}^{L-1} \widehat{\alpha}_{i-r} - \sum_{r=1}^{L-\delta-1} \widehat{\alpha}_{i-r} \tag{4.9}$$

From this we immediately see that only one of these L parameters can be chosen independent. This residual freedom denoted by $R^{(\delta)}$, shown as the green curve in Fig. 15, measures the vertical distance between two identified external legs. Similar to the parameter S, it is the same for every pair of identified legs and can be defined for a generic shift δ. It is expressed as

$$R^{(\delta)} = v_i - \sum_{r=1}^{L-\delta-1} m_{i-r} \,, \quad i = 1, \ldots, L \tag{4.10}$$

With this definition we now have a maximal set of independent Kähler parameters for $X_{L,1}$, given by $(\widehat{\alpha}_i, S, R^{(\delta)})$. In terms of these parameters we can rewrite the first expression in (3.85) as

$$\widehat{Q}^h_{i,j} = \begin{cases} \exp(-S + \sum_{r=j+\delta+1}^{L} \widehat{a}_{i-r}) & \text{if } j + \delta \leq L \\ \exp(-S - \sum_{r=1}^{j+\delta} \widehat{a}_{i-r} & \text{if } j + \delta > L \end{cases} \tag{4.11}$$

For our analysis there is no need to rewrite the other expressions defined in (3.85). Schematically the partition function associated to Fig. 15 has the following form

$$\tilde{\mathcal{Z}}^{(\delta)}_{L,1} = \sum_{\{\alpha\}} \Big(\prod_{i=1}^{L} Q_{v_i}^{|\alpha_i|} \Big) W^{\alpha_1 \dots \alpha_L}_{\alpha_{L-\delta+1} \dots \alpha_{L-\delta}}(\widehat{a}_i, S, \epsilon_1, \epsilon_2) \tag{4.12}$$

We denote the partition function here with a tilde to emphasize that is also contains the perturbative part (see 3.86), whereas we defined in (3.45) only the instanton/non-perturbative part. In order to simplify things, we chose not to introduce the parameter $R^{(\delta)}$ defined in (4.10) but instead to work with the parameters v_i, which are thus not independent of another. We could write (4.12) as a expansion in $R^{(\delta)}$, but this would then leave us with factors of m_i lingering outside of $W^{\alpha_1 \dots \alpha_L}_{\alpha_{L-\delta+1} \dots \alpha_{L-\delta}}$. The definition of $R^{(\delta)}$ will nevertheless be useful in a later section. The building block (3.86) with the external legs identified as in Fig. 15 has the explicit form

$$W^{\alpha_1 \dots \alpha_L}_{\alpha_{L-\delta+1} \dots \alpha_{L-\delta}}(\widehat{a}_i, S, \epsilon_1, \epsilon_2) = W_L(\emptyset) \cdot \Big[\Big(\frac{t}{q} \Big)^{\frac{L-1}{2}} \frac{Q_S^L}{Q_\rho^{L-\delta-1}} \Big]^{|\alpha_1|+\dots+|\alpha_L|} \prod_{i,j=1}^{L} \frac{\vartheta_{\alpha_i \alpha_j}(\widehat{Q}_{i,i-j-\delta}; \rho)}{\vartheta_{\alpha_i \alpha_j}(\overline{Q}_{i,i-j}\sqrt{q/t}; \rho)} \,, \tag{4.13}$$

where $W_L(\emptyset)$ is the perturbative contribution and $Q_S = e^{-S}$ and $Q_\rho = e^{2\pi i \rho}$. We used the identities (D.13) and (D.14) to combine the $\mathcal{J}$-functions into ϑ-functions. Our strategy for proving the invariance of the string partition function under the specific flop transformations in the case $\gcd(N, M) = 1$ is to show that the following equality between the instanton partition functions associated with two periodic strips holds

$$\mathcal{Z}^{(\delta)}_{L,1}(\omega, \epsilon_1, \epsilon_2) = \mathcal{Z}^{(\delta+1)}_{L,1}(\omega', \epsilon_1, \epsilon_2) \,, \tag{4.14}$$

where ω and ω' denote the two collective sets of Kähler parameters associated to the respective geometries. These two sets are related by the duality map (4.3). We want to emphasize that the perturbative part in 4.12 is trivially equal for the two different strips. The perturbative contribution corresponds to a strip where the legs labeled by the v_i (as shown in 15) are not glued and depend only on the trivial partition $\emptyset$. They are thus insensitive to any shift δ. In order to show that (4.14) holds, we first rewrite the building block (4.13) in a way that makes the δ dependence more explicit

$$\begin{aligned} W^{\alpha_1 \dots \alpha_L}_{\alpha_{L-\delta+1} \dots \alpha_{L-\delta}} = W_L(\emptyset) \times \Big[\Big(\frac{t}{q} \Big)^{\frac{L-1}{2}} Q_S^L \overbrace{Q_\rho^{1-K}}^{=C} \Big]^{|\alpha_1|+\dots+|\alpha_L|} \cdot \Big(\prod_{i,j=1}^{L} \frac{1}{\vartheta_{\alpha_i \alpha_j}(\overline{Q}_{i,i-j}\sqrt{q/t}; \rho)} \Big) \\ \times \overbrace{\Big(\prod_{\substack{i \le j \\ j-i<K}} \vartheta_{\alpha_i \alpha_j}(Q_{i,j}^{-1} Q_S) \Big) \Big(\prod_{\substack{i \le j \\ j-i \ge K}} \vartheta_{\alpha_i \alpha_j}(Q_{i,j}^{-1} Q_S Q_\rho) \Big)}^{=A} \\ \times \overbrace{\Big(\prod_{\substack{i > j \\ i-j \le \delta}} \vartheta_{\alpha_i \alpha_j}(Q_{j,i} Q_S) \Big) \Big(\prod_{\substack{i > j \\ i-j > \delta}} \vartheta_{\alpha_i \alpha_j}(Q_{j,i} Q_S Q_\rho^{-1}) \Big)}^{=B} \,, \end{aligned} \tag{4.15}$$

where $K = L - \delta$ and the $Q_{i,j}$ are defined as follows

$$Q_{i,j} = \prod_{k=0}^{j-i-1} \exp(-\widehat{\alpha}_{i+k}) \tag{4.16}$$

The difference between $W^{\alpha_1 \dots \alpha_L}_{\alpha_{L-\delta+1} \dots \alpha_{L-\delta}}$ for the original diagram and $W^{\alpha_1 \dots \alpha_L}_{\alpha_{L-\delta} \dots \alpha_{L-\delta-1}}$ for the diagram obtained by flop and symmetry transformations rests in the three terms A, B and C. Their respective counterparts in the shifted diagram, denoted by A', B' and C', are given by

$$\begin{aligned}
A' &= \left(\prod_{\substack{i \leq j \\ j-i<K'}} \vartheta_{\alpha_i \alpha_j}\left(\frac{Q_S}{Q_{i,j}}\right) \right) \left(\prod_{\substack{i \leq j \\ j-i \geq K'}} \vartheta_{\alpha_i \alpha_j}\left(\frac{Q_S Q_\rho}{Q_{i,j}}\right) \right), \\
B' &= \left(\prod_{\substack{i > j \\ i-j \leq \delta'}} \vartheta_{\alpha_i \alpha_j}(Q_{j,i} Q_S) \right) \left(\prod_{\substack{i > j \\ i-j > \delta'}} \vartheta_{\alpha_i \alpha_j}\left(\frac{Q_{j,i} Q_S}{Q_\rho}\right) \right), \\
C' &= Q_\rho^{1-K'},
\end{aligned} \tag{4.17}$$

where $K' = K - 1$ and $\delta' = \delta + 1$. Indeed the ϑ-functions in the denominator of (4.15) are insensitive to the shift δ. This is easily understood from the fact that their arguments consist of curves that relate upper (lower) external legs to upper (lower) external legs whose relative distances do not depend on δ. The difference between A and A' (respectively, B and B') lies in the arguments of those ϑ-functions for which $j - i = K'$ (resp. $i - j = \delta + 1$): they differ by a factor of Q_ρ. The difference between C and C' is also just a factor of Q_ρ. Finally, we also need to take account of the factors of Q_{v_i} that appear in the full partition function (4.12). In the flopped diagram, these are given by

$$Q_{v_i'} = \begin{cases} Q_{v_i} Q_S^2 & \text{if } \delta' = L \\ \dfrac{Q_{v_i} Q_S^2}{\prod_{r=\delta+2}^{L} Q_{a_{i-r}} \prod_{r=1}^{L-\delta-1} Q_{a_{i-r}}} & \text{else} \end{cases} \tag{4.18}$$

where we defined $Q_{a_i} = \exp(-\widehat{a}_i)$. In order to show that the equality (4.14) holds, we now show that the difference between $\mathcal{Z}^{(\delta)}_{L,1}(\omega, \epsilon_1, \epsilon_2)$ and $\mathcal{Z}^{(\delta+1)}_{L,1}(\omega', \epsilon_1, \epsilon_2)$ can be canceled by applying the shift identity (C.6) to the ϑ-functions mentioned above in (4.17). First, we consider the case when the shift in the external legs is $\delta' = L$. Shifting the required ϑ-functions to regain the ϑ-structure of the $\delta = L - 1$ strip gives

$$\prod_{i=1}^{L} \vartheta_{\alpha_i \alpha_i}(Q_S Q_\rho) = \prod_{i=1}^{L} (Q_S^{-2} Q_\rho^{-1})^{|\alpha_i|} \vartheta_{\alpha_i \alpha_i}(Q_S) \tag{4.19}$$

The prefactors in (4.19) resulting from the shift identity combine with (4.17) and (4.18) to reproduce the expression for $\mathcal{Z}^{(\delta)}_{L,1}(\omega, \epsilon_1, \epsilon_2)$, thus proving that (4.14) holds for $\delta = L - 1$. The computations when $\delta' \neq L$ are more involved, so we will simply sketch them. Below we present the ϑ-functions from $W^{\alpha_1 \dots \alpha_L}_{\alpha_{L-\delta} \dots \alpha_{L-\delta-1}}$ that need to be shifted in order to regain $W^{\alpha_1 \dots \alpha_L}_{\alpha_{L-\delta+1} \dots \alpha_{L-\delta}}$. We need to distinguish different cases depending on the partition α_i in question. For the sake of clarity, we focus only on terms resulting from shifts that come to the power $|\alpha_i|$ in each separate case.

1. For $i \leq \min(K', \delta')$, we shift the following ϑ-functions

$$\begin{aligned}&\vartheta_{\alpha_{i+\delta+1}\alpha_i}(Q_{i,i+\delta+1}Q_S)\vartheta_{\alpha_i\alpha_{i+K'}}\left(\frac{Q_SQ_\rho}{Q_{i,i+K'}}\right)\\ &\sim\ (Q_S^{-2}Q_{i,i+\delta+1}^{-1}Q_{i,i+K'})^{|\alpha_i|}\,\vartheta_{\alpha_{i+\delta+1}\alpha_i}\left(\frac{Q_{i,i+\delta+1}Q_S}{Q_\rho}\right)\vartheta_{\alpha_i\alpha_{i+K'}}\left(\frac{Q_S}{Q_{i,i+K'}}\right)\end{aligned} \tag{4.20}$$

2. For $i > \max(K', \delta')$, we shift the following ϑ-functions

$$\begin{aligned}&\vartheta_{\alpha_i\alpha_{i-\delta-1}}(Q_{i-\delta-1,i}Q_S)\vartheta_{\alpha_{i-K'}\alpha_i}\left(\frac{Q_SQ_\rho}{Q_{i-K',i}}\right)\\ &\sim\ (Q_S^{-2}Q_{i-\delta-1,i}^{-1}Q_{i-K',i})^{|\alpha_i|}\,\vartheta_{\alpha_i\alpha_{i-\delta-1}}\left(\frac{Q_{i-\delta-1,i}Q_S}{Q_\rho}\right)\vartheta_{\alpha_{i-K'}\alpha_i}\left(\frac{Q_S}{Q_{i-K',i}}\right)\end{aligned} \tag{4.21}$$

3. For $\min(K', \delta') < i \leq \max(K', \delta')$, we need to distinguish between two cases:

   (a) When $K' > \delta'$ we shift

$$\begin{aligned}&\vartheta_{\alpha_{i+\delta+1}\alpha_i}(Q_{i,i+\delta+1}Q_S)\vartheta_{\alpha_i\alpha_{i-\delta-1}}\,(Q_SQ_{i-\delta-1,i})\\ &\sim\ (Q_S^{-2}Q_\rho Q_{i-\delta-1,i}^{-1}Q_{i,i+\delta+1}^{-1})^{|\alpha_i|}\,\vartheta_{\alpha_{i+\delta+1}\alpha_i}\left(\frac{Q_{i,i+\delta+1}Q_S}{Q_\rho}\right)\vartheta_{\alpha_i\alpha_{i-\delta-1}}\left(\frac{Q_SQ_{i-\delta-1,i}}{Q_\rho}\right)\end{aligned} \tag{4.22}$$

   (b) For $K' < \delta'$, we shift

$$\begin{aligned}&\vartheta_{\alpha_i\alpha_{i+K'}}\left(\frac{Q_SQ_\rho}{Q_{i,i+K'}}\right)\vartheta_{\alpha_{i-K'}\alpha_i}\left(\frac{Q_SQ_\rho}{Q_{i-K',i}}\right)\\ &\sim\ (Q_S^{-2}Q_\rho^{-1}Q_{i-K',i}Q_{i,i+K'})^{|\alpha_i|}\,\vartheta_{\alpha_i\alpha_{i+K'}}\left(\frac{Q_S}{Q_{i,i+K'}}\right)\vartheta_{\alpha_{i-K'}\alpha_i}\left(\frac{Q_S}{Q_{i-K',i}}\right)\end{aligned} \tag{4.23}$$

In each case, the factors resulting from shifting the ϑ-functions combine with (4.17) and (4.18) to reproduce the expression for the partition function $\mathcal{Z}_{L,1}^{(\delta)}$. This shows that (4.14) holds. As this procedure can be iterated we have the general relation

$$\mathcal{Z}_{L,1}^{(\delta)}(\omega', \epsilon_1, \epsilon_2) = \mathcal{Z}_{L,1}(\omega, \epsilon_1, \epsilon_2) \tag{4.24}$$

where the two sets of Kähler parameters ω and ω' are related by successive application of the map (4.3), *i.e.* they are just related by linear transformations. For an explicit example of a calculation relating $\mathcal{Z}_{6,1}^{(3)}$ and $\mathcal{Z}_{6,1}$ see [36]. Whereas the calculation above has only been performed explicitly for the case $\gcd(N, M) = 1$, we conjecture that the results holds true in general

$$\mathcal{Z}_{N,M}^{(\delta)}(\omega', \epsilon_1, \epsilon_2) = \mathcal{Z}_{N,M}(\omega, \epsilon_1, \epsilon_2)\,, \tag{4.25}$$

when δ is a multiple of $\gcd(N, M)$ mod N. We recall that the latter condition is to ensure that the underlying web diagrams can indeed be related by flop. Apart from the computational complexity there is no apparent obstruction to reproducing the calculation outlined above. In

the next section we will see further arguments that underline the plausibility of the conjecture. Furthermore, as already mentioned at the beginning of this section, the authors in [48] prove the case for general N and M in a specific limit of the omega background.

An important aspect of flop transformations from the point of view of gauge theory is that, when we perform a flop on a curve that is related to the gauge coupling constant in a specific expansion of the partition function, the underlying theory gets sent through a strong coupling regime, recall relation (3.20). This means that in the adjacent Kähler cone, it should not be expected that a gauge theory associated with that specific expansion should exist, or if it does it will in general not have the same gauge group, matter content, etc. The latter should rather be seen as a strong coupling dual [145]. In the strong coupling region the full little string theory description is required. When performing the sequence of flops a number of times, the flops act alternately on two of the three sets (horizontal, vertical and diagonal) of lines in the web diagram. For example, in order to relate $X^{(\delta)}_{N,1}$ as in Fig. 15 to $X_{N,M}$, the vertical external lines never undergo flop transformation. Hence there is always an expansion whose "coupling curves" do not undergo flops. The associated theory can be safely followed through the Kähler moduli space.

We also want to emphasize that while the two topological string partition functions associated to web diagrams related by flop transitions can take the same form when written in an appropriate basis of parameters, the relation between the latter and the $3NM$ Kähler parameters describing the individual curves in the geometry is generically different. For example, the parameter Q_S defined in (4.7), which runs between pairs of identified external legs of a given $X^{(\delta)}_{N,M}$, is clearly independent of δ as can be seen by applying the duality map to the explicit expression. However, the way it depends on the Kähler parameters of individual curves is different, *e.g.* for $\delta = 0$ it depends on a single curve, for $\delta = 1$ it depends on three individual curves etc. Nevertheless, when viewed as an instanton partition function of a gauge theory these differences are not directly visible. This will be investigated further in section 5. For now, we want to provide more evidence that the diagonal expansion can really be interpreted as having a third gauge theory description associated with it.

4.3 Triality

The topological string partition function (3.45) associated to $X_{N,M}$ can be expanded in three different ways, one for each direction which is common to every vertex in the web diagram shown in Fig. 2. Schematically we thus have

$$\mathcal{Z}_{N,M}(\mathbf{h},\mathbf{v},\mathbf{m},\epsilon_1,\epsilon_2) = Z^{(N,M)}_{\text{hor}} = Z^{(N,M)}_{\text{vert}} = Z^{(N,M)}_{\text{diag}}\,, \tag{4.26}$$

where **h**,**v** and **m**, denote the collective sets of individual Kähler parameters h_i, v_i and m_i respectively. The horizontal and vertical expansions are known to correspond to instanton partition function of two supersymmetric gauge theories that are related by duality. The diagonal expansion $Z^{N,M}_{\text{diag}}$ for a given $X_{N,M}$ can be associated to a web diagram which has a non-trivial shift δ. This was illustrated for example in Fig. 23, where the diagonal expansion of $X_{3,2}$ can be reinterpreted as the vertical expansion in the equivalent representation $X^{(3)}_{6,1}$[27]. In the previous

[27]By convention, we should strictly speaking first perform a $SL(2,\mathbb{Z})$ transformation to turn diagonal legs into vertical ones and vice versa

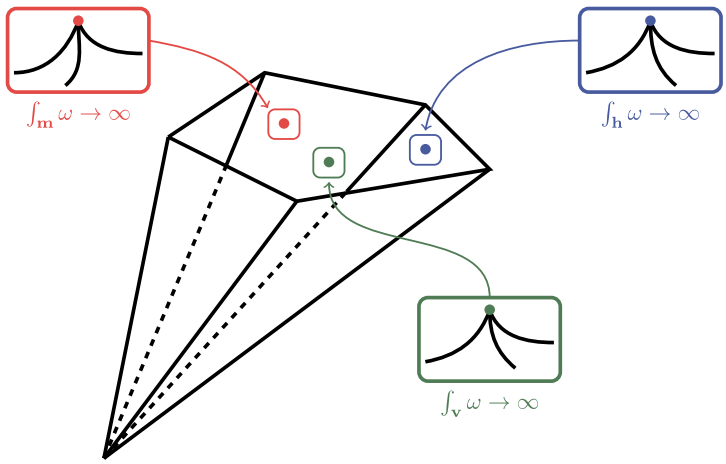

Figure 16: *Different regions in the Kähler cone of* $X_{N,M}$.

section we reviewed the result from [36], that the topological string partition function is invariant under flop transformation. A direct consequence of this result is the expression for the diagonal expansion $Z^{N,M}_{\text{diag}}$ is equal to the instanton partition function corresponding to a theory with gauge group $U[\frac{NM}{k}]^k$. However, as pointed out, the relation between the gauge theory parameters, *i.e.* coupling constants, Coulomb branch and mass parameters, and the Kähler parameters of the individual curves in the geometry is different. Thus, even if the functional expressions match, it should be verified that there exists indeed a region in the Kähler cone of $X_{N,M}$ where the weak coupling limit of the diagonal theory is realized, *i.e.* that there exists a parameter limit where the curves in the web diagram related to the coupling constants of the diagonal theory get send to infinity in a consistent way. By this we mean that there are no lines that start crossing or other inconsistencies. The existence of such a limit would provide a non-trivial check that the diagonal expansion can indeed be interpreted as a third instanton partition function associated to $X_{N,M}$. In [37], three maximal sets of $NM+2$ independent parameters were given for a generic $X_{N,M}$, one for each expansion in (4.26). With these, it was explicitly checked that the Kähler cone of $X_{N,M}$ admits three regions associated with the weak coupling regime of the horizontal, vertical and diagonal expansions of the topological string partition function respectively, providing strong evidence that there are indeed three different theories engineered by $X_{N,M}$. These theories are dual to one another as their instanton partition functions are different expansion of the same function. The presence of these three theories in a single $X_{N,M}$ was dubbed *Triality* in [37].

As remarked above, one of the key aspects of interpreting $Z^{(N,M)}_{\text{hor}}$, $Z^{(N,M)}_{\text{vert}}$ or $Z^{(N,M)}_{\text{diag}}$ in (4.26) as instanton gauge theory partition functions, is to find a region in the Kähler moduli space of $X_{N,M}$ in which either all $\mathbf{h}$ or all $\mathbf{v}$ or all $\mathbf{m}$ become infinitely large, while the remaining parameters remain finite. In order to find such a region in the moduli space, we require a particular basis for the Kähler parameters, which provides a solution for the consistency conditions discussed in section 3.4.1. While such a basis is very involved for generic $X_{N,M}$, we first consider as a simple example the configuration $X_{2,2}$ (with $k = \gcd(N,M) = 2$), to illustrate the point. Thereafter we describe the general case.

4.3.1 The specific example of $X_{2,2}$

In this case, three different parametrisations (suitable for the horizontal, vertical and diagonal gauge theory) along with a graphical interpretation of the weak coupling limit are shown in Table 4. The three different expansions (and in particular the weak coupling limit) can be interpreted as follows:

- horizontal expansion in the basis $(\rho, \widehat{b}_1; \widehat{c}_1, \widehat{c}_2, \tau; E)$

  Upon taking the limit

  $$\rho - \widehat{b}_1 \longrightarrow \infty\,, \qquad \text{and} \qquad \widehat{b}_1 \longrightarrow \infty\,, \tag{4.27}$$

  all horizontal lines of the toric diagram are effectively cut, since $h_{1,\ldots,4} \longrightarrow \infty$, while $v_{1,\ldots,4}$ and $m_{1,\ldots,4}$ remain finite.[28] The remaining diagram takes the form of two vertical strips, thus implying that the gauge group associated with the horizontal expansion is

  $$G_{\text{hor}} = U(2) \times U(2)\,. \tag{4.28}$$

  Indeed, $\rho - \widehat{b}_1$ and $\widehat{b}_1$ are related to the gauge couplings associated with each of the two $U(2)$ factors, while the parameters $\widehat{c}_{1,2}$ can be interpreted as the (simple, positive) roots of each of the two $\mathfrak{a}_1$ algebras related to the two $U(2)$ factors. Furthermore, τ can be interpreted as an additional root, that extends each of these algebras to affine $\widehat{\mathfrak{a}}_1$, while E is a parameter associated with the compactification of the toric web on a torus.

- vertical expansion in the basis $(\tau, \widehat{c}_1; \widehat{b}_1, \widehat{b}_2; \rho, D)$

  In the limit

  $$\tau - \widehat{c}_1 \longrightarrow \infty\,, \qquad \text{and} \qquad \widehat{c}_1 \longrightarrow \infty\,, \tag{4.29}$$

  all vertical lines of the toric diagram are cut, since $v_{1,\ldots,4} \longrightarrow \infty$, while $h_{1,\ldots,4}$ and $m_{1,\ldots,4}$ remain finite (and positive for certain values of $(\rho, \widehat{b}_1, \widehat{b}_2, D)$). In this way, the diagram decomposes into two horizontal strips, which implies that the gauge group associated with the vertical expansion is in fact

  $$G_{\text{vert}} = U(2) \times U(2)\,. \tag{4.30}$$

  Indeed, $\tau - \widehat{c}_1$ and $\widehat{c}_1$ can be related to the gauge couplings associated with each of the two $U(2)$ factors, and the parameters $\widehat{b}_{1,2}$ can be interpreted as the (simple, positive) roots of each of the two $\mathfrak{a}_1$ algebras related to the two $U(2)$ factors. The parameter, τ can be interpreted as an additional root, that extends each of these algebras to affine $\widehat{\mathfrak{a}}_1$, while D is a parameter associated with the compactification of the toric web on a torus.

- diagonal expansion in the basis $(V_1, V_2; \widehat{a}_1, \widehat{a}_2; F, L)$

[28] Notice in particular that there exists a region in the parameter space of $(\tau, \widehat{c}_1, \widehat{c}_2, E)$ in which $(v_1, v_2, v_3, v_4, m_1, m_2, m_3, m_4)$ are positive, which is important for their interpretation from the point of view of gauge theory as Coulomb branch parameters and hypermultiplet masses respectively.

horizontal	vertical	diagonal
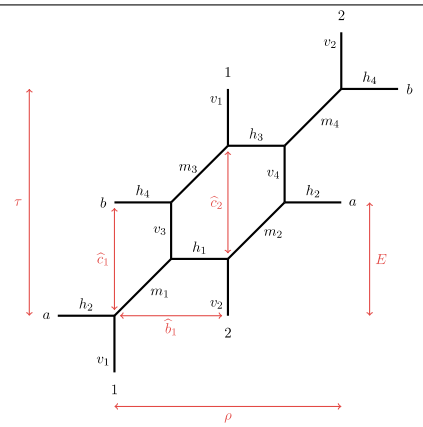	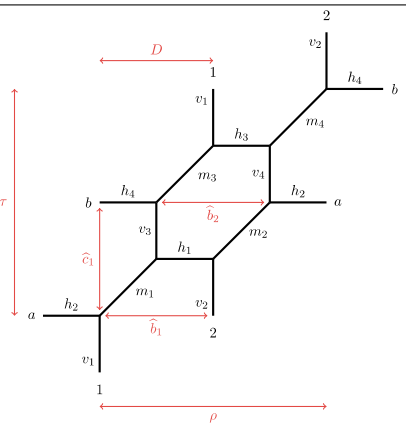	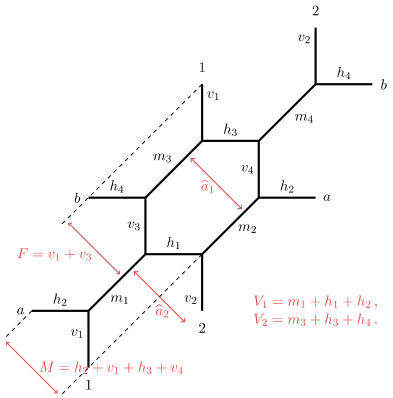
$h_1 = h_3 = \widehat{b}_1 - \frac{\widehat{c}_1 - \widehat{c}_2 + E}{2}\,,$ $h_2 = h_4 = \rho - \widehat{b}_1 + \frac{\widehat{c}_1 - \widehat{c}_2 - E}{2},$ $v_1 = v_2 = \tau - \frac{\widehat{c}_1 + \widehat{c}_2 + E}{2}\,,$ $v_3 = v_4 = \frac{\widehat{c}_1 + \widehat{c}_2 - E}{2}\,,$ $m_1 = m_4 = \frac{\widehat{c}_1 - \widehat{c}_2 + E}{2}\,,$ $m_2 = m_3 = -\frac{\widehat{c}_1 - \widehat{c}_2 - E}{2}\,,$	$h_1 = h_3 = \frac{\widehat{b}_1 + \widehat{b}_2 - D}{2}\,,$ $h_2 = h_4 = \rho - \frac{\widehat{b}_1 + \widehat{b}_2 + D}{2}\,,$ $v_1 = v_2 = \tau - \widehat{c}_1 + \frac{\widehat{b}_1 - \widehat{b}_2 - D}{2},$ $v_3 = v_4 = \widehat{c}_1 - \frac{\widehat{b}_1 - \widehat{b}_2 + D}{2}\,,$ $m_1 = m_4 = \frac{\widehat{b}_1 - \widehat{b}_2 + D}{2}\,,$ $m_2 = m_3 = -\frac{\widehat{b}_1 - \widehat{b}_2 - D}{2}\,,$	$h_1 = h_3 = \frac{\widehat{a}_1 + \widehat{a}_2 - F}{2}\,,$ $h_2 = h_4 = M - \frac{\widehat{a}_1 + \widehat{a}_2 + F}{2}\,,$ $v_1 = v_2 = -\frac{\widehat{a}_1 - \widehat{a}_2 - F}{2}\,,$ $v_3 = v_4 = \frac{\widehat{a}_1 - \widehat{a}_2 + F}{2}\,,$ $m_1 = m_4 = V_1 + F - M\,,$ $m_2 = m_3 = V_2 + F - M\,,$
$\rho - \widehat{b}_1 \longrightarrow \infty$ $\widehat{b}_1 \longrightarrow \infty$	$\tau - \widehat{c}_1 \longrightarrow \infty$ $\widehat{c}_1 \longrightarrow \infty$	$V_{1,2} \longrightarrow \infty$
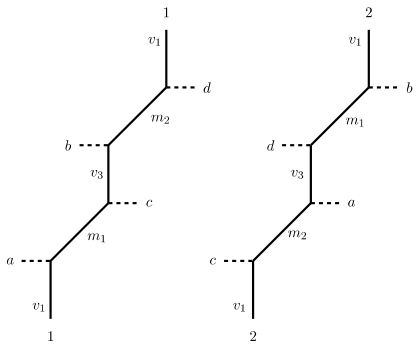	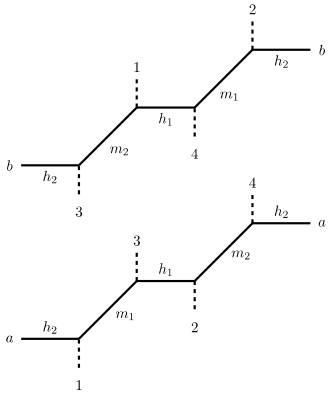	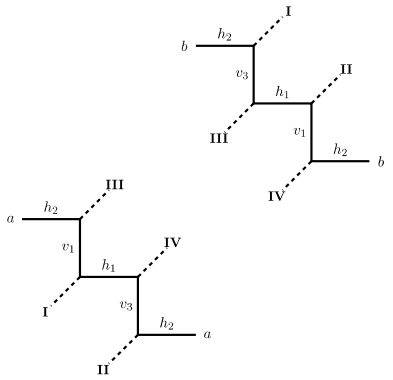

Table 4: *Three different choices of maximal sets of independent Kähler parameters for the configuration $X_{2,2}$. In each case, the 12 lines $(h_{1,\dots,4}, v_{1,\dots,4}, m_{1,\dots 4})$ are parametrised by 6 independent variables. The last row shows the weak coupling limit, which is obtained by sending two of the parameters (related to the coupling constants of the respective gauge theories) to infinity.*

In the limit $V_{1,2} \longrightarrow \infty$, all diagonal lines (along direction $(1,1)$) of the toric diagram are cut, since $m_{1,\ldots,4} \longrightarrow \infty$, while $h_{1,\ldots,4}$ and $v_{1,\ldots,4}$ remain finite (and positive for certain values). In this way, the diagram decomposes into two diagonal strips (which were called 'staircase strips' in [36]), which implies that the gauge group associated with the vertical expansion is as well

$$G_{\text{diag}} = U(2) \times U(2)\,. \tag{4.31}$$

Indeed, $V_{1,2}$ can be related to the gauge couplings associated with each of the two $U(2)$ factors, and the parameters $\widehat{a}_{1,2}$ can be interpreted as the (simple, positive) roots of each of the two $\mathfrak{a}_1$ algebras related to the two $U(2)$ factors. The parameter, L can be interpreted as an additional root, that extends each of these algebras to affine $\widehat{\mathfrak{a}}_1$, while F is a parameter associated with the compactification of the toric web on a torus.

Calculating the geometric intersection numbers between the curves and the compact divisors for the $X_{2,2}$ geometry and checking that the charges indeed furnish the right representations under the diagonal gauge group (as discussed below 3.34) would provide further evidence. However, in this case this is not necessary as the diagonal strips are geometrically identical to the horizontal and vertical ones. Thus we know in advance that the calculation works out the right way. It is important to notice that in all three cases, the connection to a certain gauge theory relies on the fact that in the weak coupling limit the web diagram decomposes into a number of *parallel* strips (either horizontally, vertically or diagonally): physically, the latter can be interpreted as parallel $NS5$ branes with semi-infinite D5-branes ending on either side in equal numbers [69]. When the strips are glued together the world-volume theory on these D5-branes is the corresponding gauge theory. This can be seen by tracing the original setup of $NS5$ branes probing a transverse orbifold singularity through the duality chain. In the current case, since the orientation of the strips can be changed through an $SL(2,\mathbb{Z})$ transformation, the diagrams in the last line of table 4 are identical up to a relabeling of the parameters. This indicates that the gauge theories engineered from the three expansions in (4.26) have the same gauge group, *i.e.*

$$G_{\text{hor}} = G_{\text{vert}} = G_{\text{diag}} = U(2) \times U(2)\,. \tag{4.32}$$

This is a peculiarity of the configuration $(N,M) = (2,2)$ (more precisely of all configurations of the form (N,N)) as in general the three gauge groups are different (albeit that their rank is the same as argued above), as we shall see from the next example $(N,M) = (3,2)$.

4.3.2 The specific example of $X_{3,2}$

The next non-trivial configuration corresponds to $(N,M) = (3,2)$ with $k = \gcd(3,2) = 1$. The corresponding web diagram contains 18 line segments which are the Kähler parameters of various rational curves in the Calabi-Yau threefold $X_{3,2}$:

$$\mathbf{h} = (h_1, \cdots, h_6)\,, \qquad \mathbf{v} = (v_1, \cdots, v_6)\,, \qquad \mathbf{m} = (m_1, \cdots, m_6)\,. \tag{4.33}$$

As discussed before, these parameters are not linearly independent but they can be parametrised by choosing 8 independent variables. Three different such parametrisations are shown in Table 5, leading to the following expansions:

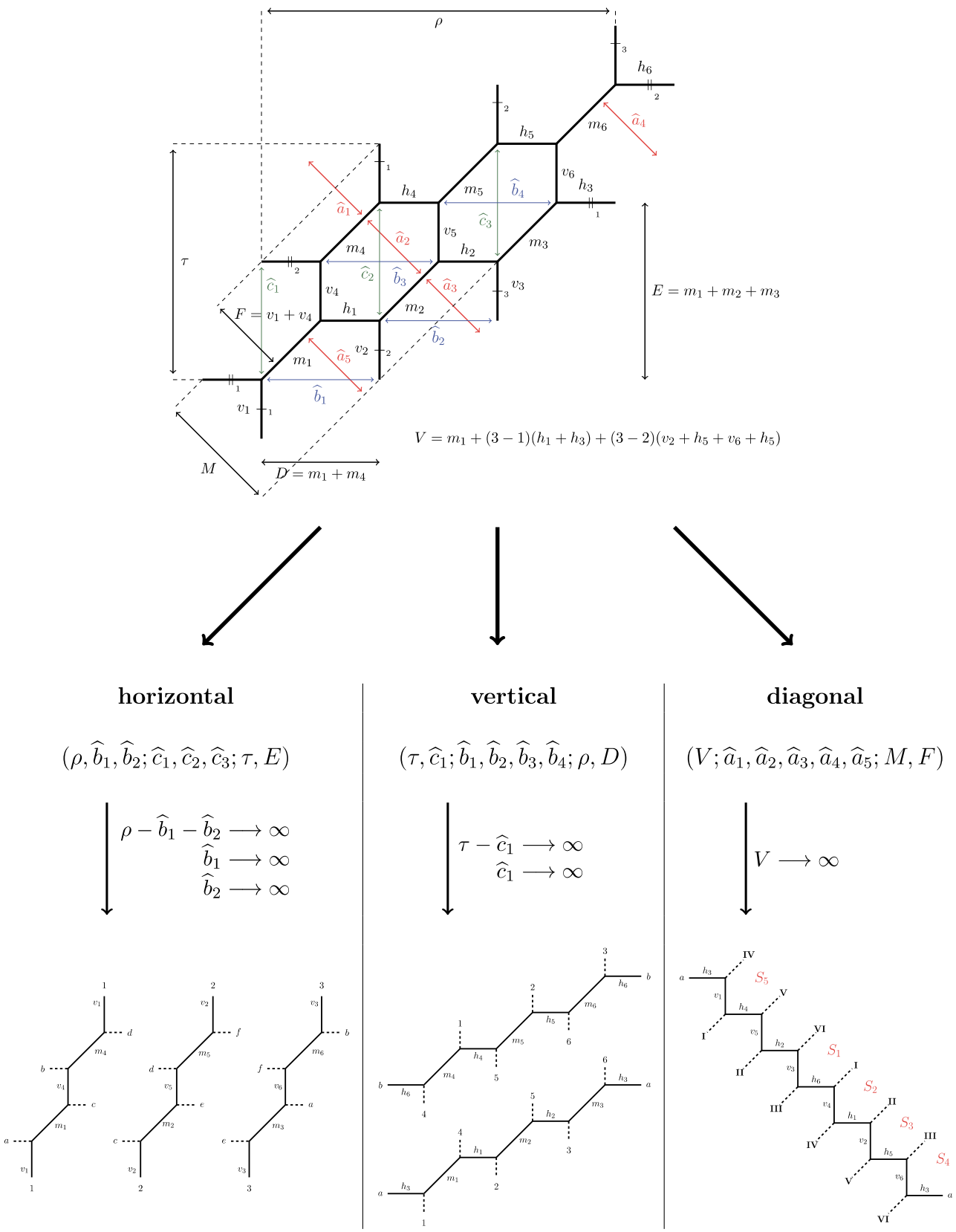

Table 5: *Three different parametrisations of the web diagram* $(N, M) = (3, 2)$*. The last line shows the decomposition of the diagram in the weak coupling limit in the horizontal, vertical and diagonal description respectively. A choice of gauge divisors for the diagonal description is highlighted in red.*

- horizontal expansion in the basis $(\rho, \widehat{b}_1, \widehat{b}_2; \widehat{c}_1, \widehat{c}_2, \widehat{c}_3; \tau, E)$

  In the limit

  $$\rho - \widehat{b}_1 - \widehat{b}_2 \longrightarrow \infty\,, \qquad \text{and} \qquad \widehat{b}_1 \longrightarrow \infty\,, \qquad \widehat{b}_2 \longrightarrow \infty\,, \tag{4.34}$$

  we find $h_{1,\dots,6} \longrightarrow \infty$, while $v_{1,\dots,6}$ and $m_{1,\dots,6}$ remain finite. Therefore, as indicated in Table 5, in the limit (4.34) the toric web diagram decomposes into 3 vertical strips, implying that the horizontal expansion gives rise to a gauge theory with gauge group

  $$G_{\text{hor}} = U(2) \times U(2) \times U(2)\,, \tag{4.35}$$

  More specifically, the parameters $(\rho - \widehat{b}_1 - \widehat{b}_2, \widehat{b}_1, \widehat{b}_2)$ are related to the gauge coupling constants, while $\widehat{c}_1$, $\widehat{c}_2$ and $\widehat{c}_3$ can be interpreted as the (simple positive) roots of $\mathfrak{a}_1$ algebras associated with each of the $U(2)$ factors. Each of these algebras is further extended to affine $\widehat{\mathfrak{a}}_1$ through the parameter τ.

- vertical expansion in the basis $(\tau, \widehat{c}_1; \widehat{b}_1, \widehat{b}_2, \widehat{b}_3, \widehat{b}_4; \rho, D)$

  In the limit

  $$\tau - \widehat{c}_1 \longrightarrow \infty\,, \qquad \widehat{c}_2 \longrightarrow \infty\,, \tag{4.36}$$

  we find $v_{1,\dots,6} \longrightarrow \infty$, while $h_{1,\dots,6}$ and $m_{1,\dots,6}$ remain finite. Therefore, the $(3,2)$ web diagram decomposes into two horizontal strips, indicating that the vertical expansion is associated with a gauge theory with gauge group

  $$G_{\text{vert}} = U(3) \times U(3)\,, \tag{4.37}$$

  In this manner, $(\tau - \widehat{c}_1, \widehat{c}_1)$ are related to the coupling constants and $(\widehat{b}_1, \widehat{b}_2)$ and $(\widehat{b}_3, \widehat{b}_4)$ correspond to the (simple positive) roots of two copies of $\mathfrak{a}_2$, associated with the to the $U(3)$ factors in (4.37). These algebras are extended to affine $\widehat{\mathfrak{a}}_2$ by the parameter ρ.

- diagonal expansion in the basis $(V; \widehat{a}_1, \widehat{a}_2, \widehat{a}_3, \widehat{a}_4, \widehat{a}_5; M, F)$

  In the limit $V \longrightarrow \infty$ we find $m_{1,\dots,6} \longrightarrow \infty$, while $h_{1,\dots,6}$ and $v_{1,\dots,6}$ remain finite, such that the web diagram decomposes into a single diagonal strip. This indicates that the diagonal expansion is associated with a gauge theory with gauge group

  $$G_{\text{diag}} = U(6)\,. \tag{4.38}$$

  Here V is related to the coupling constant, while $(\widehat{a}_1, \dots, \widehat{a}_5)$ play the role of the (simple positive) roots of $\mathfrak{a}_5$ associated with G_{diag}.

  The fact that such a gauge theory exists also outside of the weak coupling limit $V \to \infty$ can be inferred from the duality of the web diagram shown in table 5 with the toric web of $X_{6,1}$ through a series of flop- and symmetry transformations. More concretely the result (4.25) implies

  $$Z^{(6,1)}_{\text{vert}}(V, h'_{1,\dots,6}, m) = Z^{(3,2)}_{\text{diag}}(V, \widehat{a}_{1,\dots,5}, M, F)\,, \tag{4.39}$$

The vertical expansion of the partition function $\mathcal{Z}_{6,1}$ is a power series in $Q_V = e^{-V}$, which can be interpreted as the instanton partition function $Z^{(6,1)}_{\text{vert}}$ of a gauge theory with gauge group $U(6)$. In the gauge theory interpretation it is important that the flop transformations do not act on curves directly related to the coupling constants of a given gauge theory. This would send the volume associated to these curves to 0 and hence the gauge theory through a strong coupling regime making it less clear what to expect on the other side once the given curves are resolved again. Fortunately, when establishing the correspondence (4.39) no curves directly related to the gauge coupling undergo flops. This shows that $Z^{(3,2)}_{\text{diag}}$ (as a power series expansion in Q_V) can be read as the instanton partition function of a gauge theory with gauge group $U(6)$ also outside of the region $V \to \infty$.

Verifying that the geometric intersection numbers between the curves and compact divisors for the geometry $X_{3,2}$ can be assigned in a consistent way for the diagonal expansion (as discussed below 3.34) provides us with an additional non-trivial check. In contrast to the previous example of $X_{2,2}$, the diagonal strip geometry in the case at hand is different from the horizontal and vertical ones. In appendix B, we describe a way to calculate the intersection numbers for a general shifted strip geometry. We indicate our choice of gauge divisors in the diagonal strip of table 5. First we can check that the diagonal roots $\widehat{\alpha}_i$ have indeed the right weights an thus form the adjoint representation of $\mathfrak{a}_5$. We find the following weight assignment

$$\begin{aligned} &\widehat{\alpha}_1 = [2,-1,0,0,0] && \widehat{\alpha}_2 = [-1,2,-1,0,0] && \widehat{\alpha}_3 = [0,-1,2,-1,0] \\ &\widehat{\alpha}_4 = [0,0,-1,2,-1] && \widehat{\alpha}_5 = [0,0,0,-1,2] \end{aligned} \tag{4.40}$$

which is thus the correct one for all the simple roots of $\mathfrak{a}_5$. The other weights of the adjoint representation are simply obtained by taking suitable linear combinations of the simple roots. Furthermore we verify that the curves associated with the coupling constant are uncharged under the gauge group. The suggested combination[29] of curves for the coupling constant given in table 5 is

$$V = m_1 + 2(h_1 + h_3) + \widehat{\alpha}_3 + \widehat{\alpha}_0\,. \tag{4.41}$$

where we introduced the affine root $\widehat{\alpha}_0 = h_5 + v_6$ to make things more compact. By calculating the intersection of these curve with the divisors chosen for the diagonal theory we get

$$\begin{aligned} &m_1 = [-1,-1,0,1,1] \quad , \quad h_1 = [0,1,-1,-1,1] \quad , \quad h_3 = [1,0,0,1,-1] \\ &\widehat{\alpha}_0 = [-1,0,0,0,-1] \end{aligned} \tag{4.42}$$

We thus see that the combination (4.41) indeed has vanishing intersection with all the gauge divisors and is uncharged under the gauge group. Finally, it can also be checked that the horizontal and vertical curves together with their combinations give all the weights required for the adjoint representation plus a singlet.

In the case of $(N, M) = (3, 2)$, the gauge groups G_{hor}, G_{vert} and G_{diag} are different, however, as discussed in the previous section, their rank is identical. Furthermore, we stress that

[29] This combination is obtained by following the coupling for the $U(6)$ theory in $X_{6,1}$ through the flop transitions. The formula for this was originally written down in [33] and is reviewed at at later point in this section.

in all three cases the specific form of the parametrisation is not unique: Different choices of parameters leading to the same decomposition of the toric web diagram as in table 5 are possible. Indeed, in section 4.2, which is based on [36], a slightly different choice of parametrization was made as it was more suitable for the explicit computations of the general building block of the partition function.

4.3.3 The general configuration $X_{N,M}$

The discussion of the previous examples $(2,2)$ and $(3,2)$ can be generalized to a web diagram with generic (N,M). Indeed, in the following we make a proposal for three different parametrisations of the Kähler moduli space of $X_{N,M}$, facilitating the three expansions of $\mathcal{Z}_{N,M}$ that were schematically written in (4.26). In the following, we present sets – in general not unique – of $NM+2$ independent parameters (which we shall refer to as a basis in the following) suitable for the description of the horizontal, vertical and diagonal theory.[30]

The geometric interpretation of (some of) the parameters in the bases is shown in Fig. 17. The orange box in Fig. 17 highlights a generic hexagon in the (N,M) web-diagram, which can be labeled by two integers

$$r \in \{0,1\ldots,M-1\} \text{ mod } M\,, \qquad \text{and} \qquad s \in \{1,\ldots,N\} \text{ mod } N\,. \tag{4.43}$$

With the parameters shown in Fig. 17, we propose the following three (inequivalent) bases

- horizontal basis

  We propose as a basis suitable for the description of the horizontal expansion $Z_{\text{hor}}^{(N,M)}$ in (4.26) the following

  $$\mathfrak{B}_{\text{hor}} = \left\{\widehat{b}_{M-1,s=1,\ldots,N-1}\,,\rho\,,\{\widehat{c}\}_{u=1,\ldots,N}\,,\tau\,,E\right\}\,, \tag{4.44}$$

  with

  $$\{\widehat{c}\}_u = \{\widehat{c}_{r,u}|r\in\{0,1,\ldots,M-2\}\}\,, \qquad \forall u=1,\ldots,N\,. \tag{4.45}$$

  This basis indeed suggests that $Z_{\text{hor}}^{(N,M)}$ is the instanton partition function of gauge theory with gauge group $G_{\text{hor}}=[U(M)]^N$: indeed $\{c\}_{u=1,\ldots,N}$ furnish N sets of (simple positive) roots for the N factors of $U(M)$, while the N decoupling parameters,

  $$\left\{\widehat{b}_{M-1,1},\widehat{b}_{M-1,2},\ldots,\widehat{b}_{M-1,N-1}\,,\rho-\sum_{i=1}^{N-1}\widehat{b}_{M-1i}\right\} \tag{4.46}$$

  are related with the gauge coupling constants (one associated with every factor of $U(M)$ in G_{hor}), in the sense that in the limit

  $$\rho-\sum_{i=1}^{N-1}\widehat{b}_{M-1,i}\longrightarrow\infty\,, \qquad \text{and} \qquad \widehat{b}_{M-1,i}\longrightarrow\infty \qquad \forall i=1,\ldots,N-1\,, \tag{4.47}$$

[30] This choice of bases is motivated by studying numerous examples with small values of N or M. A proof of the linear independence of the parameters for generic $X_{N,M}$ is currently still missing.

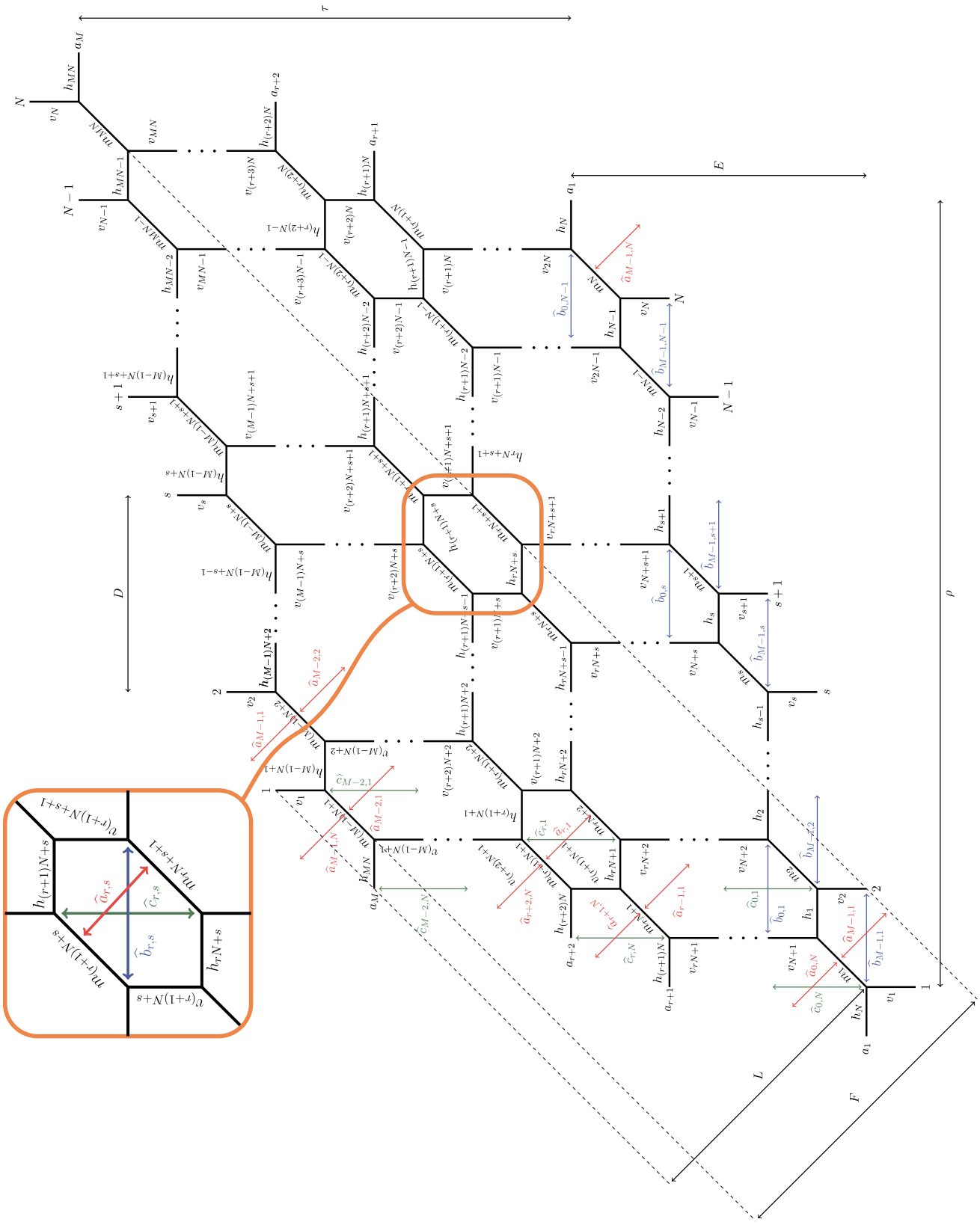

Figure 17: *Three different maximally independent sets of Kähler parameters for a generic toric web (N, M). For concreteness we assume $N \geq M$. Furthermore, for the sets $\widehat{a}$, $\widehat{b}$ and $\widehat{c}$ (which will constitute the roots in the three different gauge theory descriptions), we have only shown the first few explicitly in the diagram, along with an assignment for a generic hexagon in the web. The latter is labeled by two integers (r, s) whose range is specified in eq. (4.43).*

we have $h_{1,\ldots,NM} \longrightarrow \infty$, while $\{v_{1,\ldots,NM}, m_{1,\ldots,NM}\}$ in the diagram in Fig. 17 remain finite. Graphically, the diagram therefore composes into N vertical strips of length M, each of which associated with the theory corresponding to a single $U(M)$. The expansion of the partition function $Z^{(N,M)}_{\text{hor}}$ (schematically written in (4.26)) can therefore be more concisely be written as an instanton expansion in (4.46).

Finally, the parameter τ extends each of the algebras $\mathfrak{a}_{M-1}$ (whose roots are given in (4.45)) to affine $\widehat{\mathfrak{a}}_{M-1}$.

- vertical basis

A basis suitable for describing the vertical expansion $Z^{(N,M)}_{\text{vert}}$ in (4.26) can be found through a judicious exchange of vertical and horizontal parameters of the horizontal basis. Indeed, we propose the vertical basis to be

$$\mathfrak{B}_{\text{vert}} = \left\{ \widehat{c}_{r=0,\ldots,M-2,N}\,, \tau\,, \{\widehat{b}\}_{u=0,\ldots,M-1}\,, \rho\,, D \right\}\,, \tag{4.48}$$

with

$$\{\widehat{b}\}_u = \left\{ \widehat{b}_{u,s} | s \in \{1,\ldots,N-1\} \right\}\,, \qquad \forall\, u = 0,\ldots,M-1\,, \tag{4.49}$$

which suggests that $Z^{(N,M)}_{\text{vert}}$ can be interpreted as the instanton partition function of a gauge theory with gauge group $G_{\text{vert}} = [U(N)]^M$. Specifically $\{b\}_{u=0,\ldots,M-1}$ furnish M sets of (simple positive) roots for the M different factors of $U(N)$. Moreover, the M parameters

$$\left\{ \widehat{c}_{0,N}, \ldots, \widehat{c}_{M-2,N}\,, \tau - \sum_{i=0}^{M-2} \widehat{c}_{i,N} \right\} \tag{4.50}$$

are associated with the gauge coupling constants (one associated with each of the M factors $U(N)$) in the sense that in the limit

$$\tau - \sum_{i=0}^{M-2} \widehat{c}_{i,N} \longrightarrow \infty\,, \qquad \text{and} \qquad \widehat{c}_{i,N} \longrightarrow \infty \qquad \forall i = 0,\ldots,M-2\,, \tag{4.51}$$

we have $v_{1,\ldots,NM}$ while $\{h_{1,\ldots,NM}, m_{1,\ldots,NM}\}$ remain finite. Thus, the diagram in Fig. 17 therefore decomposes into M horizontal strips of length N each of which begin associated with the theory corresponding to a single $U(N)$. The series expansion $Z^{(N,M)}_{\text{vert}}$ (which is schematically given in (4.26)) can therefore be more concisely be written as an instanton expansion in (4.50).

Finally, the parameter ρ extends each of algebras $\mathfrak{a}_{N-1}$ (whose roots are given in (4.49)) to affine $\widehat{\mathfrak{a}}_{N-1}$.

- diagonal basis

The diagonal expansion is somewhat more involved to describe. Indeed, we propose the following $NM+2$ parameters as a basis (with $k=\gcd(N,M)$) for the diagonal expansion

$$\mathfrak{B}_{\text{diag}} = \{V_1,\dots,V_k\,,\{\widehat{a}\}_{u=0,\dots,k-1}\,,L\,,F\}\ , \tag{4.52}$$

with

$$\{\widehat{a}\}_u = \left\{\widehat{a}_{M-1-a-u,N+a}|a\in\{0,\dots,\tfrac{MN}{k}-2\}\right\}\ , \tag{4.53}$$

which suggest that $Z^{(N,M)}_{\text{diag}}$ in (4.26) is the instanton partition function of a gauge theory with gauge group $G_{\text{diag}}=[U(NM/k)]^k$. In (4.52), the parameters $V_{1,\dots,k}$ are difficult to directly identify in the web-diagram in Fig. 17. They can, however, be written as a linear combination of $(\mathbf{h},\mathbf{v},\mathbf{m})$. To this end we introduce a similar notation as in [33]: for any diagonal line of area m_a (with $a=1,\dots,NM$) stretched between two vertices A and B

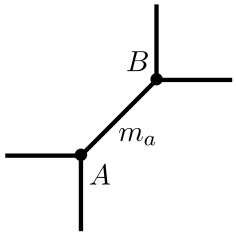

(4.54)

we define $\mathcal{P}_L(m_a)$ as the path starting at A and following N distinct horizontal and $N-1$ distinct vertical lines (going to the left), as well as $\mathcal{P}_R(m_a)$ the path starting at B and following N distinct horizontal and $N-1$ distinct vertical lines (going to the right). Furthermore, we denote $(\mathfrak{p}_L(m_a))_{i=1,\dots,2N-1}$ and $(\mathfrak{p}_R(m_a))_{i=1,\dots,2N-1}$ as the components of $\mathcal{P}_L(m_a)$ and $\mathcal{P}_R(m_a)$ respectively.[31] With this notation, we define[32] the coupling constants $(a=0,\dots,k)$

$$\begin{aligned}V_{a+1} = m_{1+aN} &+ \left(\frac{N}{k}-1\right)\left((\mathfrak{p}_L(m_{1+aN}))_1+(\mathfrak{p}_R(m_{1+aN}))_1\right)\\ &+\sum_{i=1}^{\frac{N}{k}-2}\left(\frac{N}{k}-1-i\right)\left[(\mathfrak{p}_L(m_{1+aN}))_{2i}+(\mathfrak{p}_R(m_{1+aN}))_{2i}\right]\\ &+\sum_{i=1}^{\frac{N}{k}-2}\left(\frac{N}{k}-1-i\right)\left[(\mathfrak{p}_L(m_{1+aN}))_{2i+1}+(\mathfrak{p}_R(m_{1+aN}))_{2i+1}\right]\ .\end{aligned} \tag{4.55}$$

Indeed, for $V_{1,\dots,k}\longrightarrow\infty$ we have $m_{1,\dots,NM}\longrightarrow\infty$, while $(h_{1,\dots,MN},v_{1,\dots,MN})$ remain finite. In this way, the (N,M) web-diagram decomposes into k diagonal strips of length $\frac{NM}{k}$, which can be interpreted as the weak coupling limit of a quiver gauge theory whose gauge group is $G_{\text{diag}}=[U(\frac{NM}{k})]^k$.[33] The existence of this theory outside of the weak

[31] We refer the reader to section 5 of [33], pointing out, however, that in the latter work $N<M$ had been assumed such that the roles of the horizontal and vertical lines have been exchanged.

[32] While the definition (4.55) is very abstract, it is inspired by the definition of the gauge coupling constants of the vertical expansion associated with the dual Calabi-Yau $X_{\frac{NM}{k},k}$ as explained in [33].

[33] Each strip can be associated with an individual $U(\frac{NM}{k})\subset G_{\text{diag}}$.

coupling limit can be argued by the fact that $X_{N,M}$ is dual to $X_{NM/k,k}$ through a combination of flop- and symmetry transformations proposed in [33]. Throughout this series of transformations, the diagonal lines (labeled by $m_{1,\dots NM}$) do not undergo flop transitions, such that the $V_{1,\dots,k}$ are related to the coupling constants of the $[U(\frac{NM}{k})]^k$ quiver gauge theory furnished by the vertical expansion of $\mathcal{Z}_{NM/k,k}$. Moreover, due to the fact that the partition function is expected to be invariant under the duality proposed in [33] (this was explicitly proven for $k = 1$ in [36] and also discussed above), we propose that the expansion of $\mathcal{Z}_{N,M}$ in powers of $Q_{V_a} = e^{-V_a}$ (for $a = 1, \dots, k$) can also be interpreted as the instanton partition function of a quiver gauge theory with gauge group $[U(\frac{NM}{k})]^k$. From this perspective, the $\{\widehat{a}\}_{u=0,\dots,k-1}$ in (4.53) furnish k sets of (simple positive) roots, each associated with a factor $U(\frac{NM}{k}) \subset G_{\text{diag}}$.

Finally, the parameter L extends each of algebras $\mathfrak{a}_{NM/k-1}$ (whose roots are given in (4.53)) to affine $\widehat{\mathfrak{a}}_{NM/k-1}$.

To summarize, based on the proposed bases $\mathfrak{B}_{\text{hor}}$, $\mathfrak{B}_{\text{vert}}$ and $\mathfrak{B}_{\text{diag}}$ (as well as the examples discussed above) we conjecture that for given (N, M) we can engineer three different gauge theories

- horizontal gauge theory with gauge group $G_{\text{hor}} = [U(M)]^N$
- vertical gauge theory with gauge group $G_{\text{vert}} = [U(N)]^M$
- diagonal gauge theory with gauge group $G_{\text{diag}} = [U(NM/k)]^k$ with $k = \gcd(N, M)$

whose gauge groups have the same rank. Moreover, since the partition functions of these three theories are identical (indeed, by construction they are simply different expansions of $\mathcal{Z}_{N,M}$, namely $Z^{(N,M)}_{\text{hor}}$, $Z^{(N,M)}_{\text{vert}}$ and $Z^{(N,M)}_{\text{diag}}$ respectively) they are mutually dual to each other leading to the triality

$$G_{\text{hor}} = [U(M)]^N \qquad \longleftrightarrow \qquad G_{\text{vert}} = [U(N)]^M \qquad \longleftrightarrow \qquad G_{\text{diag}} = [U(MN/k)]^k \,. \tag{4.56}$$

Notice that this duality is not limited to the weak coupling limit: This follows from the relation 4.25 and extends the duality to the full non-perturbative regime. At this point we also want to emphasize the highly non-trivial nature of the duality map that the horizontal and vertical theory have with the diagonal one. Whereas the well known fiber base duality between the horizontal and vertical theories mainly exchanges their coupling constants and their Coulomb branch parameters, the duality map to the third theory completely mixes coupling constants, Coulomb branch and mass parameters. In the next section we describe how the triality together with the result about the invariance of the partition function under flop (4.25), implies an even larger web of dualities.

4.4 Beyond Triality

The authors in [33] argued that a whole family of brane webs is related by geometric transformations

$$X_{N,M} \sim X_{N',M'} \quad \text{if} \quad \begin{cases} \gcd(N, M) = k = \gcd(N', M') \\ NM = N'M' \end{cases} \tag{4.57}$$

where the equivalence relation means that the geometries can be related by sequence of flop and $SL(2,\mathbb{Z})$ transformations. The second condition is simply the fact that the number of compact divisors (hexagons) in the web does not change under flops. As was argued in [38], the equivalence (4.57) together with the triality structure described in the previous section immediately implies a vast web of dual gauge theories. Having a triplet of theories associated to $X_{N,M}$ with gauge groups

$$G_{\text{hor}} = [U(M)]^N\,, \quad G_{\text{vert}} = [U(N)]^M\,, \quad G_{\text{diag}} = [U(MN/k)]^k \tag{4.58}$$

and another triplet associated to $X_{N',M'}$ with gauge groups

$$G'_{\text{hor}} = [U(M')]^{N'}\,, \quad G'_{\text{vert}} = [U(N')]^{M'}\,, \quad G'_{\text{diag}} = [U(M'N'/k)]^k, \tag{4.59}$$

such that the two web diagrams are related by (4.57), we can find a duality map relating their parameters by applying (4.3) a given number of times. The two sets of theories will have at least one theory in common, *i.e.* same gauge group, matter content. We can easily see from (4.58) and (4.59) that this will be theory associated to the diagonal expansion which can be safely followed through the extended Kähler moduli space (collection of adjacent Kähler cones) as the flop transformations do not act on the curves related to its coupling constants. Hence this theory is not send through a strong coupling regime where we might not trust the low-energy gauge theory description. The other theories are generically different which can also be understood from the strong coupling argument, as their coupling related curves undergo flops in general. The suggested duality structure for the Kähler cones associated to $X_{N,M}$ and $X_{N',M'}$ respectively is schematically shown in Fig. 18. From the latter figure, it is also clear that as we have to perform in general more than one flop transition, we pass through a number of different cones before reaching the final configuration. We call these the intermediate Kähler cones and they correspond to web diagrams that do not have an equivalent representation in terms of an unshifted web, *i.e.* $X^{(\delta=0)}_{N,M} = X_{N,M}$. It is a natural question to ask whether we can learn anything new from these webs. As explained above, we know that there is at least one gauge theory description associated with them, *i.e.* the gauge theory that we are following through the extended Kähler moduli space. In section 5 we will see that we can indeed get new information out of the these. As there are in general more than two web diagrams related under (4.57), the above reasoning immediately implies a vast web of dualities between circular quiver gauge theories with gauge groups such that

$$[U(N)]^M \quad \longleftrightarrow \quad [U(N')]^{M'}\,, \quad \text{with} \quad \begin{cases} \gcd(N,M) = k = \gcd(N',M') \\ NM = N'M' \end{cases} \tag{4.60}$$

We now give specific examples to illustrate and motivate the points outline above.

4.4.1 Example: The duality web associated to $X_{6,5}$

To provide evidence for the fact that the combination of equation (4.57) with the triality as implied by equation (4.56) implies an even larger web of dual theories, we look at a specific example in more detail, namely the $X_{6,5}$ geometry for which $k = \gcd(6,5) = 1$. The corresponding web diagram is depicted in Fig. 19. According to (4.57) the following web diagrams are related through flop transformations

$$X_{6,5} \sim X_{10,3} \sim X_{15,2} \sim X_{30,1} \tag{4.61}$$

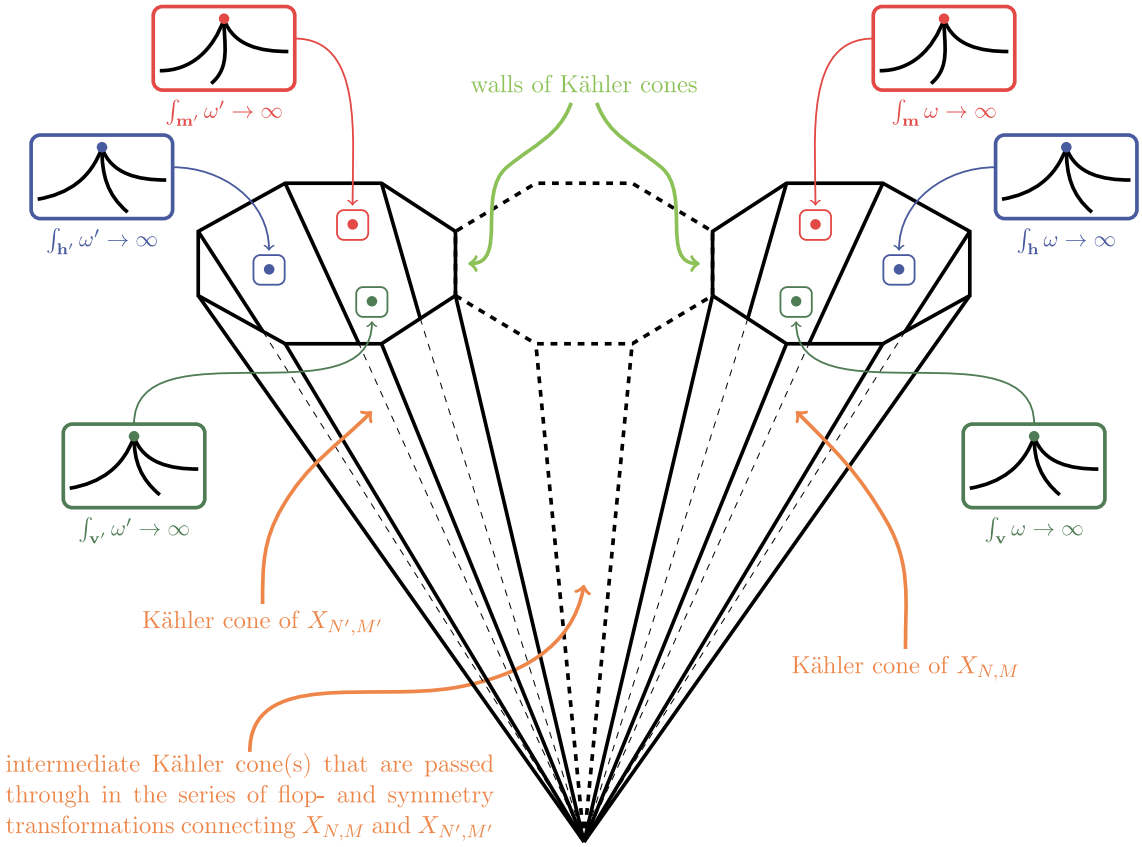

Figure 18: *Weak coupling regions in the extended moduli space of* $X_{N,M}$.

However, we will only provide explicit parametrisations and duality maps for the first two webs, *i.e.* $X_{6,5}$ and $X_{10,3}$. This should be sufficient to illustrate the proposal. Nothing fundamentally new could be learned by including the other examples. The horizontal and vertical expansions can be associated with gauge theories of gauge group $[U(5)]^6$ and $[U(6)]^5$, respectively, while according to our previous discussion, the diagonal expansion gives rise to a gauge theory with gauge group $U(30)$. To obtain the latter theory, in particular, to make the structure of $U(30)$ manifest, we need to expand $\mathcal{Z}_{6,5}$ in terms of a specific set of variables, a procedure which was proposed in full generality in the last section. Concretely, in the present case, these variables are depicted in red in Fig. 19 and consist of $(M, V, \widehat{a}_{1,\dots,30})$, where M and V are given explicitly as

$$\begin{aligned} M &= h_6 + v_1 + h_{25} + v_{26} + h_{20} + v_{21} + h_{15} + v_{16} + h_{10} + v_{11} + h_5 \,, \\ V &= m_{30} + (6-1)(h_{29} + h_{30}) + (6-2)(v_5 + h_4 + v_{25} + h_{19}) \\ &\quad + (6-3)(v_{10} + h_9 + v_{20} + h_{14}) + (6-4)(v_{15} + h_{14} + v_{15} + h_9) \\ &\quad + (6-5)(v_{20} + h_{19} + v_{10} + h_4) \,. \end{aligned} \tag{4.62}$$

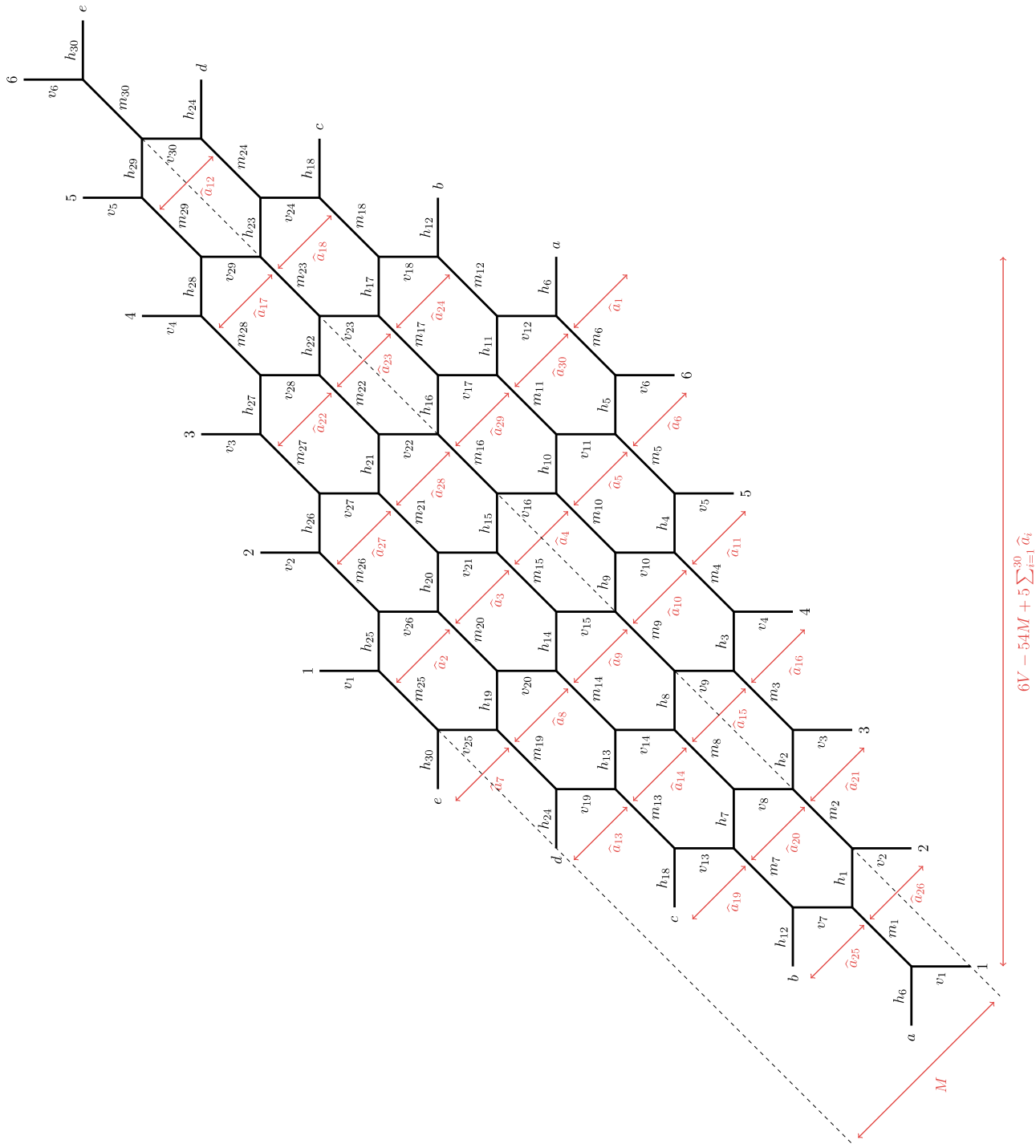

Figure 19: *Parametrisation of the* $(6, 5)$ *web diagram: out of the 90 curves* (h_i, v_i, m_i) *(for* $i = 1, \ldots, 30$*) only 32 parameters are independent. The red curves constitute a maximal set of independent parameters which makes a* $U(30)$ *symmetry visible.*

Here, the last relation follows from the general duality map relating $X_{6,5} \sim X_{30,1}$ that was initially conjectured in [33] and reviewed in the previous section. In this basis, we have[34]

$$m_i = V + p_i(M, \widehat{a}_{1,\dots,30})\,, \qquad \forall\ i = 1, \dots, 30\,, \tag{4.63}$$

where p_i are multi-linear functions in the 31 variables $(M, \widehat{a}_{1,\dots,30})$, while $h_{1,\dots,30}$ and $v_{1,\dots,30}$ are independent of V. Thus, formulated in a different manner, the diagonal expansion written schematically in (4.26), can be understood as a power series expansion in $Q_V = e^{-V}$. Furthermore, the $\widehat{a}_i$ play the role of the roots of $\widehat{\mathfrak{a}}_{29}$, *i.e.* the affine extension of the Lie algebra associated with the gauge group $U(30)$ that is associated with the diagonal expansion: indeed, in the weak coupling limit $V \to \infty$, the diagonal lines in Fig. 19 are cut (as the area of the corresponding curves in the toric Calabi-Yau threefold becomes infinite) and the remaining diagram can be presented as a single strip of length 30. According to (4.61), $X_{6,5}$ can be brought into $X_{10,3}$ by flop transformations. The web diagram of the latter is shown in Fig. 20. This was shown explicitly in [33], where also an explicit form of the duality map relating the two sets of Kähler parameters, $(\mathbf{h}, \mathbf{v}, \mathbf{m})$ and $(\mathbf{h}', \mathbf{v}', \mathbf{m}')$ was provided. This map allows us to recover the same set of parameters $(M, V, \widehat{\alpha}_{1,\dots,30})$ (drawn in red) also in Fig. 20. In terms of $(\mathbf{h}', \mathbf{v}', \mathbf{m}')$, we have explicit relations

$$\begin{aligned}
M = {} & h'_{10} + v'_1 + h'_{21} + v'_{22} + h'_{12} + v'_{13} + h'_3 + v'_4 + h'_{24} + v'_{25} + h'_{15} + v'_{16} + h'_6 + v'_7 \\
& + h'_{27} + v'_{28} + h'_{18} + v'_{19} + h'_9\,, \\
V = {} & m'_{30} + (10-1)(h'_{29} + h'_{30}) + (10-2)(v'_9 + h'_8 + v'_{21} + h'_{11}) \\
& + (10-3)(v'_{18} + h'_{17} + v'_{12} + h'_2) + (10-4)(v'_{27} + h'_{26} + v'_3 + h'_{23}) \\
& + (10-5)(v'_6 + h'_5 + v'_{24} + h'_{14}) + (10-6)(v'_{15} + h'_{14} + v'_{15} + h'_5) \\
& + (10-7)(v'_{24} + h'_{23} + v'_6 + h'_{26}) + (10-8)(v'_3 + h'_2 + v'_{27} + h'_{17}) \\
& + (10-9)(v'_{12} + h'_{11} + v'_{18} + h'_8)\,.
\end{aligned} \tag{4.64}$$

Note that, analogous to (4.63), we also have in the dual web diagram

$$m'_i = V + p'_i(M, \widehat{a}_{1,\dots,30})\,, \qquad \forall\, i = 1, \dots, 30\,, \tag{4.65}$$

for some multi-linear functions p'_i, while $h'_{1,\dots,30}$ and $v'_{1,\dots,30}$ are independent of V. Therefore, the diagonal expansions (in the sense of (4.26)) of $\mathcal{Z}_{6,5}$ and $\mathcal{Z}_{10,3}$ both give rise to gauge theories with gauge group $U(30)$, as implied by [33] and as explained above. In Fig. 20, however, we have also shown (in blue) a different set of maximally independent Kähler parameters $(D, \rho, c_{1,2,3}, \widehat{b}_{1,\dots,27})$. In terms of these variables, we have

$$v'_i = \begin{cases} c_1 + p_i^{(1)}(D, \rho, \widehat{b}_{1,\dots,27}) & \text{if} \quad 1 \le i \le 10 \\ c_2 + p_i^{(2)}(D, \rho, \widehat{b}_{1,\dots,27}) & \text{if} \quad 11 \le i \le 20 \\ c_3 + p_i^{(3)}(D, \rho, \widehat{b}_{1,\dots,27}) & \text{if} \quad 21 \le i \le 30 \end{cases} \tag{4.66}$$

for some multi-linear functions $p_i^{(1,2,3)}$, while $h'_{1,\dots,30}$ and $v'_{1,\dots,30}$ are independent of $c_{1,2,3}$. Thus, in the limit $c_i \to \infty$ for $i = 1, \dots, 3$, the vertical lines in Fig. 20 are cut and the diagram

[34] We stress that all 90 parameters (h_i, v_i, m_i) can be expressed as linear combinations of the 32 elements $(M, V, \widehat{a}_{1,\dots,30})$. However, we refrain to write down these relations explicitly, since they will not be needed for the following discussions.

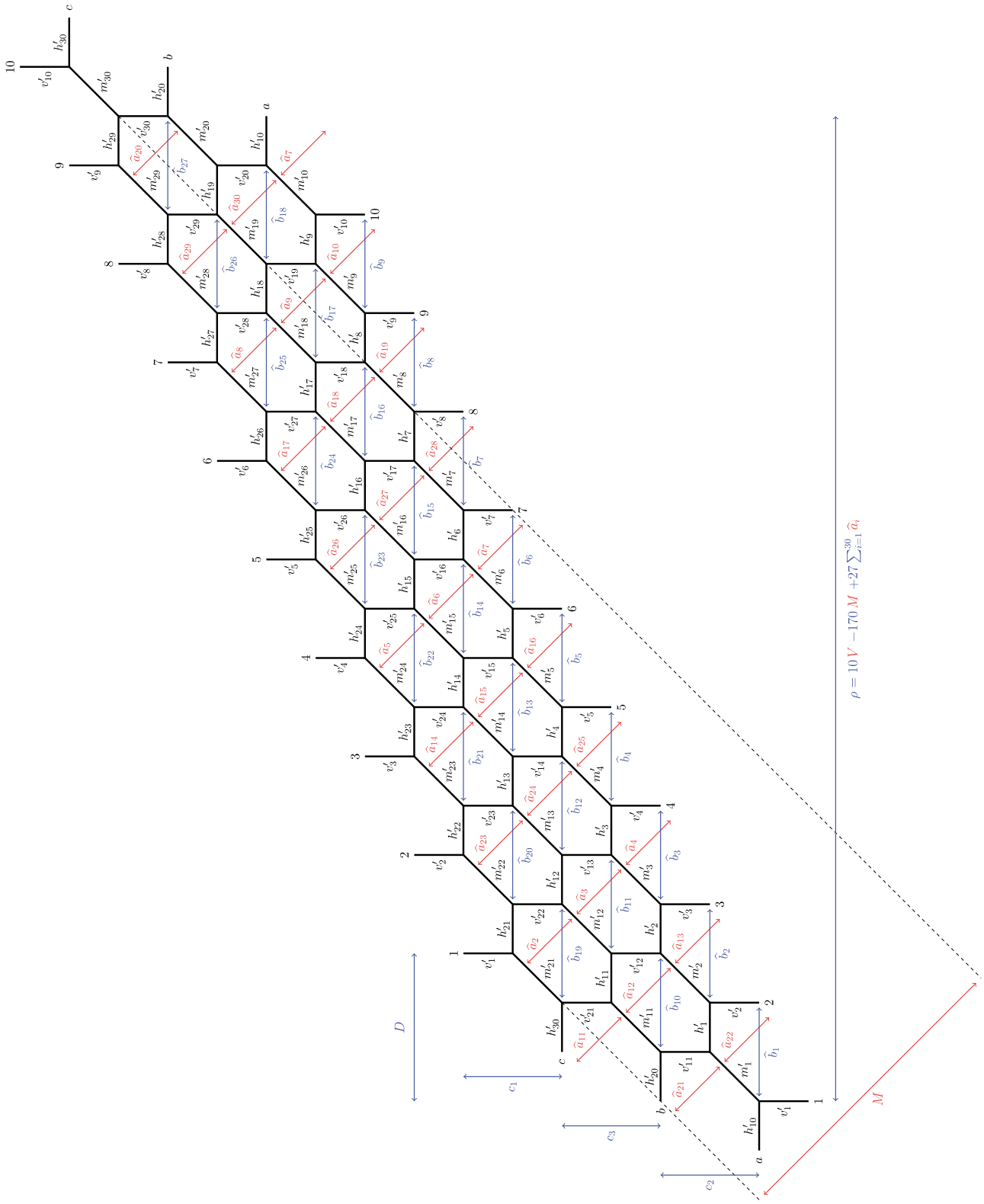

Figure 20: *Two different maximal sets of independent Kähler parameters in the* $(10, 3)$ *web diagram. After a series of suitable flop- and symmetry transformations, the red parametrisation agrees with the maximal set of independent parameters* $(M, V, \widehat{a}_{1,\ldots,30})$ *used in the* $(6, 5)$ *web diagram in Fig. 19.*

decomposes into three strips of length 10 (similarly to the examples in the previous section). We can interpret this as the weak coupling limit of a gauge theory with gauge group $[U(10)]^3$. This indicates that, upon expanding $\mathcal{Z}_{6,5}$ as a power series in e^{-c_1}, e^{-c_2} and e^{-c_3} (which is equivalent to the expansion in terms of $e^{-v_i'}$ for $i = 1, \ldots, 10$) the latter can be interpreted as an instanton expansion of a gauge theory with gauge group $[U(10)]^3$ (which via $SL(2,\mathbb{Z})$ transforms is in turn dual to a theory with gauge group $[U(3)]^{10}$). It is worth noticing that, in this manner, the $\widehat{b}_{1,\ldots,27}$ play the role of roots of Lie algebras associated with this group. Exploiting further the equivalence relation (4.61) for $X_{6,5}$ we can in the same fashion engineer a large set of dual quiver gauge theories whose gauge groups include

$$U(30)\,, \quad [U(15)]^2\,, \quad [U(10)]^3\,, \quad [U(6)]^5\,, \quad [U(5)]^6\,, \quad [U(3)]^{10}\,, \quad [U(2)]^{15}\,, \quad [U(1)]^{30}\,, \quad (4.67)$$

all of which are compatible with the condition in eq. (4.57). Although not provided, the explicit duality maps between these theories could be extracted in the same way as explained above.

4.4.2 Intermediate Kähler cones

In the following we will be interested in the intermediate Kähler cones that can be reached from a given geometry $X_{N,M}$. These intermediate cones were defined as web diagrams that do not have an equivalent representation as an unshifted web. We have argued before that the latter engineer at least one gauge theory. For two geometries $X_{N,M}$ and $X_{N',M'}$ related according to (4.57) we have seen that the theories associated to their diagonal expansions have the same gauge theory data, *i.e.* Coupling constants, Coulomb branch moduli and mass parameters. When transitioning from on web to the other, this diagonal theory is not send through a strong coupling regime (the curves related to the coupling constants do not shrink to zero size as they do not undergo flop transformations in the process). Hence this diagonal theory will also be engineered in all the intermediate cones. It is natural to ask whether there will be more than one region in a given intermediate cone that engineers a (weak coupling) description of some gauge theory. In the remainder of this section we will argue that this is the case. We give a first example that shows, along the lines of reasoning of section 4.3 that there are in general indeed more regions in the intermediate Kähler cones who can be interpreted as the weak coupling description of gauge theories. Furthermore we will see in a second example that one has to be careful when it comes to intuitions at the level of the web diagram. From a naive viewpoint, one could think that there would exist dual theories in the intermediate cones which violate the gcd condition as given in (4.60). After a more careful analysis we conclude that these descriptions which seem to violate the gcd condition can in fact not be interpreted from a gauge theory point of view.

$X_{6,1}$ and its extended moduli space

In order to motivate an answer to the questions raised about intermediate Kähler cones it is useful to study the specific example of $X_{6,1}$. The latter is schematically drawn in Fig. 21, along with a parametrisation of the Kähler parameters that is compatible with all consistency conditions. We can arrange the latter in the following form:

$$\widehat{a}_i = h_{i+1} + v\,, \qquad \widehat{b}_i = h_i + m\,, \qquad \forall i \in \{1,2,3,4,5\}\,,$$

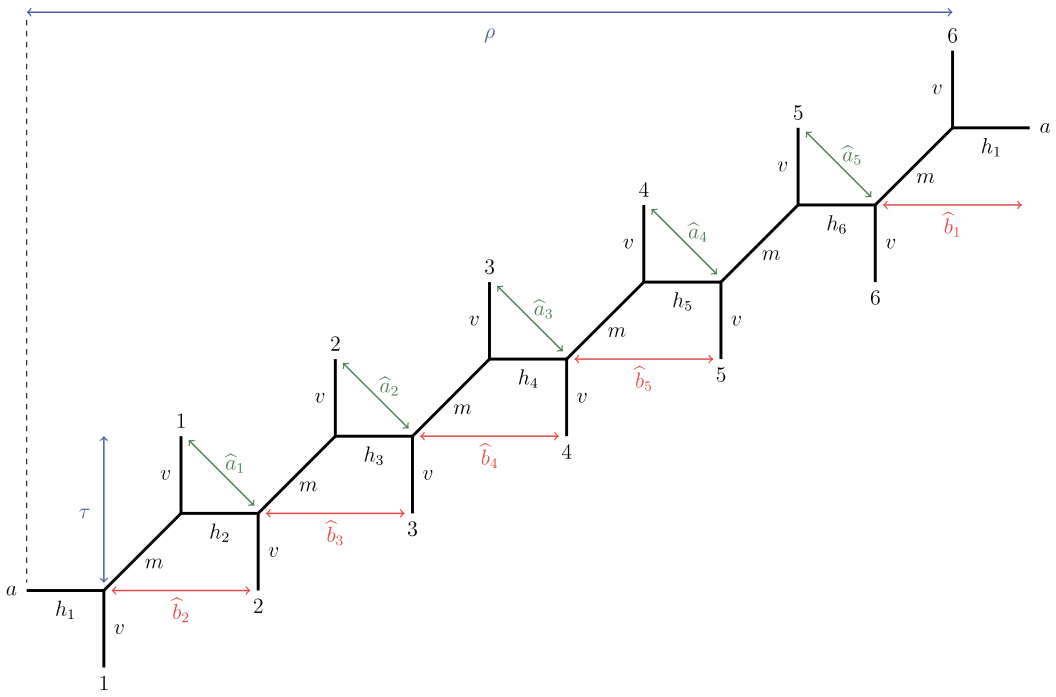

Figure 21: *Toric web diagram of $X_{6,1}$ (with shift parameter $\delta = 0$) with a consistent labeling of the areas of all curves.*

$$L = \sum_{i=1}^{5} \widehat{a}_i + h_1 + v\,, \quad \rho = \sum_{i=1}^{5} \widehat{b}_i + h_6 + m\,, \quad \tau = m + v\,, \qquad D = E/6 = m\,. \tag{4.68}$$

which is well adapted to the description of three different gauge theories engineered by $X_{N,M}$. Indeed, as can be deduced from the discussion in the previous section this web engineers the following theories

- horizontal theory of $X_{6,1}^{(\delta=0)}$

  The horizontal expansion of $\mathcal{Z}_{6,1}$ can be interpreted as the instanton partition function of a gauge theory with gauge group $[U(1)]^6$. This theory is parametrised in the following fashion:

  - coupling constants: the parameters $\widehat{b}_{1,2,3,4,5}$ and $\rho - \sum_{i=1}^{5} \widehat{b}_i$ are related to the coupling constants
  - roots: there is no finite Lie algebra associated with $U(1)$, however, the parameter τ can be interpreted as the affine root for 6 copies of the Heisenberg algebra $\widehat{\mathfrak{a}}_0$
  - mass parameter: the hypermultiplet mass scale of the theory is set by the parameter E

- vertical theory of $X_{6,1}^{(\delta=0)}$

  The vertical expansion of $\mathcal{Z}_{6,1}$ can be interpreted as the instanton partition function of a gauge theory with gauge group $U(6)$, which is parametrised in the following fashion:

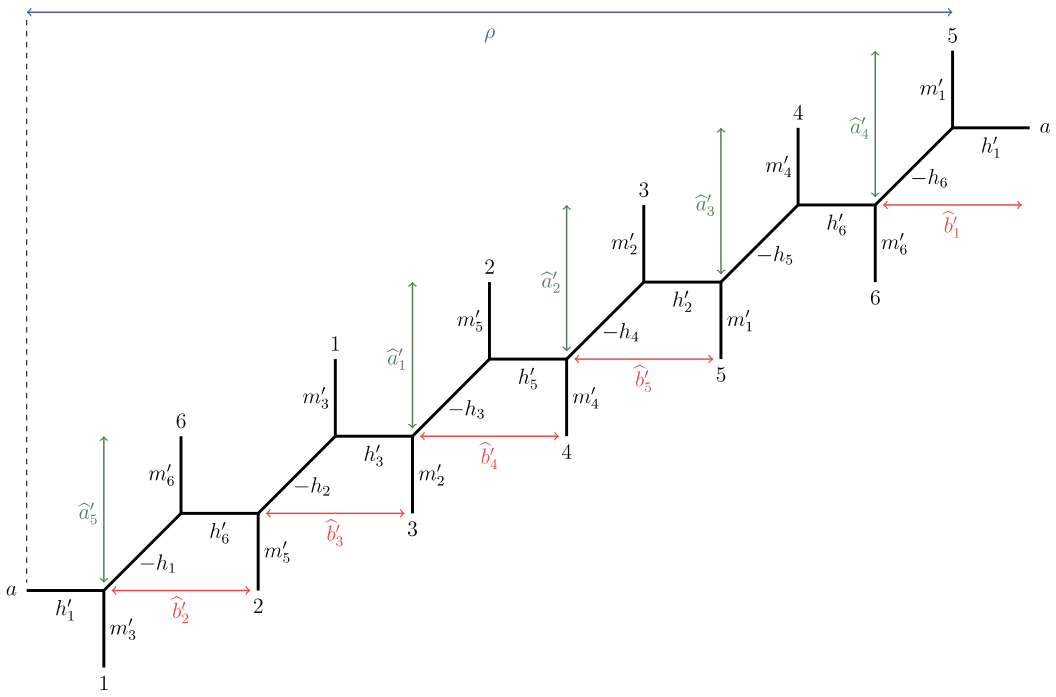

Figure 22: *Toric web diagram of* $X_{6,1}^{(\delta=5)}$ *with a consistent labeling of the areas of all curves.*

- coupling constant: the parameter v is related to the coupling constant
- roots: the parameters $\widehat{b}_{1,2,3,4,5}$ play the role of the simple positive roots of $\mathfrak{a}_5$, which is extended to $\widehat{\mathfrak{a}}_5$ by ρ
- mass parameter: the hypermultiplet mass scale of the theory is set by the parameter D

- diagonal theory of $X_{6,1}^{(\delta=0)}$

  The diagonal expansion of $\mathcal{Z}_{6,1}$ can be interpreted as the instanton partition function of a gauge theory with gauge group $U(6)$, which is parametrised in the following fashion:

  - coupling constant: the parameter m is related to the coupling constant
  - roots: the parameters $\widehat{a}_{1,2,3,4,5}$ play the role of the simple positive roots of $\mathfrak{a}_5$, which is extended to $\widehat{\mathfrak{a}}_5$ by L
  - mass parameter: the hypermultiplet mass scale of the theory is set by the parameter v

After a series of flop and $SL(2,\mathbb{Z})$ transformations, the web diagram of $X_{6,1}^{(0)}$ can be brought into the form shown in Fig. 22, which is denoted by $X_{6,1}^{(\delta=5)}$. It has an equivalent representation in the form of $X_{3,2}^{(\delta=1)}$ as shown in Fig. 23. To arrive at this presentation only $SL(2,\mathbb{Z})$ transformations were used, but in particular no flop transformations. It is important that this web diagram does not have an equivalent representation in terms of an unshifted web. It thus corresponds to an intermediate Kähler cone as defined above. With help of the map (4.3), the Kähler parameters

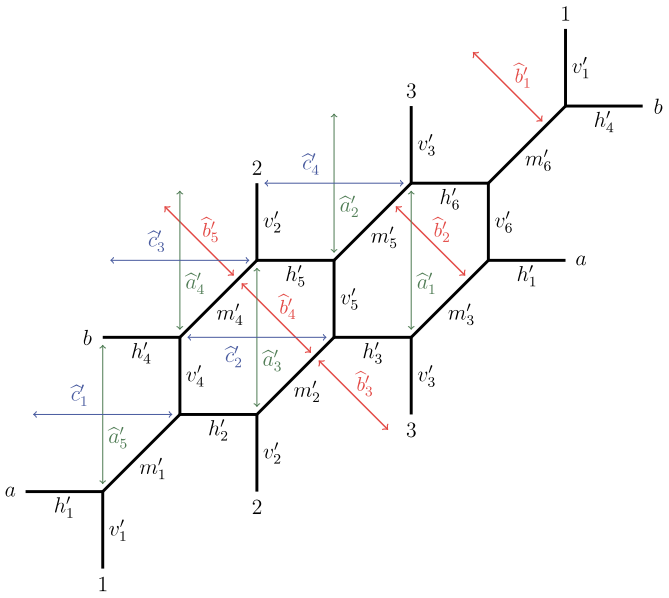

Figure 23: *Toric web diagram of* $X^{(1)}_{3,2}$ *with shift* $\delta = 1$*, and a labeling of the Kähler parameters.*

of the new web diagram in Fig. 22 (and equivalently Fig. 23) can be expressed in terms of the original Kähler parameters $\{h_{1,\dots,6}, v, m\}$. Explicitly, we have for the areas of all curves

$$
\begin{aligned}
&v'_1 = -h_6\,, && v'_2 = -h_4\,, && v'_3 = -h_2\,,\\
&v'_4 = -h_5\,, && v'_5 = -h_3\,, && v'_6 = -h_1\,,\\
&h'_1 = m + h_1 + h_6\,, && h'_2 = m + h_4 + h_5\,, && h'_3 = m + h_2 + h_3\,,\\
&h'_4 = m + h_5 + h_6\,, && h'_5 = m + h_3 + h_4\,, && h'_6 = m + h_1 + h_2\,,\\
&m'_1 = v + h_5 + h_6\,, && m'_2 = v + h_3 + h_4\,, && m'_3 = v + h_1 + h_2\,,\\
&m'_4 = v + h_4 + h_5\,, && m'_5 = v + h_2 + h_3\,, && m'_6 = v + h_1 + h_6\,.
\end{aligned}
$$

With these parameters we can furthermore define

$$
\begin{aligned}
&\widehat{b}'_1 = h'_1 + v'_1 = \widehat{b}_1\,, && \widehat{b}'_2 = h'_6 + v'_6 = \widehat{b}_2\,, && \widehat{b}'_3 = h'_3 + v'_3 = \widehat{b}_3\,,\\
&\widehat{b}'_4 = h'_5 + v'_5 = \widehat{b}_4\,, && \widehat{b}'_5 = h'_2 + v'_2 = \widehat{b}_5\,, && \qquad (4.69)
\end{aligned}
$$

$$
\begin{aligned}
&\widehat{a}'_1 = m'_3 + v'_6 = \widehat{a}_1\,, && \widehat{a}'_2 = m'_5 + v'_3 = \widehat{a}_2\,, && \widehat{a}'_3 = m'_2 + v'_5 = \widehat{a}_3\,,\\
&\widehat{a}'_4 = m'_4 + v'_2 = \widehat{a}_4\,, && \widehat{a}'_5 = m'_1 + v'_4 = \widehat{a}_5\,, && \qquad (4.70)
\end{aligned}
$$

$$
\widehat{c}'_1 = h'_1 + m'_1\,, \qquad \widehat{c}'_2 = h'_2 + m'_2\,, \qquad \widehat{c}'_3 = h'_4 + m'_4\,, \qquad \widehat{c}'_4 = h'_5 + m'_5\,,
$$

$$
L' = m'_1 + h'_1 + m'_2 + h'_2 + m'_3 + h'_3\,, \quad M' = \sum_{i=1}^{6} v'_i\,, \quad v' = v'_1 + v'_6 + m'_6\,, \qquad (4.71)
$$

$$
E' = m'_4 + m'_5 + m'_6\,, \quad D' = \sum_{i=1}^{6} m'_i\,, \quad \tau' = \sum_{i=1}^{6} (v'_i + m'_i) \qquad (4.72)
$$

which is more appropriate for their interpretation in terms of gauge theories: Indeed, in the same way as above, there are three regions in the Kähler cone of $X_{3,2}^{(\delta=1)}$ which suggest an interpretation as weak coupling regions of three gauge theories:

- horizontal theory of $X_{6,1}^{(\delta=5)}$

  In the limit $L' \to \infty$, the diagram $X_{6,1}^{(\delta=5)}$ decomposes into a single strip of length six, which suggests an interpretation as the weak coupling limit of a gauge theory with gauge group $U(6)$. In analogy to the theories with $\delta = 0$ we call this theory the *horizontal* theory, which is parametrised as follows

  - coupling constant: the parameter L' is related to the coupling constant
  - roots: the parameters $\widehat{a}'_{1,\dots,5}$ play the role of the simple positive roots of $\mathfrak{a}_5$, which is extended to $\widehat{\mathfrak{a}}_5$ by τ'
  - mass parameter: the hypermultiplet mass scale of the theory is set by the parameter D'.

- vertical theory of $X_{6,1}^{(\delta=5)}$

  In the limit $\widehat{a}'_1 \to \infty$ and $3\tau' - \widehat{a}'_1 \to \infty$, the diagram $X_{3,2}^{(\delta=1)}$ decomposes into two strips, each of length 3, which suggests an interpretation as the weak coupling limit of a gauge theory with gauge group $U(3) \times U(3)$. In analogy to the theories with $\delta = 0$ we call this theory the *vertical* theory, which is parametrised as follows

  - coupling constants: the parameters $\widehat{a}'_1$ and $3\tau' - \widehat{a}'_1$ are related to the coupling constants
  - roots: the parameters $\widehat{c}'_{1,\dots,4}$ play the role of the simple positive roots of two copies of $\mathfrak{a}_2$, which are extended to $\widehat{\mathfrak{a}}_2$ by L'
  - mass parameter: the hypermultiplet mass scale of the theory is set by the parameter E'

- diagonal theory of $X_{6,1}^{(\delta=5)}$

  In the limit $v' \to \infty$, the diagram $X_{3,2}^{(\delta=1)}$ decomposes into a single strip of length 6, which suggests an interpretation as the weak coupling limit of a gauge theory with gauge group $U(6)$. In analogy to the theories with $\delta = 0$ we call this theory the diagonal theory, which is parametrised as follows

  - coupling constant: the parameter v' is related to the coupling constant
  - roots: the parameters $\widehat{b}_{1,\dots,5}$ play the role of the simple positive roots of $\mathfrak{a}_5$, which is extended to $\widehat{\mathfrak{a}}_5$ by ρ
  - mass parameter: the hypermultiplet mass scale of the theory is set by the parameter M'

Thus, there are three regions in this intermediate Kähler cone, where the designated coupling constants vanish and the web diagram decomposes into several strips that engineer the perturbative limit of the corresponding gauge theory. This is the same argument that was already

given in section (4.3) to argue for the triality of gauge theories. We already remarked before that acting with a flop transformation on the curves that are related with the coupling constants of a given gauge theory description sends the latter through a strong coupling regime and it is a priori no clear what to expect after crossing the wall in moduli space. In the example at hand, it is the horizontal theory associated to $X_{6,1}^{(\delta=0)}$ which gets send through the strong coupling regime, *i.e.*, the flop transformations act on the parameters $h_{1,\dots,6}$. As a consequence, $X_{6,1}^{(\delta=5)}$ does not engineer a horizontal theory with gauge group $U(1)^6$ but we conjecture that it engineers a theory with gauge group $U(3) \times U(3)$ in the low energy description. The latter can be seen in a sense as the 'strong coupling dual'. We want to emphasize that this description should also hold outside the low-energy regime as $X_{3,2}^{(\delta=1)}$ can again be related to $X_{3,2}$ through flops, so the partition function are related as well according to 4.25. An analysis at the strong coupling point would require a full description in terms of little string theory. From the perspective of the remaining two gauge theories, the duality transformation acts purely in the weak coupling regime and therefore $X_{6,1}^{(\delta=5)}$ also still engineers two theories with gauge groups $U(6)$ (which we termed the horizontal and diagonal one).

Performing further flop transformation we can pass through other Kähler cones until we are back in the original cone we started in, *i.e.* associated with $X_{6,1}^{(\delta=0)}$. We can thus analyze each cone that lies in this orbit in the extended moduli space of our Calabi-Yau threefold. It can again be shown that these other cones also allow for three separate regions where a weak coupling description of a gauge theory can be expected. The gauge groups of the latter are summarized in the following table

Calabi-Yau	G_{hor}	G_{vert}	G_{diag}
$X_{6,1}^{(\delta=0)}$	$[U(1)]^6$	$U(6)$	$U(6)$
$X_{6,1}^{(\delta=5)} = \mathcal{F}(X_{6,1}^{(\delta=0)})$	$U(6)$	$[U(3)]^2$	$U(6)$
$X_{6,1}^{(\delta=4)} = \mathcal{F}^2(X_{6,1}^{(\delta=0)})$	$[U(3)]^2$	$[U(2)]^3$	$U(6)$
$X_{6,1}^{(\delta=3)} = \mathcal{F}^3(X_{6,1}^{(\delta=0)})$	$[U(2)]^3$	$[U(3)]^2$	$U(6)$
$X_{6,1}^{(\delta=2)} = \mathcal{F}^4(X_{6,1}^{(\delta=0)})$	$[U(3)]^2$	$U(6)$	$U(6)$
$X_{6,1}^{(\delta=1)} = \mathcal{F}^5(X_{6,1}^{(\delta=0)})$	$U(6)$	$[U(1)]^6$	$U(6)$

Notice that all gauge groups obtained in this fashion are of the form

$$[U(N')]^{M'} \qquad \text{with} \qquad \begin{array}{l} N'M' = 6 \text{ and} \\ \gcd(N', M') = 1\,. \end{array} \tag{4.73}$$

Thus all have the same rank and are compatible with (4.60). Moreover, all theories obtained in this way have gauge groups that can also be engineered from unshifted web diagrams that are related to $X_{6,1}$. The details of these theories might still differ and a full understanding certainly requires a more in depth analysis. A first hint will come in the next main section from analyzing the dimensional reductions of theories engineered from intermediate Kähler cones. In the following we shall discuss another example, which potentially leads to theories with new gauge groups that are not engineered by flop-related unshifted web diagrams.

$X_{4,1}$ and its extended moduli space

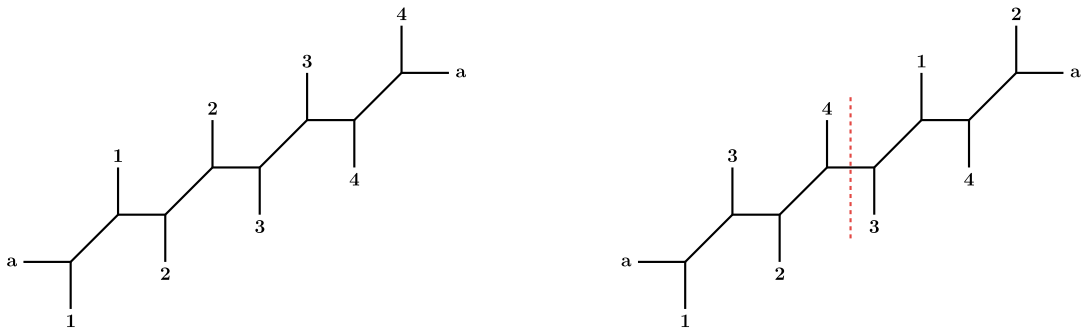

(a) $\delta = 0$ (b) $\delta = 2$

Figure 24: *Toric web diagram for the configuration* $(N, M) = (4, 1)$ *with shift* δ.

As another example we consider the case $X_{4,1}$ whose web diagram is shown in Fig. 24 (a). The latter can be related through flop transformations to $X_{4,1}^{(\delta=2)}$, whose web diagram is shown in Fig. 24 (b). Similarly to the previous example, there is a whole orbit of Kähler cones under flop transformations. Analyzing again possible parametrisations of the corresponding Kähler moduli space, along with suitable decoupling limits to search for areas that engineer weak coupling regions of potential gauge theories, we are lead to the following list of candidate gauge groups

Calabi-Yau	G_{hor}	G_{vert}	G_{diag}
$X_{4,1}^{(\delta=0)}$	$[U(1)]^4$	$U(4)$	$U(4)$
$X_{4,1}^{(\delta=3)} = \mathcal{F}(X_{4,1}^{(\delta=0)})$	$U(4)$	$[U(2)]^2$	$U(4)$
$X_{4,1}^{(\delta=2)} = \mathcal{F}^2(X_{4,1}^{(\delta=0)})$	$[U(2)]^2$	$U(4)$	$U(4)$
$X_{4,1}^{(\delta=1)} = \mathcal{F}^3(X_{4,1}^{(\delta=0)})$	$U(4)$	$[U(1)]^4$	$U(4)$

The appearance of the group $[U(2)]^2$ in this table is rather surprising since it is not of the form $U(N')^{M'}$ with $N'M' = 4$ and $\gcd(N', M') = \gcd(4, 1) = 1$. Thus, if really a quiver gauge theory with this gauge group is engineered from in the extended moduli space of $X_{4,1}$, this indicates that the web of possible dual theories is yet even further enhanced. In particular, it would indicate that the condition $\gcd(N, M) = \gcd(N', M')$ could be relaxed in (4.60) for the construction of dual gauge theories. However, in the following we will find preliminary indications that $X_{4,1}^{(\delta=2)}$ does not engineer a gauge theory that realizes the gauge group $[U(2)]^2$ in a weak coupling regime. Rather the appearance of this group seems to be linked to a strong coupling effect in the 6-dimensional description, which may be linked to the full little string theory.

To discuss this aspect in more detail, in the following we consider $X_{4,1}^{(\delta=2)}$, whose web diagram is shown in Fig. 24 (b). Upon cutting the diagram along the dashed red line and re-gluing it along the lines labeled **3** and **4**, respectively, the web diagram can be brought into the form of $X_{2,2}^{(\delta=1)}$, whose web diagram is shown in Fig. 25 along with a labeling of the Kähler parameters. In the following we will apply a geometrical analysis in terms of intersection numbers, by identifying the divisors (hexagons) $S_{1,2,3,4}$ in the web diagram Fig. 25 with the co-roots of the

gauge algebra of the supposed gauge algebra. With this, we shall be able to see if we can make a consistent assignment of charges such that a gauge theory description can be associated to it. The web diagram is shown in Fig. 25 where we have also introduced the Kähler parameters of the individual curves. As always, the parameters $\{m_i^{(j)}, v_i{}^{(j)}, h_i^{(j)}\}$ are not independent, but there are consistency conditions associated with each of the four hexagons $S_{1,2,3,4}$:

$$\begin{aligned}
S_1: &\qquad h_2^{(1)} + m_1^{(2)} = m_2^{(2)} + h_2^{(2)}\,, &&\qquad v_2^{(1)} + h_2^{(1)} = v_1^{(2)} + h_2^{(2)}\,,\\
S_2: &\qquad m_1^{(2)} + h_1^{(2)} = h_1^{(1)} + m_2^{(2)}\,, &&\qquad v_1^{(1)} + h_1^{(1)} = h_1^{(2)} + v_2^{(2)}\,,\\
S_3: &\qquad m_1^{(1)} + h_1^{(1)} = h_2^{(2)} + m_2^{(1)}\,, &&\qquad v_2^{(1)} + h_1^{(1)} = v_2^{(2)} + h_2^{(2)}\,,\\
S_4: &\qquad m_2^{(1)} + h_2^{(1)} = h_1^{(2)} + m_1^{(1)}\,, &&\qquad v_1^{(2)} + h_1^{(2)} = h_2^{(1)} + v_1^{(1)}\,.
\end{aligned} \tag{4.74}$$

If we want to interpret the horizontal expansion in Fig. 25 as corresponding to a theory with gauge group $[U(2)]^2$, we need to introduce a independent basis of 6 parameters, *i.e.* 2 coupling constants, 2 Coulomb branch parameters and 2 mass parameters. The curves associated to these parameters should then have the appropriate intersection numbers to give a consistent picture. By this we mean that the following three conditions should be satisfied:

1. The curves associated to the coupling constant should be uncharged under the gauge group, *i.e.* it should be possible to make a choice of divisors S_a and S_b (corresponding to the co-roots of the $\mathfrak{a}_1 \times \mathfrak{a}_1$ gauge algebra) such that the "coupling curves" have vanishing intersection numbers with the latter.

2. The curves associated to the Coulomb branch parameters should be charged in such a way that they fall into the adjoint representations of the respective gauge group

3. The curves associated to the mass parameters should be charged in such a way that they fall into bifundamental representations under the gauge group.

Furthermore, it is useful to have the explicit expression of the partition function for the expansion of $X_{2,2}^{(\delta=1)}$. We know that for a gauge theory it is a series expansion in the exponentiated coupling constants. It will thus give us a hint which combination of curves should be considered as candidates for the coupling constants. Different combinations are possible as the shift identity for the ϑ-functions allow us to modify the expansion parameters. The partition function associated with this web diagram can be calculated by using the general building block (3.86) and gluing it in an appropriate way. The resulting expression for the partition function takes the following form

$$\begin{aligned}
\mathcal{Z}_{2,2}^{(\delta=1)} = \sum_{\alpha_1^{(1)},\alpha_2^{(1)},\alpha_1^{(2)},\alpha_2^{(2)}} & (Q_{m_1^{(1)}} Q_{h_1^{(1)}} Q_{h_2^{(2)}} \widehat{Q}_{1,1})^{|\alpha_1^{(1)}|} (Q_{m_2^{(1)}} Q_{h_1^{(2)}} Q_{h_2^{(1)}} \widehat{Q}_{2,1})^{|\alpha_2^{(1)}|} \\
& \times (Q_{m_1^{(2)}} Q_{h_1^{(1)}} Q_{h_1^{(2)}} \widehat{Q}_{1,2})^{|\alpha_1^{(2)}|} (Q_{m_2^{(2)}} Q_{h_2^{(2)}} Q_{h_2^{(1)}} \widehat{Q}_{2,2})^{|\alpha_2^{(2)}|}\, Q_\rho^{-\frac{|\alpha_1^{(1)}|+|\alpha_2^{(1)}|+|\alpha_1^{(2)}|+|\alpha_2^{(2)}|}{2}} \\
& \times \frac{\vartheta_{\alpha_1^{(1)}\alpha_1^{(2)}}(Q_{h_1^{(1)}} \widehat{Q}_{1,2}) \vartheta_{\alpha_1^{(1)}\alpha_2^{(2)}}(Q_{h_1^{(1)}}) \vartheta_{\alpha_2^{(1)}\alpha_1^{(2)}}(Q_{h_2^{(1)}}) \vartheta_{\alpha_2^{(1)}\alpha_2^{(2)}}(Q_{h_2^{(1)}} \widehat{Q}_{2,2})}{\vartheta_{\alpha_1^{(1)}\alpha_1^{(1)}}(1) \vartheta_{\alpha_1^{(1)}\alpha_2^{(1)}}(\widehat{Q}_{2,1}) \vartheta_{\alpha_2^{(1)}\alpha_1^{(1)}}(\widehat{Q}_{1,1}) \vartheta_{\alpha_2^{(1)}\alpha_2^{(1)}}(1)} \\
& \times \frac{\vartheta_{\alpha_1^{(2)}\alpha_1^{(1)}}(Q_{h_1^{(2)}}) \vartheta_{\alpha_1^{(2)}\alpha_2^{(1)}}(Q_{h_1^{(2)}} \widehat{Q}_{2,1}) \vartheta_{\alpha_2^{(2)}\alpha_1^{(1)}}(Q_{h_2^{(2)}} \widehat{Q}_{1,1}) \vartheta_{\alpha_2^{(2)}\alpha_2^{(1)}}(Q_{h_2^{(2)}})}{\vartheta_{\alpha_1^{(2)}\alpha_1^{(2)}}(1) \vartheta_{\alpha_1^{(2)}\alpha_2^{(2)}}(\widehat{Q}_{2,2}) \vartheta_{\alpha_2^{(2)}\alpha_1^{(2)}}(\widehat{Q}_{1,2}) \vartheta_{\alpha_2^{(2)}\alpha_2^{(2)}}(1)}\,,
\end{aligned}$$

where we introduced the notation

$$\widehat{Q}_{1,1} = Q_{v_1^{(1)}} Q_{h_2^{(1)}} \,, \qquad \widehat{Q}_{2,1} = Q_{v_2^{(1)}} Q_{h_1^{(1)}} \,, \qquad \widehat{Q}_{1,2} = Q_{v_1^{(2)}} Q_{h_2^{(2)}} \,, \qquad \widehat{Q}_{2,2} = Q_{v_2^{(2)}} Q_{h_1^{(2)}} \,. \tag{4.75}$$

We can analyze the weights of the coupling constants of this expression with respect to the divisors S_1, S_2, S_3 and S_2 by computing their intersection numbers. Specifically, we have

coup.	**curve $\mathcal{C}$**	$\mathcal{C}\cdot S_4$	$\mathcal{C}\cdot S_3$	$\mathcal{C}\cdot S_1$	$\mathcal{C}\cdot S_2$
$g_1^{(1)}$	$m_1^{(1)} + h_1^{(1)} + h_2^{(2)} + v_1^{(1)} + h_2^{(1)}$	-1	-1	0	2
$g_2^{(1)}$	$m_2^{(1)} + h_1^{(2)} + h_2^{(1)} + v_2^{(1)} + h_1^{(1)}$	-1	-1	2	0
$g_1^{(2)}$	$m_1^{(2)} + h_1^{(1)} + h_1^{(2)} + v_1^{(2)} + h_2^{(2)}$	2	0	-1	-1
$g_2^{(2)}$	$m_2^{(2)} + h_2^{(2)} + h_2^{(1)} + v_2^{(2)} + h_1^{(2)}$	0	2	-1	-1

From the table we see that, as the partition function stands in (4.75), there is not one combination of the curves that is uncharged under both gauge group factors $U(2) \times U(2)$. One can try to use the shift identity of the ϑ-functions to move things around. However, we did not find any combinations which satisfies the requirements specified above. Thus, we conclude that in the present case, it is not possible to realise the full group $U(2) \times U(2)$ at the perturbative level. If at all possible, the latter can therefore only be realized non-perturbatively, thus possibly pertaining to a little string theory. This aspect requires further investigation.

4.5 Summary

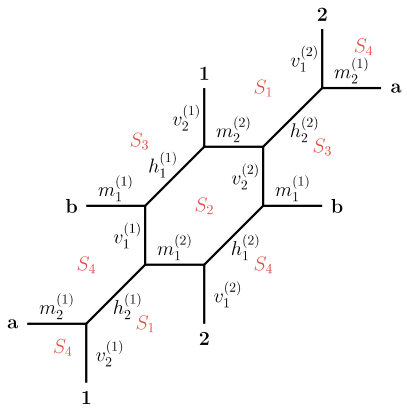

Figure 25: *Toric web diagram and parametrisation of* $X_{2,2}^{(1)}$.

In this section we studied exact dualities between little string theories of class A and thus also dualities between their low-energy descriptions as circular quiver gauge theories. The starting point for unraveling the dualities was the fact that Calabi-Yau threefolds $X_{N,M}$ and $X_{N',M'}$ with $NM = N'M'$ and $\gcd(N,M) = \gcd(N'M')$, can be related through flop transitions. This suggested relations among the theories engineered by these geometries. A crucial step for establishing these relations was to show that the associated topological string partition functions were also related. More concretely, they are invariant under the flopping procedure that connects these different geometries. This was shown explicitly in the case when $\gcd(N,M) = 1$ and we presented reasonable evidence that it holds in general. We commented on the fact that, even if the topological string partition function is invariant under flops, its relation to the individual curves in the geometries is different. In order to make sure that the partition function can really be interpreted as an instanton expansions for the low-energy gauge theories, we studied if for a given geometry $X_{N,M}$ there exist regions in the Kähler cone where the weak coupling regimes of these gauge

theories are realized. We found that in total three such regions in the Kähler cone of $X_{N,M}$, two of which corresponded to theories that were already known to be engineered by this geometry and also a third new theory with gauge group $[U(NM/k)]^k$ where $k = \gcd(N, M)$. The presence of these three theories in the Kähler cones was dubbed triality. A direct consequence of the invariance of the partition function together with the vast web of related geometries was the existence of an even larger web of dual theories residing in the Kähler cones of the different geometries. Thus theories with gauge groups $[U(N)]^M$ and $[U(N')]^{M'}$ with $NM = N'M'$ and $\gcd(N, M) = \gcd(N', M')$ were conjectured to be dual and a non-trivial example was provided to motivate the statement. Along the way, we also encountered geometries $X^{\delta}_{N,M}$ in the extended moduli space that do not have an equivalent representation in terms of unshifted web diagrams. We referred to these as intermediate Kähler cones. Upon studying specific examples we conclude that these contain as well weak coupling regions and that they should at least engineer one theory in general. The surprising fact was that just based on the web diagram, these intermediate cones also engineer theories that violate the gcd condition. However, a more careful analysis revealed that the associated expansion of the partition function could not be interpreted as an instanton series of gauge theories. It might be required to interpret this expansion from the point of view of full fledged little string theories. This point would require further study.

5 Non-trivial five-dimensional limits

In the previous section, we discussed the notion of intermediate Kähler cones and argued that the associated geometries engineer at least one little string theory whose low-energy description is in terms of a certain six dimensional supersymmetric gauge theory on $\mathbb{R}^4_{\epsilon_1,\epsilon_2} \times T^2$. The latter corresponds to a theory that can be safely followed through the Kähler moduli space when performing the sequences of flops as described in this thesis. The reason for this is that when chosen correctly, the flops do not act on the curves that control the coupling constants of this theory. The latter is thus not send through a strong coupling regime. At the end of section 4.2 it was also pointed that whereas the expression of the instanton partition function stays invariant under flops, the relation between the gauge theory parameters and the Kähler parameters associated with the individual curves changes. This fact will turn out to be crucial to the analysis performed in this section. As we are actually dealing with six dimensional theories compactified on T^2, it is natural to look at the dimensional reduction of the theories associated with intermediate Kähler cones. For the conventional theories engineered by $X_{N,M}$, the dimensional reduction was discussed in section 3.5 and shown to be rather simple from the point of view of the web diagram and also the partition function. For theories associated with an intermediate Kähler cone of $X^{(\delta)}_{N,M}$ it turns out that the dimensional reduction is not so trivial anymore.

A particularly interesting structure can already be observed in the case of the periodic strip geometry. In the case where the strip is unshifted $X_{N,1}$ and the engineered theory has $U(N)$ gauge group with adjoint matter, dimensional reduction consists in finding a simple one parameter limit which basically cuts a single line in the web diagram. The result is a five dimensional $U(N)$ theory with the same matter content compactified on S^1. It was realized in [46], that when trying the same simple argument for a periodic strip with a non-trivial shift $X^{(\delta)}_{N,M}$, it is not so simple anymore. The one parameter limit one needs to take in order to shrink the circle to zero size is more involved, meaning that there is in general more than one line in the web diagram cut. At the level of the gauge theory this translates into the fact that the rank of the gauge group gets reduced and the matter content changes. Based on [46], we will first review a specific example in detail and then conjecture the general pattern for web diagrams associated to $X^{(\delta)}_{N,M}$.

5.1 The specific example of $X^{(\delta)}_{3,1}$

We first consider the simplest non-trivial example, namely the geometry $X^{(\delta=1)}_{3,1}$. The associated web diagram is shown in Fig. 26 with the respective Kähler parameters (the meaning of the blue and red lines will be explained below). In the unshifted case, $\delta = 0$, a five dimensional limit would simply correspond to $H_1 \to \infty$. In the case when $\delta \neq 0$ the same limit cannot be taken without the curves intersecting, thus resulting in a non acceptable configuration. It turns out that there exists a different one parameter limit which produces a perfectly acceptable toric web diagram. In order to give some additional motivation for this limit, we consider the geometry of local $\mathbb{F}_1 \cup \mathbb{F}_1$ compactified on a torus, shown in Fig. 27 (a) (see [58] for the non-compact case). Here $\mathbb{F}_1$ denotes the the first Hirzebruch surface[35]. This geometry can be related to

[35]The Hirzebruch surface $\mathbb{F}_n$ can be thought of as a "twisted" $\mathbb{CP}^1$ bundle over $\mathbb{CP}^1$, where the "twisting" depends on a positive integer n. The surface $\mathbb{F}_0$ simply corresponds to the trivial bundle $\mathbb{CP}^1 \times \mathbb{CP}^1$.

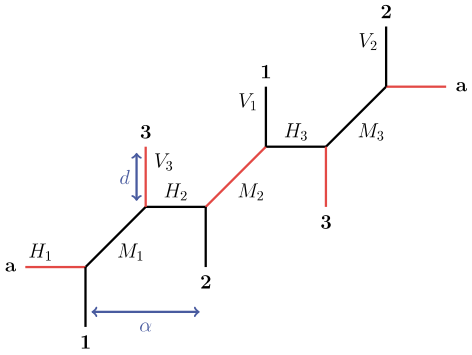

Figure 26: *Web diagram of* $X^{(1)}_{3,1}$.

the web diagram of $X^{(\delta=1)}_{3,1}$ shown in Fig. 26by flopping the curves labeled by $-E_1$ and $-E_2$. This can be seen by looking at the equivalent representation of the web diagram for $\mathbb{F}_1 \cup \mathbb{F}_1$ as shown in Fig. 27 (b). Flopping now $-E_1$ gives the web shown in 28 (a). Upon performing

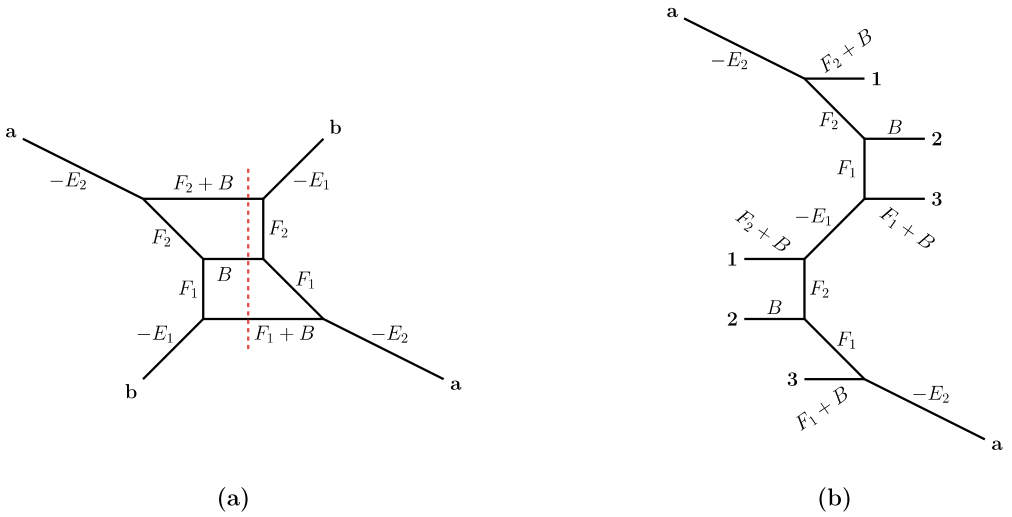

Figure 27: *(a) Gluing two copies of* $\mathbb{F}_1$. *(b) Same geometry after cutting along the red line and re-gluing along the line labeled* $-E_1$.

the appropriate $SL(2,\mathbb{Z})$ transformation, we get the web shown in Fig. 28 (b), which is related to the web diagram of $X^{(\delta=1)}_{3,1}$ shown in Fig. 26, by a flop on the curve labeled by $-E_2$. This relation gives the following identification of the Kähler parameters

$$
\begin{aligned}
&H_1 = F_2 - E_2\,, && H_2 = E_1\,, && H_3 = F_1 - E_2\,,\\
&V_1 = B\,, && V_2 = F_1 + B - E_1 - E_2\,, && V_3 = F_2 + B - E_1 - E_2\,,\\
&M_1 = F_1 - E_1\,, && M_2 = F_2 - E_1\,, && M_3 = E_2\,.
\end{aligned}
\tag{5.1}
$$

A more or less natural limit to consider for the local $\mathbb{F}_1 \cup \mathbb{F}_1$ geometry would be the so called large fiber limit. The latter can be achieved by taking for example the size of the fiber of one of the Hirzebruch surfaces to infinity, *i.e.* $F_2 \to \infty$. This limit can be translated into the web

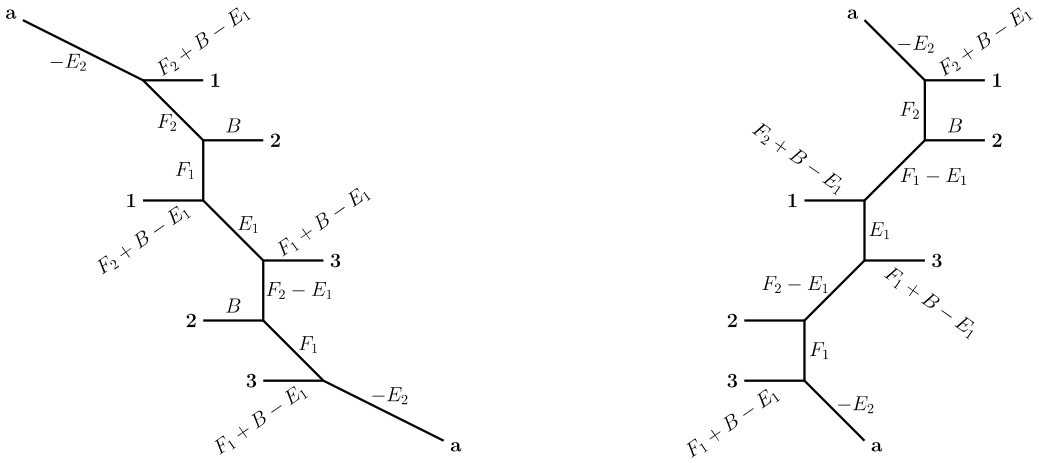

Figure 28: *(a) Geometry of Fig. 27 after a flop transformation of the line $-E_1$. (b) Same geometry after an $SL(2,\mathbb{Z})$ transformation.*

diagram of $X_{3,1}^{(\delta=1)}$ without giving any inconsistencies, *e.g.* crossing lines. From (5.1), we can see that this would give $H_1, V_3, M_2 \to \infty$. These are the lines drawn in red in Fig. 26. From the perspective of the horizontal or vertical $U(3)$ theory with adjoint matter which is engineered by $X_{3,1}^{(\delta=1)}$, this would indeed be the dimensional reduction, as the volume of the elliptic fiber gets send to infinity, at least at the graphical level of the web diagram. So we see that although a natural limit in $\mathbb{F}_1 \cup \mathbb{F}_1$, it translates into a more intricate one in the web diagram of Fig. 26. In order to study this five dimensional limit in more detail and check if it is also consistent at the level of the instanton partition function, we need to introduce a suitable basis of Kähler parameters, which as always must satisfy the consistency conditions imposed by the geometry. In hindsight, we make the following choice in terms of the parameters in Fig. 26.

$$\begin{aligned} H_1 &= 2a + d - g\,, & H_2 &= a - m_1\,, & H_3 &= a - m_2 \\ M_1 &= a + m_1\,, & M_2 &= 2a + d - g + m_1 + m_2\,, & M_3 &= a + m_2 \\ V_1 &= g - m_1 - a\,, & V_2 &= g - a - m_2\,, & V_3 &= d\,. \end{aligned} \tag{5.2}$$

In terms of this basis, the five dimensional limit of the diagram Fig. 26 is implemented by taking $d \to \infty$. In terms of the old basis of Kähler parameters this means

$$H_1 \to \infty\,, \quad V_3 \to \infty\,, \quad M_2 \to \infty\,. \tag{5.3}$$

Hence, the curves depicted in red will go off to infinity and the resulting diagram is shown in Fig. 29. The latter is still toric and corresponds to the well known local dP_3. It engineers [58] a five dimensional gauge theory with gauge group $SU(2)$ and a matter content which transforms as $N_f = 2$ copies of the fundamental representation. We will denote this theory $(SU(2), 2\mathbf{F})$. Now we look at the partition function $\mathcal{Z}_{3,1}^{(\delta=1)}$ in order to ensure that the limit $d \to \infty$ makes sense at the algebraic level. Writing the partition function $\mathcal{Z}_{3,1}^{(\delta=1)}$ using the new basis (5.2) of

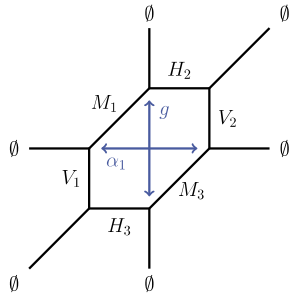

Figure 29: *Decompactified web diagram of* $X^{(1)}_{3,1}$.

Kähler parameters we get

$$\begin{aligned}\mathcal{Z}^{(\delta=1)}_{3,1} = &\sum_{\alpha_1,\alpha_2,\alpha_3} (Q_d Q_a Q_{m_1}^{1/2} Q_{m_2}^{3/2})^{|\alpha_1|} (Q_d Q_a^3 Q_{m_1}^{1/2} Q_{m_2}^{3/2})^{|\alpha_2|} (Q_a^{-2} Q_{m_1} Q_{m_2} Q_g)^{|\alpha_3|} \\ &\times \frac{\vartheta_{\alpha_1\alpha_1}(\mathcal{Q};\rho)\,\vartheta_{\alpha_2\alpha_2}(\mathcal{Q};\rho)\,\vartheta_{\alpha_3\alpha_3}(\mathcal{Q};\rho)\,\vartheta_{\alpha_1\alpha_2}(\mathcal{Q}\,Q_a^{-2};\rho)\,\vartheta_{\alpha_2\alpha_1}(\mathcal{Q}\,Q_a^{2};\rho)}{\vartheta_{\alpha_3\alpha_3}(1;\rho)\,\vartheta_{\alpha_2\alpha_3}(\mathcal{Q}^{-1}Q_a Q_{m_2};\rho)\,\vartheta_{\alpha_1\alpha_3}(\mathcal{Q}^{-1}Q_a^{-1}Q_{m_2};\rho)\,\vartheta_{\alpha_3\alpha_2}(\mathcal{Q}Q_a^{-1}Q_{m_2}^{-1};\rho)} \\ &\times \frac{\vartheta_{\alpha_2\alpha_3}(Q_a Q_{m_2};\rho)\vartheta_{\alpha_1\alpha_3}(Q_{m_2}Q_a^{-1};\rho)\vartheta_{\alpha_3\alpha_2}(Q_{m_1}Q_a^{-1};\rho)\vartheta_{\alpha_3\alpha_1}(Q_{m_1}Q_a;\rho)}{\vartheta_{\alpha_3\alpha_1}(\mathcal{Q}Q_a Q_{m_2}^{-1};\rho)\,\vartheta_{\alpha_1\alpha_1}(1;\rho)\,\vartheta_{\alpha_2\alpha_2}(1;\rho)\,\vartheta_{\alpha_1\alpha_2}(Q_a^{-2};\rho)\,\vartheta_{\alpha_2\alpha_1}(Q_a^2;\rho)}. \end{aligned} \tag{5.4}$$

where the modular parameter is $\rho = 8a + 2d - 2g + m_1 + m_2$ and we used the notation

$$Q_a = e^{-a}\,, \qquad Q_d = e^{-d}\,, \qquad Q_g = e^{-g}\,, \qquad Q_{m_{1,2}} = e^{-m_{1,2}}\,, \qquad \mathcal{Q} = Q_d Q_a^4 Q_{m_1} Q_{m_2} Q_g^{-1}\,,$$

and the summations $\alpha_1\,, \alpha_2$ and α_3 are over integer partitions of $|\alpha_1|\,, |\alpha_2|$ and $|\alpha_3|$ respectively. In order to see how the partition function reduces upon taking $d \to \infty$ it is helpful to look at the behavior of the individual $\vartheta_{\mu\nu}(x;\rho)$ functions. We must distinguish between the case where only $\rho \to i\infty$ and the case where the elliptic argument goes to zero $x \mapsto 0$ in addition to $\rho \to i\infty$. We find the following

$$\begin{aligned}\vartheta_{\mu\nu}(x;\rho) &\xrightarrow[\rho\to i\infty]{} x^{-\frac{|\mu|+|\nu|}{2}}\, t^{\frac{1}{4}(||\mu^t||^2-||\nu^t||^2)}\, q^{-\frac{1}{4}(||\mu||^2-||\nu||^2)}\, N_{\mu\nu}\Big(x\sqrt{\tfrac{t}{q}}\Big)\,, \\ \vartheta_{\mu\nu}(x;\rho) &\xrightarrow[\rho\to i\infty\,,x\mapsto 0]{} x^{-\frac{|\mu|+|\nu|}{2}}\, t^{\frac{1}{4}(||\mu^t||^2-||\nu^t||^2)}\, q^{-\frac{1}{4}(||\mu||^2-||\nu||^2)}\,, \end{aligned} \tag{5.5}$$

where the Nekrasov factor $N_{\mu\nu}$ is defined as

$$N_{\mu\nu}(x) = \prod_{(i,j)\in\mu} \Big(1 - x\, t^{\nu^t_j - i}\, q^{\mu_i - j + 1}\Big) \prod_{(i,j)\in\nu} \Big(1 - x\, t^{-\mu^t_j + i - 1}\, q^{-\nu_i + j}\Big)\,. \tag{5.6}$$

Applying 5.5 to the expression 5.4 when $d \to \infty$ we get

$$\begin{aligned}\mathcal{Z}^{5D}_{dP_3} = &\sum_{\alpha_{1,2}} (-1)^{|\alpha_1|+|\alpha_2|} \Big(Q_a^{-2}\, Q_g\, Q_{m_1}^{-1}\, Q_{m_2}^{-1}\Big)^{|\alpha_1|+|\alpha_2|} \\ &\times \frac{N_{\alpha_1\emptyset}(Q_{m_2}Q_a^{-1}\sqrt{\frac{t}{q}})N_{\emptyset\alpha_1}(Q_{m_1}Q_a\sqrt{\frac{t}{q}})N_{\alpha_2\emptyset}(Q_{m_2}Q_a\sqrt{\frac{t}{q}})N_{\emptyset\alpha_2}(Q_{m_1}Q_a^{-1}\sqrt{\frac{t}{q}})}{N_{\alpha_1\alpha_1}(\sqrt{\frac{t}{q}})N_{\alpha_2\alpha_2}(\sqrt{\frac{t}{q}})N_{\alpha_1\alpha_2}(Q_a^{-2}\sqrt{\frac{t}{q}})N_{\alpha_2\alpha_1}(Q_a^{2}\sqrt{\frac{t}{q}})}\,. \end{aligned} \tag{5.7}$$

which is indeed the partition function of the five-dimensional $\mathcal{N} = 1$ $SU(2)$ gauge theory with $N_f = 2$ [62, 146–148]. This shows that the dimensional reduction of the shifted web Fig. 26 is well behaved at the level of the partition function.

A notable feature of the dimensional reduction of the shifted web is that the rank of the gauge group gets reduced and also the matter representation changes. In contrast, for the unshifted geometry $X_{3,1}$, the resulting five dimensional theory would have the same gauge group and matter representation. By associating weights to the individual $\vartheta_{\mu\nu}$ functions in the partition function, as explained in section 3.5.1, we can analyze how the matter and the vector representation get reduced upon taking $d \to \infty$.

Starting with the vector multiplet contribution (which gives rise to the ϑ-functions in the denominator of the partition function in eq. (5.4)) we have the following weight assignments in terms of Dynkin labels $([\lambda_1], [\lambda_2])$ of $\mathfrak{su}(3)$:

$$\begin{aligned}
&\vartheta_{\alpha_1\alpha_1} \to [0,0]\,, && \vartheta_{\alpha_2\alpha_2} \to [0,0]\,, && \vartheta_{\alpha_3\alpha_3} \to [0,0] \\
&\vartheta_{\alpha_1\alpha_2} \to [2,-1]\,, && \vartheta_{\alpha_2\alpha_3} \to [-1,2]\,, && \vartheta_{\alpha_1\alpha_3} \to [1,1] \\
&\vartheta_{\alpha_2\alpha_1} \to [-2,1]\,, && \vartheta_{\alpha_3\alpha_2} \to [-1,2]\,, && \vartheta_{\alpha_3\alpha_1} \to [-1,-1]
\end{aligned} \tag{5.8}$$

As expected for a vector multiplet, we find the $\mathfrak{su}(3)$ adjoint representation plus a singlet. We can perform a similar analysis for the adjoint hypermultiplet contribution (which gives rise to the ϑ-functions in the numerator of the partition function in eq. (5.4)):

$$\begin{aligned}
&\vartheta_{\alpha_1\alpha_1} \to [0,0]\,, && \vartheta_{\alpha_2\alpha_2} \to [0,0]\,, && \vartheta_{\alpha_3\alpha_3} \to [0,0] \\
&\vartheta_{\alpha_1\alpha_2} \to [2,-1]\,, && \vartheta_{\alpha_2\alpha_3} \to [-1,2]\,, && \vartheta_{\alpha_1\alpha_3} \to [1,1] \\
&\vartheta_{\alpha_2\alpha_1} \to [-2,1]\,, && \vartheta_{\alpha_3\alpha_2} \to [-1,2]\,, && \vartheta_{\alpha_3\alpha_1} \to [-1,-1]
\end{aligned} \tag{5.9}$$

Again, as expected this gives the adjoint representation for the hypermultiplet plus a singlet. We can represent the vector and hypermultiplet representation in the weight lattices, as shown in Fig. 30. The weights that are colored in red, are related to the ϑ-functions whose argument goes to zero upon taking the $5d$ limit. These weights get projected out and we are left with an adjoint $\mathfrak{su}(2)$ representation plus a singlet for the vector multiplet and two fundamental $\mathfrak{su}(2)$ representations for the hypermultiplet. This agrees, as it should, with what one expects at the level of the web-diagram.

5.2 A two parameter series of five dimensional gauge theories

Based upon the previous example, we now describe the general structure of the non-trivial decompactification limit of twisted web diagrams corresponding to $X^{(\delta=B(A+1)-1)}_{A+B+AB,1}$ geometries, shown in Fig. 31, with $A, B \in \mathbb{N}$. Web diagrams of this type are parametrised by $A+B+AB+2$ independent parameters. As a generalization of the pattern observed in the previous examples we conjecture that there exists a one-parameter limit for which

$$H_{1+k(A+1)} \to \infty\,, \qquad V_{B+AB+r} \to \infty\,, \qquad M_{B+AB} \to \infty \qquad \forall \begin{cases} k = 0, \dots, B-1 \\ r = 1, \dots, A \end{cases} \tag{5.10}$$

with the area of the other curves kept fixed. The A vertical, B horizontal and the single diagonal curve that are decompactified in the limit (5.10) are highlighted in red in Fig. 31. The

Vector representation Matter representation

Figure 30: *The vector and matter representation of the* $(3,1)$ *web with shift* $\delta = 1$*. The weights in red get "projected" out upon taking the* 5*d limit. The circles around the weight* $[0,0]$ *indicate that the latter is threefold degenerate.*

resulting web diagram is non-compact and has the form as shown in Fig. 32. It is composed of AB compact divisors $S_{a,b}$ (with $a = 1,\ldots,A$ and $b = 1,\ldots,B$). It is well known that web diagrams of this type [58] engineer linear quiver gauge theories in five dimensions with B gauge nodes of gauge group $U(A+1)$, whose matter content consists of $B-1$ bifundamentals representations and $N_f = 2A$ fundamental representations. We denote these theories by $([U(A+1)]^B, 2A\mathbf{F}, (B-1)\mathbf{BF})$. Hence we see that the latter can be obtained as the five-dimensional limit of the six-dimensional theory with gauge group $U(A+B+AB)$ and matter in the adjoint representation that is engineered from $X^{(\delta=B(A+1)-1)}_{A+A+AB,1}$.

It must however be remarked that the five-dimensional theory is not at the most generic

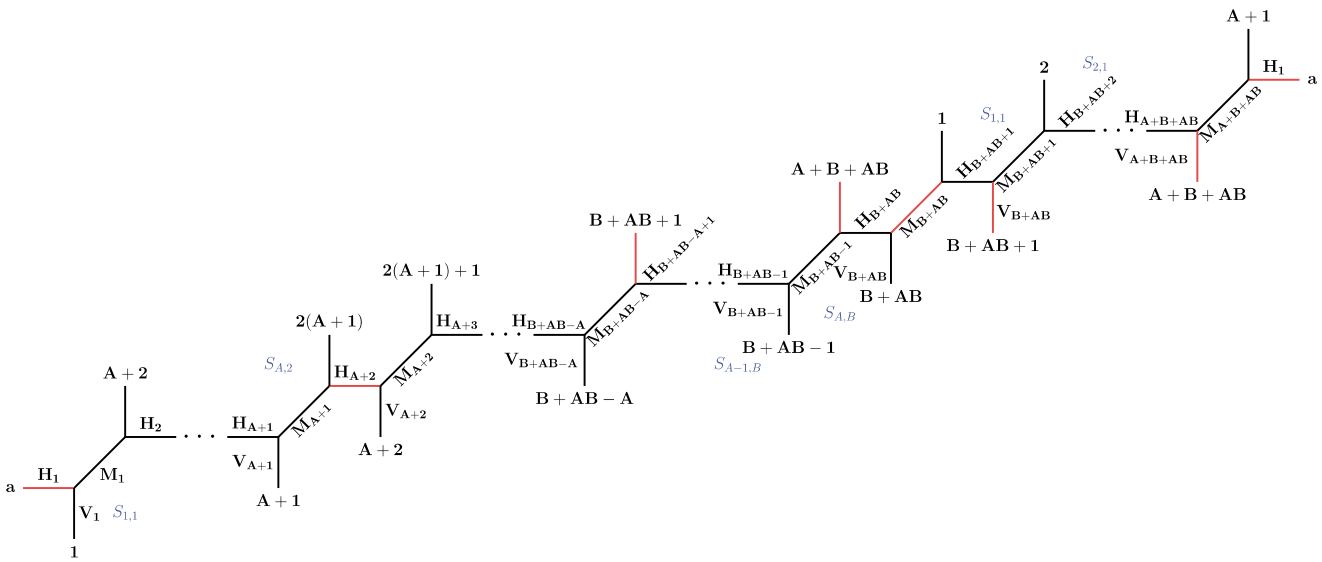

Figure 31: *Web Diagram of* $X^{(\delta=B(A+1)-1)}_{A+B+AB,1}$*. The curves drawn in red are being decompactified in the limit eq.(5.10). The blue labels* $S_{a,b}$ *indicate the same hexagons as in Fig. 32.*

point in moduli space. This can be seen by counting the independent parameters. As already mentioned above, the web diagram in Fig. 31 has a total of $A+B+AB+2$. Upon taking the

five-dimensional limit we get rid of one so the diagram in Fig. 32 has $A + B + AB + 1$. However, the most generic web of this type allows for $AB + 2(A + B) - 1$ independent parameters. Hence, the theories we obtain in the reduction process from six dimensions live in a codimension $A + B - 2$ subspace of the full moduli space. For small values of $N = A + B + AB + 2$, we list some of the non-trivial theories that can be obtained in the limit described above. A noteworthy point is that web diagrams of the same length $'N'$ (but with a different shift δ) can give rise to five-dimensional gauge theories of different rank. From the point of view of six dimensions it seems more natural to give a description of the reduction process in terms of the parameter N. In this description the possible five-dimensional theories include $[U(\frac{N+1}{D})]^{D-1}$ with $D - 2$ bifudamentals and $2(\frac{N+1}{D} - 1)$ fundamentals, where D is any positive non-trivial divisor of $N + 1$. This presentation naturally explains various gaps in table 6. Indeed when $N + 1$ is a prime number there do not exist non-trivial divisors and hence no five-dimensional limit of the type discussed above.

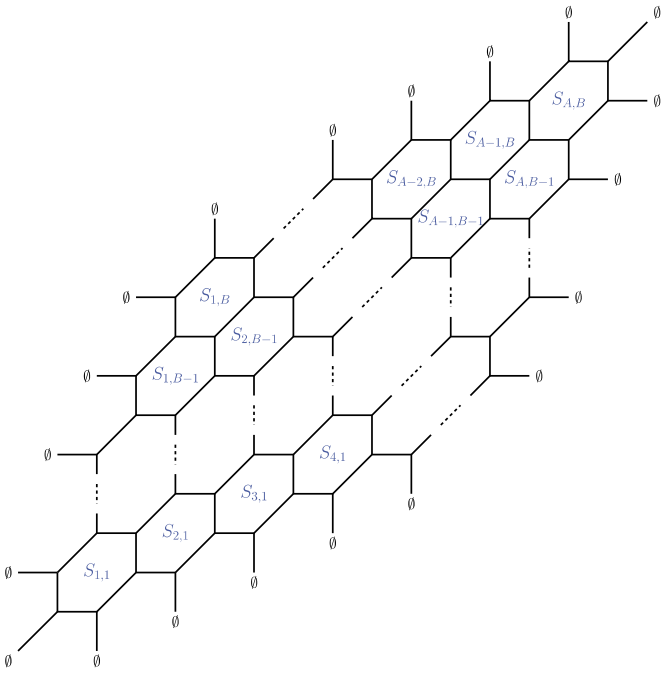

Figure 32: *Web diagram consisting of AB hexagons obtained in the decompactification limit (5.10) from Fig. 31.*

5.3 Summary

The analysis in this section was a natural consequence of the fact shown in section 4.3, namely the existence of gauge theory engineered by shifted web diagrams in the extended Kähler cone. Although our analysis was limited to geometries of the type $X^{(\delta)}_{N,1}$, there should be similar limits for general web diagrams $X^{(\delta)}_{N,M}$. We provided evidence that also these geometries engineer circle compactified theories, the radius of which is controlled by the elliptic parameter according to

	parameters of $X^{(\delta=B(A+1)-1)}_{A+B+AB,1}$			5-dim. gauge theory		
N	A	B	$\delta = B(A+1)-1$	gauge group	**F**	**BF**
3	1	1	1	$SU(2)$	2	0
5	2	1	2	$U(3)$	4	0
	1	2	3	$[U(2)]^2$	2	1
7	3	1	3	$U(4)$	6	0
	1	3	5	$[U(2)]^3$	2	2
8	2	2	5	$[U(3)]^2$	4	1
9	4	1	4	$U(5)$	8	0
	1	4	7	$[U(2)]^4$	2	3
11	5	1	5	$U(6)$	10	0
	3	2	7	$[U(4)]^2$	6	1
	2	3	8	$[U(3)]^3$	4	2
	1	5	9	$[U(2)]^5$	2	4
13	6	1	6	$U(7)$	12	0
	1	6	11	$[U(2)]^6$	2	5
14	4	2	9	$[U(5)]^2$	8	1
	2	4	11	$[U(3)]^4$	4	3
15	7	1	7	$U(8)$	14	0
	3	3	11	$[U(4)]^3$	6	2
	1	7	13	$[U(2)]^7$	2	6

Table 6: Non-trivial five-dimensional limits for $N \leq 15$

(3.11). It would be interesting to investigate this in order to see if one can come up with a similarly clear pattern in the more general case. We also want to emphasize that the limits studied in this section do not provide an exhaustive list. There are certainly the "conventional" limits for the unshifted diagrams, *i.e.* $\delta = 0$. Furthermore, other one-parameter limits can be found that completely break the gauge group from $[U(N)]$ to $[U(1)]^N$ upon dimensional reduction. We did not discuss them as they give rather trivial theories.

6 Dihedral symmetry from dual CY3 folds

In the previous sections we have used the conjecture (proven for the case when the gcd is one) that the partition function $\mathcal{Z}_{N,M}$ is invariant under specific flop transformations in order to establish a web of dualities between the different gauge theories engineered by $X^{(\delta)}_{N,M}$. Based on [47], we will take a different point of view in this section and focus on a single expansion form of the partition function which corresponds to the instanton partition function of a specific theory. For simplicity we work only with periodic strip geometries $X^{(\delta)}_{N,1}$ and we also examine the free energy $\mathcal{F}_{N,1}$, defined in (3.57), rather than the partition function. For the purpose of this discussion we expand the free energy as follows

$$\mathcal{F}_{N,1}(\widehat{a}_{1,\ldots,N}, S, R; \epsilon_1, \epsilon_2) = \sum_{n=0}^{\infty} \sum_{i_1,\ldots,i_N=0}^{\infty} \sum_{k\in\mathbb{Z}} f_{i_1,\ldots,i_N,k,n}(\epsilon_1,\epsilon_2) \widehat{Q}_1^{i_1} \ldots \widehat{Q}_N^{i_N} Q_S^k Q_R^n \tag{6.1}$$

We can combine the invariance under flop with the fact that there a numerous configurations of webs in the extended moduli space of $X_{N,1}$ such that we can associate to them a partition function that has the same gauge theory data, *i.e.* the same number of coupling constants, Coulomb branch and mass parameters respectively and thus give the same expansion form. From the specific relation between the gauge theory parameters and the individual Kähler parameters of the underlying geometry, we can write down a linear transformation relating the different choices of gauge theory parameters that give equivalent expansions

$$(\widehat{a}_1, \ldots, \widehat{a}_N, S, R)^T = G \cdot (\widehat{a}'_1, \ldots, \widehat{a}'_N, S', R')^T \tag{6.2}$$

where G is an invertible $(N+2)\times(N+2)$ matrix with integer entries. As the partition function and hence the free energy are invariant under flops transformations, the matrix G is a symmetry transformation. At the level of the expansion coefficients in (6.1) this means

$$f_{i_1,\ldots,i_N,k,n}(\epsilon_1,\epsilon_2) = f_{i'_1,\ldots,i'_N,k',n'}(\epsilon_1,\epsilon_2) \quad \text{for} \quad (i'_1,\ldots,i'_N,k',n')^T = G^T \cdot (i_1,\ldots,i_N,k,n)^T \tag{6.3}$$

The transposition of G is due to the fact, that the transformation (6.2) is a passive one from the perspective of the coefficients $f_{i_1,\ldots,i_N,k,n}$. Establishing relations of the type (6.2) for a given instanton expansion associated with $X_{N,1}$, thus allows us to extract highly non-trivial symmetries of the free energy and thus also at the level of the engineered theory. These are non-perturbative in nature as they act in a highly non-trivial way on the spectrum of the theory, mixing terms at different orders of the instanton expansion. From the point of view of the BPS counting function of little strings, they completely mix terms in different winding sectors. We also want to emphasize that they are valid for generic values of the deformation parameters ϵ_1 and ϵ_2 of the omega background. As the combination of any of two symmetries has to be itself another symmetry of the partition function, they have the structure of a group which we denote by $\widehat{\mathbb{G}}(N)$. The latter has a natural action on the vector space spanned by the independent Kähler parameters of $X_{N,1}$. In [47], the explicit examples for $N = 1, 2, 3, 4$ have been studied in detail. A pattern emerged from these examples, which made it possible to prove for generic N that $\widehat{\mathbb{G}}(N)$ has at least a subgroup of the form

$$\tilde{\mathbb{G}}(N) \cong \mathbb{G}(N) \times \mathbb{Z}_N \tag{6.4}$$

where the cyclic group $\mathbb{Z}_N$ comes from the fact that due to periodicity of the strip, there are different choices of roots possible, which only differ by cyclic rotation. More specifically, this

reflects the rotational symmetry of the affine Dynkin diagram of $\widehat{\mathfrak{a}}_{N-1}$ as we are free to choose which curves we want to associate with the affine root/node[36]. The factor $\mathbb{G}(N)$ was shown to be isomorphic to the following dihedral groups depending on the value of N

$$\mathbb{G}(N) \cong \begin{cases} \text{Dih}_3 & \text{if} \quad N = 1\,, \\ \text{Dih}_2 & \text{if} \quad N = 2\,, \\ \text{Dih}_3 & \text{if} \quad N = 3\,, \\ \text{Dih}_\infty & \text{if} \quad N \geq 4\,, \end{cases} \tag{6.5}$$

We also give an intuitive explanation at the level of the web diagram for the sudden appearance of the infinite dihedral group for $N \geq 4$. Explicit computational checks of this symmetry structure were performed in [47] for the free energy $\mathcal{F}_{N,1}$ and were all in agreement with the suggested structure. Another point of interest that will be discussed is how the the symmetries mentioned above sit inside the group $Sp(4,\mathbb{Z})$. The latter is the natural group under which genus-two modular objects transform, *i.e.* roughly speaking two modular structures that are compatible with another in a specific way (section 3.5.2). As there are at least two modular structures present in the partition function, which are basically exchanged under fiber base duality, the symmetry group of the partition function is expected to be at least a subgroup of $Sp(4,\mathbb{Z})$. This was also argued for in [48]. Indeed we find for the case $X_{1,1}$, that the symmetries discussed above together with the already present modular structure generate a group which is isomorphic to $Sp(4,\mathbb{Z})$. In the cases $X_{N,1}$ with $N \neq 1$ we conclude that at a special point in moduli space, all the combined symmetries generate at least a subgroup of $Sp(4,\mathbb{Z})$. In order to make this thesis not unnecessarily long, we simply give the specific examples of $N = 1$ and $N = 4$. From there we directly write down the general structure. We refer the reader to [47], for the worked out examples of $N = 2$ and $N = 3$. For simplicity, we denote the sequence of flops and $SL(2,\mathbb{Z})$ transformations introduced in section 4.1 that shifts the external legs by one unit (in the case $\gcd(N,M) = 1$) by $\mathcal{F}$.

6.1 Specific example of $X_{1,1}$

6.1.1 Dualities and Dih_3 Group Action

The first specific example that we provide to illustrate the ideas explained above is the configuration $(N,M) = (1,1)$. The corresponding web diagram is shown in Fig. 33(a). The later can be represented in different equivalent frames through simple $SL(2,\mathbb{Z})$ transformations and by choosing a different fundamental domain for the toric diagram. We show two such frames in Fig. 33(b) and Fig. 33(c).
Each diagram can be parametrised in terms of the parameters (h,v,m) or respectively $(\widehat{a},S,R)$, $(\widehat{a}',S',R')$ or $(\widehat{a}'',S'',R'')$. The latter can be expressed in terms of (h,v,m) as

$$\begin{aligned} \widehat{a} &= h+v\,, & S &= h\,, & R-S &= m\,, \\ \widehat{a}' &= h+m\,, & S' &= m\,, & R'-S' &= v\,, \\ \widehat{a}'' &= h+m\,, & S'' &= h\,, & R''-S'' &= v\,. \end{aligned} \tag{6.6}$$

[36] In section 3.4.1 we remarked that the zero-section divisor does not appear explicitly in the toric diagram. As a consequence the affine root is not singled out and we are free to choose it.

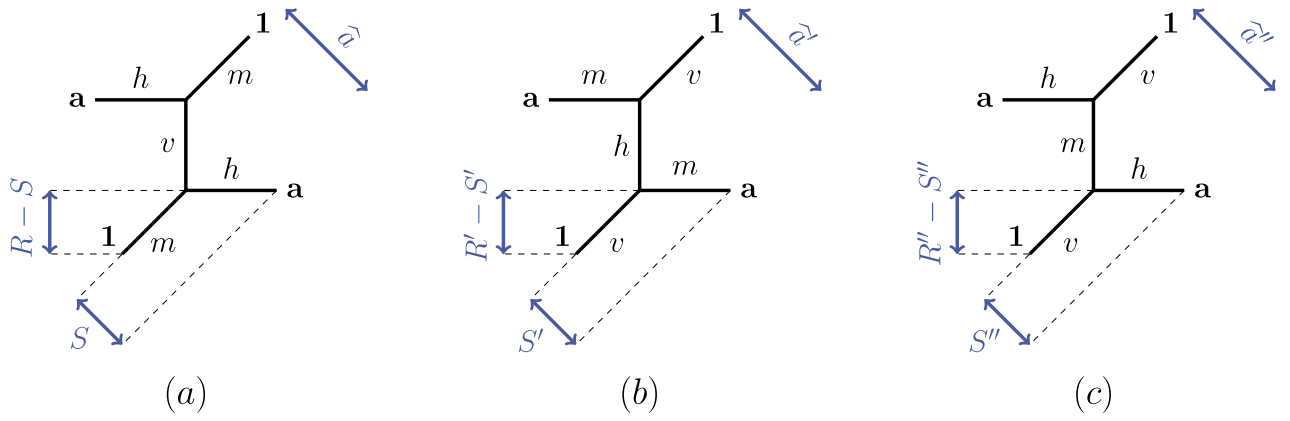

Figure 33: *Three different presentations of the web diagram of $X_{1,1}$ with a parametrisation of the areas of all curves. The parameters (h, v, m) are independent of each other and the blue parameters represent an alternative parametrisation.*

Inverting these relations, (h, v, m) can be expressed as linear combinations of $(\widehat{a}, S, R)$, $(\widehat{a}', S', R')$ or $(\widehat{a}'', S'', R'')$ respectively

$$h = S = \widehat{a}' - S' = S'' \,, \quad v = \widehat{a} - S = R' - S' = R'' - S'' \,, \quad m = R - S = S' = \widehat{a}'' - S'' \,. \tag{6.7}$$

These equations also furnish linear transformations between $(\widehat{a}, S, R)$, $(\widehat{a}', S', R')$ or $(\widehat{a}'', S'', R'')$

$$\begin{pmatrix} \widehat{a} \\ S \\ R \end{pmatrix} = G_1 \cdot \begin{pmatrix} \widehat{a}' \\ S' \\ R' \end{pmatrix} = G_2 \cdot \begin{pmatrix} \widehat{a}'' \\ S'' \\ R'' \end{pmatrix} \,, \quad \text{with} \quad G_1 = \begin{pmatrix} 1 & -2 & 1 \\ 1 & -1 & 0 \\ 1 & 0 & 0 \end{pmatrix} \,, \quad G_2 = \begin{pmatrix} 0 & 0 & 1 \\ 0 & 1 & 0 \\ 1 & 0 & 0 \end{pmatrix} \,. \tag{6.8}$$

The matrix G_1 is of order 3 (*i.e.* $G_1 \cdot G_1 \cdot G_1 = \mathbb{1}_{3\times3}$) while G_2 is of order 2 (*i.e.* $G_2 \cdot G_2 = \mathbb{1}_{3\times3}$). Thus, introducing also the matrices[37]

$$E = \mathbb{1}_{3\times3} \,, \qquad G_3 = G_1 \cdot G_1 \,, \qquad G_4 = G_1 \cdot G_2 \,, \qquad G_5 = G_2 \cdot G_1 \,, \tag{6.9}$$

the ensemble $\mathbb{G}(1) = \{E, G_1, G_2, G_3, G_4, G_5\}$ forms a finite group, whose multiplication table is

	E	G_1	G_2	G_3	G_4	G_5
E	E	G_1	G_2	G_3	G_4	G_5
G_1	G_1	G_3	G_4	E	G_5	G_2
G_2	G_2	G_5	E	G_4	G_3	G_1
G_3	G_3	E	G_5	G_1	G_2	G_4
G_4	G_4	G_2	G_1	G_5	E	G_3
G_5	G_5	G_4	G_3	G_2	G_1	E

(6.10)

from which we can read off $\mathbb{G}(1) = \{E, G_1, G_2, G_3, G_4, G_5\} \cong \mathrm{Dih}_3 \cong S_3$. The latter can be formulated more elegantly as the free group generated by the elements

$$a = G_4 = G_1 \cdot G_2 = \begin{pmatrix} 1 & -2 & 1 \\ 0 & -1 & 1 \\ 0 & 0 & 1 \end{pmatrix} \,, \quad \text{and} \quad b = G_5 = G_2 \cdot G_1 = \begin{pmatrix} 1 & 0 & 0 \\ 1 & -1 & 0 \\ 1 & -2 & 1 \end{pmatrix} \,, \tag{6.11}$$

[37] In the same manner as G_1 and G_2, these matrices can also be read off from web diagrams as in Fig. 33 with a suitable exchange of (h, v, m), which, however, we do not show explicitly.

furnishing the following presentation

$$\mathbb{G}(1) \cong \mathrm{Dih}_3 \cong \left\langle \{a, b | a^2 = b^2 = \mathbb{1}_{3\times 3}, (ab)^3 = \mathbb{1}_{3\times 3}\} \right\rangle . \tag{6.12}$$

6.1.2 Invariance of the Non-perturbative Free Energy

As a check of the fact that G_1 and G_2 as defined in (6.8) are indeed symmetry transformations of $\mathcal{Z}_{1,1}$, we can consider the coefficients in the expansion of the associated free energy $\mathcal{F}_{1,1}$. Indeed, for $N = 1$, the expansion (6.1) takes the specific form

$$\mathcal{F}_{1,1}(\widehat{a}, S, R; \epsilon_1, \epsilon_2) = \sum_{n,i=0}^{\infty} \sum_{k\in\mathbb{Z}} f_{i,k,n}(\epsilon_1, \epsilon_2)\, \widehat{Q}^i\, Q_S^k\, Q_R^n \,, \tag{6.13}$$

with $\widehat{Q} = e^{-\widehat{a}}$. As explained in the beginning of this section, in order for the matrices defined in (6.8) to be a symmetry, the coefficients $f_{i,k,n}(\epsilon_1, \epsilon_2)$ must satisfy

$$f_{i,k,n}(\epsilon_1, \epsilon_2) = f_{i',k',n'}(\epsilon_1, \epsilon_2) \qquad \text{for} \qquad (i', k', n')^T = G_\ell^T \cdot (i, k, n)^T \qquad \ell = 1, 2 \,. \tag{6.14}$$

Below we tabulate examples of coefficients $f_{i,k,n}$ with $i \leq 8$ for $n = 1$, $i \leq 4$ for $n = 2$ and $i \leq 2$ for $n = 3$ that are related by $G_{1,2}$: Table 7 shows the relations for G_1 and Table 8 for G_2.

6.1.3 Modularity and $Sp(4, \mathbb{Z})$ Symmetry

The action of $\mathbb{G}(1)$ as presented in (6.12) combines with the two modular factors $SL(2, \mathbb{Z}) \times SL(2, \mathbb{Z})$ into $Sp(4, \mathbb{Z})$, which is (a subgroup of) the automorphism group of $X_{1,1}$. To see this, instead of considering the action of $\mathbb{G}(1)$ on the vector space spanned by $(\widehat{a}, S, R)$, we consider the vector space spanned by $(\tau = h + v, \rho = m + v, v)$. Arranging the latter in the period matrix

$$\Omega = \begin{pmatrix} \tau & v \\ v & \rho \end{pmatrix} , \tag{6.15}$$

there is a natural action of $Sp(4, \mathbb{Z})$, as reviewed in appendix E. The action of $G_{1,2}$ on Ω is

$$G_1 : \quad \Omega \to \begin{pmatrix} -2v + \rho + \tau & \tau - v \\ \tau - v & \tau \end{pmatrix} , \qquad G_2 : \quad \Omega \to \begin{pmatrix} \tau & \tau - v \\ \tau - v & -2v + \rho + \tau \end{pmatrix} \tag{6.16}$$

Based on this action, we can equivalently represent the action of $\mathbb{G}(1)$ by $G'_{1,2} \in Sp(4, \mathbb{Z})$

$$G'_1 = HK = \begin{pmatrix} 1 & -1 & 0 & 0 \\ 1 & 0 & 0 & 0 \\ 0 & 0 & 0 & -1 \\ 0 & 0 & 1 & 1 \end{pmatrix} , \qquad \text{and} \qquad G'_2 = K = \begin{pmatrix} 1 & 0 & 0 & 0 \\ 1 & -1 & 0 & 0 \\ 0 & 0 & 1 & 1 \\ 0 & 0 & 0 & -1 \end{pmatrix} , \tag{6.17}$$

where K and H are defined as in appendix E. This implies that $\mathbb{G}(1) \subset Sp(4, \mathbb{Z})$. Moreover, combining $\mathbb{G}(1)$ with the $SL(2, \mathbb{Z})_\rho$ symmetry[38] acting on the modular parameter[39] ρ as

$$S_\rho : \quad (\tau, \rho, v) \longmapsto \left(\tau - \tfrac{v^2}{\rho}, -\tfrac{1}{\rho}, \tfrac{v}{\rho}\right) , \qquad T_\rho : \quad (\tau, \rho, v) \longmapsto (\tau, \rho + 1, v) \,, \tag{6.18}$$

[38] Notice that the symmetry group is isomorphic to $SL(2, \mathbb{Z})$ rather than $PSL(2, \mathbb{Z})$, since $S_\rho^2 \neq \mathbb{1}$, as can be seen from the action of S_ρ^2 on the period matrix $\Omega \to \begin{pmatrix} \tau & -v \\ -v & \rho \end{pmatrix}$.

[39] We could equally choose the modular group $SL(2, \mathbb{Z})_\tau$ acting in a similar fashion on the modular parameter τ. More precisely, $SL(2, \mathbb{Z})_\tau$ is generated by $S_\tau = HS_\rho H$ and $T_\tau = HT_\rho H$.

(i,k,n)	(i',k',n')	$f_{i,k,n}(\epsilon_{1,2}) = f_{i',k',n'}(\epsilon_{1,2})$
$(1,0,1)$	$(2,-2,1)$	$\frac{(qt+1)\left(q^2t+q(t+1)^2+t\right)}{(q-1)q(t-1)t}$
$(1,1,1)$	$(3,-3,1)$	$-\frac{(q+1)(t+1)(qt+1)}{(q-1)\sqrt{q}(t-1)\sqrt{t}}$
$(1,2,1)$	$(4,-4,1)$	$\frac{qt+1}{(q-1)(t-1)}$
$(2,-2,1)$	$(1,-2,2)$	$\frac{q^3t^2+q^2t\left(t^2+2t+2\right)+q\left(2t^2+2t+1\right)+t}{(q-1)q(t-1)t}$
$(2,1,1)$	$(4,-5,2)$	$\frac{q^4\left(-t^2\right)(t+1)-q^3t\left(t^3+3t^2+4t+1\right)-q^2\left(t^4+4t^3+7t^2+4t+1\right)-q\left(t^3+4t^2+3t+1\right)-t(t+1)}{(q-1)q^{3/2}(t-1)t^{3/2}}$
$(3,-3,1)$	$(1,-3,3)$	$-\frac{(q+1)(t+1)(qt+1)}{(q-1)\sqrt{q}(t-1)\sqrt{t}}$
$(1,-1,2)$	$(2,-1,1)$	$\frac{q^4\left(-t^2\right)(t+1)-q^3t\left(t^3+3t^2+4t+1\right)-q^2\left(t^4+4t^3+7t^2+4t+1\right)-q\left(t^3+4t^2+3t+1\right)-t(t+1)}{(q-1)q^{3/2}(t-1)t^{3/2}}$
$(1,1,2)$	$(4,-3,1)$	$\frac{q^4\left(-t^2\right)(t+1)-q^3t\left(t^3+3t^2+4t+1\right)-q^2\left(t^4+4t^3+7t^2+4t+1\right)-q\left(t^3+4t^2+3t+1\right)-t(t+1)}{(q-1)q^{3/2}(t-1)t^{3/2}}$
$(1,3,2)$	$(6,-5,1)$	$-\frac{\sqrt{qt}}{(q-1)(t-1)}$
$(2,-3,2)$	$(1,-1,2)$	$\frac{q^4\left(-t^2\right)(t+1)-q^3t\left(t^3+3t^2+4t+1\right)-q^2\left(t^4+4t^3+7t^2+4t+1\right)-q\left(t^3+4t^2+3t+1\right)-t(t+1)}{(q-1)q^{3/2}(t-1)t^{3/2}}$
$(1,-2,3)$	$(2,0,1)$	$\frac{q^5t^3+q^4t^2\left(2t^2+3t+2\right)+q^3t\left(t^4+3t^3+8t^2+6t+2\right)+q^2\left(2t^4+6t^3+8t^2+3t+1\right)+qt\left(2t^2+3t+2\right)+t^2}{(q-1)q^2(t-1)t^2}$
$(1,1,3)$	$(5,-3,1)$	$-\frac{(q+1)(t+1)\left(q^5t^3+q^4t^2(t+1)^2+q^3t\left(t^4+2t^3+6t^2+4t+1\right)+q^2\left(t^4+4t^3+6t^2+2t+1\right)+qt(t+1)^2+t^2\right)}{(q-1)q^{5/2}(t-1)t^{5/2}}$
$(1,2,3)$	$(6,-4,1)$	$\frac{q^5t^3+q^4t^2\left(2t^2+3t+2\right)+q^3t\left(t^4+3t^3+8t^2+6t+2\right)+q^2\left(2t^4+6t^3+8t^2+3t+1\right)+qt\left(2t^2+3t+2\right)+t^2}{(q-1)q^2(t-1)t^2}$
$(1,3,3)$	$(7,-5,1)$	$-\frac{(q+1)(t+1)(qt+1)}{(q-1)\sqrt{q}(t-1)\sqrt{t}}$

Table 7: *Action of G_1: the indices are related by $(i_1', i_2', k', n')^T = G_1^T \cdot (i_1, i_2, k, n)^T$.*

(i,k,n)	(i',k',n')	$f_{i,k,n}(\epsilon_{1,2}) = f_{i',k',n'}(\epsilon_{1,2})$
$(2,-3,1)$	$(1,-3,2)$	$-\frac{\sqrt{qt}}{(q-1)(t-1)}$
$(2,-2,1)$	$(1,-2,2)$	$\frac{q^3t^2+q^2t\left(t^2+2t+2\right)+q\left(2t^2+2t+1\right)+t}{(q-1)q(t-1)t}$
$(2,-1,1)$	$(1,-1,2)$	$\frac{q^4\left(-t^2\right)(t+1)-q^3t\left(t^3+3t^2+4t+1\right)-q^2\left(t^4+4t^3+7t^2+4t+1\right)-q\left(t^3+4t^2+3t+1\right)-t(t+1)}{(q-1)q^{3/2}(t-1)t^{3/2}}$
$(2,0,1)$	$(1,0,2)$	$\frac{q^5t^3+q^4t^2\left(2t^2+3t+2\right)+q^3t\left(t^4+3t^3+8t^2+6t+2\right)+q^2\left(2t^4+6t^3+8t^2+3t+1\right)+qt\left(2t^2+3t+2\right)+t^2}{(q-1)q^2(t-1)t^2}$
$(2,1,1)$	$(1,1,2)$	$\frac{q^4\left(-t^2\right)(t+1)-q^3t\left(t^3+3t^2+4t+1\right)-q^2\left(t^4+4t^3+7t^2+4t+1\right)-q\left(t^3+4t^2+3t+1\right)-t(t+1)}{(q-1)q^{3/2}(t-1)t^{3/2}}$
$(2,2,1)$	$(1,2,2)$	$\frac{q^3t^2+q^2t\left(t^2+2t+2\right)+q\left(2t^2+2t+1\right)+t}{(q-1)q(t-1)t}$
$(2,3,1)$	$(1,3,2)$	$-\frac{\sqrt{qt}}{(q-1)(t-1)}$
$(3,-3,1)$	$(1,-3,3)$	$-\frac{(q+1)(t+1)(qt+1)}{(q-1)\sqrt{q}(t-1)\sqrt{t}}$
$(3,-2,1)$	$(1,-2,3)$	$\frac{q^5t^3+q^4t^2\left(2t^2+3t+2\right)+q^3t\left(t^4+3t^3+8t^2+6t+2\right)+q^2\left(2t^4+6t^3+8t^2+3t+1\right)+qt\left(2t^2+3t+2\right)+t^2}{(q-1)q^2(t-1)t^2}$
$(3,-1,1)$	$(1,-1,3)$	$-\frac{(q+1)(t+1)\left(q^5t^3+q^4t^2(t+1)^2+q^3t\left(t^4+2t^3+6t^2+4t+1\right)+q^2\left(t^4+4t^3+6t^2+2t+1\right)+qt(t+1)^2+t^2\right)}{(q-1)q^{5/2}(t-1)t^{5/2}}$
$(3,1,1)$	$(1,1,3)$	$-\frac{(q+1)(t+1)\left(q^5t^3+q^4t^2(t+1)^2+q^3t\left(t^4+2t^3+6t^2+4t+1\right)+q^2\left(t^4+4t^3+6t^2+2t+1\right)+qt(t+1)^2+t^2\right)}{(q-1)q^{5/2}(t-1)t^{5/2}}$
$(3,2,1)$	$(1,2,3)$	$\frac{q^5t^3+q^4t^2\left(2t^2+3t+2\right)+q^3t\left(t^4+3t^3+8t^2+6t+2\right)+q^2\left(2t^4+6t^3+8t^2+3t+1\right)+qt\left(2t^2+3t+2\right)+t^2}{(q-1)q^2(t-1)t^2}$
$(3,3,1)$	$(1,3,3)$	$-\frac{(q+1)(t+1)(qt+1)}{(q-1)\sqrt{q}(t-1)\sqrt{t}}$
$(1,-3,2)$	$(2,-3,1)$	$-\frac{\sqrt{qt}}{(q-1)(t-1)}$
$(1,-2,2)$	$(2,-2,1)$	$\frac{(qt+1)\left(q^2t+q(t+1)^2+t\right)}{(q-1)q(t-1)t}$
$(1,2,2)$	$(2,2,1)$	$\frac{(qt+1)\left(q^2t+q(t+1)^2+t\right)}{(q-1)q(t-1)t}$
$(1,3,2)$	$(2,3,1)$	$-\frac{\sqrt{qt}}{(q-1)(t-1)}$
$(1,-3,3)$	$(3,-3,1)$	$-\frac{(q+1)(t+1)(qt+1)}{(q-1)\sqrt{q}(t-1)\sqrt{t}}$
$(1,3,3)$	$(3,3,1)$	$-\frac{(q+1)(t+1)(qt+1)}{(q-1)\sqrt{q}(t-1)\sqrt{t}}$

Table 8: *Action of G_2: the indices are related by $(i_1', i_2', k', n')^T = G_2^T \cdot (i_1, i_2, k, n)^T$.*

generates the complete action of $Sp(4,\mathbb{Z})$: the generators (S_ρ, T_ρ) can be expressed as $S_\rho = L^3$ and $T_\rho = L^9HL^{10}H = X_2$. Furthermore, we have $G_2'G_1' = L^5KL^7$ such that we can write

$$\begin{aligned} X_1 &= G_2'G_1'S_\rho^2\,, & X_2 &= T_\rho\,, & X_3 &= S_\rho G_1'G_1'S_\rho\,,\\ X_4 &= G_1'G_2'T_\rho G_1'G_2'\,, & X_5 &= G_1'G_2'S_\rho^2\,, & X_6 &= S_\rho^3G_1'G_2'S_\rho^2G_1'G_2'\,, \end{aligned} \tag{6.19}$$

with $X_{1,2,3,4,5,6}$ defined in (E.2). This indicates that

$$\langle G_1'\,, G_2'\,, S_\rho\,, T_\rho\rangle \supset \langle X_1\,, X_2\,, X_3\,, X_4\,, X_5\,, X_6\rangle \cong Sp(4,\mathbb{Z})\,, \tag{6.20}$$

where the last relation was shown in [149]. From (6.17), using the presentation of $Sp(4,\mathbb{Z})$ given in [150], it follows that

$$\langle G_1'\,, G_2'\,, S_\rho\,, T_\rho\rangle \subset \langle K, L\rangle \cong Sp(4,\mathbb{Z})\,, \tag{6.21}$$

which implies $\langle G_1'\,, G_2'\,, S_\rho\,, T_\rho\rangle \cong Sp(4,\mathbb{Z})$.

6.2 Specific example of $X_{4,1}$

6.2.1 Dualities and Dih_∞ Group Action

As a second example to illustrate the ideas that have been introduced in the beginning of this section, we discuss the case $X_{4,1}$. The web diagram of the latter is shown in Fig. 34 together with an appropriate parametrization. While the examples of $X_{2,1}$ and $X_{3,1}$ we not explicitly discussed in this thesis, we indicated that the group $\tilde{\mathbb{G}}(N)$ in their cases was isomorphic to Dih_2 and Dih_3 respectively. One might thus expect that the order of the group that we find for $X_{4,1}$ is larger, for example Dih_4. It is indeed true that the order grows, however it grows infinitely large and we find Dih_∞. At some later point we give an explanation for this at the level of the web diagram, but first we show that indeed $\mathbb{G}(4)$ is isomorphic to the infinite dihedral group. The consistency conditions stemming from the web diagram are

$$\begin{aligned} &S_1^{(0)}:\ h_2+m_2 = m_1+h_2\,,\ v_1+m_1 = m_2+v_2\,; \quad S_2^{(0)}:\ h_3+m_3 = m_2+h_3\,,\ v_2+m_2 = m_3+v_3\,;\\ &S_3^{(0)}:\ h_4+m_4 = m_3+h_4\,,\ v_3+m_3 = m_4+v_4\,; \quad S_4^{(0)}:\ h_1+m_1 = m_4+h_1\,,\ m_1+v_1 = m_4+v_4\,, \end{aligned} \tag{6.22}$$

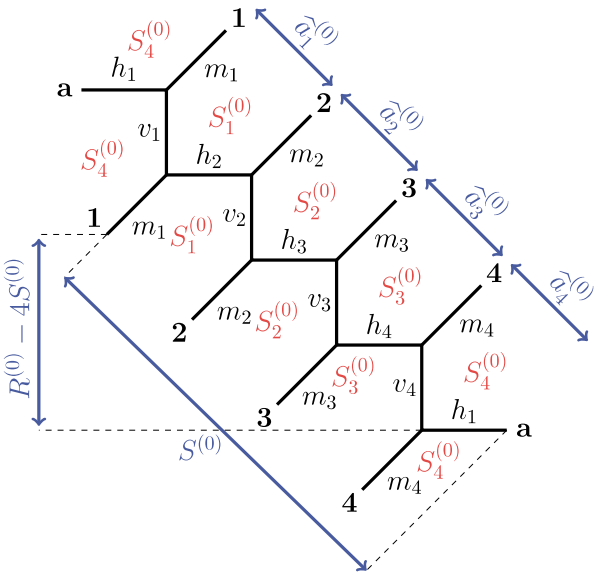

Figure 34: *Web diagram of $X_{4,1}$. An independent set of Kähler parameters is shown in blue.*

while a solution is provided by the parameters $(\widehat{a}_{1,2,3,4}^{(0)}, S^{(0)}, R^{(0)})$

$$\begin{aligned} \widehat{a}_1^{(0)} &= v_1+h_2\,, & \widehat{a}_2^{(0)} &= v_2+h_3\,,\\ \widehat{a}_3^{(0)} &= v_3+h_4\,, & \widehat{a}_4^{(0)} &= v_4+h_1\,,\\ S^{(0)} &= h_2+v_2+h_3+v_3+h_4+v_4+h_1\,,\\ R^{(0)}-4S^{(0)} &= m_1-v_2-v_3-v_4\,. \end{aligned} \tag{6.23}$$

The dihedral group found in the previous example was generated by two transformations, so we try to do the same here. The latter can in fact be obtained in a simple fashion by considering two diagrams that are obtained from Fig. 34 through a rearrangement and a flop transformation respectively:

1) rearrangement:

A simple rearrangement of Fig. 34 is shown in Fig. 35(a). The parametrisation in terms of $(\widehat{a}^{(1)}_{1,2,3,4}, S^{(1)}, R^{(1)})$ as indicated in the Fig. 35(b) is distinct to the one in Fig. 34 by $(\widehat{a}^{(0)}_{1,2,3,4}, S^{(0)}, R^{(0)})$. Indeed, the two bases are related through a linear transformation given by

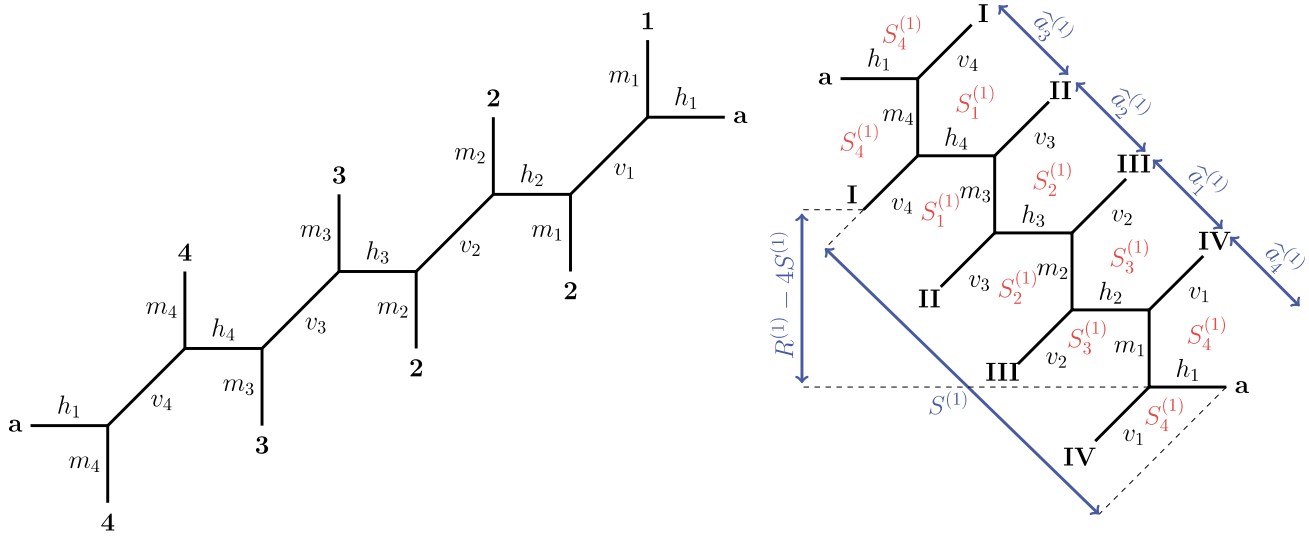

(a) (b)

Figure 35: *(a) mirrored web diagram Fig. 34 after an $SL(2,\mathbb{Z})$ transformation. (b) Same diagram after cutting the lines $v_{1,2,3,4}$ and re-gluing the lines $m_{1,2,3,4}$ (and performing an $SL(2,\mathbb{Z})$ transformation).*

$$\begin{pmatrix} \widehat{a}^{(0)}_1 \\ \widehat{a}^{(0)}_2 \\ \widehat{a}^{(0)}_3 \\ \widehat{a}^{(0)}_4 \\ S^{(0)} \\ R^{(0)} \end{pmatrix} = G_1 \cdot \begin{pmatrix} \widehat{a}^{(1)}_1 \\ \widehat{a}^{(1)}_2 \\ \widehat{a}^{(1)}_3 \\ \widehat{a}^{(1)}_4 \\ S^{(1)} \\ R^{(1)} \end{pmatrix}, \qquad \text{where} \qquad G_1 = \begin{pmatrix} 3 & 2 & 2 & 2 & -6 & 1 \\ 2 & 3 & 2 & 2 & -6 & 1 \\ 2 & 2 & 3 & 2 & -6 & 1 \\ 2 & 2 & 2 & 3 & -6 & 1 \\ 6 & 6 & 6 & 6 & -17 & 3 \\ 16 & 16 & 16 & 16 & -48 & 9 \end{pmatrix}. \tag{6.24}$$

The matrix G_1 satisfies $\det G_1 = -1$ and $G_1^2 = \mathbb{1}_{6\times 6}$.

2) transformation $\mathcal{F}$:

Another symmetry transformation can be obtained after performing suitable flop transformations on Fig. 34 that rotate the external legs. The resulting diagrams is shown in Fig. 36.

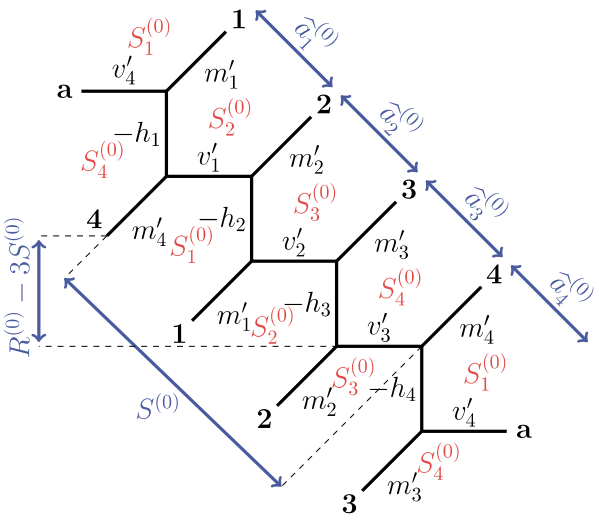

Figure 36: *Web diagram after suitable flop transformations of Fig. 34. The blue parameters are the same as defined in eq. (6.23).*

Here we have introduced the variables

$$\begin{aligned} v_1' &= v_1 + h_1 + h_2\,, & m_1' &= m_1 + h_1 + h_2\,,\\ v_2' &= v_2 + h_2 + h_3\,, & m_2' &= m_2 + h_2 + h_3\,,\\ v_3' &= v_3 + h_3 + h_4\,, & m_3' &= m_3 + h_3 + h_4\,,\\ v_4' &= v_4 + h_4 + h_1\,, & m_4' &= m_4 + h_4 + h_1\,. \end{aligned} \tag{6.25}$$

The parameters $(\widehat{a}^{(0)}_{1,2,3,4}, S^{(0)}, R^{(0)})$, shown in blue in Fig. 36 are the same as those appearing in Fig. 36, such that the flop transformation alone does not lead to a non-trivial symmetry transformation. However, starting from the web diagram Fig. 36, we can present it in the form of Fig. 37. The parametrisation in terms

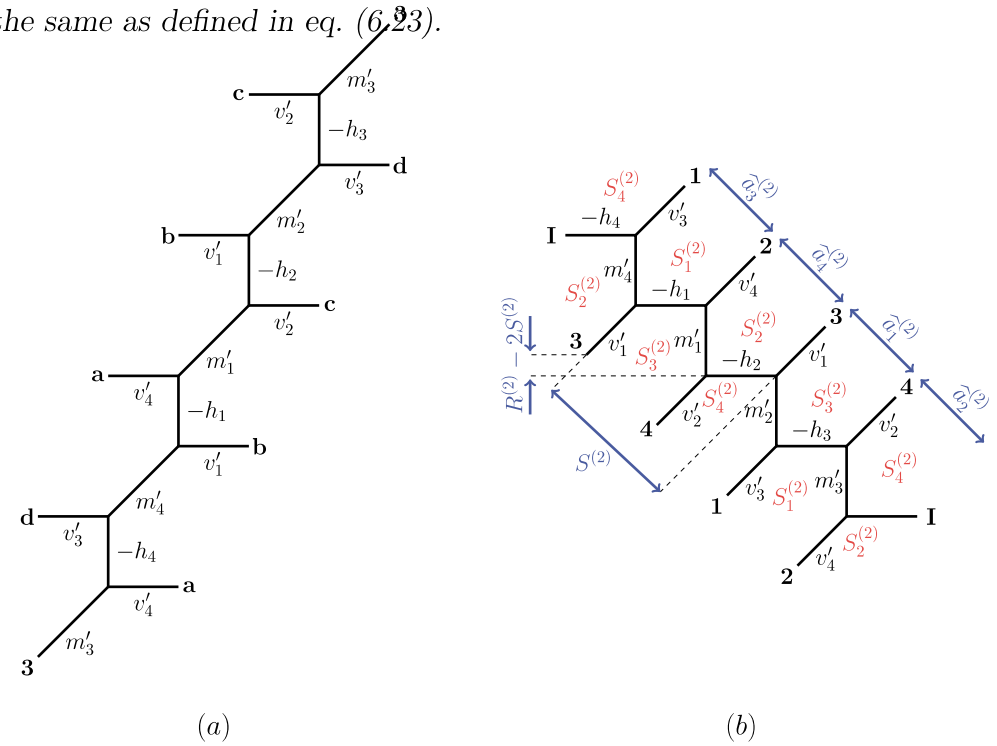

(a) (b)

Figure 37: *(a) web diagram Fig. 36 after cutting the lines $m'_{1,2,3,4}$ and re-gluing along the lines $v'_{1,2,3,4}$. (b) presentation of the web diagram after cutting along the line $-h_4$ and gluing m'_3.*

of the variables $(\widehat{a}^{(2)}_{1,2,3,4}, S^{(2)}, R^{(2)})$ used in Fig. 37(b) can be related to $(\widehat{a}^{(0)}_{1,2,3,4}, S^{(0)}, R^{(0)})$

in Fig. 34 through the transformation

$$\begin{pmatrix} \widehat{a}_1^{(0)} \\ \widehat{a}_2^{(0)} \\ \widehat{a}_3^{(0)} \\ \widehat{a}_4^{(0)} \\ S^{(0)} \\ R^{(0)} \end{pmatrix} = G_2 \cdot \begin{pmatrix} \widehat{a}_1^{(2)} \\ \widehat{a}_2^{(2)} \\ \widehat{a}_3^{(2)} \\ \widehat{a}_4^{(2)} \\ S^{(2)} \\ R^{(2)} \end{pmatrix}, \qquad \text{where} \qquad G_2 = \begin{pmatrix} 1 & 0 & 0 & 0 & -2 & 1 \\ 0 & 1 & 0 & 0 & -2 & 1 \\ 0 & 0 & 1 & 0 & -2 & 1 \\ 0 & 0 & 0 & 1 & -2 & 1 \\ 1 & 1 & 1 & 1 & -7 & 3 \\ 4 & 4 & 4 & 4 & -24 & 9 \end{pmatrix}. \tag{6.26}$$

The matrix G_2 has $\det G_2 = 1$ but does not have finite order.[40] This implies that the matrices G_1 and G_2 freely generate the group Dih_∞

$$\mathbb{G}(4) = \langle \{G_1, G_2 \cdot G_1\} \rangle \cong \mathrm{Dih}_\infty \,. \tag{6.28}$$

[40] Indeed, by complete induction one can show that

$$G_2^n = \mathbb{1}_{6\times 6} + n \begin{pmatrix} n-1 & n-1 & n-1 & n-1 & 2-4n & n \\ n-1 & n-1 & n-1 & n-1 & 2-4n & n \\ n-1 & n-1 & n-1 & n-1 & 2-4n & n \\ n-1 & n-1 & n-1 & n-1 & 2-4n & n \\ 2n-1 & 2n-1 & 2n-1 & 2n-1 & -8n & 2n+1 \\ 4n & 4n & 4n & 4n & -8(2n+1) & 4(n+1) \end{pmatrix}, \qquad \text{for} \qquad n \in \mathbb{N}\,. \tag{6.27}$$

which only resembles the identity matrix for $n = 0$.

6.2.2 A Remark on Infinite Order

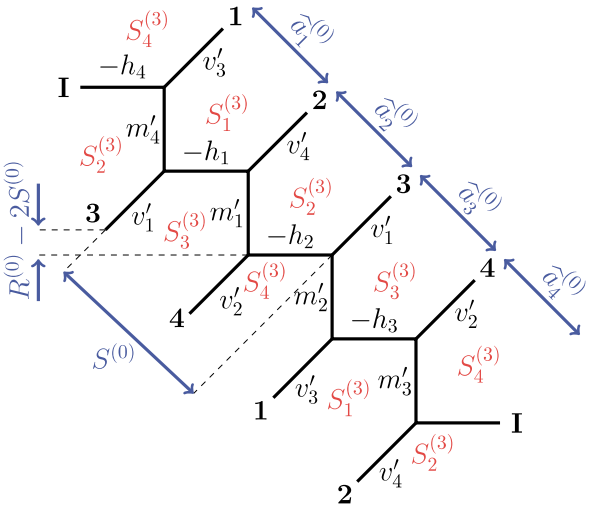

Figure 38: *Web diagram after two transformations $\mathcal{F}$ of Fig. 34. The blue parameters are the same as defined in eq. (6.23).*

We have seen in the previous section that the symmetry transformation G_2 is of infinite order, which is markedly different than what we have seen in the previous example. While we will present explicit checks that G_2 is indeed a symmetry of the free energy in the next subsection, we first want to provide an intuitive explanation of what makes the case $(N,1) = (4,1)$ different than the cases $N = 1,2,3$. Indeed, we will provide some indication that the extended moduli space of $X_{4,1}$ contains many more regions that are represented by (a priori) very different looking web diagrams. While this will not prove that G_2 is of infinite order (as we have already done in the previous section by purely algebraic means), it will indicate the novel aspect of $X_{4,1}$ (in comparison to the previous examples).

Returning to Fig. 37(b), the latter is a web diagram of the form $X_{4,1}^{(\delta=2)}$. Another way of obtaining such a diagram is to perform two transformations of the form $\mathcal{F}$ on Fig. 34, as is shown in Fig. 38, with the new parameters

$$h_1' = -h_1 + v_1' + v_4' = h_1 + h_2 + h_4 + v_1 + v_4\,, \quad h_2' = -h_2 + v_1' + v_2' = h_1 + h_2 + h_3 + v_1 + v_2\,,$$
$$h_3' = -h_3 + v_2' + v_3' = h_2 + h_3 + h_4 + v_2 + v_3\,, \quad h_4' = -h_4 + v_3' + v_4' = h_1 + h_3 + h_4 + v_3 + v_4\,,$$

as well as

$$\begin{aligned} m_1'' &= m_1' + v_4' + v_2' = 2h_1 + 2h_2 + h_3 + h_4 + m_1 + v_2 + v_4\,,\\ m_2'' &= m_2' + v_1' + v_3' = h_1 + 2h_2 + 2h_3 + h_4 + m_2 + v_1 + v_3\,,\\ m_3'' &= m_3' + v_2' + v_4' = h_1 + h_2 + 2h_3 + 2h_4 + m_3 + v_2 + v_4\,,\\ m_4'' &= m_4' + v_4' + v_1' = 2h_1 + h_2 + h_3 + 2h_4 + m_4 + v_1 + v_3\,. \end{aligned}$$

Notice that even upon imposing the consistency conditions (6.22), the parametrisation of the web diagram Fig. 38 is different than the one of the web diagram Fig. 37(b).[41] Thus, there is a duality transformation that transforms the web $X_{4,1}^{(2)} \longmapsto X_{4,1}^{(2)}$, however, with a non-trivial duality map $\mathcal{D}$ acting on the areas of all curves involved. The duality $\mathcal{D}$ can be repeatedly applied to $X_{4,1}^{(2)}$ in Fig. 37(b), thus producing an infinite number of diagrams of the type $X_{4,1}^{(2)}$, each one with an a priori different parametrisation of individual curves.

Moreover, since the blue parameters $(\widehat{a}_{1,2,3,4}^{(0)}, S^{(0)}, R^{(0)})$ in Fig. 38 are the same as in Fig. 34, the duality map $\mathcal{D}$ from the perspective of the independent Kähler parameters precisely corresponds to the symmetry transformation G_2. Therefore, the transition from Fig. 38 to Fig. 37(b) gives (a new) geometric representation of G_2 at the level of web diagrams, which readily allows to also compute arbitrary powers of G_2. The above discussion does not generalise to the cases

[41] This can be seen by choosing the solution $v_1 = v_2 = v_3 = v_4 = v$ and $m_1 = m_2 = m_3 = m_4 = m$.

$N = 2, 3$ (but can be extended to $N > 4$). Indeed, web diagrams with shifts $\delta \geq 2$ for $N = 2, 3$ can readily be related (possibly through simple cutting and re-gluing operations) to web diagrams with $\delta \in \{0, 1\}$, which only gave rise to symmetry transformations of finite order. In other words, in the cases $N = 2, 3$, the equivalents of the diagrams Fig. 37 and Fig. 38 are of the type $\delta \leq 1$, which we have seen to provide only transformations of finite order.

6.2.3 Invariance of the Non-perturbative Free Energy

As non-trivial check for the fact that G_1 and G_2 are indeed symmetries of $\mathcal{Z}_{4,1}$, we consider the non-perturbative free energy associated with the latter. For simplicity, we restrict ourselves to the leading term in $\epsilon_{1,2}$. To this end, we define

$$\lim_{\epsilon_{1,2}\to 0} \epsilon_1\, \epsilon_2\, \mathcal{F}_{4,1}(\widehat{a}_{1,2,3,4}, S, R; \epsilon_1, \epsilon_2) = \sum_{n,i_a=0}^{\infty} \sum_{k\in\mathbb{Z}} f^{\text{NS}}_{i_1,i_2,i_3,i_4,k,n}\, \widehat{Q}_1^{i_1}\, \widehat{Q}_2^{i_2}\, \widehat{Q}_3^{i_3}\, \widehat{Q}_3^{i_4}\, Q_S^k\, Q_R^n\,, \tag{6.29}$$

where $f^{\text{NS}}_{i_1,i_2,i_3,i_4,k,n} \in \mathbb{Z}$ and $\widehat{Q}_i = e^{-\widehat{a}_i}$ (for $i = 1, 2, 3, 4$), $Q_S = e^{-S}$ and $Q_R = e^{-R}$. The symmetry transformations G_1 and G_2 act in the following manner on the coefficients $f^{\text{NS}}_{i_1,i_2,i_3,i_4,k,n}$

$$f^{\text{NS}}_{i_1,i_2,i_3,i_4,k,n} = f^{\text{NS}}_{i'_1,i'_2,i'_3,i'_4,k',n'} \quad \text{for} \quad (i'_1, i'_2, i'_3, i'_4, k', n')^T = G_\ell^T \cdot (i_1, i_2, i_3, i_4, k, n)^T \quad \forall \ell = 1, 2\,. \tag{6.30}$$

We can explicitly check the relations (6.30) by computing the relevant expansions of the free energies. However, since the matrix G_1 in (6.24) contains very large numbers, the relations are easier to check for the matrices $G_1 \cdot G_2$ and G_2 with

$$G_1 \cdot G_2 = \begin{pmatrix} 1 & 0 & 0 & 0 & 0 & 0 \\ 0 & 1 & 0 & 0 & 0 & 0 \\ 0 & 0 & 1 & 0 & 0 & 0 \\ 0 & 0 & 0 & 1 & 0 & 0 \\ 1 & 1 & 1 & 1 & -1 & 0 \\ 4 & 4 & 4 & 4 & -8 & 1 \end{pmatrix}. \tag{6.31}$$

In Table 9 and Table 10 we tabulate examples of coefficients $f^{\text{NS}}_{i_1,i_2,i_3,i_4,k,n}$ with $i_1+i_2+i_3+i_4 \leq 6$ for $n = 1$ and $n = 2$ that are related by $G_1 \cdot G_2$ and G_2 respectively.

6.2.4 Modularity at a Particular Point of the Moduli Space

Similarly to the case $N = 1$, we can analyse how the group $\mathbb{G}(4)$ is related to $Sp(4, \mathbb{Z})$ at the particular region in the moduli space, which is characterized by $\widehat{a}_1^{(0)} = \widehat{a}_2^{(0)} = \widehat{a}_3^{(0)} = \widehat{a}_4^{(0)} = \widehat{a}$, which implies $h_1 = h_2 = h_3 = h_4 = h$ (while the consistency conditions (**??**) impose $v_1 = v_2 = v_3 = v_4 = v$ and $m_1 = m_2 = m_3 = m_4 = m$). We can introduce the period matrix

$$\Omega = \begin{pmatrix} \tau & v \\ v & \rho \end{pmatrix}, \qquad \text{with} \qquad \begin{aligned} \tau &= m + v\,, \\ \rho &= h + m\,. \end{aligned} \tag{6.32}$$

$(i_1, i_2, i_3, i_4, k, n)$	$(i'_1, i'_2, i'_3, i'_4, k', n')$	$f^{\rm NS}_{i_1,i_2,i_3,i_4,k,n}$
$(0, 0, 1, 0, -2, 1)$	$(2, 2, 2, 3, -6, 1)$	2
$(0, 0, 1, 0, -1, 1)$	$(3, 3, 4, 3, -7, 1)$	-8
$(0, 0, 1, 1, -3, 1)$	$(1, 1, 2, 2, -5, 1)$	-1
$(0, 0, 1, 2, -2, 1)$	$(2, 2, 3, 4, -6, 1)$	18
$(0, 0, 1, 2, -1, 1)$	$(3, 3, 4, 5, -7, 1)$	-45
$(0, 0, 1, 3, -3, 1)$	$(1, 1, 2, 4, -5, 1)$	-5
$(0, 0, 1, 3, -2, 1)$	$(2, 2, 3, 5, -6, 1)$	30
$(0, 0, 1, 4, -3, 1)$	$(1, 1, 2, 5, -5, 1)$	-7
$(0, 0, 1, 4, -2, 1)$	$(2, 2, 3, 6, -6, 1)$	42
$(0, 0, 1, 5, -3, 1)$	$(1, 1, 2, 6, -5, 1)$	-9
$(0, 0, 1, 5, -2, 1)$	$(2, 2, 3, 7, -6, 1)$	54
$(0, 0, 0, 6, -2, 1)$	$(2, 2, 2, 8, -6, 1)$	12

Table 9: *Action of* $G_1 \cdot G_2$*:* $(i'_1, i'_2, i'_3, i'_4, k', n')^T = (G_1 \cdot G_2)^T \cdot (i_1, i_2, i_3, i_4, k, n)^T$.

$(i_1, i_2, i_3, i_4, k, n)$	$(i'_1, i'_2, i'_3, i'_4, k', n')$	$f^{\rm NS}_{i_1,i_2,i_3,i_4,k,n}$
$(0, 0, 1, 1, -3, 1)$	$(1, 1, 2, 2, -7, 2)$	-1
$(0, 1, 2, 2, -4, 1)$	$(0, 1, 1, 2, -6, 2)$	2
$(1, 1, 1, 2, -4, 1)$	$(1, 1, 1, 2, -6, 2)$	4
$(1, 1, 2, 3, -5, 1)$	$(0, 0, 1, 2, -3, 1)$	-3
$(1, 1, 2, 4, -5, 1)$	$(0, 0, 1, 3, -5, 2)$	-5
$(1, 1, 3, 3, -5, 1)$	$(0, 0, 2, 2, -5, 2)$	-4

Table 10: *Action of* G_2*:* $(i''_1, i''_2, i''_3, i''_4, k'', n')^T = G_2^T \cdot (i_1, i_2, i_3, i_4, k, n)^T$.

Using the parametrisation (6.28) of $\mathbb{G}(4)$, it is sufficient to analyse the relation of the generators G_1 and $G_2' = G_2 \cdot G_1$ to $Sp(4,\mathbb{Z})$. The restriction of these generators to the subspace $(\widehat{a}, S, R)$ can be written in the form

$$G_1^{(\text{red})} = \begin{pmatrix} 1 & -2 & 1 \\ 0 & -1 & 1 \\ 0 & 0 & 1 \end{pmatrix}, \qquad \text{and} \qquad G_2'^{,(\text{red})} = \begin{pmatrix} 1 & 0 & 0 \\ 4 & -1 & 0 \\ 16 & -8 & 1 \end{pmatrix}, \tag{6.33}$$

Rewriting them furthermore to act as elements of $Sp(4,\mathbb{Z})$ in the form of (E.3) on the period matrix Ω in (6.32), they take the form

$$\widetilde{G}_1^{(\text{red,Sp})} = HKL^6KL^6HKHL^6KL^6KH\,, \quad \text{and} \quad \widetilde{G}_2'^{,(\text{red,Sp})} = HKL^6KL^6KL^6KH\,, \tag{6.34}$$

where K, L and H are defined in appendix E. As in the cases of $N = 2, 3$, this implies that the restriction of $\mathbb{G}(3)$ to the particular region of the Kähler moduli space $(\widehat{a}, S, R)$ is a subgroup of $Sp(4,\mathbb{Z})$. However, unlike the case $N = 1$, we cannot conclude that the freely generated group $\langle \widetilde{G}_1^{(\text{red,Sp})}, \widetilde{G}_2'^{,(\text{red,Sp})}, S_\rho, T_\rho, S_\tau, T_\tau \rangle$ is isomorphic to $Sp(4,\mathbb{Z})$.

6.3 General pattern

We show a general web diagram for $X_{N,1}^{(\delta)}$ with a suitable prametrization in 39. The $2N$ consistency conditions are given by

$$h_i + m_i = h_i + m_{i+1} \quad , \quad v_i + m_i = v_{i+\delta} + m_{i+1}\,, \tag{6.35}$$

where $m_{i+N} = m_i$ and $v_{i+N} = v_i$.

6.3.1 Symmetry Transformations of Generic Webs

We can summarise all previous examples by introducing the following matrices

$$\mathcal{G}_2(N) = \begin{pmatrix} & & & 0 & 0 \\ & \mathbb{1}_{N\times N} & & \vdots & \vdots \\ & & & 0 & 0 \\ 1 & \cdots & 1 & -1 & 0 \\ N & \cdots & N & -2N & 1 \end{pmatrix}, \tag{6.36}$$

as well as

$$\mathcal{G}_\infty(N) = \begin{pmatrix} & & & -2 & 1 \\ & \mathbb{1}_{N\times N} & & \vdots & \vdots \\ & & & -2 & 1 \\ 1 & \cdots & 1 & -2N+1 & N-1 \\ N & \cdots & N & -2N(N-1) & (N-1)^2 \end{pmatrix}. \tag{6.37}$$

The matrices $\mathcal{G}_2(N)$ and $\mathcal{G}_\infty(N)$ for the examples corresponding to $N = 1, 2, 3, 4$ are given explicitly as

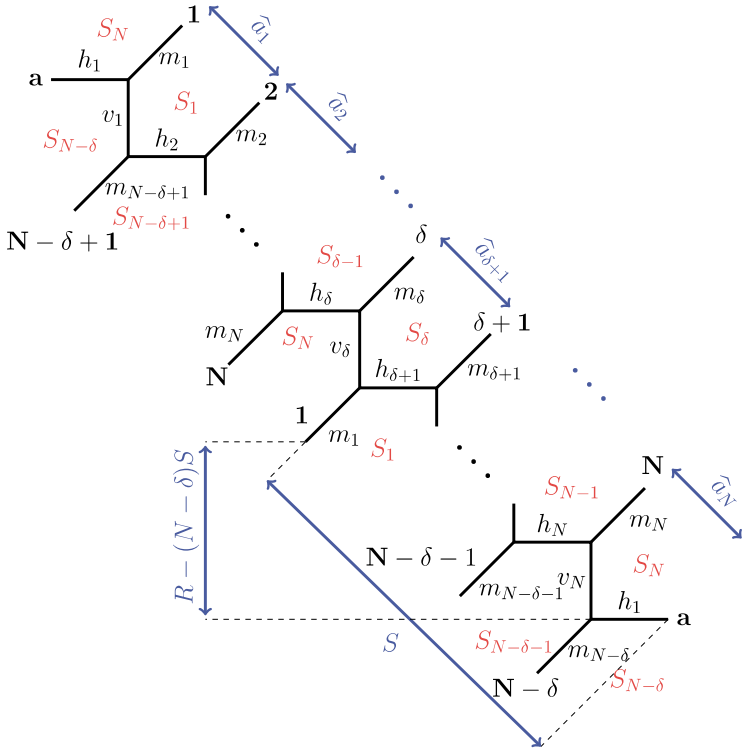

Figure 39: *Web diagram of* $X^{(\delta)}_{N,1}$.

N	$\mathcal{G}_2(N)$	$\mathcal{G}_\infty(N)$	**defined in**
1	b	G_1	eq. (6.11) and eq. (6.8)
2	G_2	G_3	eq. (4.6) and eq. (4.12) in [47]
3	G_3	$G_3 \cdot G_2$	eq. (5.10) and eq. (5.14) in [47]
4	$G_1 \cdot G_2$	G_2	eq. (6.24) and eq. (6.26)

where the equation numbers refer to the definitions of the matrices in the individual cases. The matrices $\mathcal{G}_2$ and $\mathcal{G}_\infty(N)$ furnish two symmetry relations for a web diagram of the type $(N, 1)$. To see this, in the following we shall check explicitly the combinations of $\mathcal{G}_\infty(N) \cdot \mathcal{G}_2(N)$ and $\mathcal{G}_\infty(N)$, which at the level of the web diagrams are generated by the same transformations we already discussed in the example of $(N, 1) = (4, 1)$ and which can be generalized for generic N:

1) rearrangement:

We first verify that $\mathcal{G}_\infty(N) \cdot \mathcal{G}_2(N)$ is a symmetry. To this end, we start from the configuration shown in Fig. 39 for $\delta = 0$, which (after mirroring and performing an $SL(2, \mathbb{Z})$ transformation) can be presented as in Fig. 40(a). The latter in turn can alternatively be presented in the form. Fig. 40(b). The matrix $\mathcal{G}_\infty(N) \cdot \mathcal{G}_2(N)$ (defined in (6.36) and (6.37) respectively) relates the parameters in the web diagram Fig. 39 to those in Fig. 40(b) in the following way

$$(\widehat{a}_1\,, \ldots\,, \widehat{a}_N\,, S\,, R)^T = \mathcal{G}_2(N) \cdot \mathcal{G}_\infty(N) \cdot (\widehat{a}'_1\,, \ldots\,, \widehat{a}'_N\,, S'\,, R')^T\,, \tag{6.38}$$

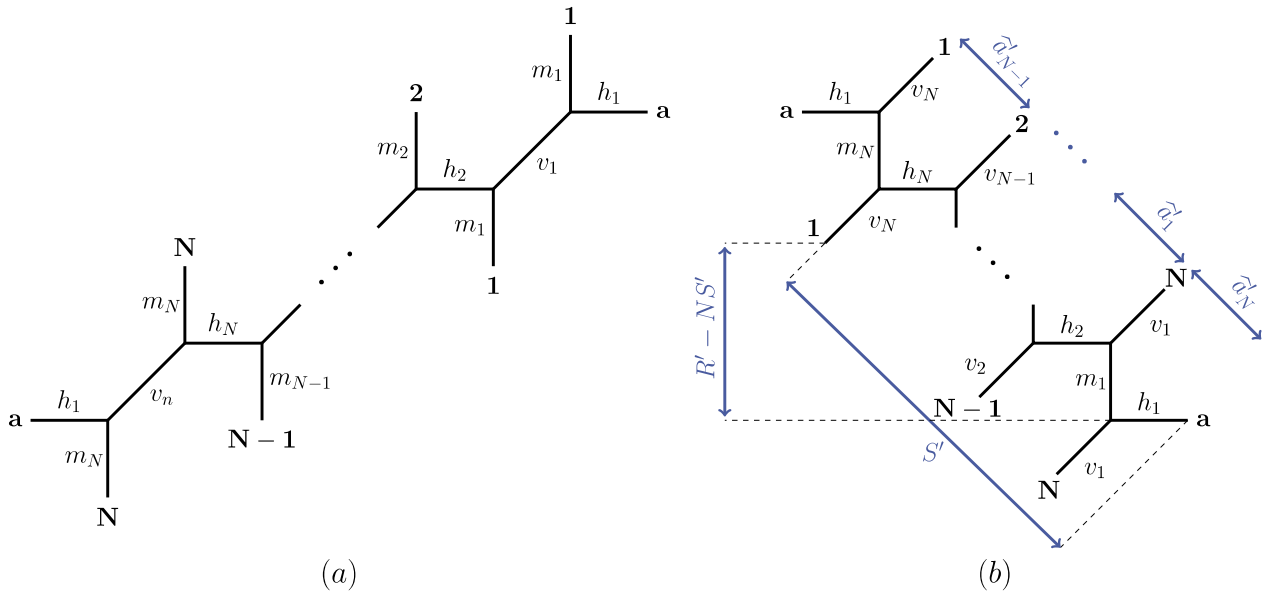

(a) (b)

Figure 40: *Two alternative presentations of the web diagram of* $X^{(\delta=0)}_{N,1}$ *from 39.*

where

$$\mathcal{G}_\infty(N)\cdot\mathcal{G}_2(N) = \begin{pmatrix} & \mathbb{A}_{N\times N} & & -2N+2 & 1 \\ & & & \vdots & \vdots \\ & & & -2N+2 & 1 \\ N^2-3N+2 & \cdots & N^2-3N+2 & -2N^2+4N-1 & N-1 \\ N(N-2)^2 & \cdots & N(N-2)^2 & -2N(2-3N+N^2) & (N-1)^2 \end{pmatrix}, \tag{6.39}$$

with $\mathbb{A}_{N\times N} = (N-2)\begin{pmatrix} 1 & \cdots & 1 \\ \vdots & & \vdots \\ 1 & \cdots & 1 \end{pmatrix} + \mathbb{1}_{N\times N}$. Upon using the following solution of the consistency conditions in (6.35)

$$v_1 = v_2 = \ldots = v_N = v\,, \qquad \text{and} \qquad m_1 = m_2 = \ldots = m_N = m\,, \tag{6.40}$$

which implies from Fig. 39 and Fig. 40(b) (for $i = 1,\ldots,N$)

$$\begin{aligned} &\widehat{a}_i = h_{i+1} + v\,, && \widehat{a}'_i = h_{i+1} + m \\ &S = \sum_{k=1}^{N} h_k + (N-1)v\,, && S' = \rho' - m = \sum_{k=1}^{N}\widehat{a}'_k = \sum_{k=1}^{N} h_k + (N-1)m\,, \\ &R - NS = m - (N-1)v\,, && R' - NS' = v - (N-1)m\,, \end{aligned} \tag{6.41}$$

we have indeed (with $\rho' = \sum_{k=1}^{N}\widehat{a}'_k = \sum_{k=1}^{N} h_k + Nm$)

$$\widehat{a}_i = \widehat{a}'_i + (N-2)\rho' - (2N-2)S' + R' = h_{i+1} + v\,,$$

$$S = (N^2-3N+2)\rho' - (2N^2-4N+1)S' + (N-1)R' = \sum_{k=1}^{N} h_k + (N-1)v\,,$$

$$R = N(N-2)^2\rho' - 2N(2-3N+N^2)S' + (N-1)^2R' = N\sum_{k=1}^{N} h_k + m + (N-1)^2 v\,,$$

which proves (6.38).

2) transformation $\mathcal{F}$:

In a similar fashion we can show that $\mathcal{G}_\infty(N)$ is a symmetry transformation. To this end, we first consider a transformation of the type $\mathcal{F}$ acting on the web diagram Fig. 39 for $\delta = 0$ which results in the web diagram shown in Fig. 41, representing $X^{(\delta=1)}_{N,1}$. The blue parameters in Fig. 41

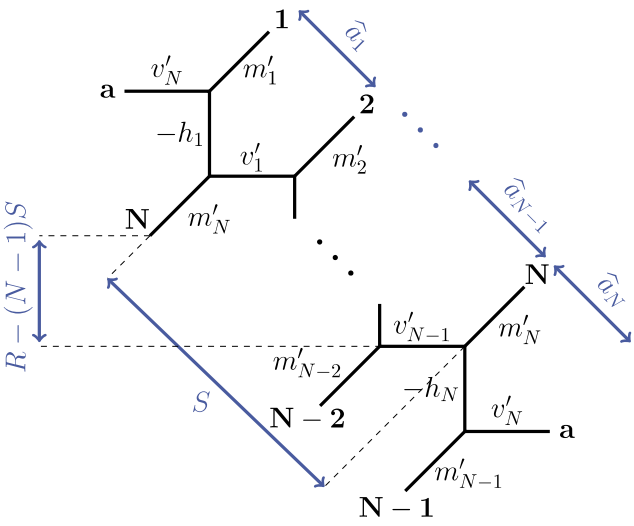

Figure 41: *Web diagram of* $X^{(1)}_{N,1}$.

are the same as in Fig. 39, while we also have introduced

$$\begin{aligned} v'_1 &= v_1 + h_1 + h_2\,, & m'_1 &= m_1 + h_1 + h_2\,,\\ v'_2 &= v_2 + h_2 + h_3\,, & m'_2 &= m_2 + h_2 + h_3\,,\\ &\vdots & &\vdots\\ v'_N &= v_N + h_N + h_1\,, & m'_N &= m_N + h_N + h_1\,. \end{aligned}$$

Cutting the diagram Fig. 41 along the lines $v'_{1,\ldots,N-1}$ and re-gluing it along the lines $m'_{1,\ldots,N}$ we obtain the web diagram shown in Fig. 42(a). Cutting the latter diagram furthermore along the line $-h_N$ it can also be represented in the form Fig. 42(b), which corresponds to a staircase diagram with shift $\delta = N-2$. The set of independent Kähler parameters $(\widehat{a}''_{1,\ldots,N}, S'', R'')$ can be related to $(\widehat{a}_{1,\ldots,N}, S, R)$ in the following manner

$$(\widehat{a}_1\,,\ldots,\widehat{a}_N\,,S\,,R)^T = \mathcal{G}_\infty(N)\cdot(\widehat{a}''_1\,,\ldots,\widehat{a}''_N\,,S''\,,R'')^T\,, \tag{6.42}$$

To show this, we use (6.37) and (6.40) along with

$$\widehat{a}''_i = m'_{i+1} - h_{i+2} = m + h_{i+1}\,, \qquad S'' = m\,, \qquad R'' - 2S'' = v - m \tag{6.43}$$

to compute (with $\rho'' = \sum_{k=1}^{N}(m'_k - h_k) = Nm + \sum_{k=1}^{N} h_k$)

$$\begin{aligned} \widehat{a}_i &= \widehat{a}''_i - 2S'' + R'' = m + h_{i+1} + v - m = h_{i+1} + v\,,\\ S &= \rho'' - (2N-1)S'' + (N-1)R'' = \sum_{k=1}^{N} h_k + (N-1)v\,,\\ R &= N\rho'' - 2N(N-1)S'' + (N-1)^2R'' = N\sum_{k=1}^{N} h_k + m + (N-1)^2 v\,, \end{aligned} \tag{6.44}$$

which matches (6.41) and therefore shows that $\mathcal{G}_\infty(N)$ is a symmetry transformation.

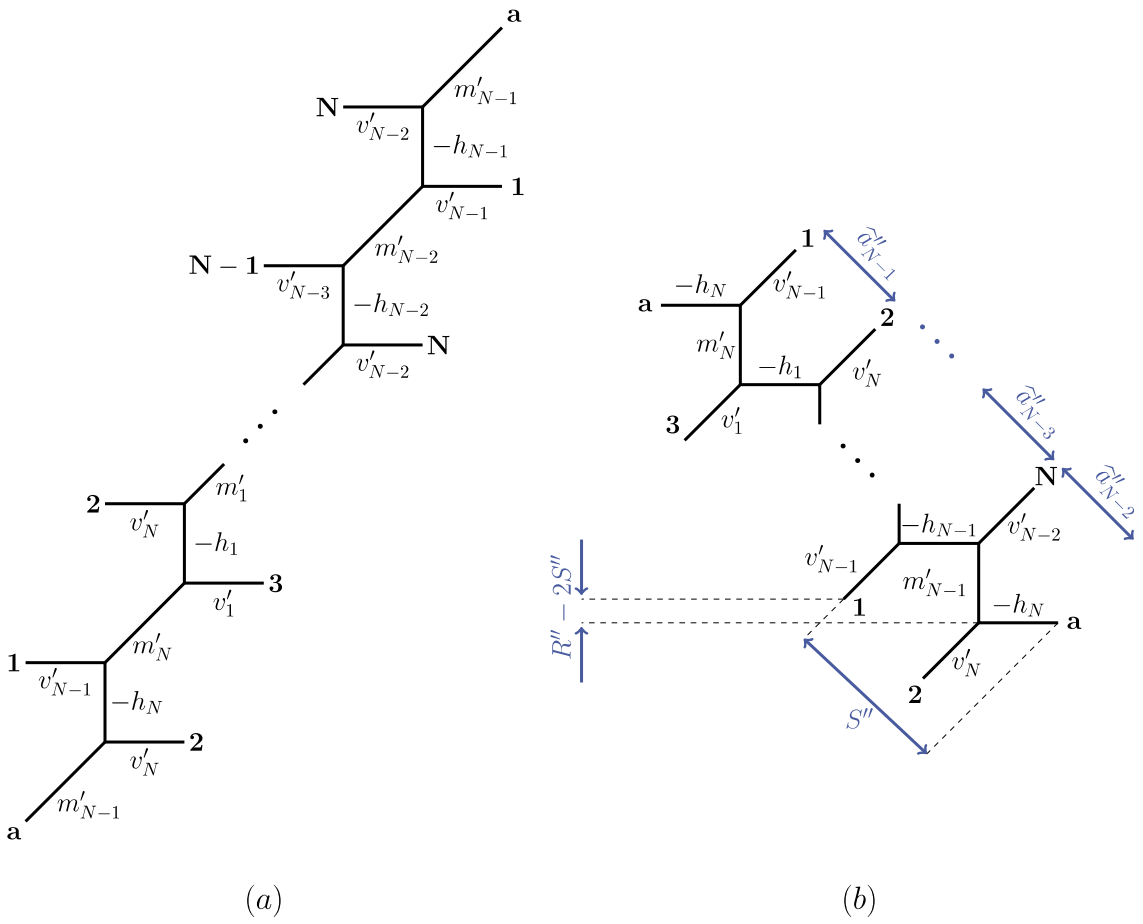

Figure 42: *(a) Alternative presentations of the web diagram in Fig. 41. (b) Further presentation in the form of a shifted web diagram with $\delta = N - 2$.*

6.3.2 Generators of the Dihedral Group

After having shown that the transformations $\mathcal{G}_\infty(N) \cdot \mathcal{G}_2(N)$ and $\mathcal{G}_\infty(N)$ (and thus also $\mathcal{G}_2(N)$) are symmetry transformations of the partition function $\mathcal{Z}_{N,1}$, we shall now discuss the group structure they are generating. The matrix $\mathcal{G}_2(N)$ has order 2 (*i.e.* $\mathcal{G}_2(N).\mathcal{G}_2(N) = \mathbb{1}_{(N+2)\times(N+2)}$), while $\mathcal{G}_\infty(N)$ has the following order

$$\operatorname{ord} \mathcal{G}_\infty(N) = \begin{cases} 3 & \text{if} \quad N = 1\,, \\ 2 & \text{if} \quad N = 2\,, \\ 3 & \text{if} \quad N = 3\,, \\ \infty & \text{if} \quad N \geq 4\,. \end{cases} \tag{6.45}$$

Here infinite order means $\nexists\, m \in \mathbb{N}$ such that $(\mathcal{G}_\infty(N))^m = \mathbb{1}_{(N+2)\times(N+2)}$. While we have shown all cases $N \leq 4$ explicitly in previous sections, for $N > 4$ it is sufficient to realise that

$$\vec{v}_N = \Big(\underbrace{1, \ldots, 1}_{N \text{ times}}, \frac{N + \sqrt{N(N-4)}}{2}, \frac{N}{2}(N - 2 + \sqrt{N(N-4)}) \Big)^T\,, \tag{6.46}$$

is an eigenvector of $\mathcal{G}_\infty(N)$ for the eigenvalue[42]

$$\lambda_N = \frac{1}{2}\left((N-2)^2 - 2 + \sqrt{N(N-4)}(N-2)\right) \in \mathbb{R}\,. \tag{6.47}$$

Since $\lambda_N > 1$ for $N \geq 5$ (and $\mathcal{G}_\infty(N)$ is diagonalizable for $N \geq 5$) it follows that $\mathcal{G}_\infty(N)$ is not of finite order in these cases. Thus, upon introducing the matrix

$$\mathcal{G}_2'(N) = \mathcal{G}_2(N)\cdot\mathcal{G}_\infty(N) = \begin{pmatrix} & & & -2 & 1 \\ & \mathbb{1}_{N\times N} & & \vdots & \vdots \\ & & & -2 & 1 \\ 0 & \cdots & 0 & -1 & 1 \\ 0 & \cdots & 0 & 0 & 1 \end{pmatrix}, \tag{6.48}$$

which is of order 2 (*i.e.* $\mathcal{G}_2'(N).\mathcal{G}_2'(N) = \mathbb{1}_{N+2\times N+2}$), we find that $\mathcal{G}_2(N)$ and $\mathcal{G}_2'(N)$ freely generate a dihedral group

$$\mathbb{G}(N) = \langle\{\mathcal{G}_2(N)\,,\mathcal{G}_2'(N)\}\rangle \cong \begin{cases} \text{Dih}_3 & \text{if} \quad N=1\,, \\ \text{Dih}_2 & \text{if} \quad N=2\,, \\ \text{Dih}_3 & \text{if} \quad N=3\,, \\ \text{Dih}_\infty & \text{if} \quad N\geq 4\,. \end{cases} \tag{6.49}$$

For $N \geq 4$, eq. (6.45) shows that $\nexists\, n \in \mathbb{N}$ with $(\mathcal{G}_2(N)\cdot\mathcal{G}_2'(N))^n = \mathbb{1}_{(N+2)\times(N+2)}$ (which also implies $\nexists\, n \in \mathbb{N}$ with $(\mathcal{G}_2'(N)\cdot\mathcal{G}_2(N))^n = \mathbb{1}_{(N+2)\times(N+2)}$). Furthermore, since $(\mathcal{G}_2(N))^2 = \mathbb{1}_{(N+2)\times(N+2)} = (\mathcal{G}_2'(N))^2$, this also implies $\nexists\, n \in \mathbb{N}$ with $\mathcal{G}_2'(N)\cdot(\mathcal{G}_2(N)\cdot\mathcal{G}_2'(N))^n = \mathbb{1}_{(N+2)\times(N+2)}$ or $(\mathcal{G}_2(N)\cdot\mathcal{G}_2'(N))^n\cdot\mathcal{G}_2(N) = \mathbb{1}_{(N+2)\times(N+2)}$.[43] This means that there are no non-trivial (braid) relations between $\mathcal{G}_2(N)$ and $\mathcal{G}_2'(N)$, which indeed shows that the group $\mathbb{G}(N) \cong \text{Dih}_\infty$ for $N \geq 4$.

Notice that $\mathcal{G}_2(N)$ is a lower diagonal matrix, while $\mathcal{G}_2'(N)$ is an upper diagonal $(N+2)\times(N+2)$ matrix. Furthermore, the partition function is invariant under the action of the group $\mathbb{Z}_N$, which is generated by matrices of the form

$$R(M) = \begin{pmatrix} & & & 0 & 0 \\ & M & & \vdots & \vdots \\ & & & 0 & 0 \\ 0 & 0 & 0 & 1 & 0 \\ 0 & 0 & 0 & 0 & 1 \end{pmatrix}, \tag{6.50}$$

where M is an $N\times N$ matrix that acts by permuting the $\widehat{a}_{1,\ldots,N}$. One can check that matrices of the form $R(M)$ commute with both $\mathcal{G}_2(N)$ and $\mathcal{G}_2'(N)$, such that we have the following symmetry group of the partition function $\widetilde{G}(N) \cong \mathbb{G}(N)\times\mathbb{Z}_N$.

[42]The remaining eigenvalues are $+1$ (with degeneracy N) and λ_N^{-1}.

[43]For example, the former relation is equivalent to $(\mathcal{G}_2(N)\cdot\mathcal{G}_2'(N))^n = \mathcal{G}_2'(N)$. Squaring this relation (due to the fact that $\mathcal{G}_2'(N)$ is of order 2) would be equivalent to $(\mathcal{G}_2(N)\cdot\mathcal{G}_2'(N))^{2n} = \mathbb{1}_{(N+2)\times(N+2)}$, which does not agree with (6.45).

6.3.3 Modularity at a Particular Point of the Moduli Space

Using the general parametrisation of the group $\mathbb{G}(N)$ in (6.49), we once again ask the question how the latter is related to $Sp(4,\mathbb{Z})$ at the particular region in the moduli space, which is characterized by $\widehat{a}^{(0)}_{1,\dots,N} = \widehat{a}^{(0)}_4 = \widehat{a}$, which implies $h_{1,\dots,N} = h$ (while the consistency conditions already impose $v_{1,\dots,N} = v$ and $m_{1,\dots,N} = m$). We can similarly introduce the period matrix

$$\Omega = \begin{pmatrix} \tau & v \\ v & \rho \end{pmatrix}, \qquad \text{with} \qquad \begin{matrix} \tau = m + v\,, \\ \rho = h + m\,. \end{matrix} \tag{6.51}$$

Using the parametrisation (6.49) of $\mathbb{G}(4)$, it is sufficient to analyse the relation of the generators $\mathcal{G}_2(N)$ and $\mathcal{G}'_2(N)$ to $Sp(4,\mathbb{Z})$. The restriction of these generators to the subspace $(\widehat{a}, S, R)$ can be written in the form

$$\mathcal{G}_2^{(\mathrm{red})}(N) = \begin{pmatrix} 1 & -2 & 1 \\ 0 & -1 & 1 \\ 0 & 0 & 1 \end{pmatrix}, \qquad \text{and} \qquad \mathcal{G}_2^{\prime,(\mathrm{red})}(N) = \begin{pmatrix} 1 & 0 & 0 \\ N & -1 & 0 \\ N^2 & -2N & 1 \end{pmatrix}, \tag{6.52}$$

or on the space (τ, ρ, v)

$$\widetilde{\mathcal{G}}_2^{(\mathrm{red})}(N) = D_N^{-1} \cdot \mathcal{G}_2^{(\mathrm{red})}(N) \cdot D_N = \begin{pmatrix} (N-1)^2 & (N-2)^2N^2 & -2N\,(N^2-3N+2) \\ 1 & (N-1)^2 & 2(1-N) \\ N-1 & N\,(N^2-3N+2) & -2N^2+4N-1 \end{pmatrix},$$

$$\widetilde{\mathcal{G}}_2^{\prime,(\mathrm{red})}(N) = D_N^{-1} \cdot \mathcal{G}_2^{\prime,(\mathrm{red})}(N) \cdot D_N = \begin{pmatrix} 1 & 4 & -4 \\ 0 & 1 & 0 \\ 0 & 2 & -1 \end{pmatrix}, \qquad \text{with} \quad D_N = \begin{pmatrix} 0 & 1 & 0 \\ 0 & N & -1 \\ 1 & N^2 & -2N \end{pmatrix}.$$

Rewriting these generators furthermore to act as elements of $Sp(4,\mathbb{Z})$ in the form of (E.3) on the period matrix Ω in (6.51), they take the form

$$\widetilde{\mathcal{G}}_2^{(\mathrm{red,Sp})}(N) = (HKL^6H)^{N-2}K(HL^6KH)^{N-2} = \begin{pmatrix} N-1 & 1-(N-1)^2 & 0 & 0 \\ 1 & 1-N & 0 & 0 \\ 0 & 0 & N-1 & 1 \\ 0 & 0 & 1-(N-1)^2 & 1-N \end{pmatrix},$$

$$\widetilde{\mathcal{G}}_2^{\prime,(\mathrm{red,Sp})}(N) = HK(L^6K)^{N-1}H = \begin{pmatrix} -1 & N & 0 & 0 \\ 0 & 1 & 0 & 0 \\ 0 & 0 & -1 & 0 \\ 0 & 0 & N & 1 \end{pmatrix}, \tag{6.53}$$

where K, L and H are defined in appendix E. For $N \in \mathbb{N}$, the restriction of $\mathbb{G}(N)$ to the particular region of the Kähler moduli space $(\widehat{a}, S, R)$ is a subgroup of $Sp(4,\mathbb{Z})$. However, for $N > 1$, we cannot conclude that the freely generated group $\langle \widetilde{\mathcal{G}}_2^{(\mathrm{red,Sp})}(N), \widetilde{\mathcal{G}}_2^{\prime,(\mathrm{red})}(N), S_\rho, T_\rho, S_\tau, T_\tau \rangle$ is isomorphic to $Sp(4,\mathbb{Z})$.

6.4 Summary

In this section, we analyzed the consequences of the vast duality web from the point of view of a specific expansion of the topological string partition function. We find that the different

expansions of the same form, *i.e.* same number of coupling constants, Coulomb branch and mass parameters respectively, are related by linear transformations acting on the Kähler moduli space. By representing these transformation as matrices, we find that they generate a dihedral groups whose order depends on the specific geometry $X^{(\delta)}_{N,1}$. We show that these groups have finite order for $N \leq 3$ and that for $N \geq 4$ they are isomorphic to the infinite dihedral group. We give an argument for the appearance of the infinite dihedral group based on the web diagram. Furthermore, we analyzed how these new symmetries combines with the already present modular structure and how they sit inside $Sp(4, \mathbb{Z})$.

7 Conclusions

The main goal of this thesis was to establish and study exact dualities among little string theories of type A, which naturally implies dualities between their low-energy descriptions as circular quiver gauge theories. Important for a good understanding of these theories and gaining hints about what duality relations one might expect, was the plethora of alternative viewpoints on little string theories of type A. The F-theory construction gives valuable insights into how the geometry of the Calabi-Yau threefold $X_{N,M}$ is related to the different physical parameters such as coupling constants, Coulomb branch and mass parameters, that we encounter in the engineered theories. The brane configuration in M-theory is important to be able to calculate the BPS counting function of the little strings. Through the relation to closed topological string theory, the BPS counting function for the little strings in $\mathbb{R}^4_{\epsilon_1,\epsilon_2} \times T^2$ is related to the closed topological string amplitude associated with the Calabi-Yau threefold $X_{N,M}$, for which we have the powerful topological vertex method at our disposal. The duality between the M-theory configuration with he (p,q) brane web representation in type IIB string theory provided an important framework to systematically apply the vertex method. The equivalence between the toric diagram of $X_{N,M}$ and the (p,q) brane web made it possible to use the graphical simplicity and the powerful methods of toric geometry to look for dualities in a systematic way by applying flop transitions and thus relating different geometries. The interpretation of certain web diagrams that were encountered in this process was rather tricky but the correspondence between the geometric elements in the F-theory construction and their counterparts in the toric graph of $X_{N,M}$ helped to shed light on this issue.

The fact that different web diagrams of the type $X_{N,M}$ can be related through flop transitions was important to get first hints of what kind of duality relations can be expected. From these purely geometric considerations one would expect relations between theories with gauge groups $[U(N)]^M$ and $[U(N')]^{M'}$ with $NM = N'M'$ and $\gcd(N,M) = \gcd(N',M)'$. In order to verify these expectations, the associated topological string partition functions were compared. In a first step, the behavior of the partition function under a specific sequence of flops was studied and explicitly shown to be invariant in the when $\gcd(N,M) = 1$. A well motivated conjecture was made for the case $\gcd(N,M) > 1$. From this result it follows that the partition functions associated with geometries related through flop transitions have the same form as a series expansion in a suitable basis of independent Kähler parameters. The way this basis depends on the individual curves in the underlying geometry can however be different, a fact that led to new insights at a later point in the thesis that we will discuss below.

In a given geometry $X_{N,M}$ it was known that the topological vertex allowed for three different choices of preferred direction, horizontal, vertical and diagonal. The first two choices were already well studied but this was not the case for the diagonal one. Through the geometric relation under flops between $X_{N,M}$ and $X_{\frac{NM}{l},k}$ (with $k = \gcd(N,M)$) and the result of invariance of the partitions functions, it was concluded that the diagonal expansion has an interpretation as an instanton partition function associated with a theory that has gauge group $[U(NM/k)]^k$. As the relation between the gauge theory parameters to the individual curves in the two geometries was different, it was also checked that there is a region in the Kähler moduli space of $X_{N,M}$ where the weak coupling regime is realized. This was done by providing three suitable gauge theory parametrizations of the web diagram and the presence

of these three theories in the single Kähler cone was dubbed triality. From the combination of these results we also concluded that there was an extended web of dualities among theories engineered by geometries $X^{(\delta)}_{N,M}$ that can be related through flops. The study of the extended Kähler moduli space led naturally to what we called intermediate Kähler cones. These were defined to correspond to web diagrams $X^{(\delta)}_{N,M}$ that do not admit an equivalent representation in terms of an unshifted diagram (*i.e.* $\delta = 0$). We argued that even these geometries engineer at least one theory, which is the one that does not get send through a strong coupling regime as the associated curves do not undergo flops on this path through Kähler moduli space. We also encountered configurations which seem at a first glance to engineer theories which violate the gcd-condition described above. A more in depth analysis showed that the associated partition function expansion can not be interpreted in terms of an instanton series of a gauge theory. It would be interesting to see if one can make sense out of this expansion in the framework of full fledged little string theory. Another interesting direction based on the results mentioned so far, would be to see if a similar analysis can be performed for little string theories of some other ADE type. This would require that the underlying geometry admits a description as a toric variety and furthermore that we know the explicit construction in terms of a toric fan. In general, these will be more elaborate as one needs for example to include $O5$ planes if one eventually wants to build a configuration corresponding to other little string theories [40]. However, advances in vertex technology in the presence of $O5$ planes [151] make this a possible direction for further investigation.

Another new insight gained in this thesis that followed from the fact that even when the partitions functions of geometries $X^{(\delta)}_{N,M}$ with different shift that related through flops agree, the relation between the expansion parameters and the individual curves in the geometry is different. If a given shifted geometry engineers a honest to good theory compactified on $\mathbb{R}^4_{\epsilon_1,\epsilon_2} \times T^2$, there should exist a limit which induces the dimensional reduction to $\mathbb{R}^4_{\epsilon_1,\epsilon_2} \times S^1$. In terms F-theory, this means that we have to find a limit in which we take the volume of a given curve to infinity, which in turn takes the volume of the elliptic fiber to infinity resulting thus in dimensional reduction. In the unshifted case, this limit has a very simple realization for the theories we are interested in. We end up with five-dimensional theories that have the same gauge group and matter content. However, once a non-trivial shift is present the story, turns out to be more complicated. In the periodic strip case $X^{(\delta)}_{N,1}$, we managed to find such limits first at the level of the web diagram by analyzing the associated consistency conditions. We were able to write down the general pattern of these kinds of limit for a periodic strip geometry. Further studying the behavior of the partition function under this limit, we were able to confirm its consistency. We were able to write down the general pattern of these kinds of limit for a periodic strip geometry. The resulting five-dimensional theories have in general a gauge group of reduced rank and a different matter content than their six-dimensional parent theory. In a first step, one could try to extend this result to more general geometries $X^{(\delta)}_{N,M}$ in order to see if one could establish a pattern in this more general case. Furthermore, it would be interesting to capture these non-trivial limits in the F-theory construction of the little string theories. The above mentioned results indicate that there a clearly differences in the geometry $X^{(\delta)}_{N,M}$ with respect to $X_{N,M}$ that makes the F-theory interpretation less clear. It seems that now the volume of the elliptic fiber cannot be taken to infinity without taking also the volume of the elliptic base curve to infinity. One might be led to consider more general spaces, such as for example genus-one fibrations [152] in order to fully capture the F-theory compactification

on $X^{(\delta)}_{N,M}$. We leave this direction for further studies.

Another result of this thesis is the presence of a dihedral symmetry in the topological string partition function associated to the periodic strip geometry $X^{(\delta)}_{N,1}$. This follows from the observation that a such a web diagram all the webs diagrams that can be reached by flops allows for numerous different but equivalent expansions of the topological string partition function that have the same structure, *i.e.* same number of coupling constant, Coulomb branch and mass parameters respectively. This is a direct consequence of the invariance under flop transformations. Each basis of these equivalent expansions is related to another one by linear transformation, which can be conveniently encode into a matrix. As this transformation constitutes a symmetry of the partition function and as the combination of two such symmetries has to be another symmetry, they form a group. We explicitly showed that this matrices provide a representation of the dihedral groups acting on the Kähler moduli space. We described explicitly how the order of the dihedral group depends on the value of N and proved that for $N > 3$ the symmetry group is isomorphic to the infinite dihedral group. It was also analyzed how these newly discovered symmetries combine with the modular structure of the partition function and how this combination is embedded into $Sp(4, \mathbb{Z})$ at a specific point in moduli space. There are a few interesting directions one can take from here. First, there is the rather natural question of what happens for more general geometries than the periodic strip. Upon a preliminary analysis of a few simple examples it seems that one obtains again dihedral symmetry groups in that case. It is however not clear if or for what geometries the symmetry will be the infinite dihedral group. It would also be interesting to understand the dihedral symmetry at the level of the BPS counting function of the little string. Some terms in in a given winding sector are mapped to terms in a different winding sector, while other terms do not get mapped outside of their winding sector under the dihedral symmetry. So it is natural to ask whether this distinction is arbitrary or if it has some deeper physical meaning to it.

The results in this thesis illustrate the power of string theoretic constructions in the study of supersymmetric gauge theories. The geometrical tools at our disposal allowed for the discovery of a web of dualities whose existence is rather difficult to infer from a purely gauge-theoretic viewpoint. Furthermore the non-perturbative techniques allowed us to devise exact results. One could hope that the advancement and the study of non-perturbative methods will allow us to apply them to scenarios that are more realistic from a phenomenological point of view. Furthermore, as the little string theories arise as worldvolume theories in string and M-theory, the duality web that we established makes it clear that brane configurations which seem a priori very different have the same information encoded in their BPS spectrum of little strings.

A A few elements of toric geometry

We introduce some basic concepts from toric geometry that are used to define the so called fan. The latter is used in the main part of this work. This exposition is not meant to be exhaustive and we will certainly ignore a lot of subtleties. We follow mostly [153]. For a more complete introduction, see [124].

A toric variety X_Δ of complex dimension m can be defined as a holomorphic quotient of $\mathbb{C}^n$

$$X_\Delta = \frac{(\mathbb{C}^n / Z_\Delta)}{G} \tag{A.1}$$

where $G \cong (\mathbb{C}^*)^{n-m} \times \Gamma$ is direct product of an algebraic torus $(\mathbb{C}^*)^{n-m}$ and a discrete abelian group Γ. The set of fixed points Z_Δ is removed from $\mathbb{C}^n$ so that G can act freely. For non-trivial Γ, the variety has so called orbifold singularities. This will be explained at a later point in this section. The construction of a toric variety is in a sense a generalization of the construction of weighted projective space, which is actually a simple example of a toric variety. The $\mathbb{C}^*$ action on X is defined as

$$(z_1, \ldots, z_n) \quad \mapsto \quad (\lambda^{k_1} z_1, \ldots, \lambda^{k_n} z_n)\,, \quad \text{with } \lambda \in \mathbb{C}^*\,, \quad k_i \in \mathbb{Z} \tag{A.2}$$

The toric fan

The data associated with a toric variety can conveniently be packaged in an object called a fan. We consciously try to avoid describing explicitly the algebraic geometry viewpoint on toric varieties as these concepts are not used in this thesis and will just make things unnecessarily complicated. We first start by explaining the construction of a fan an then describe the relation to the toric variety.

The fundamental building blocks of a fan are called cones. Consider a lattice $N \cong \mathbb{Z}^n$ and the associated vector space $N_\mathbb{R} = N \otimes \mathbb{R}$, obtained by allowing for real coefficients. For a finite set of vectors S in the lattice N, a strongly convex polyhedral cone σ is defined by

$$\sigma = \text{Cone}(S) = \{\sum_{u \in S} \lambda_u u \,|\, \lambda_u \in \mathbb{R}_{\geq 0}\} \tag{A.3}$$

and the condition $\sigma \cap (-\sigma) = \{0\}$, which assures strong convexity, *i.e.* a cone does not contain any line tough the origin. Given a cone $\sigma \in N_\mathbb{R}$, we can define the dual cone $\sigma^\vee$ living in the dual space $M_\mathbb{R}$ as

$$\sigma^\vee = \{m \in M_\mathbb{R} \,|\, \langle u, m\rangle \geq 0\,, \quad \forall u \in \sigma\} \tag{A.4}$$

Using the dual lattice M, we can define the faces of a cone σ. For a dual lattice point $m \in M$ we have the half-space

$$H_m^+ = \{u \in N_\mathbb{R} \,|\, \langle v, m\rangle \geq 0\} \tag{A.5}$$

A half-space H_m^+ is said to support a cone σ if it fully contains that cone. A face of a cone is then defined to be the intersection of the cone with a supporting half-space H_m^+. When τ

is a face of σ we write $\tau \prec \sigma$. A cone is thus a face of itself, it's intersection with H_0. We give special names to two categories of faces. Firstly, faces of dimension 1 are called edges. They are generated by the set of vectors $u \in S$ that generate the cone itself. Secondly, faces of codimension 1 are called facets. We consider a simple example shown in Fig. 43 in order to illustrate the concepts introduced so far.

Figure 43: *(a) A cone σ spanned by the lattice vectors $u_1 = (0, 1)$ and $u_2 = (1, 1)$. (b) The dual cone $\sigma^\vee$ spanned by $v_1 = (1, 0)$ and $v_2 = (-1, 1)$.*

A fan Δ in $N_\mathbb{R}$ is given by a collection of cones in $N_\mathbb{R}$ such that two conditions are satisfied:

1. A face of a cone in Δ is again a cone in Δ.
2. The intersection of two cones in Δ is a face of each.

The associated toric variety is denoted by X_Δ. This explains in hindsight the choice of notation in (A.1). It should be emphasized that each cone σ is a fan by itself. In the language of algebraic geometry, a cone defines a so called affine variety. These are in some sense the open subsets of our toric variety. The fan tells us how these affine varieties must be patched together, *i.e.* it encodes the transition functions. However, we will not describe how to extract the transition functions as this is not needed and avoids an unnecessary detour into algebraic geometry. A good illustrative example of the machinery described above is that of $\mathbb{CP}^2$. The fan of the latter is depicted in Fig. 44. It is spanned by the three vectors $u_1 = (1, 0)$, $u_2 = (0, 1)$ and $u_3 = (-1, -1)$. Each of the cones σ_1, σ_2 and σ_3 defines an affine patch $U_{\sigma_i} \cong \mathbb{C}^2$. Using the fan it is then possible to extract the usual transition function of $\mathbb{CP}^2$. The action of the algebraic torus $(\mathbb{C}^*)^{n-m}$ can be easily read of from the fan of a toric variety. To each vector $u_i \in \Delta$ corresponds a homogeneous coordinate $z_i \in \mathbb{C}^n$. There are $n - m$ relations among the vectors in the fan of the form

$$\sum_i Q_i^a u_i = 0\,, \quad \text{where} \quad Q_i^a \in \mathbb{Z}\,, \quad a = 1, \ldots, n-m \tag{A.6}$$

Every such relation gives rise to a $\mathbb{C}^*$-action

$$(z_1, \ldots, z_n) \mapsto (\lambda_a^{Q_1^a} z_1, \ldots, \lambda_a^{Q_n^a} z_n) \tag{A.7}$$

which has been introduced in A.2. For the example of $\mathbb{CP}^2$ in Fig. 44 there is a single relation which immediately gives rise to the known $\mathbb{C}^*$ action $(z_1, z_2, z_3) \mapsto (\lambda z_1, \lambda z_2, \lambda z_3)$.

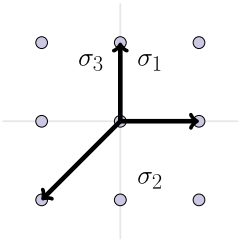

Figure 44: *Toric fan associated to* $\mathbb{CP}^2$

All the toric varieties that we consider in this work are non-compact. At the level of the fan this has a simple manifestation. A toric variety X_Δ is compact if and only if its fan Δ spans the whole $N_\mathbb{R}$. It is thus easy to see from the fan in Fig. 44 that the associated toric variety, *i.e.* $\mathbb{CP}^2$ is compact. In addition to being non-compact, the varieties in this thesis are Calabi-Yau, which imposes further constraints on the form of the toric fan. We will not provide any details here but the Calabi-Yau condition, as described in section 2.1, can be neatly translated into the language of toric geometry. A toric variety X_Δ is Calabi-Yau if and only if for every relation (A.6) satisfied by the vectors in the fan Δ we have

$$\sum_i Q_i^a = 0\,, \quad a = 1, \ldots, n-m \tag{A.8}$$

This condition can be translated into the equivalent statement that all vectors in the fan must end on the same hyperplane. We immediately deduce that a toric Calabi-Yau variety cannot be compact. As we are dealing with Calabi-Yau threefolds in this thesis whose toric fan lives in $\mathbb{R}^3$, it is sufficient to for us to only represent the hyperplane on which all the vectors end. Hence the toric fan of a Calabi-Yau threefold can be conveniently encoded into a two dimensional graph with the vertices representing a vector ending at that point. We show the example of the so called conifold in Fig. 45 (a). The four vertices shown in the $z = 1$ plane correspond to the vectors $v_1 = (0, 0, 1)$, $v_2 = (1, 0, 1)$, $v_3 = (0, 1, 1)$ and $v_4 = (1, 1, 1)$.

Singularities and Flop transition

Algebraically the conifold is defined by the following equation

$$P = xy - uv = 0\,, \quad (x, y, u, v) \in \mathbb{C}^4 \tag{A.9}$$

The conifold is a singular variety. From the algebraic perspective this means that there are points for which

$$P = 0 \quad \text{and} \quad dP = 0 \tag{A.10}$$

For the conifold, we have that $(0, 0, 0, 0) \in \mathbb{C}^4$ is a singular point. There is more than one way for obtaining a non-singular variety by smoothing out the singularity. The method that will be of interest to us, is a so called resolution[44]. In order to do so, we introduce projective

[44]More specifically, a crepant resolution, meaning that it preserves the Calabi-Yau condition [124].

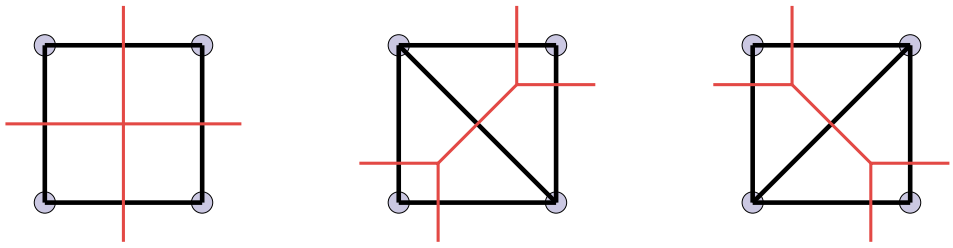

(a) (b) (c)

Figure 45: *(a) Toric diagram of the conifold. Due to the Calabi-Yau condition it is sufficient to show only the plane at $z = 1$. (b) and (c) Two different resolution of the conifold. They are related by flop transition. The respective dual toric diagrams are drawn in red.*

coordinates $[a : b] \in \mathbb{CP}^1$ and describe the space in the following way

$$ax = bu \quad \text{and} \quad by = av \tag{A.11}$$

For points $(x, y, u, v) \neq (0, 0, 0, 0)$, the coordinates $[a : b]$ are uniquely determined and we just get the usual conifold. However, when $(x, y, u, v) = (0, 0, 0, 0)$ the coordinates $[a : b]$ parametrize the full $\mathbb{CP}^1$. Instead of the singular point, we now have a sphere and the total space is smooth. We could also have made a different choice and introduced the coordinates $[a : b]$ as

$$ax = bv \quad \text{and} \quad by = au \tag{A.12}$$

This other choice of resolution gives a different total space in general. However, due to the simplicity of the example, the two spaces are isomorphic. The passage from one choice to the other is known as flop transition. We now describe how these concepts translate into the language of toric fans.

In a general toric fan, given a cone σ its associated affine variety X_σ is singular if σ is not generated by an integral basis of the lattice N. For our purposes, it suffices to say that variety will be non-singular if and only if the toric diagram is triangulated. Thus, resolving the singularity boils down to triangulation. In general, different triangulations correspond to different different resolutions of the singularities. For example, in Fig. 45 (b) and (c) we show the two possible triangulations of the conifold (these correspond to the two possible choice for the resolution described in the algebraic description). As mentioned above, the process that relates different resolutions is called flop transition. At the level of the toric diagram this procedure amounts simply to replacing a given triangulation with a different one. Further implications for the geometry are discussed in the main text. There is a dual representation of toric diagrams which makes contact with the so called (p, q)-brane webs discussed in section 3.4.1. In order to get the dual toric diagram we simply draw the perpendiculars to each edge in the diagram. These are drawn in red in Fig. 45.

B Toric Varieties of infinite type

In the following we give a very rough calculation of the intersection numbers in the elliptic Calabi-Yau threefold $X^{(\delta)}_{N,M}$, relying mostly on known results in the literature.

Infinite toric fan

As in [123], we start by considering an infinite toric fan, which can be decomposed into the following set of maximal cones in $\mathbb{R}^3$:

$$\begin{aligned}\sigma^1_{i,j} &= \mathbb{R}_{\geq 0}(i,j,1) + \mathbb{R}_{\geq 0}(i+1,j,1) + \mathbb{R}_{\geq 0}(i,j+1,1)\,,\\ \sigma^2_{i,j} &= \mathbb{R}_{\geq 0}(i+1,j,1) + \mathbb{R}_{\geq 0}(i,j+1,1) + \mathbb{R}_{\geq 0}(i+1,j+1,1)\,, \quad i,j \in \mathbb{Z}\end{aligned} \tag{B.1}$$

where the triples $(i,j,k) \in \mathbb{Z}^3$ are called ray generators in the following. Since all ray generators in (B.1) end on the same plane defined by $z = 1$ in $\mathbb{R}$ (*i.e.* $k = 1$ in all cases), the resulting geometry is Calabi-Yau and non-compact. A local region of the toric fan looks as shown in Fig. 46, where it is sufficient to show only the $x - y$ plane at $z = 1$ due to the Calabi-Yau condition. Each wall, that is the intersection of two maximal cones, defines an irreducible toric

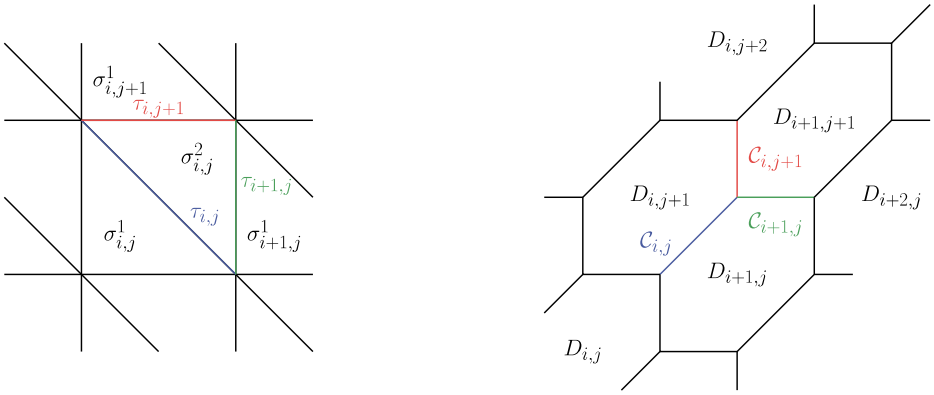

Figure 46: *(a) A local view of the $x - y$ plane at $z = 1$ of an infinite toric fan with some maximal cones σ and walls τ labeled. (b) A local view of the dual diagram to our infinite fan with some curves and divisors labeled.*

curve. There are three families of curves, diagonal (blue), horizontal (green), and vertical (red) (the orientations are defined with respect to the dual toric graph Fig. 46 (b)). The walls have the following form:

$$\begin{aligned}\tau_{i,j} &= \sigma^1_{i,j} \cap \sigma^2_{i,j} = \mathbb{R}_{\geq 0}(i+1,j,1) + \mathbb{R}_{\geq 0}(i,j+1,1)\,,\\ \tau_{i+1,j} &= \sigma^2_{i,j} \cap \sigma^1_{i+1,j} = \mathbb{R}_{\geq 0}(i+1,j,1) + \mathbb{R}_{\geq 0}(i+1,j+1,1)\,,\\ \tau_{i,j+1} &= \sigma^2_{i,j} \cap \sigma^1_{i,j+1} = \mathbb{R}_{\geq 0}(i,j+1,1) + \mathbb{R}_{\geq 0}(i+1,j+1,1)\,.\end{aligned} \tag{B.2}$$

Due to $SL(2,\mathbb{Z})$ symmetry, the three families of curves are equivalent to each other, i.e. they are mapped into another in different $SL(2,\mathbb{Z})$ frames. It is thus sufficient to focus on one class of curves. We choose the diagonal (blue) one. In the following, we shall follow [124] for a general result (reduced to a three-dimensional fan) and apply it directly to the specific construction above: Let $u_{i=0,1,2,3}$ be four ray generators in a smooth three-dimensional toric fan. If $\tau = \sigma \cap \sigma'$ is a wall in the latter, which is defined through

$$\tau = \mathbb{R}_{\geq 0}u_1 + \mathbb{R}_{\geq 0}u_2\,, \qquad \sigma = \mathbb{R}_{\geq 0}u_0 + \mathbb{R}_{\geq 0}u_1 + \mathbb{R}_{\geq 0}u_2\,, \qquad \sigma' = \mathbb{R}_{\geq 0}u_1 + \mathbb{R}_{\geq 0}u_2 + \mathbb{R}_{\geq 0}u_3\,,$$

there exist integers $b_{1,2}$ such that the wall relation

$$u_0 + b_1 u_1 + b_2 u_2 + u_3 = 0 \tag{B.3}$$

is satisfied. The intersection number of the irreducible curve $\mathcal{C}_\tau$ associated to τ with the divisor D_u associated to any ray generator u of the fan is then given by:

$$D_u \cdot \mathcal{C}_\tau = \begin{cases} 1 & \text{if } u = u_0, u_3\,, \\ b_i & \text{if } u = u_i \text{ for } i = 1,2\,, \\ 0 & \text{else}\,. \end{cases} \tag{B.4}$$

Specifically, for the toric fan (B.1), we have the wall relation for $\tau_{i,j}$ defined in (B.2):

$$(i,j,1) - 1(i+1,j,1) - 1(i,j+1,1) + (i+1,j+1,1) = 0\,, \quad \text{with} \quad b_1 = b_2 = -1\,. \tag{B.5}$$

Thus (B.4) directly yields the following intersection numbers for the curves associated to $\tau_{i,j}$ in (B.2), with all divisors (associated with the ray generators u)

$$D_u \cdot \mathcal{C}_{\tau_{i,j}} = \begin{cases} 1 & \text{if } u = u_0, u_3 \\ -1 & \text{if } u = u_k \text{ for } k = 1,2 \\ 0 & \text{else} \end{cases} \tag{B.6}$$

By $SL(2,\mathbb{Z})$ symmetry, we thus have the following non-zero intersection numbers for the dual toric diagram in Fig. 46 (b):

$$D \cdot \mathcal{C}_{i,j} = \begin{cases} 1 & \text{if } D = D_{i,j}, D_{i+1,j+1}\,, \\ -1 & \text{if } D = D_{i+1,j}, D_{i,j+1}\,, \end{cases} \qquad D \cdot \mathcal{C}_{i+1,j} = \begin{cases} 1 & \text{if } D = D_{i,j+1}, D_{i+2,j}\,, \\ -1 & \text{if } D = D_{i+1,j}, D_{i+1,j+1}\,, \end{cases}$$
$$D \cdot \mathcal{C}_{i,j+1} = \begin{cases} 1 & \text{if } D = D_{i+1,j}, D_{i,j+2}\,, \\ -1 & \text{if } D = D_{i,j+1}, D_{i+1,j+1}\,. \end{cases} \tag{B.7}$$

Summarizing these results in words, we can say: The intersection of a curve $\mathcal{C}$ with a divisor D is 1 if $\mathcal{C}$ sticks out D and it is -1 if $\mathcal{C}$ lies inside D.

$X^{(\delta)}_{N,M}$ and intersection numbers

In [123], the authors gave a toric construction of $X_{N,M}$. Roughly speaking, they consider an infinite toric fan quotiented by $N\mathbb{Z}\times M\mathbb{Z}$ to impose periodic identifications in the web diagram. In the following we assume[45] that there exists a similar quotient, which gives rise to the periodic identifications required in the web diagram $X^{(\delta)}_{N,M}$. It should be noted that different choices of the fundamental domain give different but equivalent representations of a given geometry. For most curves and divisors, this quotient does no change the intersection numbers as devised in the previous section. Nevertheless, in the webs $X^{(\delta)}_{N,M}$ with $N = 1$ or $M = 1$ some curves will see

[45] Although we have not checked explicitly the existence of a quotient that satisfies all consistency conditions given in [123], we have checked our results for the intersection numbers (B.8) and (B.9) in various cases through other methods. In particular, for the cases $X^{(\delta)}_{2,1}$, $X^{(\delta)}_{2,2}$ (for $\delta = 0,1$) and $X^{(\delta)}_{2,N}$ (for $\delta = 0,1,\ldots,N-1$) we have calculated them independently by representing the geometry locally as (combinations of) $\mathbb{P}^1 \times \mathbb{P}^1$ and found complete agreement. This leads us to believe that a quotient procedure as detailed below can be employed to compute the intersection numbers.

their intersections numbers modified due to the fact that a given curve $\mathcal{C}$ can now intersect two irreducible divisors D and D' that are identified under the quotient procedure. We will discuss in the following the two special situations that may arise for N or M equal to 1, thus changing the effective rule given at the end of the previous section. It is sufficient to focus on configurations of type $X_{N,1}$ as the $X_{1,M}$ configuration will follow the same pattern by $SL(2,\mathbb{Z})$ symmetry.

• **Case 1:** The curve $\mathcal{C}$ lies inside two divisors which get identified under the quotient action. In the infinite fan we can consider the intersection of the toric curve $\mathcal{C}$ with the divisor $D = D_1 + D_2$ in Fig. B:

$$\mathcal{C} \cdot D = \mathcal{C} \cdot D_1 + \mathcal{C} \cdot D_2 = 1 + 1 = 2 \tag{B.8}$$

Under the quotient action, the two irreducible divisors get identified $D_1 \sim D_2$, leading to the result above.

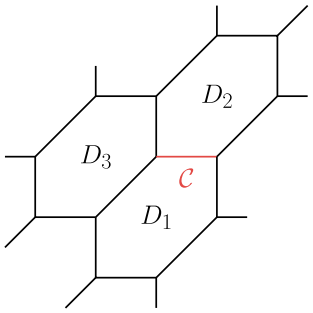

Figure 47: *A curve $\mathcal{C}$ and divisors D_1, D_2 and D_3.*

• **Case 2:** The curve $\mathcal{C}$ lies in one divisor and sticks out of another one and both get identified under the quotient. In terms of the infinite fan we are interested in the intersection of $\mathcal{C}$ with the divisor $D' = D_1 + D_3$ (see Fig. B)

$$\mathcal{C} \cdot D' = \mathcal{C} \cdot D_1 + \mathcal{C} \cdot D_3 = 1 - 1 = 0\,. \tag{B.9}$$

C Jacobi forms

This section is meant to introduce the definition and some basic properties of Jacobi forms. We also define the well known Jacobi theta function θ_1 which appears in numerous instances in the main part of this work. For a good reference on the subject of Jacobi forms we refer the reader to [154].

Jacobi forms

A Jacobi form of weight k and index m is a holomorphic function

$$\phi : \mathcal{H} \times \mathbb{C} \to \mathbb{C}\,,$$

where $\mathcal{H}$ denotes the complex upper half-plane, *i.e.* $\mathcal{H} = \{\rho \in \mathbb{C} \,|\, \mathrm{Im}(\rho) > 0\}$. Furthermore, the function $\phi(\rho, z)$ satisfies the following two transformation properties

$$\phi\Big(\frac{a\rho+b}{c\rho+d}, \frac{z}{c\rho+d}\Big) = (c\rho+d)^k e^{2\pi i m \frac{cz}{c\rho+d}} \phi(\rho,z)\,, \quad \text{where} \quad \begin{pmatrix} a & b \\ c & d \end{pmatrix} \in SL(2,\mathbb{Z}) \tag{C.1}$$

and

$$\phi(\rho, z+\lambda\rho+\mu) = e^{-2\pi i m(\lambda^2\rho + 2\lambda z)} \phi(\rho,z)\,, \quad \text{where} \quad (\lambda,\mu) \in \mathbb{Z}^2 \tag{C.2}$$

By specializing the transformation properties (C.1) and (C.2) we can see that $\phi(\rho+1,z) = \phi(\rho,z+1) = \phi(\rho,z)$, which implies that the function $\phi(\rho,z)$ has a Fourier expansion. We say that $\phi(\rho,z)$ is a holomorphic Jacobi form if this Fourier expansion is of the form

$$\phi(\rho,z) = \sum_{n=0}^{\infty} \sum_{\substack{r\in\mathbb{Z} \\ r^2\leq 4nm}} a(n,r) Q_\rho^n Q_z^r \tag{C.3}$$

where $Q_\rho = e^{2\pi i\rho}$ and $Q_z = e^{2\pi i z}$. In the case we have the stronger condition $r^2 - 4nm < 0$ it is called a Jacobi cusp form. If there is no condition at all on the second sum in the Fourier expansion it is called a weak Jacobi form. It follows from the second transformation law (C.2) that two Fourier coefficients $a(n,r)$ and $a(n',r')$ are equal when

$$r^2 - 4nm = (r')^2 - 4n'm \quad \text{and} \quad r' = r \pmod{2m} \tag{C.4}$$

Jacobi theta function θ_1

In this work we are exclusively interested in a very specific Jacobi form known as Jacobi theta function θ_1. The subscript is conventional and it meant to distinguish it from similar Jacobi forms that bear the same name. It is defined as follows

$$\theta_1(\rho,z) = 2iQ_\rho^{1/8}\sin(\pi z)\prod_{r=1}^{\infty}(1-Q_\rho^r)(1-Q_\rho^r Q_z)(1-Q_\rho^r Q_z^{-1}) \tag{C.5}$$

In addition to the transformation properties (C.1) and (C.2), θ_1 satisfies a variety of other relations. Among these the most useful for us is what we call the shift identity, given by

$$\theta_1(\rho, z+n\,\rho) = Q_\rho^{-\frac{n^2}{2}}\,(-e^{-2\pi i z})^n\,\theta_1(\rho,z) \quad n\in\mathbb{Z}\,. \tag{C.6}$$

This identity is of great importance to us in section 4.2. It allows us to show that certain topological string partitions functions are actually the same expression written in different ways and related through equation C.6.

D Integer partitions and related objects

In this appendix, we define our notation concerning integer partitions. Furthermore, we introduce we introduce different functions that depend on these partitions and which are used in the main body of this work.

Integer partition

A partition of a positive integer n is defined to be an ordered set of positive integers $\lambda = \{\lambda_1,\lambda_2,\ldots,\lambda_{\ell(\lambda)}\}$ such that

$$\lambda_1\geq\lambda_2\geq\cdots\geq\lambda_{\ell(\lambda)}>0 \quad \text{and} \quad |\lambda| = \sum_{i=1}^{\ell(\lambda)}\lambda_i = n\,. \tag{D.1}$$

We furthermore define

$$||\lambda||^2 = \sum_{i=1}^{\ell(\lambda)} \lambda_i^2 \,. \tag{D.2}$$

Integer partitions are represented graphically by using Young diagrams, *e.g.* the following partition partition $\eta = \{3, 3, 1\}$ would be represented by

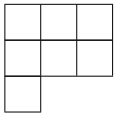

With the help of the Young diagrams we can naturally define the transpose of a partition λ^t by the Young diagram that is a reflection along the diagonal of the original diagram. In terms of the previous example $\lambda = \{3, 3, 1\}$, the transposed diagram would be

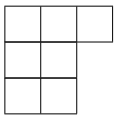

(D.3)

The transpose in this case is $\lambda^t = \{3, 2, 2\}$. Analogously to D.2, we define

$$||\lambda^t||^2 = \sum_{i=1}^{\ell(\lambda^t)} (\lambda_i^t)^2 \tag{D.4}$$

Given two partitions μ of m and ν of n such that $\ell(\mu) \geq \ell(\nu)$, $\mu_i > \nu_i$ for $i = 1, \ldots, \ell(\nu)$, we can define the skew partition μ/ν, which is obtained by formally subtracting the Young diagrams from another, *e.g.*

$\mu =$ 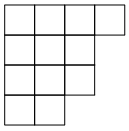 , $\nu =$ 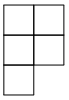 , $\mu/\nu =$ 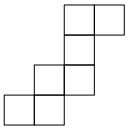 (D.5)

A pair of coordinates (i, j) can be associated to a box in a given Young diagram, where the first entry denotes the row and the second the column. The box in the most upper left corner has the coordinates $(1, 1)$ for example.

Schur Functions

Schur functions are symmetric polynomials in n variables $\mathbf{x} = (x_1, \ldots, x_n)$, that are indexed by integer partitions λ. They are defined as

$$s_\lambda(\mathbf{x}) = \sum_T \mathbf{x}^T = \sum_T x_1^{t_1} \ldots x_n^{t_n} \tag{D.6}$$

where the summation is over all semistandard Young tableaux T that can be associated with the partition λ. Each t_i counts the occurrences of the number i in T. Skew Schur functions

depend on skew partitions λ/η and they can be defined in terms of the conventional Schur functions as follows

$$s_{\lambda/\eta}(\mathbf{x}) = \sum_{\mu} N^{\lambda}_{\eta\mu} s_{\mu}(\mathbf{x})\,, \tag{D.7}$$

where $N^{\lambda}_{\eta\mu}$ are the Littlewood-Richardson coefficients. Two very useful identities when performing sums of skew Schur functions [155] are

$$\begin{aligned}\sum_{\eta} s_{\eta^t/\mu}(\mathbf{x}) s_{\eta/\nu}(\mathbf{y}) &= \prod_{i,j=1}^{\infty}(1+x_i y_j)\sum_{\tau} s_{\nu^t/\tau}(\mathbf{x}) s_{\mu^t/\tau^t}(\mathbf{y}) \\ \sum_{\eta} s_{\eta/\mu}(\mathbf{x}) s_{\eta/\nu}(\mathbf{y}) &= \prod_{i,j=1}^{\infty}(1-x_i y_j)^{-1}\sum_{\tau} s_{\nu^t/\tau}(\mathbf{x}) s_{\mu/\tau}(\mathbf{y})\end{aligned} \tag{D.8}$$

Special functions and useful identities

A set of special functions depending on partitions are the $\mathcal{J}$-functions. In the main text of this work they appear in section 3.5.5 when calculating a universal building block for the instanton partition function associated to the geometries $X_{N,M}$. They are indexed by two integer partitions μ and ν and have the following explicit form

$$\mathcal{J}_{\mu\nu} = (x;t,q) = \prod_{k=1}^{\infty} J_{\mu\nu}(Q_{\rho}^{k-1}x;t,q)\,, \tag{D.9}$$

where

$$J_{\mu\nu}(x;t,q) = \prod_{(i,j)\in\mu}\left(1-xt^{\nu^t_j-i+\frac{1}{2}}q^{\mu_i-j+\frac{1}{2}}\right)\prod_{(i,j)\in\nu}\left(1-xt^{-\mu^t_j+i-\frac{1}{2}}q^{-\nu_i+j-\frac{1}{2}}\right) \tag{D.10}$$

In this expression the product runs over the coordinates of the Young diagrams associated to the respective partitions. Another set of special functions are the ϑ-functions. They naturally appear in the expression of the instanton partition function $\mathcal{Z}^{(\delta)}_{N,M}$ and are defined as

$$\vartheta_{\mu\nu}(x;\rho) = \prod_{(i,j)\in\mu}\vartheta\left(x^{-1}q^{-\nu^t_j+i-\frac{1}{2}}t^{-\mu_i+j-\frac{1}{2}};\rho\right)\prod_{(i,j)\in\nu}\vartheta\left(x^{-1}q^{\mu^t_j-i+\frac{1}{2}}t^{\nu_i-j+\frac{1}{2}};\rho\right) \tag{D.11}$$

where

$$\vartheta(x;\rho) = (x^{\frac{1}{2}}-x^{-\frac{1}{2}})\prod_{k=1}^{\infty}(1-x\,Q_{\rho}^{k})(1-x^{-1}Q_{\rho}^{k}) = \frac{i\,Q_{\rho}^{-\frac{1}{8}}\theta_1(\rho;z)}{\prod_{k=1}^{\infty}(1-Q_{\rho}^{k})}\,. \tag{D.12}$$

Here θ_1 is the Jacobi theta function defined in (C.5). Pairs of $\mathcal{J}$-functions can be combined into ϑ-functions in by utilizing the following identities

$$\mathcal{J}_{\mu\nu}(x;q,t)\mathcal{J}_{\nu\mu}(Q_{\rho}x^{-1};q,t) \;= x^{\frac{|\mu|+|\nu|}{2}}q^{\frac{||\nu^t||^2-||\mu^t||^2}{4}}t^{\frac{||\mu||^2-||\nu||^2}{4}}\,\vartheta_{\mu\nu}(x;\rho)\,, \tag{D.13}$$

as well as

$$\frac{(-1)^{|\mu|}t^{\frac{||\mu||^2}{2}}q^{\frac{||\mu^t||^2}{2}}\tilde{Z}_\mu(q,t)\tilde{Z}_{\mu^t}(t,q)}{\mathcal{J}_{\mu\mu}(Q_\rho\sqrt{\frac{t}{q}};q,t)\mathcal{J}_{\mu\mu}(Q_\rho\sqrt{\frac{q}{t}};q,t)} = \frac{1}{\vartheta_{\mu\mu}(\sqrt{\frac{q}{t}};\rho)} = \frac{1}{\vartheta_{\mu\mu}(\sqrt{\frac{t}{q}};\rho)}\,. \tag{D.14}$$

These identities are used when explicitly gluing the M universal building blocks $W^{\alpha_1\ldots\alpha_N}_{\beta_1\ldots\beta_N}$ together to form a specific web diagram $X^{(\delta)}_{N,M}$. From (C.6) and (D.12) it is clear that the ϑ-functions also satisfy a so called shift identity

$$\begin{aligned}\vartheta_{\alpha\beta}(Q_xQ_\rho^{\pm};\rho) &= (-Q_x^{\mp}Q_\rho^{-\frac{1}{2}})^{|\alpha|+|\beta|}q^{\mp\frac{|\alpha|+||\alpha||^2-|\beta|-||\beta||^2}{2}}\Big(\prod_{(i,j)\in\alpha}q^{\pm i}\Big)\Big(\prod_{(i,j)\in\beta}q^{\mp i}\Big)\vartheta_{\alpha\beta}(Q_x;\rho)\\ &= (-Q_x^{\mp}Q_\rho^{-\frac{1}{2}})^{|\alpha|+|\beta|}q^{\pm\frac{\kappa(\beta)-\kappa(\alpha)}{2}}\vartheta_{\alpha\beta}(Q_x;\rho)\end{aligned} \tag{D.15}$$

Upon changing the order of the indexing partitions in ϑ, we simply have

$$\vartheta_{\alpha\beta}(Q_x;\rho) = (-1)^{|\alpha|+|\beta|}\vartheta_{\beta\alpha}(Q_x^{-1};\rho) \tag{D.16}$$

Another set of identities that are used in the main text to convert infinite products into products over integer partition coordinates are the following

$$\begin{aligned}\prod_{i,j=1}^{\infty}\frac{1-Qq^{-\mu_j^t+i-1}t^{-\nu_i+j}}{1-Qq^{i-1}t^j} &= \prod_{(i,j)\in\nu}(1-Qq^{-\mu_j^t+i-1}t^{-\nu_i+j})\prod_{(i,j)\in\mu}(1-Qq^{\nu_j^t-i}t^{\mu_i-j+1})\\ \prod_{i,j=1}^{\infty}\frac{1-Qq^{-\mu_j^t+i-1}t^{-\mu_i+j}}{1-Qq^{i-1}t^j} &= \prod_{(i,j)\in\mu}(1-Qq^{-\mu_j^t+i-1}t^{-\mu_i+j})(1-Qq^{\mu_j^t-i}t^{\mu_i-j+1})\end{aligned} \tag{D.17}$$

E Presentation of $Sp(4,\mathbb{Z})$ and Modularity

In [150] a presentation of $Sp(4,\mathbb{Z})$ in terms of 2 generators (satisfying 8 defining relations) has been given. The latter are of order 2 and 12 respectively

$$K = \begin{pmatrix}1&0&0&0\\1&-1&0&0\\0&0&1&1\\0&0&0&-1\end{pmatrix}, \qquad \text{and} \qquad L = \begin{pmatrix}0&0&-1&0\\0&0&0&-1\\1&0&1&0\\0&1&0&0\end{pmatrix}, \tag{E.1}$$

which satisfy

$$\begin{aligned}&K^2 = L^{12} = \mathbb{1}_{4\times4}\,, \quad (KL^7KL^5K)L = L(KL^5KL^7K)\,, \quad (L^2KL^4)H = H(L^2KL^4)\,,\\ &(L^3KL^3)H = H(L^3KL^3)\,, \quad (L^2H)^2 = (HL^2)^2\,, \quad L(L^6H)^2 = (L^6H)^2L\,, \quad (KL^5)^5 = (L^6H)^2\,,\end{aligned}$$

where $H = KL^5KL^7K$. We also mention that another presentation [149] (in terms of 6 generators and 18 defining relations) is given by $X_{1,2,3,4,5,6}$, which can be expressed in terms of L and K as follows

$$X_1 = L^5KL\,, \qquad X_2 = L^9HL^{10}H\,, \qquad X_3 = L^8KL^{10}\,,$$

$$X_4 = HL^9HL^{10}\,, \qquad X_5 = HL^6\,, \qquad X_6 = L^9HL^6H\,. \tag{E.2}$$

Furthermore, the group $Sp(4,\mathbb{Z})$ acts in a very natural form on the period matrix $\Omega = \begin{pmatrix} \tau & v \\ v & \rho \end{pmatrix}$ of a genus 2 Riemann surface

$$\begin{pmatrix} A & B \\ C & D \end{pmatrix}: \qquad \Omega \longmapsto (A\Omega + B)(C\Omega + D)^{-1}\,. \tag{E.3}$$

Here A, B, C, D are 2×2 matrices that satisfy

$$A^TD - C^TB = \mathbb{1}_{2\times 2} = DA^T - CB^T\,, \qquad A^TC = C^TA\,, \qquad B^TD = D^TB\,. \tag{E.4}$$

For convenience, we provide the action of some of the generators on the period matrix Ω

$$K: \ \Omega \to \begin{pmatrix} \tau & \tau - v \\ \tau - v & -2v + \rho + \tau \end{pmatrix}, \qquad L^3: \ \Omega \to \begin{pmatrix} \tau - \frac{v^2}{\rho} & \frac{v}{\rho} \\ \frac{v}{\rho} & -\frac{1}{\rho} \end{pmatrix},$$

$$L^6: \ \Omega \to \begin{pmatrix} \tau & -v \\ -v & \rho \end{pmatrix}, \qquad L^9: \ \Omega \to \begin{pmatrix} \tau - \frac{v^2}{\rho} & -\frac{v}{\rho} \\ -\frac{v}{\rho} & -\frac{1}{\rho} \end{pmatrix},$$

$$H: \ \Omega \to \begin{pmatrix} \rho & v \\ v & \tau \end{pmatrix}, \qquad L^2KL^4: \ \Omega \to \begin{pmatrix} \tau & v - 1 \\ v - 1 & \rho \end{pmatrix},$$

$$L^9HL^{10}H: \ \Omega \to \begin{pmatrix} \tau & v \\ v & \rho + 1 \end{pmatrix}, \qquad HL^9HL^{10}: \ \Omega \to \begin{pmatrix} \tau + 1 & v \\ v & \rho \end{pmatrix}. \tag{E.5}$$

F Résumé en français

Depuis sa découverte la théorie des cordes est considérée comme un des meilleurs candidats pour une théorie quantique de la gravitation. Après de nombreuses années d'efforts cet entreprise n'a malheureusement pas encore mené à un modèle réaliste de notre réalité. Malgré tout, on a appris beaucoup de nouvelles choses sur la quête de comprendre cette théorie mystérieuse. Il se trouve que la théorie des cordes fait intervenir un bon nombre de structures mathématiques très sophistiquées et peut fournir des point de vue alternatif ainsi que de nouveaux résultats de ce côté. Parc contre, ce qui va être l'utilité majeure pour nous dans cette thèse et le fait qu'elle donne aussi nouvelle approche aux théories de jauges. Ces dernières sont une classe de théories quantique, dont le célèbre modèle standard des particules en fait partie. C'est ce modèle qui reste à nos jours et cela avec beaucoup de succès, notre meilleur description de la physique des particules telle qu'on la observe dans les collisionneurs. Pourtant on sait que le modèle standard ne donne pas l'image complète de notre réalité physique. Parmi d'autres défauts, la gravité n'y figure pas par example. Cela était donc clairement une parmi plusieurs sources de motivation pour chercher ailleurs. Revenons à la théorie des cordes et aux théories de jauges en général. A travers des modèle de cordes quantique on peut modéliser une classe particulière de théories de jauges, à savoir les théories de jauges supersymétriques. La supersymétrie est un concept qui relie bosons et fermions les un avec les autres. Sous elle, un boson va avoir un

fermion associé à lui, son superparténaire, et vice versa. Même si à ce jour, il n'y a pas de vérification expérimentale de la supersymétrie, cette dernière reste néanmoins un outil de calcul puissant. Comme elle impose des relations entre bosons et fermions, elle rend la théorie plus rigide (contenu en champs réduit, moins de paramètres libres, etc.) et nous fournit avec des outils de calcul puissants. Le résultat est donc que dans ces théories, beaucoup de quantités sont plus facile à calculer. Le point important de cette histoire est que si on n'arrive pas à résoudre un modèle ou à calculer une certaine quantité en présence de supersymétrie, on n'y arrivera probablement pas sans. D'où une bonne raison de s'intéresser à cette classe de théories même si la supersymétrie ne sera jamais observée expérimentalement.

Le sujet principal de cette thèse porte sur les "Little string theories" (LST). Ce sont des théories en six dimensions qui ont des degrés de libertés non locaux données par des cordes mais ne contiennent pas de gravité. Leur existence était établie pour une première fois lors de la réalisation que la théorie dans le volume d'univers de la brane NS5 pouvait être découplé de la gravité sans pour autant devenir trivial. Cela est dû au fait que la tension des branes NS5 dépend d'une telle manière de la constante de couplage de la corde g_s que la limite $g_s \to 0$ avec $M_s =$ fixe, supprime les interactions entre cordes propageant sur la brane et cordes qui se propagent dans l'espace-temps hors brane. Parmi les dernières il y a notamment les cordes fermées dont les modes vibratoires correspondent aux gravitons. En plus les LST sont liés aux fameuses théories de champ superconformes (SCFT) en six dimensions. Superconforme veut dire que ces théories sont supersymétriques et qu'en plus il n'y a pas de paramètre dimensionnée qui pourra donner une échelle physique. La raison pour le statut de célébrité de ces théories est que six est la dimension la plus élevée pour laquelle on peut avoir une symétrie superconforme. Dans ce sens, ces SCFT en six dimensions sont donc en quelque sorte les théories mères des SCFT en dimensions inférieurs. Ces dernières peuvent être obtenues par compactification. Les SCFT en six dimensions contiennent également des degrés de liberté cordes, mais ces cordes peuvent être de tension nulle. La relation avec les LST est que dans les LST il y a exactement une échelle qui est donnée par la tension finie et non-nul du "little string". Il existe alors une limite pour se débarrasser cet échelle et d'atteindre ainsi une SCFT associé. Les LST admettent une description effective en terme de théories de jauges supersymétrique de type quiver. Cela veut dire qu'il y a plusieurs groupe de jauges différents et qu'il y a de la matière qui est couplé à un ou à plusieurs de ces facteurs de jauge. Cette structure peut être facilement représentée sous forme d'un graphe qu'on appelle quiver, par example 1. Chaque groupe de jauge est représentée par un noeud et la matière par différents segments qui connectent les facteurs de jauge (noeuds) auxquels ils sont couplés.

Tout comme les théorie des cordes de type IIA et IIB en dix dimensions d'espace-temps, les LST ont la propriété de T-dualité. Par T-duality entre IIA et IIB, on entend le fait que si on compactifie par example une dimension spatiale de la théorie IIA sur un cercle à un rayon fixé, la théorie physique qu'on obtient est la même que si on prenait la type IIB avec la même dimension spatiale compactifié sur un cercle de rayon inversé. Comme les quantités calculable dans ces deux théories sont reliées, on dit que les théories sont duales, plus spécifiquement T-dual dans ce cas. Cette même notion de T-dualité est vraie pour les LST en six dimensions, encore une qualité qui soulignent le caractère non-local des ces théories. Pour vérifier la dualité par le calcul, il existe différentes méthodes. Une méthode particulièrement intéressant est par comparaison des fonctions de partitions de Nekrasov. Ces fonctions sont des objects non-

perturbative. Cela veut dire que toutes les corrections quantiques, notamment celles dues aux instantons sont comprises dedans. Donc, établir une relation entre des fonctions de partitions pour deux théories à priori distinctes, fournit une preuve de dualité exacte à tout ordre. Ces fonctions de partitions ont été initialement introduites pour des théories supersymétriques en quatre dimensions. Le calcul repose sur une technique appelée localisation supersymétrique, laquelle est basé sur la description lagrangienne de la théorie en question. Malheureusement, les théories auxquelles nous nous intéressons dans cette thèse, ne disposent pas de description lagrangienne. Il faut donc avoir recours à une autre méthode pour calculer ces fonctions de partitions. Par une chaîne de dualités en théories des cordes on peut relier les configurations de branes qui donnent les LST à une configurations de branes en ce qu'on appelle théorie M. Cette dernière est une théorie dans un espace-temps en onze dimensions et les théories des cordes peuvent obtenues à partir de la théorie M par compactification et dualités. Sa description de basse énergie est donnée par la supergravité en onze dimensions. Dans cette configuration de branes en théories M, il existe une technique systématique, appelée le vertex topologique, pour calculer les fonctions de partitions pour les LST qui sont le sujet de cette thèse.

Le but de cette thèse est d'analyser si la classe de LST à laquelle on s'intéresse, admet encore des dualités autre que la T-dualité décrite plus haut. Pour cela nous disposons d'outils géométrique issus de la géométrie torique. La puissance de cette approche est qu'elle est très graphique. Des éléments importants de la structure des LST peuvent ainsi être représenté par des simple graphique en deux dimensions. Cette représentation graphique nous fournit des premières indications de présence d'un réseau the théories duales beaucoup plus important que seulement la T-dualité. En calculant, les fonctions de partitions associées, nous sommes capables que ces dualité sont effectivement réalisées. En terme de théorie de jauges supersymétrique, le résultat est également intéressant dans le sens ou ces nouvelles dualités mélangent les paramètres des théories d'une manière hautement non-trivial. Donc si on ne dispose pas de l'approche de construction par la théorie des cordes, ce serait quasi impossible de deviner ces relations entre ces différents théories.

Nous étudions également différentes conséquences de ce réseau de dualités. Nous en tirons des nouvelles limites de réduction dimensionnelle de six à cinq dimensions pour ces théories. Les limites conventionnelles pour ces théories donnent en général des théories en cinq dimensions ayant le même groupe de jauge et le même contenu en matière. Les nouvelles limites que nous décrivons, réduisent également la dimensionalité mais aussi en même temps le rang du groupe de jauge et changent le contenu en matière. Tout cela est vérifié sur le plan calculatoire à l'aide de la fonction de partition de Nekrasov. Un autre résultat que nous tirons du réseau de dualités est la présence d'une symétrie dihédrale pour la fonction de partition même et par conséquence aussi pour les théories de jauges associées. Cette symétrie agit d'une façon hautement non-perturbative au niveau des théories de jauge. Elle relie des termes à different ordre dans l'expansion instantonique (non-perturbative). Encore une fois, sans l'approche de la théorie des cordes, cette symétrie serait très difficile, voire impossible, à trouver.

S'il y a donc une leçon importante à tirer de cette thèse, c'est que la construction de théories de jauges supersymétriques en théories des cordes peut nous fournir des informations qui sont quasi impossible d'obtenir du seul point de vue de la théorie da jauge. La puissance des méthodes géometriques disponible en théories des cordes ainsi que les différents points de vue alterna-

tive nous permettent d'analyser des questions pertinentes, comme par example la dualité entre différentes théories, par des angles multiples et d'obtenir des résultats étonnants.

References

[1] J. Polchinski, *String theory. Vol. 1: An introduction to the bosonic string,* doi:10.1017/CBO9780511816079

[2] J. Polchinski, *String theory. Vol. 2: Superstring theory and beyond,* doi:10.1017/CBO9780511618123

[3] R. Blumenhagen, D. Lüst and S. Theisen, *Basic concepts of string theory,*

[4] J. H. Schwarz, *Physical States and Pomeron Poles in the Dual Pion Model,* Nucl. Phys. B **46** (1972) 61.

[5] P. Goddard and C. B. Thorn, *Compatibility of the Dual Pomeron with Unitarity and the Absence of Ghosts in the Dual Resonance Model,* Phys. Lett. **40B** (1972) 235.

[6] J. Polchinski, *Dirichlet Branes and Ramond-Ramond charges,* Phys. Rev. Lett. **75** (1995) 4724 [hep-th/9510017].

[7] E. Witten, *String theory dynamics in various dimensions,* Nucl. Phys. B **443** (1995) 85 [hep-th/9503124].

[8] M. Dine, P. Y. Huet and N. Seiberg, *Large and Small Radius in String Theory,* Nucl. Phys. B **322** (1989) 301.

[9] J. Dai, R. G. Leigh and J. Polchinski, *New Connections Between String Theories,* Mod. Phys. Lett. A **4** (1989) 2073.

[10] A. Sen, *Electric magnetic duality in string theory,* Nucl. Phys. B **404** (1993) 109 doi:10.1016/0550-3213(93)90475-5 [hep-th/9207053].

[11] C. Vafa, *Evidence for F theory,* Nucl. Phys. B **469** (1996) 403 [hep-th/9602022].

[12] E. Witten, *Topological Sigma Models,* Commun. Math. Phys. **118** (1988) 411.

[13] R. Gopakumar and C. Vafa, *M theory and topological strings. 1.,* hep-th/9809187.

[14] R. Gopakumar and C. Vafa, *M theory and topological strings. 2.,* hep-th/9812127.

[15] Y. A. Golfand and E. P. Likhtman, *Extension of the Algebra of Poincare Group Generators and Violation of p Invariance,* JETP Lett. **13** (1971) 323 [Pisma Zh. Eksp. Teor. Fiz. **13** (1971) 452].

[16] J. Wess and B. Zumino, *Supergauge Transformations in Four-Dimensions,* Nucl. Phys. B **70** (1974) 39.

[17] R. Haag, J. T. Lopuszanski and M. Sohnius, *All Possible Generators of Supersymmetries of the s Matrix,* Nucl. Phys. B **88** (1975) 257.

[18] E. Witten and D. I. Olive, *Supersymmetry Algebras That Include Topological Charges,* Phys. Lett. **78B** (1978) 97.

[19] C. Montonen and D. I. Olive, *Magnetic Monopoles as Gauge Particles?,* Phys. Lett. **72B** (1977) 117.

[20] H. Osborn, *Topological Charges for N=4 Supersymmetric Gauge Theories and Monopoles of Spin 1,* Phys. Lett. **83B** (1979) 321.

[21] A. Sen, *Dyon - monopole bound states, selfdual harmonic forms on the multi - monopole moduli space, and SL(2,Z) invariance in string theory,* Phys. Lett. B **329** (1994) 217 [hep-th/9402032].

[22] E. Witten, *Some comments on string dynamics,* hep-th/9507121.

[23] N. Seiberg, *New Theories in Six-Dimensions and Matrix Description of M Theory on T^5 and T^5/Z_2*, Phys. Lett. B **408** (1997) 98 [hep-th/9705221].

[24] O. Aharony, *A Brief Review of 'Little String Theories'*, Class. Quant. Grav. **17** (2000) 929 [hep-th/9911147].

[25] D. Kutasov, *Introduction to Little String Theory*, in Superstrings and related matters. Proceedings, Spring School, Trieste, Italy, April 2-10, 2001, pp. 165–209, 2001.

[26] W. Nahm, *Supersymmetries and their Representations,* Nucl. Phys. B **135** (1978) 149.

[27] L. Bhardwaj, *Classification of 6d $\mathcal{N} = (1,0)$ gauge theories,* JHEP **1511** (2015) 002 [arXiv:1502.06594 [hep-th]].

[28] L. Bhardwaj, M. Del Zotto, J. J. Heckman, D. R. Morrison, T. Rudelius and C. Vafa, *F-theory and the Classification of Little Strings,* Phys. Rev. D **93** (2016) no.8, 086002 [arXiv:1511.05565 [hep-th]].

[29] P. Pasti, D. P. Sorokin and M. Tonin, *On Lorentz invariant actions for chiral p forms,* Phys. Rev. D **55** (1997) 6292 [hep-th/9611100].

[30] M. Aganagic and N. Haouzi, *ADE Little String Theory on a Riemann Surface (and Triality),* arXiv:1506.04183 [hep-th].

[31] S. Hohenegger, A. Iqbal and S. J. Rey, *Instanton-monopole correspondence from M-branes on $\mathbb{S}^1$ and little string theory,* Phys. Rev. D **93** (2016) no.6, 066016 [arXiv:1511.02787 [hep-th]].

[32] S. Hohenegger, A. Iqbal and S. J. Rey, *Self-Duality and Self-Similarity of Little String Orbifolds,* Phys. Rev. D **94** (2016) no.4, 046006 [arXiv:1605.02591 [hep-th]].

[33] S. Hohenegger, A. Iqbal and S. J. Rey, *Dual Little Strings from F-Theory and Flop Transitions,* JHEP **1707** (2017) 112 [arXiv:1610.07916 [hep-th]].

[34] B. Bastian and S. Hohenegger, *Five-Brane Webs and Highest Weight Representations,* JHEP **1712** (2017) 020 [arXiv:1706.08750 [hep-th]].

[35] N. Haouzi and C. Kozçaz, *The ABCDEFG of Little Strings,* arXiv:1711.11065 [hep-th].

[36] B. Bastian, S. Hohenegger, A. Iqbal and S. J. Rey, *Dual little strings and their partition functions,* Phys. Rev. D **97** (2018) no.10, 106004 [arXiv:1710.02455 [hep-th]].

[37] B. Bastian, S. Hohenegger, A. Iqbal and S. J. Rey, *Triality in Little String Theories,* Phys. Rev. D **97** (2018) no.4, 046004 doi:10.1103/PhysRevD.97.046004 [arXiv:1711.07921 [hep-th]].

[38] B. Bastian, S. Hohenegger, A. Iqbal and S. J. Rey, *Beyond Triality: Dual Quiver Gauge Theories and Little String Theories,* JHEP **1811** (2018) 016 [arXiv:1807.00186 [hep-th]].

[39] J. Kim, S. Kim and K. Lee, *Little strings and T-duality,* JHEP **1602** (2016) 170 [arXiv:1503.07277 [hep-th]].

[40] J. Kim and K. Lee, *Little strings on D_n orbifolds,* JHEP **1710** (2017) 045 [arXiv:1702.03116 [hep-th]].

[41] M. Aganagic, E. Frenkel and A. Okounkov, *Quantum q-Langlands Correspondence,* Trans. Moscow Math. Soc. **79** (2018) 1 [arXiv:1701.03146 [hep-th]].

[42] I. Antoniadis, A. Delgado, C. Markou and S. Pokorski, *The effective supergravity of Little String Theory,* Eur. Phys. J. C **78** (2018) no.2, 146 [arXiv:1710.05568 [hep-th]].

[43] A. Ahmed, S. Hohenegger, A. Iqbal and S. J. Rey, *Bound states of little strings and symmetric orbifold conformal field theories,* Phys. Rev. D **96** (2017) no.8, 081901 [arXiv:1706.04425 [hep-th]].

[44] J. Hayling, R. Panerai and C. Papageorgakis, *Deconstructing Little Strings with $\mathcal{N} = 1$ Gauge Theories on Ellipsoids,* SciPost Phys. **4** (2018) no.6, 042 [arXiv:1803.06177 [hep-th]].

[45] B. Haghighat, J. Kim, W. Yan and S. T. Yau, *D-type fiber-base duality,* JHEP **1809** (2018) 060 [arXiv:1806.10335 [hep-th]].

[46] B. Bastian, S. Hohenegger, A. Iqbal and S. J. Rey, *Five-Dimensional Gauge Theories from Shifted Web Diagrams,* Phys. Rev. D **99** (2019) no.4, 046012 [arXiv:1810.05109 [hep-th]].

[47] B. Bastian and S. Hohenegger, *Dihedral Symmetries of Gauge Theories from Dual Calabi-Yau Threefolds,* Phys. Rev. D **99** (2019) no.6, 066013 [arXiv:1811.03387 [hep-th]].

[48] B. Haghighat and R. Sun, *M5 branes and Theta Functions,* arXiv:1811.04938 [hep-th].

[49] L. Bhardwaj, *Revisiting the classifications of 6d SCFTs and LSTs,* arXiv:1903.10503 [hep-th].

[50] B. Haghighat, A. Iqbal, C. Kozçaz, G. Lockhart and C. Vafa, *M-Strings,* Commun. Math. Phys. **334** (2015) no.2, 779 [arXiv:1305.6322 [hep-th]].

[51] B. Haghighat, C. Kozcaz, G. Lockhart and C. Vafa, *Orbifolds of M-strings,* Phys. Rev. D **89** (2014) no.4, 046003 [arXiv:1310.1185 [hep-th]].

[52] S. Hohenegger and A. Iqbal, *M-strings, elliptic genera and $\mathcal{N} = 4$ string amplitudes,* Fortsch. Phys. **62** (2014) 155 [arXiv:1310.1325 [hep-th]].

[53] M. R. Douglas, *Branes within branes,* NATO Sci. Ser. C **520** (1999) 267 [hep-th/9512077].

[54] N. Seiberg, *Notes on theories with 16 supercharges,* Nucl. Phys. Proc. Suppl. **67** (1998) 158 [hep-th/9705117].

[55] R. Dijkgraaf, C. Vafa and E. Verlinde, *M-theory and a topological string duality,* hep-th/0602087.

[56] M. Aganagic, A. Klemm, M. Marino and C. Vafa, *The Topological vertex,* Commun. Math. Phys. **254**, 425 (2005) [hep-th/0305132].

[57] A. Iqbal, C. Kozcaz and C. Vafa, *The Refined topological vertex,* JHEP **0910** (2009) 069 [hep-th/0701156].

[58] O. Aharony, A. Hanany and B. Kol, *Webs of (p,q) five-branes, five-dimensional field theories and grid diagrams,* JHEP **9801** (1998) 002 doi:10.1088/1126-6708/1998/01/002 [hep-th/9710116].

[59] M. Nakahara, *Geometry, Topology and Physics,* Second edition, Institute of Physics Publishing, 2003

[60] K. Hori et al. *Mirror Symmetry* Clay Mathematics Monographs, 2003

[61] N. Seiberg and E. Witten, *Electric - magnetic duality, monopole condensation, and confinement in N=2 supersymmetric Yang-Mills theory,* Nucl. Phys. B **426** (1994) 19 Erratum: [Nucl. Phys. B **430** (1994) 485] [hep-th/9407087].

[62] N. A. Nekrasov, *Seiberg-Witten prepotential from instanton counting,* Adv. Theor. Math. Phys. **7** (2003) no.5, 831 [hep-th/0206161].

[63] L. Alvarez-Gaume and S. F. Hassan, *Introduction to S duality in N=2 supersymmetric gauge theories: A Pedagogical review of the work of Seiberg and Witten,* Fortsch. Phys. **45** (1997) 159 [hep-th/9701069].

[64] N. Seiberg and E. Witten, *Monopoles, duality and chiral symmetry breaking in N=2 supersymmetric QCD,* Nucl. Phys. B **431** (1994) 484 [hep-th/9408099].

[65] P. C. Argyres, M. R. Plesser and N. Seiberg, *The Moduli space of vacua of N=2 SUSY QCD and duality in N=1 SUSY QCD,* Nucl. Phys. B **471** (1996) 159 [hep-th/9603042].

[66] N. Marcus and A. Sagnotti, *The Ultraviolet Behavior of $N = 4$ Yang-Mills and the Power Counting of Extended Superspace,* Nucl. Phys. B **256** (1985) 77.

[67] N. Seiberg, *Naturalness versus supersymmetric nonrenormalization theorems,* Phys. Lett. B **318** (1993) 469 [hep-ph/9309335].

[68] N. Seiberg, *Supersymmetry and Nonperturbative beta Functions,* Phys. Lett. B **206** (1988) 75.

[69] E. Witten, *Solutions of four-dimensional field theories via M theory,* Nucl. Phys. B **500** (1997) 3 [hep-th/9703166].

[70] A. Klemm, W. Lerche, P. Mayr, C. Vafa and N. P. Warner, *Selfdual strings and N=2 supersymmetric field theory,* Nucl. Phys. B **477** (1996) 746 [hep-th/9604034].

[71] A. Losev, N. Nekrasov and S. L. Shatashvili, *Issues in topological gauge theory,* Nucl. Phys. B **534** (1998) 549 [hep-th/9711108].

[72] A. Lossev, N. Nekrasov and S. L. Shatashvili, *Testing Seiberg-Witten solution,* NATO Sci. Ser. C **520** (1999) 359 [hep-th/9801061].

[73] E. Witten, *Topological Quantum Field Theory,* Commun. Math. Phys. **117** (1988) 353.

[74] Y. Tachikawa, *A review on instanton counting and W-algebras,* arXiv:1412.7121 [hep-th].

[75] A. A. Belavin, A. M. Polyakov, A. S. Schwartz and Y. S. Tyupkin, *Pseudoparticle Solutions of the Yang-Mills Equations,* Phys. Lett. B **59** (1975) 85 [Phys. Lett. **59B** (1975) 85]. doi:10.1016/0370-2693(75)90163-X

[76] M. F. Atiyah, N. J. Hitchin, V. G. Drinfeld and Y. I. Manin, *Construction of Instantons,* Phys. Lett. A **65** (1978) 185.

[77] M. F. Atiyah and R. Bott, *The Moment map and equivariant cohomology,* Topology **23** (1984) 1.

[78] N. Nekrasov and A. Okounkov, *Seiberg-Witten theory and random partitions,* Prog. Math. **244** (2006) 525 [hep-th/0306238].

[79] D. Gaiotto, *N=2 dualities,* JHEP **1208** (2012) 034 [arXiv:0904.2715 [hep-th]].

[80] L. F. Alday, D. Gaiotto and Y. Tachikawa, *Liouville Correlation Functions from Four-dimensional Gauge Theories,* Lett. Math. Phys. **91** (2010) 167 [arXiv:0906.3219 [hep-th]].

[81] I. Antoniadis, E. Gava, K. S. Narain and T. R. Taylor, *Topological amplitudes in string theory,* Nucl. Phys. B **413** (1994) 162 [hep-th/9307158].

[82] T. Eguchi and H. Kanno, *Topological strings and Nekrasov's formulas,* JHEP **0312** (2003) 006 [hep-th/0310235].

[83] A. Iqbal and A. K. Kashani-Poor, *Instanton counting and Chern-Simons theory,* Adv. Theor. Math. Phys. **7** (2003) no.3, 457 [hep-th/0212279].

[84] A. Iqbal and A. K. Kashani-Poor, *SU(N) geometries and topological string amplitudes,* Adv. Theor. Math. Phys. **10** (2006) no.1, 1 [hep-th/0306032].

[85] M. Berkooz, M. Rozali and N. Seiberg, *Matrix Description of M theory on T^4 and T^5,* Phys. Lett. B **408** (1997) 105 [hep-th/9704089].

[86] K. A. Intriligator, *New string theories in six-dimensions via branes at orbifold singularities,* Adv. Theor. Math. Phys. **1** (1998) 271 [hep-th/9708117].

[87] M. R. Douglas and G. W. Moore, *D-branes, quivers, and ALE instantons,* hep-th/9603167.

[88] J. D. Blum and K. A. Intriligator, *New phases of string theory and 6-D RG fixed points via branes at orbifold singularities,* Nucl. Phys. B **506** (1997) 199 doi:10.1016/S0550-3213(97)00449-5 [hep-th/9705044].

[89] T. Weigand, *F-theory,* PoS TASI **2017** (2018) 016 [arXiv:1806.01854 [hep-th]].

[90] M. Cvetič and L. Lin, *TASI Lectures on Abelian and Discrete Symmetries in F-theory,* PoS TASI **2017** (2018) 020 doi:10.22323/1.305.0020 [arXiv:1809.00012 [hep-th]].

[91] J. J. Heckman, *More on the Matter of 6D SCFTs,* Phys. Lett. B **747** (2015) 73 [arXiv:1408.0006 [hep-th]].

[92] J. J. Heckman, D. R. Morrison and C. Vafa, *On the Classification of 6D SCFTs and Generalized ADE Orbifolds,* JHEP **1405**, 028 (2014) Erratum: [JHEP **1506**, 017 (2015)] [arXiv:1312.5746 [hep-th]].

[93] M. Del Zotto, J. J. Heckman, D. R. Morrison and D. S. Park, *6D SCFTs and Gravity,* JHEP **1506** (2015) 158 [arXiv:1412.6526 [hep-th]].

[94] J. J. Heckman, D. R. Morrison, T. Rudelius and C. Vafa, *Atomic Classification of 6D SCFTs,* Fortsch. Phys. **63**, 468 (2015) [arXiv:1502.05405 [hep-th]].

[95] E. Witten, *Bound states of strings and p-branes,* Nucl. Phys. B **460** (1996) 335 [hep-th/9510135].

[96] B. R. Greene, A. D. Shapere, C. Vafa and S. T. Yau, *Stringy Cosmic Strings and Non-compact Calabi-Yau Manifolds,* Nucl. Phys. B **337** (1990) 1.

[97] M. R. Douglas and M. Li, *D-brane realization of N=2 superYang-Mills theory in four-dimensions,* hep-th/9604041.

[98] F. Denef, *Les Houches Lectures on Constructing String Vacua,* Les Houches **87** (2008) 483 [arXiv:0803.1194 [hep-th]].

[99] M. Bianchi, A. Collinucci and L. Martucci, *Magnetized E3-brane instantons in F-theory,* JHEP **1112** (2011) 045 [arXiv:1107.3732 [hep-th]].

[100] D. R. Morrison and D. S. Park, *F-Theory and the Mordell-Weil Group of Elliptically-Fibered Calabi-Yau Threefolds,* JHEP **1210** (2012) 128 [arXiv:1208.2695 [hep-th]].

[101] K. Kodaira, *On compact analytic surfaces,* II, Annals of Math. **77** (1964) 563-626

[102] A. Néron, *Modèles minimaux des variétés abéliennes sur les corps locaux et globaux,* Annals of Math. **82** (1965) 249-331

[103] S. H. Katz and C. Vafa, *Matter from geometry,* Nucl. Phys. B **497** (1997) 146 [hep-th/9606086].

[104] C. Beasley, J. J. Heckman and C. Vafa, *GUTs and Exceptional Branes in F-theory - II: Experimental Predictions,* JHEP **0901** (2009) 059 [arXiv:0806.0102 [hep-th]].

[105] C. Cordova, *Decoupling Gravity in F-Theory,* Adv. Theor. Math. Phys. **15** (2011) no.3, 689 [arXiv:0910.2955 [hep-th]].

[106] M. Bertolini, P. R. Merkx and D. R. Morrison, *On the global symmetries of 6D superconformal field theories,* JHEP **1607** (2016) 005 [arXiv:1510.08056 [hep-th]].

[107] H. Grauert, *Über Modifikationen und exzeptionelle analytische Mengen,* Math. Ann. **146** (1962) 331-368

[108] M. Artin, *Some numerical criteria for contractibility of curves on algebraic surfaces,* Amer. J. Math. **84** (1962) 485-496

[109] J. J. Heckman and T. Rudelius, *Top Down Approach to 6D SCFTs,* J. Phys. A **52** (2019) no.9, 093001 [arXiv:1805.06467 [hep-th]].

[110] M. Esole, S. H. Shao and S. T. Yau, *Singularities and Gauge Theory Phases,* Adv. Theor. Math. Phys. **19** (2015) 1183 [arXiv:1402.6331 [hep-th]].

[111] M. Esole, S. H. Shao and S. T. Yau, *Singularities and Gauge Theory Phases II,* Adv. Theor. Math. Phys. **20** (2016) 683 [arXiv:1407.1867 [hep-th]].

[112] M. Esole and S. H. Shao, *M-theory on Elliptic Calabi-Yau Threefolds and 6d Anomalies,* [arXiv:1504.01387 [hep-th]]

[113] A. Grassi and D. R. Morrison, *Group representations and the Euler characteristic of elliptically fibered Calabi-Yau threefolds,* math/0005196 [math.AG].

[114] D. R. Morrison and W. Taylor, *Matter and singularities,* JHEP **1201** (2012) 022 [arXiv:1106.3563 [hep-th]].

[115] A. Neitzke and C. Vafa, *Topological strings and their physical applications,* hep-th/0410178.

[116] M. Marino, *Chern-Simons theory and topological strings,* Rev. Mod. Phys. **77** (2005) 675 doi:10.1103/RevModPhys.77.675 [hep-th/0406005].

[117] T. J. Hollowood, A. Iqbal and C. Vafa, *Matrix models, geometric engineering and elliptic genera,* JHEP **0803** (2008) 069 [hep-th/0310272].

[118] G. W. Gibbons and S. W. Hawking, *Gravitational Multi - Instantons,* Phys. Lett. **78B** (1978) 430.

[119] B. Andreas, G. Curio and D. Lust, *The Neveu-Schwarz five-brane and its dual geometries,* JHEP **9810** (1998) 022 [hep-th/9807008].

[120] N. Seiberg and E. Witten, *Comments on string dynamics in six-dimensions,* Nucl. Phys. B **471** (1996) 121 [hep-th/9603003].

[121] D. Tong, *NS5-branes, T duality and world sheet instantons,* JHEP **0207** (2002) 013 [hep-th/0204186].

[122] N. C. Leung and C. Vafa, *Branes and toric geometry,* Adv. Theor. Math. Phys. **2** (1998) 91 [hep-th/9711013].

[123] A. Kanazawa, S.C. Lau, *Local Calabi-Yau manifolds of type $\tilde{A}$ and open Yau-Zaslow formula via SYZ mirror symmetry,* [arXiv:1605.00342v2 [math.AG]]

[124] D. Cox, J. Little, H. Schenck, *Toric Varieties,* American Mathematical Society - 2010

[125] J. Hayling, C. Papageorgakis, E. Pomoni and D. Rodríguez-Gómez, *Exact Deconstruction of the 6D (2,0) Theory,* JHEP **1706** (2017) 072 [arXiv:1704.02986 [hep-th]].

[126] S. Hohenegger, A. Iqbal and S. J. Rey, *M-strings, monopole strings, and modular forms,* Phys. Rev. D **92** (2015) no.6, 066005 [arXiv:1503.06983 [hep-th]].

[127] B. Haghighat, *From strings in 6d to strings in 5d,* JHEP **1601** (2016) 062 [arXiv:1502.06645 [hep-th]].

[128] J. H. Bruinier, G. van der Geer, G. Harder, D. Zagier *The 1-2-3 of Modular Forms* Springer Verlag, 2008

[129] B. Feng, A. Hanany and Y. H. He, *Counting gauge invariants: The Plethystic program,* JHEP **0703** (2007) 090 [hep-th/0701063].

[130] N. A. Nekrasov and S. L. Shatashvili, *Quantization of Integrable Systems and Four Dimensional Gauge Theories,* arXiv:0908.4052 [hep-th]

[131] M. Taki, *Refined Topological Vertex and Instanton Counting,* JHEP **0803** (2008) 048 [arXiv:0710.1776 [hep-th]].

[132] H. Hayashi and K. Ohmori, *5d/6d DE instantons from trivalent gluing of web diagrams,* JHEP **1706** (2017) 078 [arXiv:1702.07263 [hep-th]].

[133] H. Hayashi, S. S. Kim, K. Lee and F. Yagi, *5-brane webs for 5d $\mathcal{N} = 1$ G_2 gauge theories,* JHEP **1803** (2018) 125 [arXiv:1801.03916 [hep-th]].

[134] R. Gopakumar and C. Vafa, *On the gauge theory / geometry correspondence,* Adv. Theor. Math. Phys. **3** (1999) 1415 [AMS/IP Stud. Adv. Math. **23** (2001) 45] [hep-th/9811131].

[135] P. Candelas, P. S. Green and T. Hubsch, *Rolling Among Calabi-Yau Vacua,* Nucl. Phys. B **330** (1990) 49.

[136] E. Witten, *Quantum Field Theory and the Jones Polynomial,* Commun. Math. Phys. **121** (1989) 351.

[137] M. Aganagic, M. Marino and C. Vafa, *All loop topological string amplitudes from Chern-Simons theory,* Commun. Math. Phys. **247** (2004) 467 [hep-th/0206164].

[138] A. Iqbal, *All genus topological string amplitudes and five-brane webs as Feynman diagrams,* hep-th/0207114.

[139] P. S. Aspinwall, B. R. Greene and D. R. Morrison, *Multiple mirror manifolds and topology change in string theory,* Phys. Lett. B **303** (1993) 249 [hep-th/9301043].

[140] M. Reid, *The moduli space of 3-folds with $K = 0$ may nevertheless be irreducible,* Math. Ann. 287 (1987) 329-334.

[141] P. S. Green and T. Hübsch, *Connecting moduli spaces of Calabi-Yau threefolds,* Commun. Math. Phys. 119 (1988) 431-441.

[142] P. S. Green and T. Hübsch, *Phase transitions among (many of) Calabi-Yau compactifications,* Phys. Rev. Lett. 61 (1988) 1163.

[143] P. Candelas, P. S. Green, and T. Hübsch, *Finite Distances Between Distinct Calabi-Yau Vacua: (Other Worlds Are Just Around The Corner),* Phys. Rev. Lett. 62 (1989) 1956.

[144] P. Candelas, P. S. Green, and T. Hübsch, *Rolling Among Calabi-Yau Vacua,* Nucl. Phys. B330 (1990) 49.

[145] A. Hanany and E. Witten, *Type IIB superstrings, BPS monopoles, and three-dimensional gauge dynamics,* Nucl. Phys. B **492** (1997) 152 [hep-th/9611230].

[146] H. Nakajima and K. Yoshioka, *Instanton counting on blowup. II. K-theoretic partition function,* math/0505553 [math-ag].

[147] H. Awata and Y. Yamada, *Five-dimensional AGT Relation and the Deformed beta-ensemble,* Prog. Theor. Phys. **124**, 227 (2010) doi:10.1143/PTP.124.227 [arXiv:1004.5122 [hep-th]].

[148] M. Taki, *Seiberg Duality, 5d SCFTs and Nekrasov Partition Functions,* arXiv:1401.7200 [hep-th].

[149] H. Behr, *Eine endliche Präsentation der symplektischen Gruppe $Sp(4, \mathbb{Z})$.* Math.Z. **141** (1975), 47-56.

[150] P. Bender, *Eine Präsentation der symplektischen Gruppe $Sp(4, \mathbf{Z})$ mit 2 Erzeugenden und 8 definierenden Relationen.* J.Algebra **65**(2), 328-331 (1980).

[151] S. S. Kim and F. Yagi, *Topological vertex formalism with O5-plane,* Phys. Rev. D **97** (2018) no.2, 026011 [arXiv:1709.01928 [hep-th]].

[152] T. W. Grimm, A. Kapfer and D. Klevers, *The Arithmetic of Elliptic Fibrations in Gauge Theories on a Circle,* JHEP **1606** (2016) 112 [arXiv:1510.04281 [hep-th]].

[153] C. Closset, *Toric geometry and local Calabi-Yau varieties: An Introduction to toric geometry (for physicists)*, arXiv:0901.3695 [hep-th].

[154] M. Eichler and D. Zagier, *The Theory of Jacobi Forms,* Springer Verlag, 1985

[155] I. G. Macdonald, *Symmetric Functions and Hall Polynomials,* (second edition, 1995), Oxford Mathematical Monographs, Oxford Science Publications

.